PETER VAN DE KAMP

Principles of Astrometry

VAN DE KAMP

Principles of Astrometry

FREEMAN

PRINCIPLES OF ASTROMETRY

A Series of Books in Mathematics

Editors *R. A. Rosenbaum, G. Philip Johnson*

PRINCIPLES OF ASTROMETRY

With special emphasis on long-focus photographic astrometry

PETER VAN DE KAMP
Sproul Observatory, Swarthmore College

W. H. FREEMAN AND COMPANY
San Francisco and London

Printed in the United States of America.

Library of Congress Catalog Card Number 66-22077

Preface

In this book are presented some basic features of the space-time relations of stellar positions on the celestial sphere, often referred to as the field of astrometry, and, in more detail, the concepts and methods of long-focus astrometry. Mathematical principles rather than observational techniques are stressed. The reader is assumed to be acquainted with the elements of solid geometry, trigonometry, and calculus, and to have had at least an introductory course in astronomy. I have attempted to present the principles of astrometry in the simplest manner possible, using both the geometric approach and analytical derivations.

The positions of the stars on the celestial sphere have been studied for more than two millennia, in the course of which the problems of positional astronomy have appeared in the following sequence. The precession of the equinoxes, which accounts for secular changes in the equatorial coordinates of celestial objects, was discovered by Hipparchus as early as 125 B.C. because of its large angular value, 50″ yearly, but the true angular changes in position, or proper motions, of individual stars were not observed until 1718, when Edmund Halley noted that some bright stars showed relative displacements from the positions recorded for them by Ptolemy in the second century A.D. Stellar aberration due to the finite velocity of light and the earth's annual orbital motion around the sun was discovered and explained in 1726 by James Bradley (its total yearly amplitude is nearly 41″) who, a few years later found the periodic precessional term, the nutation. Solar motion was first established by William Herschel in 1783 from his observations of secular parallactic effect in stellar proper motions. In 1803 Herschel also established relative orbital motion for the components of Castor and other binary stars.

Annual parallactic motion was successfully measured in 1838 by Friedrich Wilhelm Bessel for the double star 61 Cygni. Star streaming, or preferential motion, was discovered by Jacobus Kapteyn in 1905 but not explained until Bertil Lindblad developed the theory of galactic rotation in 1926. This theory, in turn, led to Jan Oort's simple mathematical formulation for differential rotation in 1927.

Orbital motion and parallax of stars had thus already been measured in the first half of the nineteenth century. The invention of photography made possible the attainment of greater accuracy—through the combination of long-focus telescope and photographic plate—in studies of parallax and orbital motion; in fact, in all astrometric studies that involve the measurement of very small angular displacements. But although a photograph of the moon was taken in 1840, it was not until the early years of the twentieth century that the first successful precision work in long-focus photographic astrometry was done by Frank Schlesinger and by Ejnar Hertzsprung. Schlesinger developed both technique and methods as applied to the problems of stellar parallax; Hertzsprung did the same for photographically resolved double stars, i.e., the relative positions of binary star components.

The first part of this book introduces the subject of spherical astrometry. It begins with a brief survey of the most used relations of spherical trigonometry (Chapter 1). Next follows a survey of celestial coordinate systems, of definitions and formulae of spherical astrometry, and an elementary treatment of the effects of atmospheric refraction (Chapter 2). Precession, stellar parallax, and aberration are then discussed (Chapter 3), as are solar motion and galactic rotation (Chapter 4).

The second part begins with a survey of the relations between spherical and plane astrometry (Chapter 5). Next follows a presentation of the field of long-focus astrometry. A discussion of the technique (Chapter 6) is followed by an examination of the plane reduction of stellar paths and of the spherical reduction of the positions of planets, comets, asteroids, and satellites (Chapter 7). The long-focus determination of stellar parallaxes is then discussed (Chapter 8). Particular attention is given to the reduction effects and transfer problems arising for stellar paths covering long time intervals, and the problem of secular perspective acceleration of relatively nearby stars with both appreciable proper motion and radial velocity (Chapter 9).

The orbital analysis of visual binaries, together with a brief outline of the long-focus multiple exposure technique, comes next (Chapter 10). The long-focus photographic method is used to establish the mass ratio of double-star components. If the total mass of the binary system is known, the separate masses may thus be obtained. (Stellar luminosities and masses are basic desiderata in astronomical research, and, if only for this reason, the techniques and methods of long-focus photographic astrometry are important.) Ac-

curate luminosities and masses are known for several dozen binary stars and have contributed to our knowledge of the mass-luminosity relation (Chapter 11).

Of particular interest are the discovery and subsequent observation of departures from uniform rectilinear motion, or perturbations, for what appears to be a "single" star. Several perturbations with total amplitudes of $0''.04$ or more have been observed, indicating the presence of unseen companions of very low masses. The search for unseen companion objects includes the search for planetary companions of stars (Chapter 12).

Finally, a brief survey of the application of the long-focus technique to star fields, clusters, and widely separated components of binaries is given (Chapter 13).

The third part of the book comprises a brief outline of the theory of errors (Chapter 14) and the method of least squares (Chapter 15), both of perennial importance in the analysis of astrometric observations.

For a more advanced treatment of spherical astrometry the reader is referred to any of the classical works on the subject that are listed at the end of Chapter 1.

I am indebted to Dr. Freeman Miller of the astronomy department of the University of Michigan for encouragement and many useful suggestions.

May, 1966

PETER VAN DE KAMP

Contents

I
SPHERICAL ASTROMETRY

II
PLANE ASTROMETRY

III

ANALYSIS OF OBSERVATIONS

I

SPHERICAL ASTROMETRY

1 Spherical Trigonometry

1. Celestial and terrestrial spheres; spherical triangle

The celestial sphere is a useful, illusory concept, which provides a convenient surface on which to draw and study the relation between directions from the point chosen to be the center of the sphere to celestial objects, such as the stars. The radius of the celestial sphere is indeterminate, and may often conveniently be taken as unity. Thus, as long as we are concerned with directions only, and not with distances, spherical geometry plays an exclusive role, as it does also for the relation between points on the earth's surface, for an assumed spherical shape of the earth. Angular relationships on both celestial and terrestrial spheres are studied by the methods of spherical trigonometry.

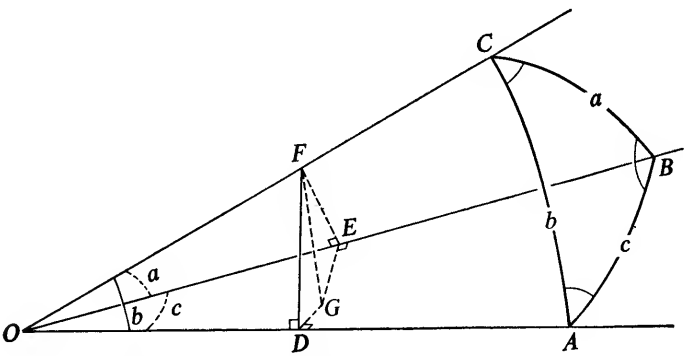

Fig. 1.1. *Sine formula in spherical trigonometry.*

In Figure 1.1, the directions OA, OB, OC correspond to the points A, B, and C on the sphere with center O. The planes OBC, OAC and OAB intersect the sphere in *great circles*, which define the *spherical triangle* ABC. The arcs $BC = a$, $AC = b$, and $AB = c$, named the *sides* of the spherical triangle, equal the angles BOC, COA, and AOB, respectively; this tacitly implies a radius

unity for the radius of the celestial sphere. The angles between the planes OAB and OAC, OAB and OBC, and OBC and OAC appear as the *angles* A, B, and C of the spherical triangle.

There are several trigonometric relations between the sides and the angles of a spherical triangle. Three basic relationships are most useful and may be established in a number of ways. A simple geometric derivation will be given first.

2. Sine formula

In Figure 1.1, let the planes FDG and FEG be perpendicular to the directions OA and OB, respectively; their intersection FG is perpendicular to the plane OAB. We have

$$\sin A = \sin FDG = \frac{FG}{DF}, \qquad \sin B = \sin FEG = \frac{FG}{EF},$$

hence

$$\frac{\sin A}{\sin B} = \frac{EF}{DF}. \tag{1.1}$$

Also

$$\sin a = \frac{EF}{OF}, \qquad \sin b = \frac{DF}{OF},$$

hence

$$\frac{\sin a}{\sin b} = \frac{EF}{DF}. \tag{1.2}$$

Equations (1.1) and (1.2) yield

$$\sin a \sin B = \sin b \sin A.$$

Similarly

$$\sin a \sin C = \sin c \sin A, \tag{1.3}$$

and

$$\sin b \sin C = \sin c \sin B,$$

or, also

$$\frac{\sin A}{\sin a} = \frac{\sin B}{\sin b} = \frac{\sin C}{\sin c}. \tag{1.4}$$

Equations (1.3) and (1.4) represent the *sine formula* of spherical trigonometry.

3. Cosine formula

The plane perpendicular to the direction OA intersects OB at the point H (Fig. 1.2). Both DF and DH are perpendicular to OD. Note that HF is common to the two triangles OHF and DHF. The cosine formula of plane trigonometry applied to these two triangles yields

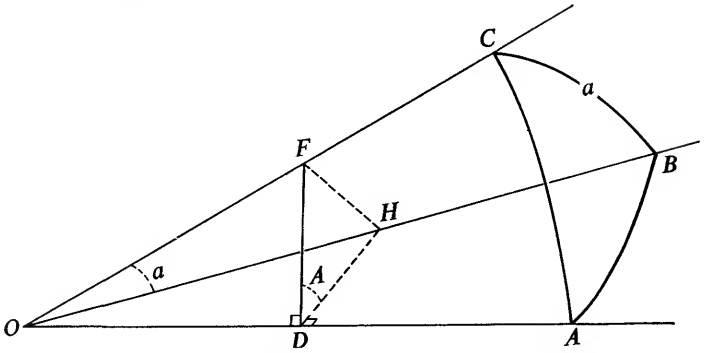

Fig. 1.2. *Cosine formula in spherical trigonometry.*

$$HF^2 = OH^2 + OF^2 - 2\,OF\,OH\cos a$$

and

$$HF^2 = DH^2 + DF^2 - 2\,DF\,DH\cos A,$$

whence

$$0 = 2\,OD^2 - 2\,OF\,OH\cos a + 2\,DF\,DH\cos A,$$

or

$$\cos a = \frac{OD}{OF}\frac{OD}{OH} + \frac{DF}{OF}\frac{DH}{OH}\cos A,$$

i.e.,

$$\left.\begin{aligned} \cos a &= \cos b\cos c + \sin b\sin c\cos A. \\ \text{Similarly} \\ \cos b &= \cos a\cos c + \sin a\sin c\cos B \\ \text{and} \\ \cos c &= \cos a\cos b + \sin a\sin b\cos C. \end{aligned}\right\} \quad (1.5)$$

This is the *cosine formula* of spherical trigonometry.

4. Extended cosine formula

A third set of useful formulae is obtained as follows.

Multiplication of first equation (1.5) with cos c yields

$$\cos a\cos c = \cos b\cos^2 c + \sin b\sin c\cos c\cos A.$$

The second equation (1.5) may be written as

$$\cos a\cos c = \cos b - \sin a\sin c\cos B.$$

By equating, we find

$$\sin a\sin c\cos B = \cos b(1 - \cos^2 c) - \sin b\sin c\cos c\cos A,$$

or, dividing by sin c,

$$\sin a \cos B = \cos b \sin c - \sin b \cos c \cos A,$$

and similarly

$$\sin a \cos C = \cos c \sin b - \sin c \cos b \cos A$$

and two related pairs of formulae:

$$\left.\begin{aligned} \sin b \cos A &= \cos a \sin c - \sin a \cos c \cos B \\ \sin b \cos C &= \cos c \sin a - \sin c \cos a \cos B \\ \sin c \cos A &= \cos a \sin b - \sin a \cos b \cos C \\ \sin c \cos B &= \cos b \sin a - \sin b \cos a \cos C. \end{aligned}\right\} \quad (1.6)$$

Equations (1.6) represent the *extended cosine formula* of spherical trigonometry.

5. Alternate derivation of fundamental formulae

The three basic formulae may be derived in a brief, elegant manner through the intermediary of rectangular coordinates. In the spherical triangle ABC (Fig. 1.3) let the z-axis point to A, the yz-plane pass through AB, while x is perpendicular to yz. For an assumed unit radius of the sphere the three rectangular coordinates are

$$x = \sin b \sin A, \qquad y = \sin b \cos A, \qquad z = \cos b. \quad (1.7)$$

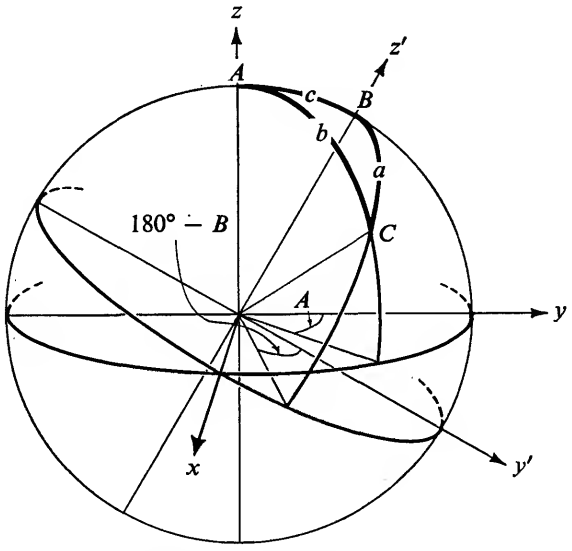

Fig. 1.3. *Relation between spherical triangle and two rectangular coordinate systems.*

Now consider another rectangular coordinate system obtained by a rotation through an angle c around the x-axis so that the z'-axis points to B; the $y'z'$-plane obviously coincides with the yz-plane. It is easily seen that the corresponding rectangular coordinates are

$$x' = \sin a \sin B, \qquad y' = -\sin a \cos B, \qquad z' = \cos a. \tag{1.8}$$

The two rectangular coordinate systems are related as follows

$$x' = x, \qquad y' = y \cos c - z \sin c, \qquad z' = z \cos c + y \sin c. \tag{1.9}$$

Substitution of (1.7) and (1.8) into (1.9) yields the basic formulae

$$\sin a \sin B = \sin b \sin A, \tag{1.3}$$

$$\sin a \cos B = \cos b \sin c - \sin b \cos c \cos A, \tag{1.6}$$

$$\cos a = \cos b \cos c + \sin b \sin c \cos A, \tag{1.5}$$

which thus prove to have special geometric significance.

A practical illustration of this derivation is the relation between equatorial and ecliptic coordinates (Chapter 2, section 4). In that case x points to the vernal equinox, y to a point on the equator at 6^h right ascension, y' to a point on the ecliptic at 90° longitude, z to the north equatorial pole, and z' to the north ecliptic pole.

6. Spherical right triangle

For a rectangular spherical triangle ($C = 90°$) the three fundamental formulae become

$$\sin c \sin A = \sin a, \qquad \sin c \cos A = \cos a \sin b, \qquad \cos c = \cos a \cos b, \tag{1.10}$$

relations which are frequently employed (see for example Chapter 3, Section 4).

7. Analogy between formulae of plane and spherical trigonometry

There are obvious analogies between the formulae of plane and spherical trigonometry, or, to put it differently, the above formulae of spherical trigonometry contain the corresponding formulae of plane trigonometry. For small angular values we may use the following close approximations:

$$\sin \theta \to \theta, \qquad \cos \theta \to 1 - \frac{\theta^2}{2},$$

where θ is expressed in radians. Hence, for small values of the sides a, b, c, i.e. near-plane triangles, formula (1.4) becomes the well-known sine formula of plane trigonometry:

$$\frac{\sin A}{a} = \frac{\sin B}{b} = \frac{\sin C}{c}.$$

Similarly, for small values of a, b, and c, formula (1.5) may be written as

$$1 - \frac{a^2}{2} = \left(1 - \frac{b^2}{2}\right)\left(1 - \frac{c^2}{2}\right) + bc \cos A,$$

which, at the limit, as a, b, and c approach zero, leads to another well-known formula of plane trigonometry,

$$a^2 = b^2 + c^2 - 2bc \cos A.$$

Finally, the extended cosine formula leads to the trivial expression

$$a \cos B + b \cos A = c.$$

There are also interesting analogies between the formulae of spherical and plane trigonometry for a right triangle. We shall simply list these relations,

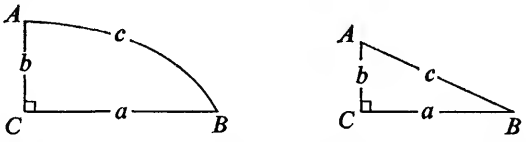

Fig. 1.4. *Right triangles:* left, *spherical;* right, *plane.*

which are easily derived. Again it may be shown that the formulae of plane trigonometry are contained in those of spherical trigonometry.

Plane right triangle	*Spherical right triangle*	
$\sin A = \frac{a}{c}$	$\sin A = \frac{\sin a}{\sin c}$	(1.11)
$\cos A = \frac{b}{c}$	$\cos A = \frac{\tan b}{\tan c}$	(1.12)
$\tan A = \frac{a}{b}$	$\tan A = \frac{\tan a}{\sin b}$	(1.13)
$\sin A = \cos B$	$\sin A = \frac{\cos B}{\cos b}$	(1.14)
$c^2 = a^2 + b^2$	$\cos c = \cos a \cos b$	(1.15)
$1 = \cot A \cot B$	$\cos c = \cot A \cot B$	(1.16)

and so on.

8. Haversine formula

Any angle of a spherical triangle may be expressed in terms of the three sides. The cosine formula (1.5) yields

$$\cos A = \frac{\cos a - \cos b \cos c}{\sin b \sin c}. \tag{1.17}$$

We shall now introduce the so-called *haversine*

$$\frac{1 - \cos A}{2} = \sin^2 \frac{A}{2}. \tag{1.18}$$

From (1.17) we see that

$$1 - \cos A = \frac{\sin b \sin c + \cos b \cos c - \cos a}{\sin b \sin c} = \frac{\cos (b - c) - \cos a}{\sin b \sin c},$$

which may be reduced to

$$\frac{1 - \cos A}{2} = \frac{\sin \frac{a + b - c}{2} \sin \frac{a - b + c}{2}}{\sin b \sin c}, \tag{1.19}$$

making use of the well-known, easily derived formula

$$\cos x - \cos y = -2 \sin \frac{x + y}{2} \sin \frac{x - y}{2}. \tag{1.20}$$

Introduce

$$a + b + c = 2s$$

and we find

$$\sin \frac{A}{2} = \sqrt{\frac{\sin (s - b) \sin (s - c)}{\sin b \sin c}}. \tag{1.21}$$

Corresponding formulae may be derived for $\cos A/2$ and $\tan A/2$:

$$\cos \frac{A}{2} = \sqrt{\frac{\sin s \sin (s - a)}{\sin b \sin c}}, \tag{1.22}$$

$$\tan \frac{A}{2} = \sqrt{\frac{\sin (s - b) \sin (s - c)}{\sin s \sin (s - a)}}. \tag{1.23}$$

For small values of the sides, formulae (1.21), (1.22), and (1.23) become the well-known formulae of plane trigonometry,

$$\sin \frac{A}{2} = \sqrt{\frac{(s - b)(s - c)}{bc}},$$

$$\cos \frac{A}{2} = \sqrt{\frac{s(s - a)}{bc}},$$

$$\tan \frac{A}{2} = \sqrt{\frac{(s - b)(s - c)}{s(s - a)}}.$$

9. Polar triangle and formulae

Each point of a sphere has a corresponding "equatorial" great circle. Any spherical triangle ABC has its polar counterpart, resulting from the intersection of the "equators" of the vertices A, B, and C.

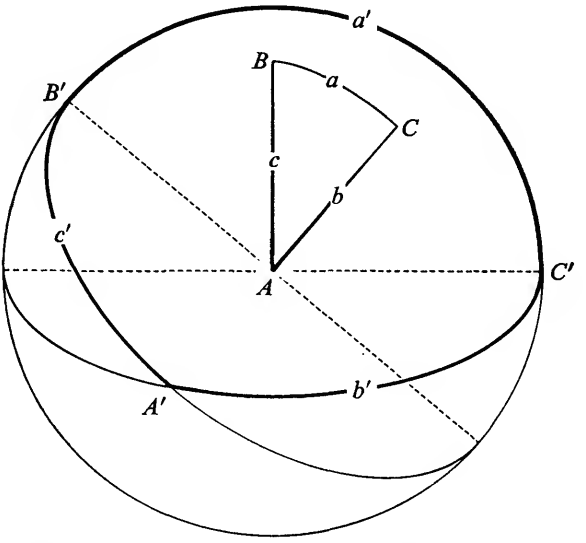

Fig. 1.5. *Polar triangle. In the perspective of this diagram the sides b and c appear as straight lines, as in 1.4,* left.

In Figure 1.5, the vertices A, B, C of the spherical triangle ABC are the poles of the sides $B'C' = a'$, $C'A' = b'$, and $A'B' = c'$ of the spherical triangle $A'B'C'$. Conversely, the vertices A', B', C' of the polar triangle $A'B'C'$ are the poles of the sides $BC = a$, $AC = b$, and $AB = c$ of the spherical triangle ABC. Since $B'A' \perp b$ and $A'C' \perp c$ it follows that $B'AC' = \pi - BAC$. Similar relations exist throughout and thus we have

$$a' = \pi - A, \qquad b' = \pi - B, \qquad c' = \pi - C, \tag{1.24}$$

and also

$$a = \pi - A', \qquad b = \pi - B', \qquad c = \pi - C'. \tag{1.25}$$

Thus, *the formulae of spherical trigonometry may be extended by replacing the sides and angles by the corresponding supplements of the angles and sides, respectively.*

The sine formula obviously remains the same; the cosine and the extended cosine formulae become

$$\begin{aligned} \cos A &= -\cos B \cos C + \sin B \sin C \cos a, \\ \cos B &= -\cos A \cos C + \sin A \sin C \cos b, \\ \cos C &= -\cos A \cos B + \sin A \sin B \cos c, \end{aligned} \tag{1.26}$$

and

$$\begin{aligned} \sin A \cos b &= \cos B \sin C + \sin B \cos C \cos a, \\ \sin A \cos c &= \cos C \sin B + \sin C \cos B \cos a, \\ \sin B \cos a &= \cos A \sin C + \sin A \cos C \cos b, \\ \sin B \cos c &= \cos C \sin A + \sin C \cos A \cos b, \\ \sin C \cos a &= \cos A \sin B + \sin A \cos B \cos c, \\ \sin C \cos b &= \cos B \sin A + \sin B \cos A \cos c. \end{aligned} \tag{1.27}$$

10. Isosceles spherical triangle; angular distance between two great circles

Astrometric problems frequently involve the angular value of the great circle base of an isosceles spherical triangle (Fig. 1.6).

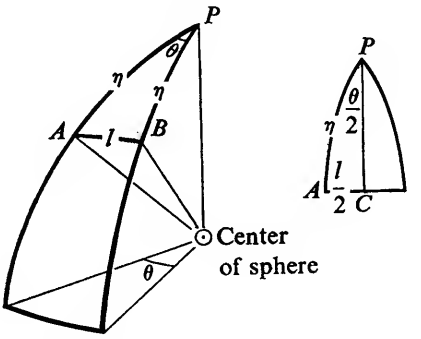

Fig. 1.6. *Isosceles spherical triangle. Length of great circle base.*

Let l be the length of the great circle arc AB, η the length of the sides, and θ the angle at the vertex, or pole P, of the isosceles triangle. In other words, θ is the angle between the planes of the great circles PA and PB, centered at O, the center of the sphere, and l is the angle between the radii OA and OB.

The cosine rule yields

$$\begin{aligned} \cos l &= \cos^2 \eta + \sin^2 \eta \cos \theta \\ &= \cos^2 \eta + \sin^2 \eta - \sin^2 \eta (1 - \cos \theta), \end{aligned}$$

whence

$$1 - \cos l = \sin^2 \eta (1 - \cos \theta).$$

This may be written as

$$\sin \frac{l}{2} = \sin \frac{\theta}{2} \sin \eta. \tag{1.28}$$

The same result is obtained by applying the sine rule (1.11) to the spherical right triangle ACP.

The great circle arc is the shortest distance between any two points. This can be demonstrated in a number of ways. It is of particular interest to compare the result for l with the length l_s of the small circle AB, whose length obviously is (Fig. 1.7)

$$l_s = \theta \sin \eta \tag{1.29}$$

(again, for unit value of the radius of the sphere).

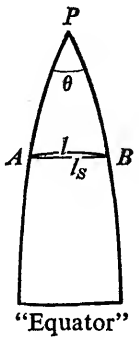

Fig. 1.7.
Isosceles spherical triangle. Relation between lengths of great circle and small circle base.

The great circle arc l is always shorter than the small circle arc l_s. This is easily seen:
if

$$0 < x_1 < x_2 < \pi,$$

then

$$\frac{\sin x_2}{x_2} < \frac{\sin x_1}{x_1}, \tag{1.30}$$

since the derivative of $\sin x/x$ is $(\cos x/x^2)\ (x - \tan x)$ and therefore negative for $0 < x < \pi$ (this is also easily understood by studying the graph $y = \sin x$). Now put

$$x_1 = \frac{\theta}{2} \sin \eta,$$

$$x_2 = \frac{\theta}{2}.$$

Substitution in (1.30) yields

$$\frac{\sin\frac{\theta}{2}}{\frac{\theta}{2}} < \frac{\sin\left(\frac{\theta}{2}\sin\eta\right)}{\frac{\theta}{2}\sin\eta},$$

i.e.,

$$\sin\frac{\theta}{2}\sin\eta < \sin\left(\frac{\theta}{2}\sin\eta\right).$$

Or, substituting (1.28) and (1.29):

$$\sin\frac{l}{2} < \frac{l_s}{2}$$

hence

$$l < l_s, \tag{1.31}$$

Q.E.D.

11. Approximation of small by great circle for small arcs

For small values of θ, (1.28) may be written with a very high degree of approximation as (1.29).

The formulae of spherical trigonometry hold for great circles, i.e., the intersections of planes that pass through the center of the sphere. They may not be applied to triangles involving small circles. For slender triangles, whose base is a very small section of a small circle, the length of the base may, however, with a very high degree of precision, be replaced by the arc of a great circle through the end points of the small segment of the small circle. This is a very useful relationship frequently used where small angular displacements are involved. For example, if in Figure 1.7 P represents the celestial pole, the sides PA and PB equal 90° minus the declination δ, and for small values of θ the length of the arc AB may be expressed by $\theta \cos\delta$.

12. Useful relations

The following approximations are frequently used. The adjective "small" has relative meaning only, and its significance has to be established for each problem to which it is desired to apply the approximations.

For value of a, small compared with 1:

$$(1 \pm a)^n = 1 \pm na. \tag{1.32}$$

For example

$$\frac{1}{1 \pm a} = 1 \mp a, \qquad \sqrt{1 \pm a} = 1 \pm \frac{a}{2}.$$

For small values of $\Delta\theta$:

$$\sin(\theta \pm \Delta\theta) = \sin\theta \pm \Delta\theta\cos\theta, \qquad \cos(\theta \pm \Delta\theta) = \cos\theta \mp \Delta\theta\sin\theta. \tag{1.33}$$

For small values of θ:

$$\sin\theta = \theta - \frac{\theta^3}{3!} \quad \text{or sometimes} \quad \sin\theta = \theta, \tag{1.34}$$

$$\cos\theta = 1 - \frac{\theta^2}{2} \quad \text{or sometimes} \quad \cos\theta = 1, \tag{1.35}$$

$$\tan\theta = \theta + \frac{\theta^3}{3} \quad \text{or sometimes} \quad \tan\theta = \theta. \tag{1.36}$$

Suggested readings

William Chauvenet, *Spherical and Practical Astronomy*, 5th ed. (1891). (Reprinted by Dover Publications, New York.) 2 vols.

André Danjon, *Astronomie Générale: Astronomie Sphérique et Eléments de Méchanique Céleste*. Paris, J. and R. Sennac, 1959.

J. J. Nassau, *Practical Astronomy*. New York, McGraw-Hill, 1948.

Simon Newcomb, *A Compendium of Spherical Astronomy* (1906). (Reprinted by Dover Publications, New York.)

W. M. Smart, *Spherical Astronomy*. Cambridge University Press, 1944.

E. W. Woolard and G. M. Clemence, *Spherical Astronomy*. New York, Academic Press, 1966.

2 Celestial Sphere

A. CELESTIAL COORDINATES

1. Coordinate systems: horizontal, equatorial, ecliptic, galactic

A direction, i.e. a point on the celestial sphere, is defined and determined by two spherical coordinates referred to a fundamental great circle and a point on that circle. One coordinate is measured perpendicular to the fundamental circle along an auxiliary great circle, passing through the star S and the pole of the fundamental circle. The other is measured from a zero point on the fundamental circle to the intersection of the auxiliary circle with the fundamental circle. There are four coordinate systems in use in spherical astrometry.

The horizontal coordinate system (Fig. 2.1)

Fundamental circle:	horizon
Zero point:	north

The two coordinates are (1) *altitude* h, measured along vertical (great) circle from horizon to point S, counted positive above the horizon, negative below it, and (2) *azimuth* A, measured along the horizon from the north point, through the east, to the intersection of the vertical circle. Instead of altitude h, its complement measured from the zenith Z, the *zenith distance* ζ, is frequently used.

The equatorial coordinate system (Fig. 2.2)

Fundamental circle:	equator
Zero point:	vernal equinox

The equator is an extension of the earth's equator, and the poles are defined by the earth's axis. The vernal equinox is the point at which the sun ascends from below to above the equator, or in other words, the *ascending node* Υ of the ecliptic on the equator. The ecliptic, or sun's path, is inclined 23°27′ to the

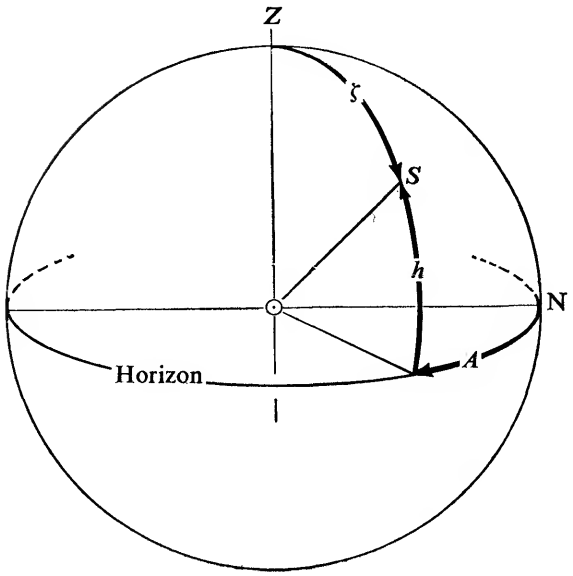

Fig. 2.1. *Horizontal coordinate system.*

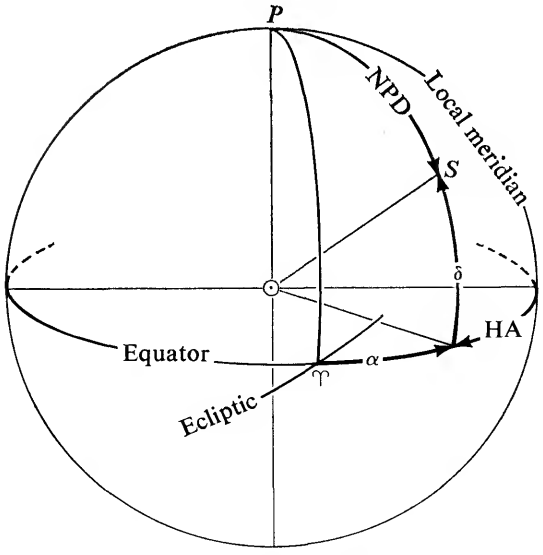

Fig. 2.2. *Equatorial coordinate system.*

equator. Both equator and equinox will be studied in more detail in Chapter 3.

The two coordinates are: (1) *Declination* δ, measured along the great circle through star and pole, named *hour circle*, from equator to star, counted positive north of the equator, negative south of it. The *north polar distance* (NPD) is sometimes used; this is the complement of the declination, i.e., $90° - \delta$. (2) *Right ascension* α, measured from the vernal equinox, along the equator in the west-east direction, i.e., opposite the apparent rotation of the celestial sphere. Of special interest is the *hour angle*, the angle counted positive westward from the local meridian to the hour-circle of the star.

By definition, the hour angle of the vernal equinox is the *sidereal time*, and we thus have the simple relation,

$$\text{right ascension} + \text{hour angle} = \text{sidereal time}.$$

For a star on the meridian the right ascension equals the sidereal time.

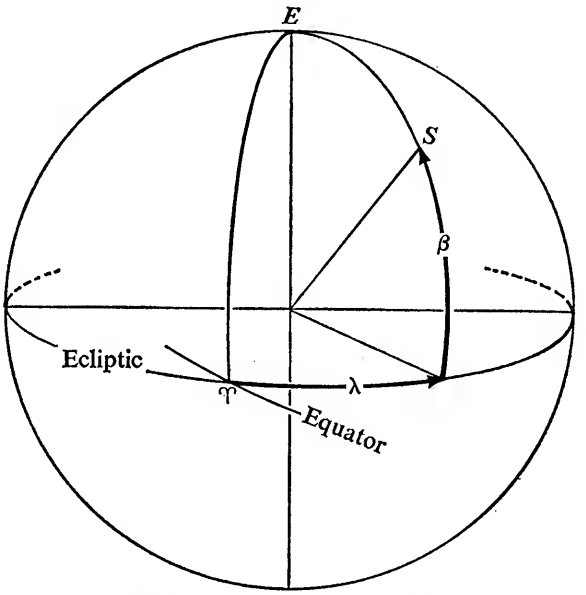

Fig. 2.3. *Ecliptic coordinate system.*

The ecliptic coordinate system (Fig. 2.3)

Fundamental circle:	ecliptic
Zero point:	vernal equinox

Here the coordinates are (1) *celestial latitude* β, measured along the so-called *latitude* circle through star and ecliptic pole E, and counted either north (+) or

south (−), with respect to the ecliptic, and (2) *celestial longitude* λ, measured from the vernal equinox, along the ecliptic in the direction of increasing right ascension.

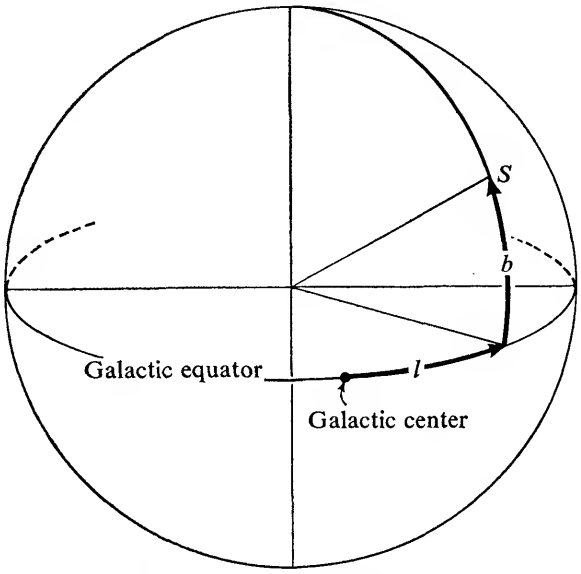

Fig. 2.4. *Galactic coordinate system.*

The galactic coordinate system (Fig. 2.4)

Fundamental circle:	galactic equator
Zero point:	galactic center

In studies involving the structure of our stellar system, it is often desirable to use *galactic* coordinates. Here the fundamental line is the galactic circle, a great circle represented by the course of the "Milky Way." The *galactic circle*, or *galactic equator*, intersects the celestial equator at an angle of 62°20′ at ascending node RA = $18^h46^m.6$.

The coordinates are (1) *galactic latitude b*, measured on the great circle through star and galactic pole, and counted north (+) or south (−) with respect to the galactic equator, and (2) *galactic longitude l*, measured along the galactic equator eastward. The logical choice of zero point is the galactic center, which is assumed to be at right ascension $17^h39^m.3$ declination −28°54′. All these coordinates are valid for the equator and equinox of 1900.0 (see Chapter 4).

The galactic coordinates as defined above are currently referred to as the

"new" International Astronomical Union (IAU) system and frequently referred to as l^{II} and b^{II} to distinguish them from the "old" coordinates l^{I} and b^{I}, referred to a slightly different galactic equator and a zero point defined by the ascending node of the galactic on the celestial equator.[1]

2. The concentric celestial and terrestrial spheres; navigation[2]

The earth is nearly spherical, hence as a close approximation the terrestrial sphere is considered concentric with the celestial sphere. This results in important simple relationships.

At any given time any location on earth has a corresponding zenith on the celestial sphere, and any celestial object, such as a star S, has a corresponding substellar point F on the earth's surface. Both zenith and substellar point play a basic role in determining terrestrial and celestial positions and in navigation.

Note that these radial relationships between star and substellar point, or between zenith and observer, or between terrestrial and celestial pole, can be illustrated in diagrams containing both the concentric terrestrial and celestial spheres. As soon as directions other than these are considered, only one sphere can accurately be represented in a diagram. For example, directions to the same star from different points on the earth's surface can be drawn as parallel lines from a terrestrial sphere of finite dimensions to an infinitely distant point on the celestial sphere. Similarly, directions to different stars, or points on the celestial sphere, as seen from a single point on earth, can be illustrated for a celestial sphere of finite dimensions, with the observer at the center; the earth may now be reduced to a point, since the rest of the earth's surface is not involved.

Figure 2.5 shows that the following important relationship exists: *The terrestrial longitude and latitude of a substellar point equal the Greenwich Hour Angle (GHA) and declination of the star.* The GHA and declination are listed directly and indirectly for a number of bright stars and the bright planets in astronomical almanacs, as a function of the time at Greenwich. Hence, if we know the time at Greenwich, we know the location of all substellar points.

If the star is in the observer's zenith, his location *is* the substellar point. In general this will not be so; however, the observer, by measuring the zenith distance of the star, knows that he must be located on a small circle (*circle of position*), whose radius equals the zenith distance and whose center is the

[1] A. Blaauw, C. S. Gum, J. L. Pawsey, and G. Westerhout, "The New I.A.U. System of Galactic Coordinates (1958 revision)," *Monthly Notices of the Royal Astronomical Society*, 121 (1960): 123–131.

[2] Although this section is not strictly relevant to the main topics of this book, its importance in the realm of the horizontal and equatorial coordinate systems warrants its inclusion. For further information see Bart J. Bok and Frances W. Wright, *Basic Marine Navigation*, Boston, New York, Houghton Mifflin, 1944.

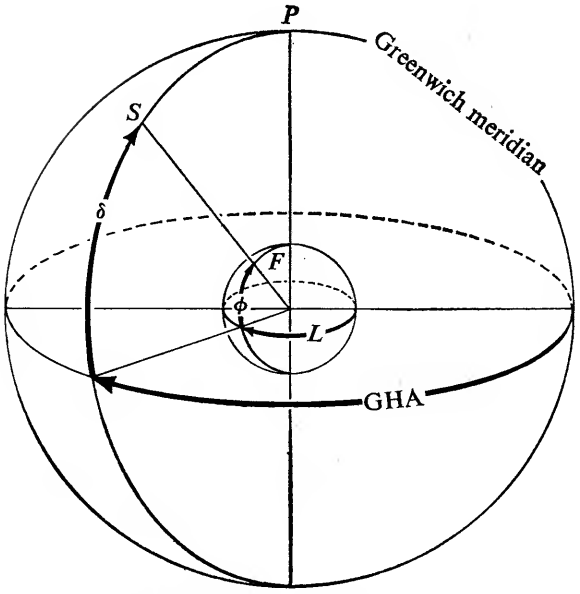

Fig. 2.5. *Relation between concentric terrestrial and celestial spheres.*

substellar point (Fig. 2.6); from each point on this small circle, the star will have the same zenith distance.

The substellar point of the north pole star (Polaris) is always close to the terrestrial north pole, and the above statement reduces to the well-known

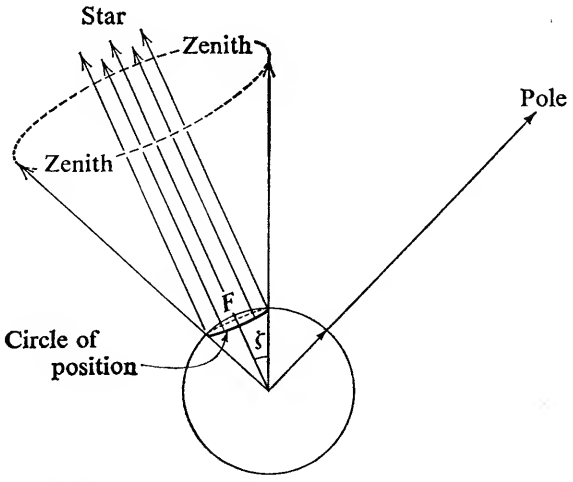

Fig. 2.6. *Circle of position around substellar point.*

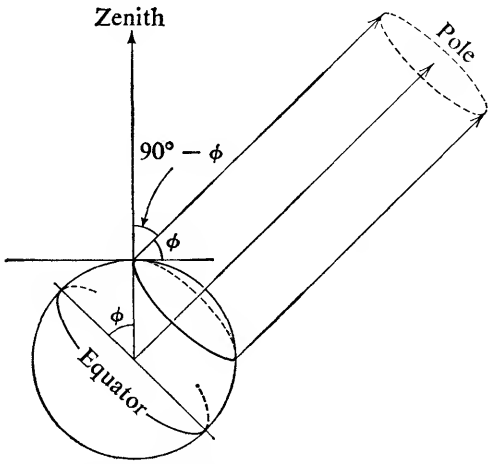

Fig. 2.7. *The altitude of the elevated pole equals the latitude of the observer.*

facts that the zenith distance of the elevated pole—in the northern hemisphere closely approximated by Polaris—equals the co-latitude (90° − latitude) of the observer, and hence that the altitude of the elevated pole equals the latitude of the observer (Fig. 2.7): the declination of the zenith also equals the latitude of the observer.

It is thus seen that, in general, navigation implies the observation of the zenith distance of two different stars, in order to establish two circles of position, which reduce the possible location of the observer to the two inter-

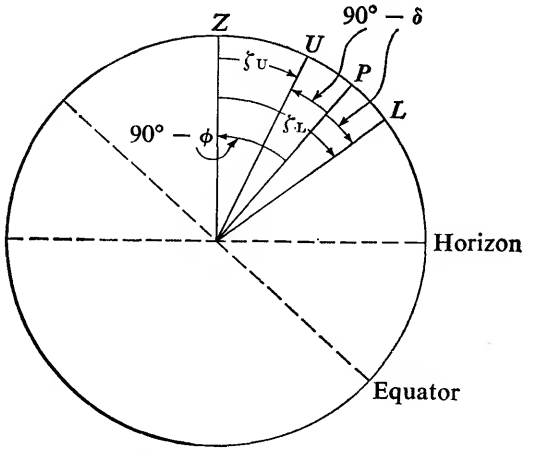

Fig. 2.8. *Relation of upper and lower culmination to latitude and declination.*

sections of the two circles. If need be, observations of a third star (or more) will provide a unique answer.

Of particular interest are observations of zenith distance (or altitude) made on the *meridian* of the observer. If the diurnal path of a star is completely above the horizon, observations of the zenith distance may be made at both upper (U) and lower (L) culminations. A diagram (Fig. 2.8) of the meridian section of the celestial sphere shows that these observations yield two observational equations:

$$\zeta_U = \delta - \phi, \qquad \zeta_L = 180° - \delta - \phi, \tag{2.1}$$

from which we find

$$\phi = 90° - \frac{\zeta_U + \zeta_L}{2}, \qquad \delta = 90° - \frac{\zeta_U - \zeta_L}{2}. \tag{2.2}$$

Similar relationships hold for an upper culmination south of the zenith, and for southern latitudes.

Observations of circumpolar stars thus permit the determination of both latitude and declination, subject to corrections due to refraction, instrumental errors, the nonspherical shape of the earth, and the like. For other than circumpolar stars, if only one culmination can be observed, either declination or latitude can be determined, provided the other is known.

3. Relation between equatorial and horizontal coordinates

The relations in section 2 were studied through concepts of solid and plane geometry. The most general approach to the relationship between celestial and terrestrial coordinates involves the methods and formulae of spherical trigonometry.

Relations between coordinates in the equatorial and horizontal system are conveniently studied in the so-called *astronomical* (sometimes called

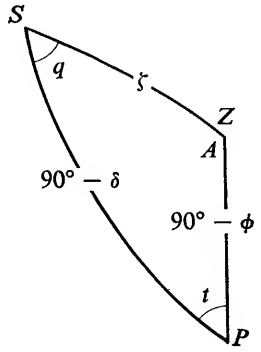

Fig. 2.9.
The astronomical triangle, as seen from inside of celestial sphere: ζ = zenith distance; δ = declination; ϕ = latitude; t = hour angle; A = azimuth; q = parallactic angle.

"parallactic") *triangle*, formed by the star S, the celestial (north) pole, and the zenith Z (Fig. 2.9). A few examples follow.

a) Given ϕ, δ, and t, calculate ζ and A. The cosine rule gives

$$\cos \zeta = \sin \phi \sin \delta + \cos \phi \cos \delta \cos t, \tag{2.3}$$

$$\sin \delta = \sin \phi \cos \zeta + \cos \phi \sin \zeta \cos A. \tag{2.4}$$

The first relation yields ζ, and A may be calculated from the second relation.

b) Given ϕ, ζ, and A, calculate δ and t. The same formulae now permit the calculation of δ and t.

c) Later we shall need the angle $ZSP = q$, named the *parallactic angle*. The sine rule gives

$$\sin q = \cos \phi \frac{\sin t}{\sin \zeta}. \tag{2.5}$$

d) Given ϕ, δ, and ζ, calculate the hour-angle t. Using the haversine formula (1.21), we find

$$\sin \frac{t}{2} = \sqrt{\frac{\sin \dfrac{\zeta - \phi + \delta}{2} \sin \dfrac{\zeta + \phi - \delta}{2}}{\cos \phi \cos \delta}}. \tag{2.6}$$

e) To calculate the time (hour angle) and azimuth of rising and setting, simple relations exist, since $\zeta = 90°$. In formula (2.3) $\cos \zeta = 0$, hence the hour angle is found from the simple relation

$$\cos t = -\tan \phi \tan \delta. \tag{2.7}$$

Formula (2.4) yields

$$\sin \delta = \cos \phi \cos A,$$

whence

$$\cos A = \sin \delta \sec \phi, \tag{2.8}$$

a simple expression for calculating the azimuth at rising and setting.

However, these formulae are only approximate since all celestial objects are appreciably lifted by refraction at the horizon, and for the sun the extended disk must be taken into account.

It must also be pointed out that sine (or cosine) functions are not universally useful for determining an angle, since they vary little near 90° (or 0°). Hence tangent or cotangent formulae, derived from the basic formula, may be preferable, since these functions vary greatly for all values of the angle, large or small.

For example: for the simplified case of rising or setting, (2.7) may be written as

$$\cos t = -\frac{\sin \phi \sin \delta}{\cos \phi \cos \delta},$$

from which

$$2\sin^2\frac{1}{2}t = 1 - \cos t = \frac{\cos\phi\cos\delta + \sin\phi\sin\delta}{\cos\phi\cos\delta} = \frac{\cos(\phi - \delta)}{\cos\phi\cos\delta},$$

$$2\cos^2\frac{1}{2}t = 1 + \cos t = \frac{\cos\phi\cos\delta - \sin\phi\sin\delta}{\cos\phi\cos\delta} = \frac{\cos(\phi + \delta)}{\cos\phi\cos\delta}.$$

Hence

$$\tan\frac{1}{2}t = \sqrt{\frac{\cos(\phi - \delta)}{\cos(\phi + \delta)}}. \tag{2.9}$$

4. Relation between equatorial and ecliptic coordinates

The spherical triangle formed by star S and the poles P and E of equator and ecliptic (Fig. 2.10), respectively, yields the following relations between coordinates in the equatorial and the ecliptical coordinate systems

$$\sin\beta = \cos\epsilon\sin\delta - \sin\epsilon\cos\delta\sin\alpha, \tag{2.10}$$

$$\cos\beta\sin\lambda = \sin\epsilon\sin\delta + \cos\epsilon\cos\delta\sin\alpha, \tag{2.11}$$

$$\cos\beta\cos\lambda = \cos\delta\cos\alpha, \tag{2.12}$$

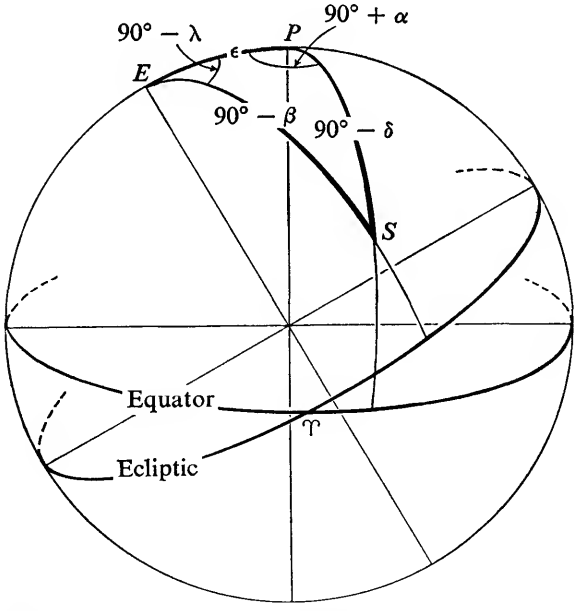

Fig. 2.10. *Relation between equatorial and ecliptic coordinates.*

and, conversely

$$\sin \delta = \cos \epsilon \sin \beta + \sin \epsilon \cos \beta \sin \lambda, \tag{2.13}$$

$$\cos \delta \sin \alpha = -\sin \epsilon \sin \beta + \cos \epsilon \cos \beta \sin \lambda, \tag{2.14}$$

$$\cos \delta \cos \alpha = \cos \beta \cos \lambda. \tag{2.15}$$

Here ϵ is the inclination (23°27′) of the ecliptic on the equator (Section 1), also referred to as the *obliquity* of the ecliptic.

For another derivation of these formulae see Chapter 1, Section 5.

5. Change in position angle with hour circle

The change in position angle (Fig. 2.11) as a great circle S_1S_2 passes successive hour circles is obtained as follows. Applying the sine rule to the spherical triangle PS_1S_2, we have

$$\frac{\sin \theta'}{\sin \theta} = \frac{\cos \delta}{\cos \delta'}$$

or

$$\frac{\sin (\theta + \Delta\theta)}{\sin \theta} = \frac{\cos \delta}{\cos (\delta + \Delta\delta)}.$$

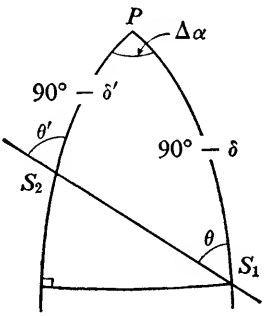

Fig. 2.11. *Change in position angle with hour circle, as seen from inside of celestial sphere.*

If $\Delta\delta$ and $\Delta\theta$ are small,

$$\frac{\sin \theta + \Delta\theta \cos \theta}{\sin \theta} = \frac{\cos \delta}{\cos \delta - \Delta\delta \sin \delta} = \frac{1}{1 - \Delta\delta \tan \delta},$$

or

$$1 + \Delta\theta \cot \theta = 1 + \Delta\delta \tan \delta,$$

whence

$$\Delta\theta = \Delta\delta \tan \delta \tan \theta. \tag{2.16}$$

For small arcs (Fig. 2.12) we may express $\Delta\delta$ in terms of the great circle value $\Delta\alpha \cos \delta$ and the position angle θ by

$$\tan \theta = \frac{\Delta\alpha \cos \delta}{\Delta\delta} \tag{2.17}$$

hence

$$\Delta\theta = \Delta\alpha \sin \delta. \tag{2.18}$$

This formula proves significant, for example, in comparing observations made at different epochs of the position angle of a double star having a large proper motion. (Chapter 10, Section 2)

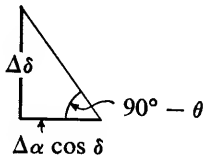

Fig. 2.12.
Change in position angle for small changes in right ascension and declinations.

B. ASTRONOMICAL REFRACTION

6. Refraction formula

Surface observations of the altitude h, or zenith distance ζ, are affected by the *refraction* of light as it passes through the earth's atmosphere. For the simplified case of plane parallel layers (Fig. 2.13) of gradually increasing density

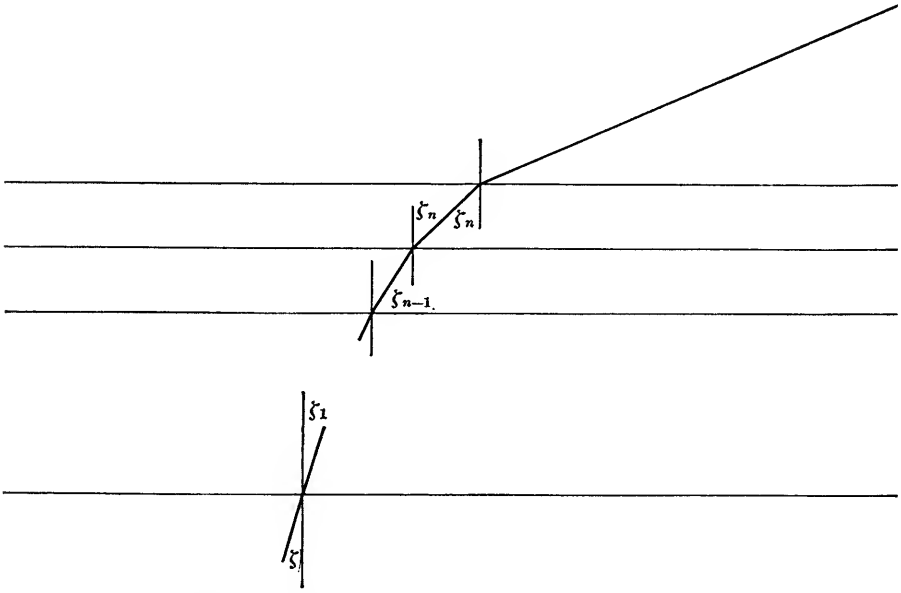

Fig. 2.13. *Astronomical refraction in earth's atmosphere.*

toward the earth's surface, we see that the direction to the star undergoes successive changes as follows:

$$\frac{\sin z}{\sin \zeta_n} = \mu_n, \qquad \frac{\sin \zeta_n}{\sin \zeta_{n-1}} = \frac{\mu_{n-1}}{\mu_n}, \ \ldots$$

$$\ldots \frac{\sin \zeta_1}{\sin \zeta} = \frac{\mu}{\mu_1}.$$

Here z is the zenith distance unaffected by refraction, ζ is the zenith distance as observed from the earth's surface, and μ the index of refraction near the earth's surface. Obviously

$$\sin z = \mu \sin \zeta. \tag{2.19}$$

It is seen that the relation between ζ and z depends only on the value of μ near the earth's surface.

Since μ is more than 1, the observed zenith distance is always less than the true zenith distance of entry, i.e., all stars are lifted up toward the zenith. Formula (2.19) may be written as

$$\sin (\zeta + r) = \mu \sin \zeta, \tag{2.20}$$

where r is the amount of *astronomical refraction.*
Or, since r is small,

$$\sin \zeta + r \cos \zeta = \mu \sin \zeta,$$

whence

$$r = (\mu - 1) \tan \zeta, \tag{2.21}$$

or

$$r = R \tan \zeta, \tag{2.22}$$

where R is the *constant of refraction.*

Thus, as a first approximation, the vertical astronomical refraction is proportional to the tangent of the zenith distance. For many purposes the simple formula (2.21) may be used for zenith distances not exceeding 45°. Since $\mu = 1.00029$, formula (2.21), expressed in seconds of arc, may be approximately written as

$$r = 60'' \tan \zeta.$$

For spherical layers concentric with the earth's surface, the refraction formula is found to be represented by

$$r = A \tan \zeta + B \tan^3 \zeta, \tag{2.23}$$

where

$$A = (\mu - 1) + B$$

and

$$B \text{ is close to } -''.07.$$

Both A and B depend on temperature, pressure, and local conditions. Moreover, the refraction varies, of course, with the wavelength of the radiation. In practice, A and B are derived from astronomical observations.

7. Refraction in right ascension and declination

On the meridian, the astronomical refraction affects declination only, but off the meridian, both right ascension and declination are affected. The effect is

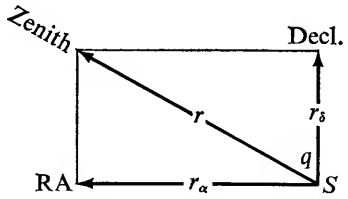

Fig. 2.14. *Astronomical refraction in equatorial coordinates.*

found from studying the astronomical triangle (Fig. 2-9). The equatorial components (Fig. 2.14) of the refraction effect r amount to,

$$\begin{aligned} &\text{In right ascension (great circle):} \quad r_\alpha = r \sin q \\ &\text{In declination:} \quad r_\delta = r \cos q \end{aligned} \tag{2.24}$$

where the parallactic angle q is related to latitude ϕ, zenith distance ζ, and hour angle t by the relation

$$\sin q = \cos \phi \frac{\sin t}{\sin \zeta}. \tag{2.5}$$

First, we shall study the effect in RA, which is of particular interest in photographic astrometry (Chapter 6, Section 6). For the simple case of

$$r = R \tan \zeta, \tag{2.22}$$

the refraction effect r_α, measured along a great circle arc, may be written as

$$r_\alpha = r \sin q = r \cos \phi \frac{\sin t}{\sin \zeta} = R \cos \phi \sin t \sec \zeta. \tag{2.25}$$

For the refraction effect in declination the coefficient $\cos q$ may be found from the cosine formula, as follows,

$$\sin \phi = \sin \delta \cos \zeta + \cos \delta \sin \zeta \cos q, \tag{2.26}$$

hence

$$\cos q = \frac{\sin \phi - \sin \delta \cos \zeta}{\cos \delta \sin \zeta} = \frac{\sin \phi}{\cos \delta \sin \zeta} - \frac{\tan \delta}{\tan \zeta}.$$

Or, substituting $r = R \tan \zeta$,

$$r_\delta = R\left(\frac{\sin \phi}{\cos \delta \cos \zeta} - \tan \delta\right) \tag{2.27}$$

8. Refraction for small hour angles

Of particular interest are the changes in r_α and r_δ for relatively small changes in hour angle, such as are customary in long-focus photographic astrometry. For observations near the meridian, we may replace $\sin t$ by t and ζ by $(\phi - \delta)$, so that the refraction effect in right ascension may be written as

$$Rt \cos \phi \sec (\phi - \delta). \tag{2.28}$$

To study the effect r_δ, we eliminate ζ in (2.27) by using the expression

$$\cos \zeta = \sin \phi \sin \delta + \cos \phi \cos \delta \cos t, \tag{2.3}$$

which may be written as

$$\cos \zeta = \sin \phi \sin \delta + \cos \phi \cos \delta - (1 - \cos t) \cos \phi \cos \delta,$$

or

$$\cos \zeta = \cos (\phi - \delta) - \frac{t^2}{2} \cos \phi \cos \delta, \tag{2.29}$$

for small values of t.

Substitution in (2.27) yields

$$r_\delta = R\left\{\frac{\sin \phi}{\cos \delta\left\{\cos (\phi - \delta) - \frac{t^2}{2} \cos \phi \cos \delta\right\}} - \tan \delta\right\}$$

or, again for small values of t,

$$r_\delta = R\left\{\frac{1}{\cos (\phi - \delta)} \frac{\sin \phi\left(1 + \frac{t^2}{2} \frac{\cos \phi \cos \delta}{\cos (\phi - \delta)}\right)}{\cos \delta} - \tan \delta\right\}$$

$$= R\left\{\frac{\sin \phi - \sin \delta \cos (\phi - \delta)}{\cos (\phi - \delta) \cos \delta} + \frac{t^2}{2} \frac{\sin \phi \cos \phi}{\cos (\phi - \delta)}\right\}.$$

The first terms in brackets may be transformed as follows:

$$\frac{\sin \phi - \sin \delta \cos (\phi - \delta)}{\cos (\phi - \delta) \cos \delta} = \frac{\sin \phi - \sin \delta (\cos \phi \cos \delta + \sin \phi \sin \delta)}{\cos (\phi - \delta) \cos \delta}$$

$$= \frac{\sin \phi \cos^2 \delta - \cos \phi \sin \delta \cos \delta}{\cos (\phi - \delta) \cos \delta} = \frac{\sin \phi \cos \delta - \cos \phi \sin \delta}{\cos (\phi - \delta)}$$

$$= \frac{\sin (\phi - \delta)}{\cos (\phi - \delta)} = \tan (\phi - \delta).$$

Hence for small values of t

$$r_\delta = R\left\{\tan(\phi - \delta) + \frac{t^2 \sin 2\phi}{\cos(\phi - \delta)}\right\}. \tag{2.30}$$

For small hour angles the refraction in declination consists therefore of a constant meridian term plus a term which varies with the square of the hour angle.

On the meridian, $\zeta = \phi - \delta$, and the above expression becomes, of course,

$$r = R \tan(\phi - \delta) = R \tan \zeta.$$

3 Stellar Positions and Their Changes, Secular and Annual

1. Fundamental astronomy

Fundamental astronomy consists basically of the establishment of a system of coordinates of stars (and planets) on the celestial sphere. Positions are measured with respect to a reference frame, which in turn must be obtained from cosmic objects. The natural choice for a fundamental plane is the equator; the choice of a zero point in this plane is arbitrary, the use of the vernal equinox is traditional.

Equator and equinox are determined from frequent observation of the declination of the sun. Basically, the equinox and the obliquity of the ecliptic are determined from solar positions, using the equation

$$\sin \alpha = \cot \epsilon \tan \delta. \tag{3.1}$$

The value of ϵ is determined from the observed maximum and minimum values of δ. Using the determination of ϵ, observations of the declination of the sun near the equinox then serve to locate the equinox.

The instruments commonly used for measuring stellar positions are the transit, vertical circle, and transit or meridian circle, which is a combination of a transit instrument and a vertical circle. Right ascensions and declinations may be observed simultaneously with the transit circle, whereas the other two are single coordinate instruments. The right ascensions of stars are obtained by comparing the transits of stars and sun. The measurement of right ascension requires a sidereal clock as an accessory. The pole is determined from observations of circumpolar stars at upper and lower culminations. The declinations are determined from observations at upper and/or lower culminations. All observations are corrected for refraction and instrumental errors. Since neither the coordinate system nor the stars are fixed, the study of the positions of stars invariably implies the study of their annual change due to

precession (Section 2), aberration (Section 5), and proper motion (Section 3).

The systematic patterns that exist in stellar motions, such as solar motion and galactic rotation (Chapter 4), can be represented by appropriate mathematical models. In addition, there is the perennially troublesome effect of systematic errors in the observed positions and proper motions of stars.[1]

2. Precession and nutation

The earth's flattening, combined with the obliquity of the ecliptic, results in a slow turning of the equator on the ecliptic due to the differential gravitational effect of moon and sun. Since these effects are proportional to the mass and inversely proportional to the cube of the distance of the perturbing body, the moon's effect averages over twice that of the sun (as it does also for the tides).

Luni-solar, planetary, and general precession; general considerations

The secular retrogression, i.e., in the direction of decreasing longitude, of the vernal equinox along the ecliptic is named the *luni-solar precession* p; it amounts to $50''.3708$ for the epoch 1900. The obliquity of the ecliptic ϵ for the same epoch amounts to $23°27'8''.26$. Both values, like most astronomical constants, are subject to small secular changes. The luni-solar precession results in the celestial poles describing small circles with a radius of $23°27'$ and a period of about 25,725 years around both the north and south ecliptic poles. These circles are referred to as *precessional circles*.

In addition to the *luni-solar* precession, there is the *planetary* precession l, the slow turning of the ecliptic on the equator, caused by the gravitational effect of the planets on the earth's orbit. The result is a motion of the vernal equinox along the equator in the direction of increasing right ascension. The combined luni-solar and planetary precession, i.e., the motion of the equinox along the moving ecliptic, is named the *general precession* χ, which equals $p - l \cos \epsilon$.

Newcomb introduced a quantity P, named *precessional constant*, which equals $(p + p_g) \sec \epsilon$. Here p_g is the so-called geodesic precession, a small, direct, relativistic motion of the equinox amounting to $+0''.0192$ per year. Its size is determined by the inertial properties of the earth, the masses of earth, moon, and sun, and the elements of the earth's and moon's orbits.

The precessional constant amounts to $P = 54''.9272$ for the epoch 1900; its centennial change is only $-0''.00004$ as contrasted with the centennial changes of $+0''.0050$ in p, and of $-46''.84$ in ϵ.

Associated with the secular terms of the precession are periodic terms known as *nutations*. Of these, the principal effect is related to the retrogression of

[1] J. C. Kapteyn, "On the Proper Motions of the Faint Stars and the Systematic Errors of the Boss Fundamental System," *Bulletin of the Astronomical Institutes of the Netherlands*, 1 (1922): 69–78.

the line of nodes of the moon's orbit on the ecliptic. It may be represented by an elliptical motion of the celestial poles with a semi-axis major of 9″.2 perpendicular to the precessional motion, and a semi-axis minor of 6″.8 along the precessional circle, in a period of 18.6 years.

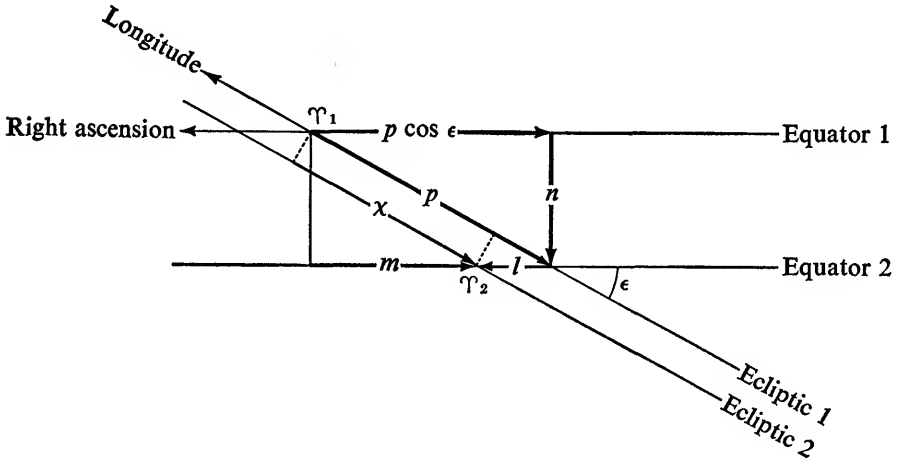

Fig. 3.1. *Effects of precession on vernal equinox, equator, and ecliptic, as seen from inside of celestial sphere.*

The annual rates of the precession terms in different coordinates are summarized below. The size of these quantities applies both to the motion of the equinox (counted positive in the direction of decreasing coordinates: longitude, right ascension, and declination) and to the effects of these quantities on the coordinates measured with respect to the equinox. T is expressed in tropical centuries since 1900.

Luni-solar precession in longitude:	$p = +50''.3708 + 0''.0050\ T$
Planetary precession in longitude:	$-l \cos \epsilon = -0''.1144 + 0''.0172\ T$
General precession in longitude:	$\chi = p - l \cos \epsilon = +50''.2564 + 0''.0222\ T$
Luni-solar precession in RA:	$p \cos \epsilon = +46''.2098 + 0''.0046\ T$
Planetary precession in RA:	$-l = -0''.1247 + 0''.0188\ T$
General precession in RA:	$m = p \cos \epsilon - l = +46''.0851 + 0''.0279\ T$
General precession in declination:	$n = p \sin \epsilon = +20''.0468 - 0''.0085\ T$

These values are due to Simon Newcomb and continue to be the official values used, though small corrections appear to be needed.

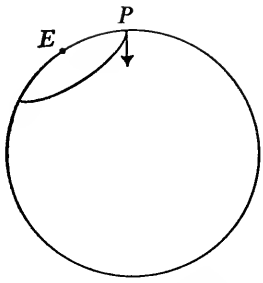

Fig. 3.2. *Motion of celestial pole P on precessional circle centered on pole E of the ecliptic.*

Note that the celestial pole moves continually toward the equinox at an annual rate of $n = p \sin \epsilon$, measured along the great circle (Fig. 3.2).

Although l can be obtained from theoretical considerations (secular perturbations), p can be found only from a discussion of proper motions.

Effect of luni-solar precession on hour circle and position angle

Precession causes a slow change in the hour circle for any star S, and in the equatorial coordinates α and δ (Fig. 3.3).

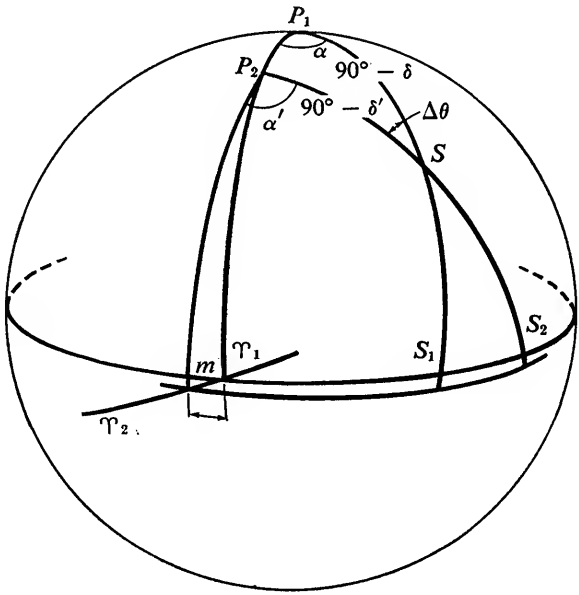

Fig. 3.3. *Effect of precession on hour circle, position angle, and on right ascension and declination.*

The annual rate $\Delta\theta$, at which the hour circle turns, follows from the spherical triangle SP_1P_2, where P_1 and P_2 are the poles of the equator, one year apart and separated by $n = p \sin \epsilon$, measured along the great circle,

$$\frac{\sin \Delta\theta}{\sin n} = \frac{\sin \alpha}{\cos \delta'}.$$

Or, since $\Delta\theta$ and n are small, and replacing δ' by δ,

$$\Delta\theta = n \frac{\sin \alpha}{\cos \delta} = +0^{\circ}00557 \frac{\sin \alpha}{\cos \delta} \text{ yearly.} \tag{3.2}$$

The quantity $\Delta\theta$ represents a change in position angle at the star's location (Fig. 3.4). This effect plays a significant role, for example, in comparing the

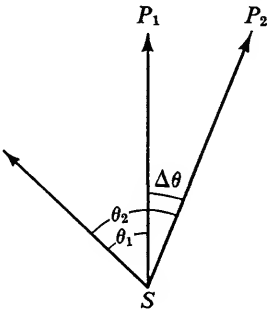

Fig. 3.4. *Change in position angle due to precession.*

position angles of double stars made at different epochs (see Chapter 10, Section 2).

Effect of precession on star positions

The effect of precession on celestial longitude and latitude is very simple. All longitudes increase at the annual rate of χ, and minor changes occur in β because of the planetary precession.

Of particular interest is the effect of precession on the right ascension and declination of a star. We shall limit ourselves to short term effects, i.e., the first order time effects only. A simple approach is the following (Fig. 3.3):

Let P_1 and P_2 be the poles of the equator, one year apart, Υ_1 and Υ_2 the corresponding equinoxes; the two poles are separated by $n = p \sin \epsilon$, measured along the great circle.

The increase in right ascension due to precession consists of two parts: (1) the amount m due to the general precession of the equinox, (2) the quantity S_1S_2 where S_1 and S_2 are the intersections of the two successive hour circles with the equator (either equator in this first approximation). It is easily seen from the spherical triangle SS_1S_2, that

$$S_1S_2 = \Delta\theta \sin \delta.$$

Or, since

$$\Delta\theta = n \frac{\sin \alpha}{\cos \delta}, \tag{3.2}$$

we find

$$S_1S_2 = n \sin \alpha \tan \delta. \tag{3.3}$$

Hence the total precession effect on right ascension is

$$pr_\alpha = m + n \sin \alpha \tan \delta. \tag{3.4}$$

The quantity pr_α refers to the precession effect on the coordinate α (RA). If it is desired to express this amount, at the star's location, as measured along the great circle, multiplication with cos δ gives

$$pr_\alpha \cos \delta = m \cos \delta + n \sin \alpha \sin \delta. \tag{3.5}$$

To derive the precession effect in declination we apply the cosine rule to the spherical triangle P_1P_2S;

$$\sin \delta' = \cos n \sin \delta + \sin n \cos \delta \cos \alpha. \tag{3.6}$$

Also,

$$\sin \delta' = \sin (\delta + pr_\delta), \tag{3.7}$$

where pr_δ is the annual change in declination due to precession. Or, since n and pr_δ are very small we may write (3.6) as:

$$\sin \delta' = \sin \delta + n \cos \delta \cos \alpha \tag{3.8}$$

and (3.7) as

$$\sin \delta' = \sin \delta + pr_\delta \cos \delta. \tag{3.9}$$

We see that

$$pr_\delta = n \cos \alpha, \tag{3.10}$$

the first order term of the precessional effect in declination.

3. Proper motions. Annual variations.

In addition to the continuous changes that precession causes in the positions of the stars, as measured on the fundamental equatorial coordinate system, the stars have motions of their own, known as *proper motions*. Precession and proper motion combined are called the *annual variation* of a star.

By comparing observations of right ascension and declination made at different epochs, annual variations are derived. The secular part of these variations consists of (1) the proper motion of the star, (2) the effect of precession of the reference system, (3) errors of observation. The reference system can only be an internal one because it is defined by the limited number of stars whose annual variations have been observed. The cosmic distribution of these motions is one of the factors limiting the attainable accuracy of the

precessional constants.[2] The ideal way of determining the precessional corrections would be from the observed annual variations of distant galaxies, at present an impractical procedure, however. Conventional meridian circle observations alone cannot establish an extragalactic reference system. Such a system must be based on photographic observations, the meridian circle observations serving to transfer the reference system to regions in the sky that are inadequately provided with galaxies.

A system of absolute motions in a restricted sense can always be obtained by deriving the precessional corrections from the stars themselves, using the assumption that the proper motions of the stars "average zero." Assuming the observed annual variations to be corrected for an adopted precession (Newcomb's values, for example), the resulting proper motions can be represented by the sum of the precessional corrections and any systematic motions that can be approximately expressed in analytical form, like galactic rotation and parallactic motion (Chapter 4). The question of finding the precessional constants is thus intimately tied up with the cosmic laws governing stellar motions.

The precessional corrections appear in the form

$$\text{In } \mu_\alpha \cos\delta: \qquad \Delta m \cos\delta + \Delta n \sin\alpha \sin\delta, \tag{3.4}$$

$$\text{In } \mu_\delta: \qquad \Delta n \cos\alpha. \tag{3.10}$$

Here Δm is normally considered a correction of the luni-solar precession $p \cos\epsilon$, and a separate correction Δl for the planetary precession is introduced. In addition, the proper motions in right ascension are usually considered to be affected by a constant error Δe, called the "motion of the equinox." This is partly a linear time effect due to changes in observational technique, partly an error of cosmic origin due to the different distribution of the proper motions of the stars used in any particular solution for precessional corrections.

In any comprehensive analysis the $\mu_\alpha \cos\delta$ are thus considered subject to a correction $\Delta k \cos\delta$ where

$$\Delta k = \Delta m - \Delta e - \Delta l.$$

The separation of these component quantities of Δk is beyond our scope. The effects of solar motion and galactic rotation will be discussed in the next chapter.

4. Annual Parallax

Parallax, parallactic displacement, and parallax factor

The orbital motion of the earth results in an annual parallactic orbit for any star. The unforeshortened semi-axis major of this orbit equals the annual

[2] Peter van de Kamp, "Remarks on the Attainable Accuracy of the Precessional Constants," *The Astronomical Journal*, 48 (1939): 21–23.

parallax of the star, which is related to the distance r by the relation (Fig. 3.5) $p = 1/r$, where p is expressed in seconds of arc and r in parsecs; 1 parsec = 206265 a.u.

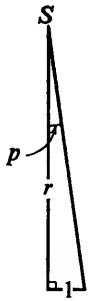

Fig. 3.5.
Relation between annual parallax p (in seconds of arc), semi-axis major of earth's orbit 1 (in astronomical units), and distance r (in parsecs): $p = 1/r$.

The momentary displacement of the geocentric from the heliocentric position of the star depends on the direction of star and sun (Fig. 3.6). This parallactic displacement may be expressed as

$$p_t = \frac{R \sin \theta}{r}, \tag{3.11}$$

where R is the radius vector of the sun expressed in astronomical units of distance, i.e., the semi-axis major of the earth's orbit, also called the mean

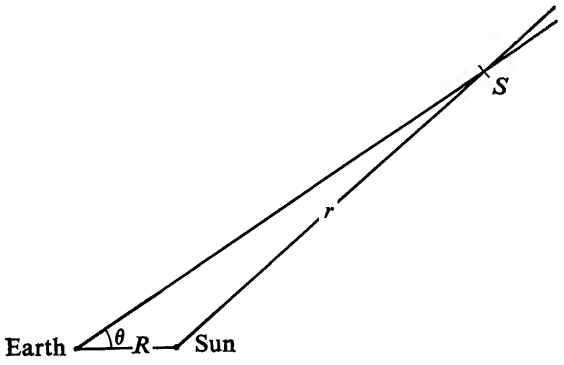

Fig. 3.6. *Annual parallactic displacement.*

distance, and θ is the angle between the direction to the sun and to the star. R and θ vary with the time of the year; in addition, θ depends on the position of the star on the celestial sphere.

The *parallactic displacement* p_t at any one time may be written as

$$p_t = pR \sin \theta = pP_t, \tag{3.12}$$

where p is the annual parallax, and

$$P_t = R \sin \theta \tag{3.13}$$

is the annual *parallax factor*. We shall now derive expressions for the components of the parallactic displacement, or rather the components of the parallax factor P_t, in both the ecliptic and the equatorial coordinate systems.

Effect in longitude and latitude

Note (Fig. 3.6) that the parallactic shift is *toward the sun*, directed along the great circle passing through sun and star. The parallactic factors are:

$$\begin{aligned} &\text{In longitude (great circle):} && P_\lambda = R \sin \theta \sin \phi, \\ &\text{In latitude:} && P_\beta = -R \sin \theta \cos \phi, \end{aligned} \tag{3.14}$$

where ϕ is the angle at the star's location from the arc $S\odot$, joining star and sun, to the star's latitude circle (Fig. 3.7). The rectangular spherical triangle $SS'\odot$ yields the trigonometric relations,

$$\sin \theta \sin \phi = \sin (\odot - \lambda), \qquad \sin \theta \cos \phi = \cos (\odot - \lambda) \sin \beta, \tag{3.15}$$

where λ and β are the celestial longitude and latitude of the star, and $\odot$ is the longitude of the sun.

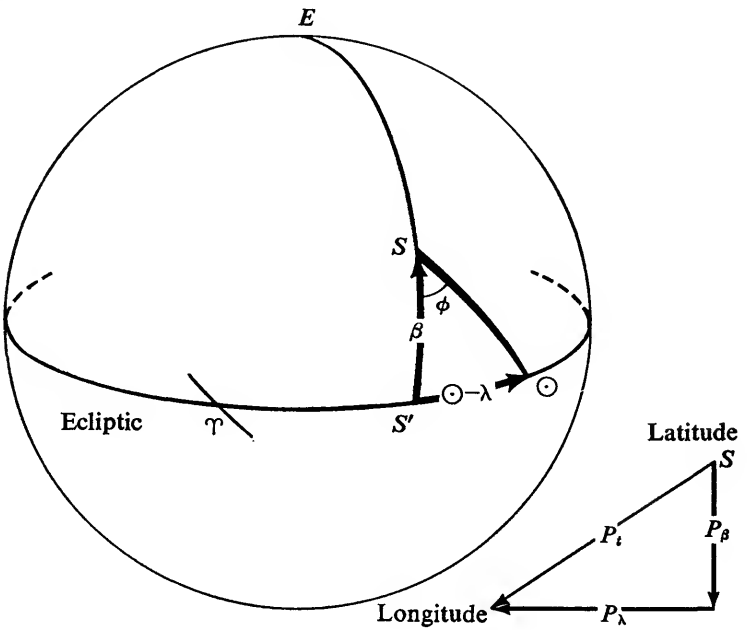

Fig. 3.7. *Parallax in longitude and latitude: S = star; $\odot$ = sun; Υ = vernal equinox.* Small diagram: *As seen from inside of celestial sphere.*

We thus find,

$$P_\lambda = R \sin (\odot - \lambda), \qquad P_\beta = -R \cos (\odot - \lambda) \sin \beta. \tag{3.16}$$

The polar coordinates R and $\odot$ of the sun's elliptical path are listed in astronomical almanacs. We see that R and $\odot - \lambda$ are the polar coordinates of the parallax factors for the unforeshortened parallactic orbit of the star. At any latitude β the parallax factors P_λ and P_β define the unit parallactic ellipse, unforeshortened in longitude but foreshortened in latitude by the factor $\sin \beta$.

Effect in right ascension and declination

In current parallax determinations it is customary to carry out the measurements in right ascension, and preferably declination also. Owing to the small inclination of the ecliptic on the equator, the major portion of the parallactic displacement, as a rule, occurs in right ascension. The parallactic factors in the equatorial coordinate system are:

$$\begin{aligned} &\text{In right ascension (great circle):} && P_\alpha = R \sin \theta \sin \chi, \\ &\text{In declination:} && P_\delta = R \sin \theta \cos \chi, \end{aligned} \tag{3.17}$$

where χ is the position angle at the star of the arc $S\odot$ (Fig. 3.8). To eliminate

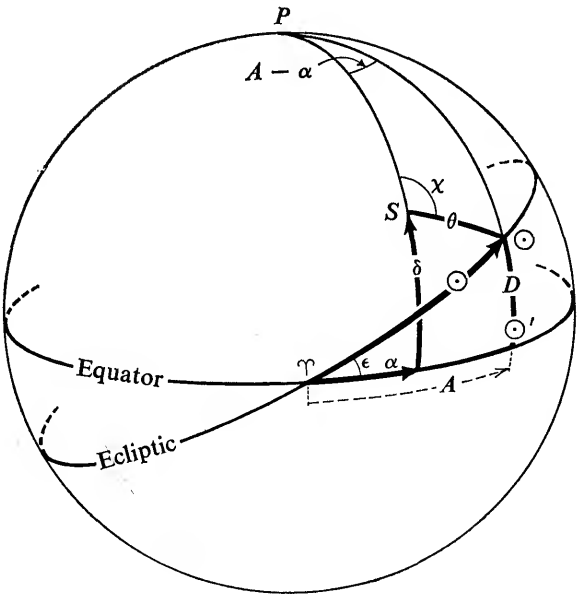

Fig. 3.8. *Parallax in right ascension and declination: S = star; $\odot$ = sun, $\odot'$ = intersection of hour circle of sun with equator; Υ = vernal equinox.*

χ we introduce the right ascension A and declination D of the sun. The spherical triangle $S\odot P$ yields the trigonometric relations,

$$\begin{aligned} \sin\theta \sin\chi &= \cos D \sin(A - \alpha), \\ \sin\theta \cos\chi &= \cos D \sin\delta \cos(A - \alpha) - \sin D \cos\delta. \end{aligned} \tag{3.18}$$

The rectangular spherical triangle $\Upsilon \odot \odot'$, where $\odot'$ is the intersection of the hour circle of the sun with the equator, yields,

$$\begin{aligned} \cos\odot &= \cos A \cos D, \\ \sin\odot \sin\epsilon &= \sin D, \\ \sin\odot \cos\epsilon &= \sin A \cos D, \end{aligned} \tag{3.19}$$

where $\epsilon = 23°27'$ is the obliquity of the ecliptic. Combining (3.18), (3.19), and (3.17) we find

$$\begin{aligned} P_\alpha &= R(\cos\epsilon \cos\alpha \sin\odot - \sin\alpha \cos\odot) \\ P_\delta &= R[(\sin\epsilon \cos\delta - \cos\epsilon \sin\alpha \sin\delta)\sin\odot - \cos\alpha \sin\delta \cos\odot] \end{aligned} \tag{3.20}$$

In practice (Chapter 8) the right ascension, α, and declination, δ, of the star are reduced to the equator and equinox of, say, the year 2000; any appreciable effect of proper motion is applied up to the epoch of the observation. A precession correction of $+0'.838$ (2000 − Epoch) is applied to the values of $\odot$ to refer them also to the equinox of the year 2000.

The formulae for the parallax factors are simplified by the following substitutions:

$$\begin{aligned} p &= +0.9174 \cos\alpha, & a &= +0.3979 \cos\delta - 0.9174 \sin\alpha \sin\delta, \\ q &= -\sin\alpha, & b &= -\cos\alpha \sin\delta, \end{aligned}$$

whence

$$P_\alpha = R(p \sin\odot + q \cos\odot), \qquad P_\delta = R(a \sin\odot + b \cos\odot).$$

Here p, q, a, b, R, $\sin\odot$, and $\cos\odot$ are calculated to four decimal places. The final values for P_α and P_δ are used to three or two places.

The same result may be obtained by a rotation from ecliptic to equatorial coordinates; in this case the equatorial coordinates of the sun need not be introduced. To convert from ecliptic to equatorial parallax factors, we have the relations (Fig. 3.9),

$$P_\alpha = P_\lambda \cos h - P_\beta \sin h, \qquad P_\delta = P_\lambda \sin h + P_\beta \cos h, \tag{3.21}$$

where h is the angle of rotation between the two coordinate systems for a particular star.

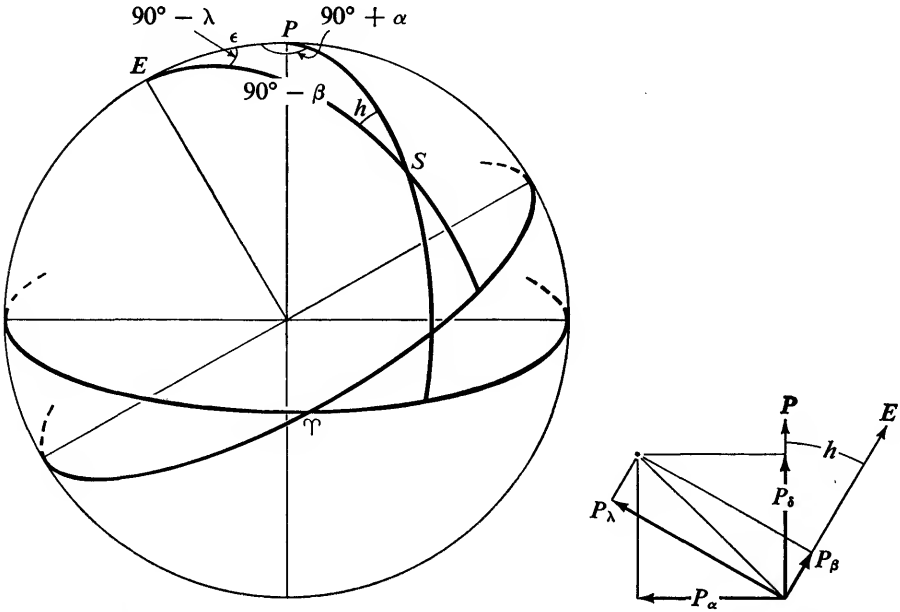

Fig. 3.9. *Relation between parallactic displacements in ecliptic and equatorial coordinates.* Small diagram: *As seen from inside of celestial sphere.*

Substitution of (3.16) in (3.21) yields

$$\begin{aligned} P_\alpha &= R \sin (\odot - \lambda) \cos h + R \cos (\odot - \lambda) \sin \beta \sin h, \\ P_\delta &= R \sin (\odot - \lambda) \sin h - R \cos (\odot - \lambda) \sin \beta \cos h. \end{aligned} \tag{3.22}$$

From the spherical triangle formed by the star and the equatorial and ecliptic poles we find, using the sine relation,

$$\sin h = \sin \epsilon \frac{\cos \alpha}{\cos \beta}, \tag{3.23}$$

and, using the polar cosine relation,

$$\cos h = \sin \lambda \sin \alpha + \cos \lambda \cos \alpha \cos \epsilon, \tag{3.24}$$

and after some complicated transformations (3.22) may be reduced to (3.20).

5. Annual aberration

Aberration circle, hodograph

The finite velocity of light leads to the effect of *stellar aberration*, a tilting of the apparent direction of the star *toward* the direction of the motion of the observer (Fig. 3.10).

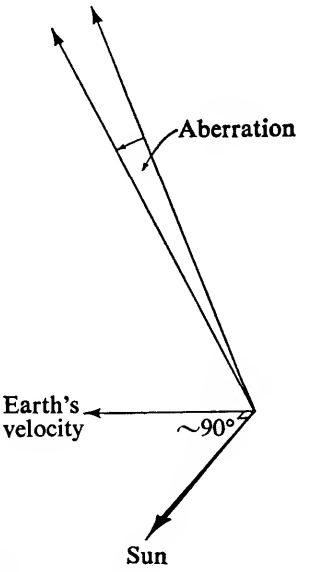

Fig. 3.10. *Annual aberration of star light.*

Of particular interest is the *annual aberration* resulting from the earth's orbital motion around the sun. The total orbital velocity V is the resultant of the components V_θ and V_r, perpendicular to and along the radius vector earth–sun. The following relations[3] hold:

$$V_\theta = \frac{2A}{p}(1 + e\cos v), \tag{3.25}$$

$$V_r = \frac{2A}{p} e \sin v, \tag{3.26}$$

where A and p represent the areal velocity and the parameter of the orbit and e and v the eccentricity and true anomaly.

It proves convenient to introduce the circular velocity V_c corresponding to an idealized earth's orbit with a radius equal to the mean distance a, and a period equal to the sidereal year,

$$V_c = \frac{2\pi a}{P}. \tag{3.27}$$

Since by definition the parameter

$$p = a(1 - e^2) \tag{3.28}$$

[3] Peter van de Kamp, *Elements of Astromechanics*, San Francisco and London, W. H. Freeman and Company, 1964, equations 3.38 and 3.16.

and the areal velocity

$$A = \frac{\pi a^2(1 - e^2)^{1/2}}{P} \tag{3.29}$$

we find

$$\frac{2A}{p} = \frac{2\pi a}{P}(1 - e^2)^{-1/2}$$

or

$$\frac{2A}{p} = V_c(1 - e^2)^{-1/2}. \tag{3.30}$$

Hence (3.25) and (3.26) may be written as

$$V_\theta = V_c(1 - e^2)^{-1/2}(1 + e \cos v) \tag{3.31}$$

$$V_r = V_c(1 - e^2)^{-1/2} e \sin v. \tag{3.32}$$

These rectangular vector components may be written as

$$V_\theta = K + eK \cos v, \tag{3.33}$$

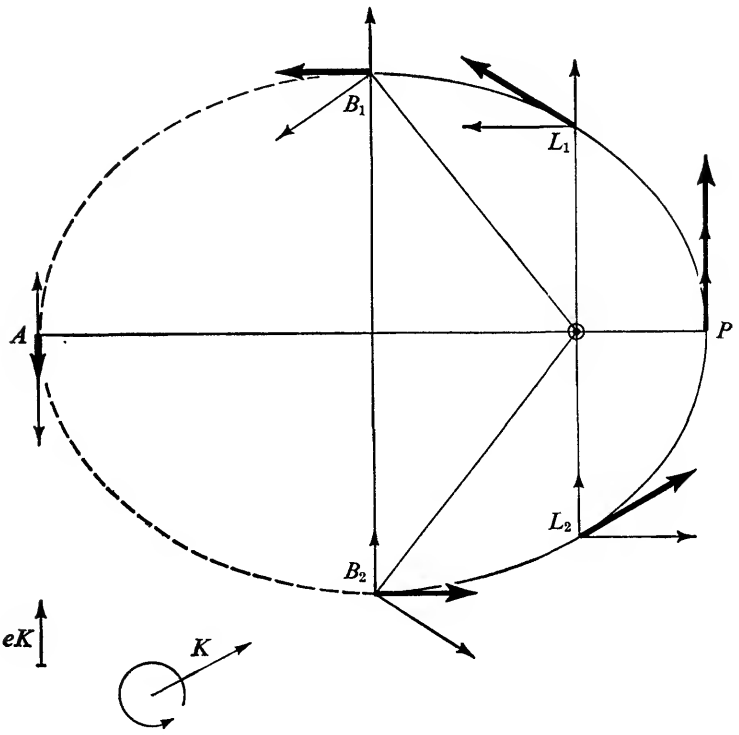

Fig. 3.11. *Velocity vectors at periastron, apastron, ends of latus rectum, and ends of minor axis, for* $e = 0.6$.

$$V_r = eK \sin v, \tag{3.34}$$

where

$$K = V_e(1 - e^2)^{-1/2}. \tag{3.35}$$

Note that V_θ consists of a constant term K, directed perpendicular to the radius vector, plus a term $eK \cos v$ which together with $V_r = eK \sin v$ defines a constant term eK in the direction $v = 90°$. Hence V may be considered the resultant of a constant circular velocity K perpendicular to the radius vector, hence constantly turning, and a velocity eK in the constant direction $v = 90°$, perpendicular to the major axis (Figs. 3.11 and 3.12).

Thus the velocity vectors V define a circle with radius K, the vectors originating at a point O that lies at a distance eK from the center of the circle opposite the direction $v = 90°$. The true anomaly v appears at the center of the circle, indicating the direction of V_θ. The velocity vectors at periastron P, apastron A, and the ends of the latus rectum L_1 and L_2 are represented by OP, OA, OL_1, and OL_2, representing $v = 0°$, 180°, 90°, and 270°, respectively. The velocity vectors at the ends of the minor axis B_1 and B_2 are represented by OB_1 and OB_2. These vectors equal the radius $K = V_e(1 - e^2)^{-1/2}$ of the circle (Fig. 3.13).

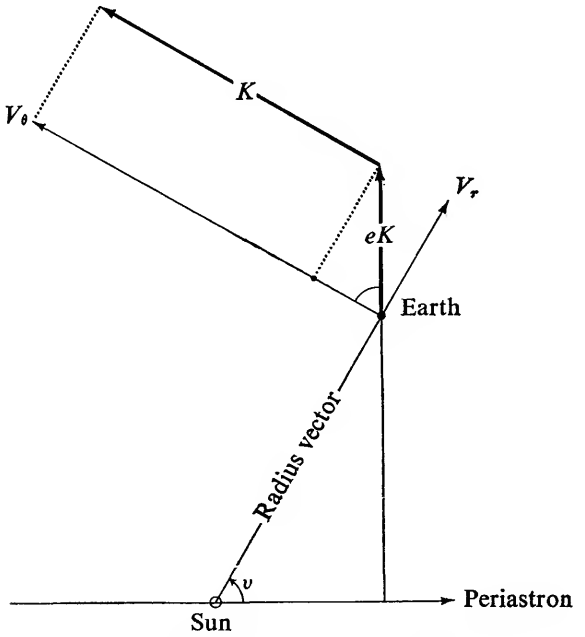

Fig. 3.12. *Components of earth's velocity along and perpendicular to radius vector.*

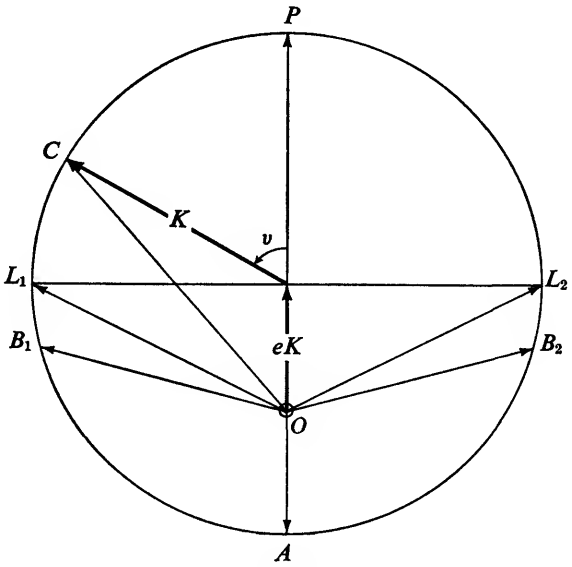

Fig. 3.13. *Hodograph showing orbital velocities as resultant of component K perpendicular to radius vector and component eK perpendicular to major axis.*

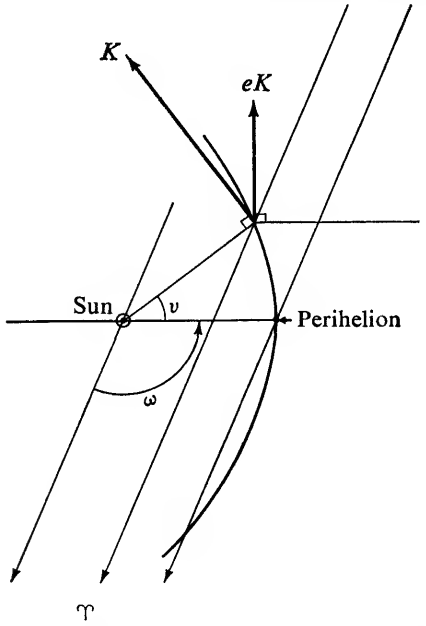

Fig. 3.14. *Relation between true anomaly, sun's longitude ☉, and heliocentric longitude ω of perihelion.*

Such a velocity-vector diagram is called a *hodograph.*

The directions, i.e., longitudes, of the velocity vectors K and eK are related to the sun's longitude $\odot$ and the heliocentric longitude ω of the perihelion (the value of ω is close to 100°, it differs 180° from the geocentric longitude of the perigee). It is easily seen (Fig. 3.14) that:

Longitude of velocity vector K: $\odot - 90°$,

Longitude of velocity vector eK: $\omega + 90°$.

The momentary aberrational effect depends on the direction of the star and the position of the earth in its orbit. The unforeshortened aberrational effect

Fig. 3.15.
Relation between aberration constant k, velocity K, and velocity of light c.

at the pole of the ecliptic is obviously a circle, and the heliocentric position of the star differs from the center of the aberration circle by the amount

$$eK = eV_e(1 - e^2)^{-1/2}.$$

The scale of the stellar aberration effect in angular measure (Fig. 3.15) is given by the so-called "constant of aberration"

$$k = \frac{K}{c} = \frac{V_e(1 - e^2)^{-1/2}}{c} = 20''.49, \tag{3.36}$$

where $V_e = 29.8$ km/sec is the "circular" velocity in the earth's orbit, $e = 0.01675$ is the eccentricity of the earth's orbit, and $c = 299{,}792.5$ km/sec is the velocity of light. The corresponding effect $ek = eK/c$ amounts to only $0''.34$.

The aberration effect of a star in any other direction will now be considered the resultant of the two effects due to the orbital velocity components: that perpendicular to the radius vector and that perpendicular to the major axis of the earth's orbit. The unforeshortened value of the two effects are k and eK, respectively. Both effects are foreshortened by the factor $\sin\theta$, where θ is the angle between the direction to the star and the direction of the velocity vector considered. The problem is analogous to that of parallax (Section 4).

Effect in longitude and latitude

Effect due to velocity vector K.—As a result of the velocity vector K the star is displaced by the amount $k \sin\theta$ toward a point F on the ecliptic in longitude $\odot - 90°$ (Fig. 3.16). The resulting aberrational effect is:

$$\begin{aligned} &\text{In longitude (great circle):} && k \sin\theta \sin\phi, \\ &\text{In latitude:} && k \sin\theta \cos\phi, \end{aligned}$$

where ϕ is the angle at the star's location from the arc SF to the star's latitude circle. Note that the arc FS' equals $(\odot - \lambda) - 90°$.

The rectangular spherical triangle $SS'F$ yields

$$\begin{aligned} \sin\theta \sin\phi &= \sin(\odot - \lambda - 90°) = -\cos(\odot - \lambda), \\ \sin\theta \cos\phi &= \cos(\odot - \lambda - 90°)\sin\beta = -\sin(\odot - \lambda)\sin\beta. \end{aligned} \tag{3.37}$$

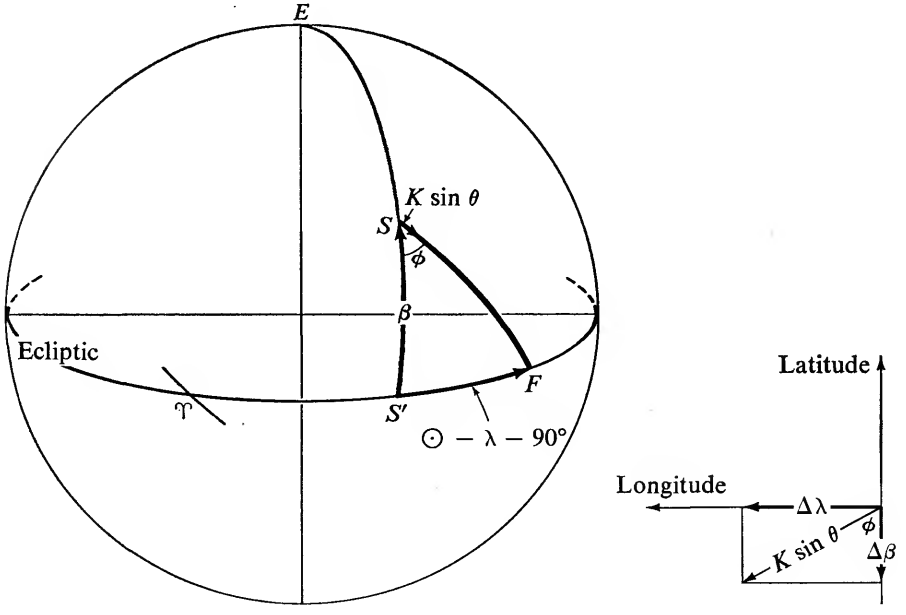

Fig. 3.16. *Aberration in longitude and latitude.* Small diagram: *As seen from inside of celestial sphere.*

We thus find:

$$\begin{aligned} &\text{Aberration in longitude (great circle):} && -k \cos (\odot - \lambda), \\ &\text{Aberration in latitude:} && -k \sin (\odot - \lambda) \sin \beta. \end{aligned} \tag{3.38}$$

Effect due to the constant velocity vector eK.—As a result of the constant velocity vector eK, the star is displaced forward by the amount $eK \sin \theta$ toward a point on the ecliptic in longitude $\omega + 90°$. Substituting $\omega + 90°$ for $\odot - 90°$, i.e., $(\omega - \lambda - 180°)$ for $(\odot - \lambda)$, and following the earlier procedure we find:

$$\begin{aligned} &\text{Aberration in longitude (great circle):} && +ek \cos (\omega - \lambda), \\ &\text{Aberration in latitude:} && +ek \sin (\omega - \lambda) \sin \beta. \end{aligned} \tag{3.39}$$

Effect in right ascension and declination

Effect due to velocity vector K.—From Figure 3.17 we note that the aberrational effects are:

$$\begin{aligned} &\text{In right ascension (great circle):} && k \sin \theta \sin \chi \\ &\text{In declination:} && k \cos \theta \cos \chi \end{aligned}$$

where χ is the position angle at the star of the arc SF. Note that the situation is analogous to that for parallax except that in (3.20) $\odot$ is replaced by $\odot - 90°$. It is easily seen that the aberrations effect are:

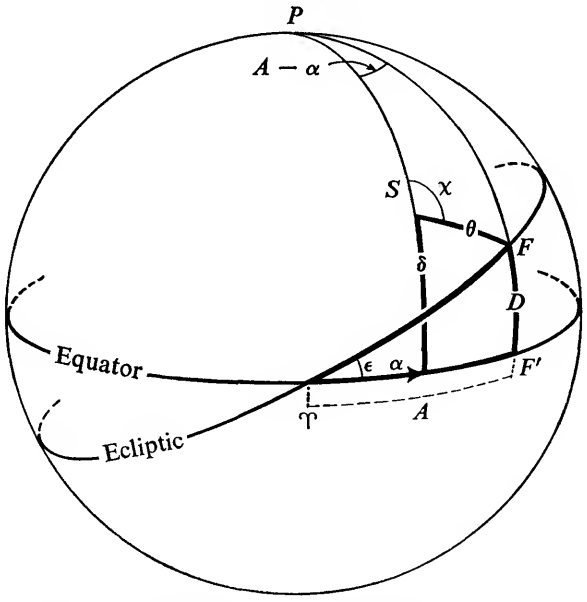

Fig. 3.17. *Aberration in right ascension and declination.*

In right ascension (great circle):

$$-k(\cos\epsilon\cos\alpha\cos\odot+\sin\alpha\sin\odot),$$

In declination: (3.40)

$$-k\{(\sin\epsilon\cos\delta-\cos\epsilon\sin\alpha\sin\delta)\cos\odot+\cos\alpha\sin\delta\sin\odot\}.$$

Effect due to constant velocity vector eK.—By substituting $\omega+90°$ for $\odot-90°$ i.e., $\omega+180°$ for $\odot$, we find:

Aberration in right ascension (great circle):

$$+ek(\cos\epsilon\cos\alpha\cos\omega+\sin\alpha\sin\omega),$$

(3.41)

Aberration in declination:

$$+ek\{(\sin\epsilon\cos\delta-\cos\epsilon\sin\alpha\sin\delta)\cos\omega+\cos\alpha\sin\delta\sin\omega\}.$$

Effect of eccentricity of earth's orbit

The center of the projected aberrational ellipse differs from the true position of the star by the constant factors (3.39) (in longitude and latitude) or (3.41) (in right ascension and declination).

By convention the quantities containing e are omitted, i.e., the eccentricity of the earth's orbit is ignored. The error thus introduced is at most 0".3 and very nearly constant for any one star through the centuries.

6. Stellar positions

We distinguish between the *mean* equator and equinox, defined by the secular precession terms, and the *true* equator and equinox, which include also the nutation for the epoch considered.

Stellar positions are defined accordingly. The *mean position* as given in most catalogues is the heliocentric position referred to the mean equator and equinox of a stated epoch, usually the beginning of the year. The heliocentric position is that which would be determined by an imaginary observer at the sun, and thus contains no parallax, nor is aberration included. The beginning of the year refers to that of the fictitious Besselian year, which corresponds to a right ascension of $18^h40^m(280°)$ of the mean sun, affected by aberration and measured from the mean equinox. It is always nearly the same as the beginning of the calendar year.

The *true position* is the heliocentric position referred to the true equator and equinox of the moment. It is obtained by adding to the *mean position* the accumulated precessional and nutational effects since the date of the mean position.

The *apparent place* is the *observed* position as seen from (the center of) the earth, as referred to the true equator and equinox of the moment. It is obtained by adding to the true position the effects of annual aberration and of parallax, which is often negligibly small.

Planetary positions present a different problem altogether, since the planets are so very close to the earth, compared with the stars. Geocentric parallax as well as *light time* must now be taken into account. Light time varies rapidly because of the orbital motion of earth and of the planets, and therefore plays an entirely different role than it does for stars, with their virtually constant motions throughout the centuries.

7. Positional accuracy

Over the centuries, the accuracy with which stellar positions can be determined has increased gradually. In order to appreciate many of the derivations that will be presented, it will be useful to have some knowledge of the accuracy involved. Current star catalogues, based on meridian circle observations, give stellar positions with an accuracy represented by probable errors of about $0''.1$. However, systematic errors may be rather larger than the probable errors.

In Part II of this book we shall discuss the photographic techniques and methods of obtaining stellar positions. Photographic positions derived from wide-angle, short-focus instruments yield about the same accuracy as meridian circle observations. Long-focus photographs give star positions with a probable error of about $0''.04$ for a triple exposure. The average of several exposures, on several plates on several nights, may yield a probable error as small as $0''.01$.

Multiple-exposure photographs of wide double stars yield relative positions with probable errors as small as $0''.003$ (Chapter 10).

Suggested readings

The American Ephemeris and Nautical Almanac. Washington, D. C., Government Printing Office. (Published annually).

Explanatory Supplement to The Astronomical Ephemeris and The American Ephemeris and Nautical Almanac. London, Her Majesty's Stationery Office, 1961.

G. M. Clemence, "Astronomical Reference Systems," *in* K. Aa. Strand, ed., *Basic Astronomical Data* (Stars and Stellar Systems, Vol. III). University of Chicago Press, 1963, pp. 1–10.

F. P. Scott, "The System of Fundamental Proper Motions," *in* K. Aa. Strand, ed., *Basic Astronomical Data* (Stars and Stellar Systems, Vol. III). University of Chicago Press, 1963, pp. 11–29.

4 Systematic Patterns in Proper Motions

A. SOLAR MOTION

1. Introduction

Within a neighborhood extending up to a small fraction of the sun's distance to the galactic center, say $<10\%$, stellar motions show two simple distinctive patterns.

1. The sun's motion with respect to its neighboring stars results in a *secular parallactic* motion for the stars. The *apex* and *antapex* of the direction of solar motion are located in the constellations Hercules and Columba respectively.

2. The sun's motion and stellar motions are the local manifestation of the differences in their huge galactic orbits around the galactic center some 10,000 parsecs distant in the direction of Sagittarius; the galactic velocity of the sun is about 250 km/sec in the approximate direction of Cygnus. The individual galactic velocities of stars or sun depend on the gravitational field of the galaxy. As seen from the sun the effects of differential galactic rotation may be expressed in a simple manner (part B of this chapter).

In terms of location in the sky solar motion effects are revealed as single periodic functions, differential galactic rotation as double periodic functions. The solar motion effects are of prime importance because they permit us to determine statistical stellar distances beyond the limits of the conventional annual parallax method, and the galactic rotation effects contribute to our knowledge of dynamical properties of the galactic system.

2. Annual and secular parallax

If we express the star's distance r in parsecs we have the following fundamental relations:

$$\begin{aligned} \text{Annual parallax} &= \frac{1}{r}, \\ \text{Secular parallax} &= \frac{h}{r}. \end{aligned} \tag{4.1}$$

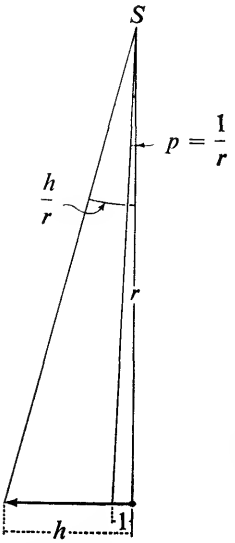

Fig. 4.1.
Annual and secular parallax for star on parallactic equator, i.e., at right angles from apex ($\lambda = 90°$).

Here the parallax values are expressed in seconds of arc; h is the motion of the solar system expressed in astronomical units per year. If desired, a transition to metric measure is given through the relation

$$1 \text{ a.u./year} = 4.74 \text{ km/sec.}$$

3. Solar motion: solar velocity and apex

It is important to consider closely what is meant by *solar motion.* The convenient observational origin for stellar velocities is the sun. The only possible definition of solar motion in the galactic system is that it is the equal and opposite of the group motion of stars. The latter can be determined only if the stellar space velocities are known from proper motions, radial velocities, and parallaxes.

The relation between rectangular and equatorial polar coordinates is

$$\begin{aligned} x &= r \cos\delta \cos\alpha \text{ where } + x \text{ points to the vernal equinox,} \\ y &= r \cos\delta \sin\alpha \text{ where } + y \text{ points to RA } 6^h \text{ on the equator,} \\ z &= r \sin\delta \quad\quad \text{where } + z \text{ points to the celestial north pole.} \end{aligned} \tag{4.2}$$

Here x, y, z, and r are expressed in parsecs.

The annual variations are given by

$$\begin{aligned} \frac{dx}{dt} &= -r \cos\delta \sin\alpha\, \mu_\alpha - r \sin\delta \cos\alpha\, \mu_\delta + \cos\delta \cos\alpha \frac{dr}{dt} \\ \frac{dy}{dt} &= \quad r \cos\delta \cos\alpha\, \mu_\alpha - r \sin\delta \sin\alpha\, \mu_\delta + \cos\delta \sin\alpha \frac{dr}{dt} \\ \frac{dz}{dt} &= \quad r \cos\delta\, \mu_\delta + \sin\delta \frac{dr}{dt}. \end{aligned} \tag{4.3}$$

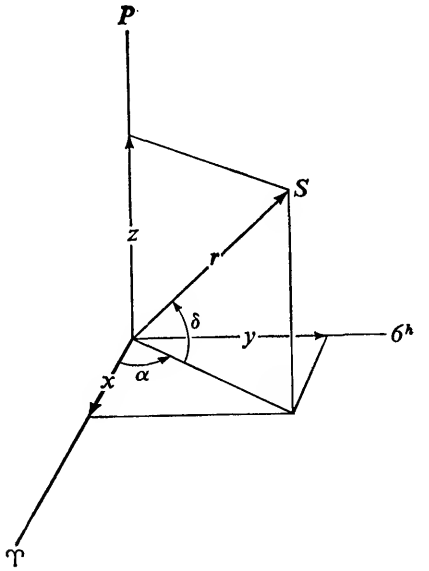

Fig. 4.2. *Relation between rectangular and polar equatorial coordinates of star.*

Here $\frac{dx}{dt}$, $\frac{dy}{dt}$, $\frac{dz}{dt}$, and $\frac{dr}{dt}$ are expressed in a.u./year; μ_α and μ_δ are the proper motion components expressed in seconds of arc per year.

For a certain group of stars therefore the group motion is given by the rectangular components $\left(\overline{\frac{dx}{dt}}\right)$, $\left(\overline{\frac{dy}{dt}}\right)$, $\left(\overline{\frac{dz}{dt}}\right)$, the solar motion by the equal and opposite values h_x, h_y, h_z, so that

$$h_x = -\left(\overline{\frac{dx}{dt}}\right), \qquad h_y = -\left(\overline{\frac{dy}{dt}}\right), \qquad h_z = -\left(\overline{\frac{dz}{dt}}\right). \tag{4.4}$$

From this the solar velocity h and the right ascension A and declination D of the apex easily follow:

$$\begin{aligned} h &= \sqrt{h_x^2 + h_y^2 + h_z^2}, \\ \tan A &= \frac{h_y}{h_x}, \\ \tan D &= \frac{h_z}{\sqrt{h_x^2 + h_y^2}}. \end{aligned} \tag{4.5}$$

The parallactic parts of the velocity components of the individual stars are given by

$$\begin{aligned} \mu_{\alpha,p} \cos \delta &= \frac{h_x}{r} \sin \alpha - \frac{h_y}{r} \cos \alpha, \\ \mu_{\delta,p} &= \frac{h_x}{r} \cos \alpha \sin \delta + \frac{h_y}{r} \sin \alpha \sin \delta - \frac{h_z}{r} \cos \delta, \\ -\frac{dr}{dt} &= h_x \cos \alpha \cos \delta + h_y \sin \alpha \cos \delta + h_z \sin \delta. \end{aligned} \tag{4.6}$$

Here h_x/r, h_y/r, and h_z/r are the rectangular components of the secular parallax h/r and shall be denoted by X, Y, Z. If also we express the third equation in metric units, we obtain the commonly used formulae for the polar components of parallactic motion:

$$\begin{aligned} \mu_{\alpha,p} \cos \delta &= X \sin \alpha - Y \cos \alpha, \\ \mu_{\delta,p} &= X \cos \alpha \sin \delta + Y \sin \alpha \sin \delta - Z \cos \delta, \\ -V_p &= V_x \cos \alpha \cos \delta + V_y \sin \alpha \cos \delta + V_z \sin \delta. \end{aligned} \tag{4.7}$$

4. Mean secular parallax: v and τ components

The problem of secular parallax becomes important only for stars whose individual distances are unknown. Assuming that for a group of stars in a limited portion of the sky the residual proper motions cancel with respect to their mean parallactic motion; the mean proper motion gives the following equations:

$$\begin{aligned} \overline{\mu_\alpha \cos \delta} &= X \sin \alpha - Y \cos \alpha, \\ \overline{\mu_\delta} &= X \cos \alpha \sin \delta + Y \sin \alpha \sin \delta - Z \cos \delta, \end{aligned} \tag{4.8}$$

where X, Y, and Z now represent the rectangular coordinates of the *mean secular parallax* of the stars:

$$\left(\frac{\overline{h}}{r}\right).$$

A number of groups of stars well distributed over the sky furnish a number of pairs of equations of conditions (4.8): a least-squares solution gives values of X, Y, and Z. Their relation to the mean secular parallax and the position of the apex is then given by

$$\begin{aligned} X &= \left(\frac{\overline{h}}{r}\right) \cos A \cos D & \left(\frac{\overline{h}}{r}\right) &= \sqrt{X^2 + Y^2 + Z^2}, \\ Y &= \left(\frac{\overline{h}}{r}\right) \sin A \cos D & \tan A &= \frac{Y}{X}, \\ Z &= \left(\frac{\overline{h}}{r}\right) \sin D, & \tan D &= \frac{Z}{\sqrt{X^2 + Y^2}}. \end{aligned} \tag{4.9}$$

If only radial velocities are known formula (4.7) can be used on the assumption that the residual radial velocities cancel. In that case a least-squares solution gives values for the rectangular components V_x, V_y, V_z of the solar velocity V_0 and we have:

$$\begin{aligned} V_x &= V_0 \cos A \cos D, & V_0 &= \sqrt{V_x^2 + V_y^2 + V_z^2}, \\ V_y &= V_0 \sin A \cos D, & \tan A &= \frac{V_y}{V_x}, \\ V_z &= V_0 \sin D, & \tan D &= \frac{V_z}{\sqrt{V_x^2 + V_y^2}}. \end{aligned} \tag{4.10}$$

Either solution (4.9) or (4.10) is based on the assumption that the solar motion is sufficiently exhibited by either the transverse or radial components of the space motions. Formula (4.9) therefore enables us to obtain the mean secular parallax and solar apex for a group of stars whose proper motions are known; formula (4.10) gives us the solar velocity and solar apex for a group of stars whose radial velocities are known; either method thus yields an apex determination.

In order to obtain the three rectangular components of the solar motion, any systematic effects must, of course, be properly taken into account. For radial velocities, possible red shift will have to be considered; for proper motions, precession corrections may be in order. In either case the effects of differential galactic rotation are present. Systematic errors of observational origin are of serious consequence, especially for small proper motions. In Sections 8, 9, and 10 of this chapter the various significant effects will be further discussed for the case of proper motions.

Solar motion is inherently a relative concept, depending on the stars involved. The conventional value refers to the stars for which radial velocity and proper motion data are readily available. This *standard solar motion*[1] is given by

$$\begin{aligned} V_0 &= 19.5 \text{ km/sec} \\ A &= 18^h.0 & (l &= 56°) \\ D &= +30° & (b &= +23°). \end{aligned}$$

The *basic solar motion*[2] refers to the velocities of stars in the solar neighborhood; it is given by

$$\begin{aligned} V_0 &= 15.4 \text{ km/sec} \\ A &= 17^h.8 & (l &= 51°) \\ D &= +25° & (b &= +23°). \end{aligned}$$

[1] J. Delhaye, "Solar Motion and Velocity Distribution of Common Stars," *in* A. Blaauw and M. Schmidt, eds., *Galactic Structure* (Stars and Stellar Systems, Vol. V). University of Chicago Press, 1965, p. 73.

[2] *Ibid.*, p. 74.

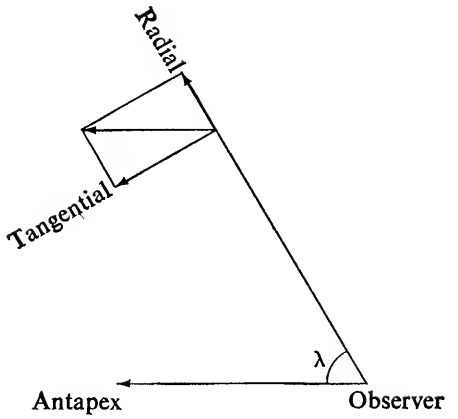

Fig. 4.3. *Tangential and radial effects in secular parallactic motion.*

For the sake of completeness the formulae will now be given for deriving mean secular parallax and solar velocity if the apex is considered as known.

If λ is the angular distance of the star from the antapex, it follows that the *secular parallax factor* of the total parallactic proper motion equals $\sin \lambda$; the secular parallax factor P_r of the parallactic radial velocity is $\cos \lambda$. If, moreover, χ is the position angle of the direction to the antapex, measured at the star, then the secular parallax factors in right ascension (great circle) and

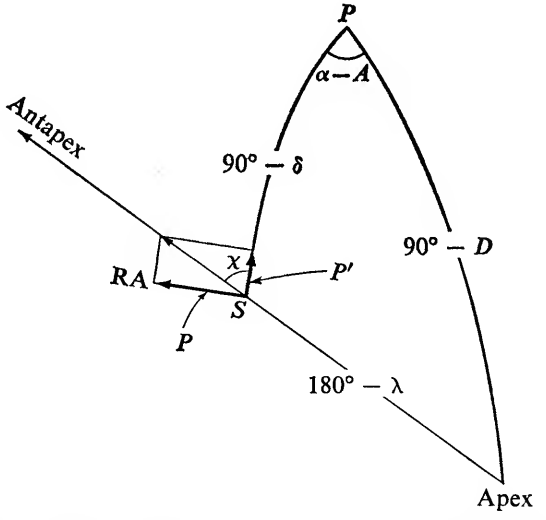

Fig. 4.4. *Angular distance* λ *of star from apex and position angle* χ *of antapex, as seen from inside of celestial sphere.*

declination amount to $P = \sin\lambda \sin\chi$ and $P' = \sin\lambda \cos\chi$, respectively. Applying the sine, extended cosine, and cosine rules to the spherical triangle formed by star, antapex, and north celestial pole, we see that:

$$\begin{aligned} P = \sin\lambda \sin\chi &= \sin(\alpha - A)\cos D, \\ P' = \sin\lambda \cos\chi &= \cos(\alpha - A)\cos D \sin\delta - \sin D \cos\delta, \\ P_r = \cos\lambda &= -\cos(\alpha - A)\sin D \cos\delta - \sin D \sin\delta. \end{aligned} \tag{4.11}$$

The same relations are easily derived by combining the relation (4.7) with (4.9) and (4.10).

The secular parallax factors[3] may be calculated directly from the equatorial positions of star or apex, or from the quantities λ and χ. The relations (4.11) have been used to calculate λ and χ as functions of α or δ; the resulting tabulations or diagrams are conveniently used.[4]

Limiting ourselves for the moment to the proper motions, we may now write

$$\overline{\mu_\alpha \cos\delta} = P\left(\frac{\bar{h}}{r}\right), \qquad \overline{\mu_\delta} = P'\left(\frac{\bar{h}}{r}\right). \tag{4.12}$$

Generally these relations would hold for an average of several stars in a limited group of stars, and the formulae may of course be used for separate stars. A least-squares solution yields

$$[P^2]\left(\frac{\bar{h}}{r}\right) = [P\overline{\mu_\alpha \cos\delta}], \qquad [P'^2]\left(\frac{\bar{h}}{r}\right) = [P'\overline{\mu_\delta}]. \tag{4.13}$$

It is also possible and often desirable to introduce the total parallactic proper motion, rather than its equatorial components. We observe that the total proper motion is the resultant of the *parallactic proper motion* μ_p and the star's own or *peculiar proper motion* μ_i. We know that $\mu_p = h/r \sin\lambda$, but unless the distance to the star is known, we cannot separate μ_p and μ_i. The following procedure is very useful. We introduce the so-called v *component* directed toward the antapex, and the τ *component*, perpendicular to the direction of the parallactic motion. We know then that the τ component is due to the star's own motion, while for a large number of stars the v components, within some statistical uncertainty, may be expected to represent the parallactic motion μ_p.

We now write

$$v = \mu\cos(\theta - \chi), \qquad \tau = \mu\sin(\theta - \chi), \tag{4.14}$$

[3] P. J. van Rhijn and B. J. Bok, *The Secular Parallax of the Stars of Different Apparent Magnitude and Galactic Latitude*, (Groningen Publication 45), 1931. (Abbreviated tabulations of P and P' are given in tables 11 and 12.)

[4] W. M. Smart, "The Construction of a Chart Giving the Angular Distances of Stars from, and the Position Angles Relative to, the Ant-apex of the Solar Motion," *Monthly Notices of the Royal Astronomical Society*, 83 (1923): 465–469.

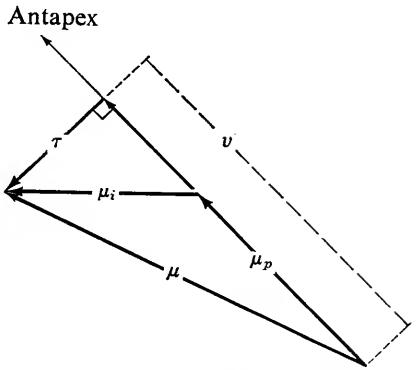

Fig. 4.5. *Total* (μ), *parallactic* (μ_p), *and peculiar* (μ_i) *proper motions;* v *and* τ *components.*

where θ is the position angle of the total proper motion μ, measured at the star. Or since

$$\mu \sin\theta = \mu_\alpha \cos\delta, \qquad \mu \cos\theta = \mu_\delta, \tag{4.15}$$

we may express v and τ directly in terms of $\mu_\alpha \cos\delta$ and μ_δ, as follows,

$$v = \mu_\alpha \cos\delta \sin\chi + \mu_\delta \cos\chi, \qquad \tau = \mu_\alpha \cos\delta \cos\chi - \mu_\delta \sin\chi. \tag{4.16}$$

On the assumption that for a group of stars the residual motions of the separate stars are random and cancel, the quantity μ_p is considered given by the v component. Similarly, $V_p = V_0 \cos\lambda$ may be set equal to the observed radial velocity V. We thus have $h/r \sin\lambda = v$, $V_0 \cos\lambda = V$. Therefore, least-squares solutions lead to the following simple expressions for mean secular parallax and solar velocity,

$$\left(\frac{\bar{h}}{r}\right) = \frac{[v \sin\lambda]}{[\sin^2\lambda]}, \qquad V_0 = \frac{[V \cos\lambda]}{[\cos^2\lambda]}. \tag{4.17}$$

It is clear that the secular parallax method will be most successful if the residual motions are small compared with the mean parallax. It is also obvious

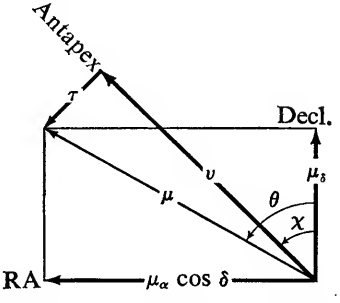

Fig. 4.6. *Equatorial, and* v *and* τ *components of total proper motions.*

that regions near the apex and antapex have greatest weight in determining the directions of solar motion, and that those near the "parallactic equator," 90° from the apex, have highest weight in the determination of mean secular parallax. An inherent weakness of mean secular parallaxes is therefore the lack of equivalence in accuracy in different parts of the sky. Since the solar apex lies not far from the galactic circle the secular parallax factors, and hence the parallactic motions, are large in high galactic latitudes but relatively small in lower latitudes. A determination of mean secular parallaxes in low latitudes has, therefore—other things being equal—less accuracy than one in high latitudes, and is also more sensitive to uncertainties in the reference system of proper motions.[5]

The following sections, 5, 6, and 7, are not strictly astrometric in character. They have been included because of their close relationship to the subject matter of this book.

5. Mean annual parallax and mean distance

The mean annual parallax for a group of stars may be obtained by dividing the solar velocity into the mean secular parallax, i.e.,

$$\bar{p} = \frac{1}{h}\left(\frac{\bar{h}}{r}\right)$$

or, more commonly,

$$\bar{p} = \frac{4.74}{V_0}\left(\frac{\bar{h}}{r}\right). \tag{4.18}$$

The standard value of V_0 is 19.5 km/sec, corresponding to $h = 4.1$ a.u./year. The mean parallax may also be derived by comparing the mean value of τ components with the mean absolute value of the peculiar radial velocities V_i, i.e., the observed radial velocities, after correction for solar motion. The formula is

$$\bar{p} = 4.74\,\frac{|\bar{\tau}|}{|\bar{V}_i|}. \tag{4.19}$$

The mean annual parallax may be reduced to mean distance by allowing for the dispersion in distance. This is, at best, difficult. For any dispersion in distance (or parallax) it is obvious that

$$\bar{r} \neq \frac{1}{\bar{p}}.$$

Allowance for the dispersion may be made, for example, for the simple case in which a Gaussian distribution is adopted. This may be justifiable for a group of stars with a limited range in both apparent magnitude m and absolute M.

[5] W. Fricke, "The Influence of Proper Motion Systems on the Determination of Statistical Parallaxes," *Vistas in Astronomy*, 8 (1966): 205–214.

Since the *distance modulus* is given by $m - M = 5 \log r - 5$, for a single value of m, a dispersion (root mean square deviation) of σ_M in the value of M corresponds to a dispersion of $0.2\,\sigma_M$ in $\log r$.

It can be shown[6] that the following relations exist:

$$\bar{p} = p_0 \exp \frac{(0.2\,\sigma_M)^2}{2\,\mathrm{mod}^2}, \tag{4.20}$$

$$\bar{r} = r_0 \exp \frac{(0.2\,\sigma_M)^2}{2\,\mathrm{mod}^2}, \tag{4.21}$$

$$\bar{r} = \frac{1}{\bar{p}} \exp \frac{(0.2\,\sigma_M)^2}{\mathrm{mod}^2}, \tag{4.22}$$

where p_0 and r_0 are the most probable values of p and r, and $\mathrm{mod} = \log e_{10} = 0.4343$. The conversion factor is not necessarily negligible, as may be seen from the following tabulation:

σ_M	$\exp \frac{(0.2\,\sigma_M)^2}{\mathrm{mod}^2}$
0.5	1.05
1.0	1.24
1.5	1.61
2.0	2.33
2.5	3.8
3.0	6.7

B. GALACTIC ROTATION

The discovery of galactic rotation by Lindblad and Oort led to a mathematical formulation that is significant in astrometric studies involving the proper motions of stars on the celestial sphere, or major portions thereof. We shall limit ourselves here to the classical differential galactic rotation terms, first presented by Oort, which are valid for comparatively nearby stars and should be taken into account in all proper-motion studies of them.

6. Differential galactic rotation: effects on tangential and radial velocities

We shall first consider a plane rotating system. The distance from the sun to the center of rotation, or galactic center, is R; the circular velocity at the sun's location is V. The velocity of rotation is assumed to depend only on the dis-

[6] E. v. d. Pahlen, *Lehrbuch der Stellarstatistik*, Leipzig, J. A. Barth, 1937, pp. 317–320. (Discusses the relation between mean parallax and mean distance.)

tance to the center, its radial gradient is $\partial V/\partial R$. The circular velocity V' at a distance $R + dR$ from the galactic center is given by

$$V' = V + \frac{\partial V}{\partial R} dR. \tag{4.23}$$

Let us now study the effects of rotation as observed from an object at the sun's location that is in circular motion around the galactic center. What is the effect for a star (in the galactic plane) at a distance r? Assume that r is small compared with R (say 1,000 parsecs, as compared with an assumed value of 10,000 parsecs for R).

Toward the center—i.e., at a distance $R - r$ from the center—the circular velocity is

$$V - \frac{\partial V}{\partial R} r. \tag{4.24}$$

Away from the center—i.e., toward the anti-center at a distance $R + r$ from the center—the circular velocity is

$$V + \frac{\partial V}{\partial R} r. \tag{4.25}$$

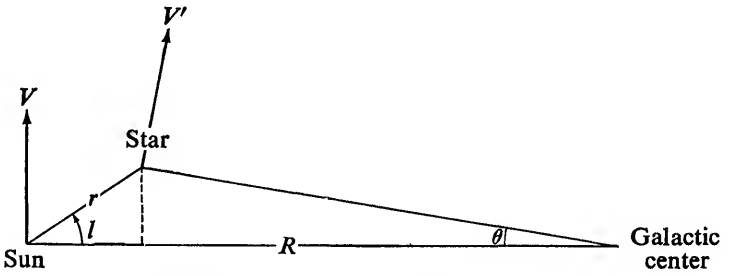

Fig. 4.7. *Galactic rotation in galactic plane.*

For a star at distance r, in a direction at galactic longitude l, the circular velocity V' is given by

$$V' = V - \frac{\partial V}{\partial R} r \cos l, \tag{4.26}$$

since, for this star, to a high degree of approximation

$$dR = -r \cos l. \tag{4.27}$$

To study the effects of differential galactic rotation as observed from a circular orbit at the sun's location, we note that the components toward (x) the galactic center and in the forward direction (y) are

$$v_x = V' \sin \theta, \qquad v_y = V' \cos \theta - V, \tag{4.28}$$

where θ is the difference in galactocentric longitude of sun and star. If r/R is sufficiently small, say <0.1 radian, $(r/R)^2$ may be neglected as compared with r/R. Since $\sin\theta \leq (r/R)$, the minimum value of $\cos\theta$ is $1 - \frac{1}{2}(r/R)^2$: i.e., $\cos\theta$ may be taken as 1.

Equations (4.28) may now be simplified by neglecting second order terms. In the first equation we substitute V for V', thereby neglecting $(\partial V/\partial R)\, dR \sin\theta$ (see 4.23). In the second equation we replace $\cos\theta$ by 1, thereby neglecting $\frac{1}{2}(r/R)^2 V'$. Hence

$$\begin{aligned} v_x &= V \sin\theta, \\ v_y &= V' - V. \end{aligned} \tag{4.29}$$

To a high approximation we may write

$$\sin\theta = \frac{r \sin l}{R}. \tag{4.30}$$

Equations (4.29) may be transformed by substituting (4.30) in the first equation, and (4.26) in the second equation, with the following result:

$$v_x = \frac{V}{R} r \sin l, \qquad v_y = -\frac{\partial V}{\partial R} r \cos l. \tag{4.31}$$

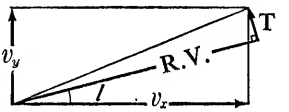

Fig. 4.8. *Radial and tangential components of differential galactic rotation.*

The radial and tangential components (counted positive in the direction of increasing l) of the differential rotational velocity are given by

$$R.V. = v_x \cos l + v_y \sin l, \qquad T = -v_x \sin l + v_y \cos l. \tag{4.32}$$

Substituting (4.30) in (4.31) gives

$$\begin{aligned} R.V. &= \left(\frac{V}{R} \sin l \cos l - \frac{\partial V}{\partial R} \sin l \cos l\right) r, \\ T &= \left(-\frac{V}{R} \sin^2 l - \frac{\partial V}{\partial R} \cos^2 l\right) r. \end{aligned} \tag{4.33}$$

7. Oort constants; solid and Keplerian rotation

The above relations may be reduced to

$$R.V. = Ar \sin 2l, \qquad T = Ar \cos 2l + Br, \tag{4.34}$$

where

$$A = \frac{1}{2}\left(\frac{V}{R} - \frac{\partial V}{\partial R}\right), \qquad B = \frac{1}{2}\left(-\frac{V}{R} - \frac{\partial V}{\partial R}\right), \tag{4.35}$$

are the so-called *Oort constants* of differential galactic rotation. In these formulae r and R are expressed in parsecs, V in km/sec. Hence A and B are expressed in km/sec/parsec. As mentioned before, the formulae are first approximations and hold for values of r that are small compared with R.

Note that

$$A - B = \frac{V}{R} = \omega, \tag{4.36}$$

where ω is the angular rotation in km/sec/parsec. Also

$$-(A + B) = \frac{\partial V}{\partial R}. \tag{4.37}$$

It is of interest to evaluate A and B for two special theoretical cases of rotation.

For a *solid rotation*

$$V = \omega R, \tag{4.38}$$

where ω is constant, hence

$$\frac{\partial V}{\partial R} = \omega \tag{4.39}$$

and

$$A = 0, \qquad B = -\frac{V}{R}, \tag{4.40}$$

i.e., there are no double periodic effects either in the radial or tangential velocities, only a constant rotation term in proper motion.

For a *Keplerian rotation*

$$V^2 = \frac{C}{R}, \tag{4.41}$$

where C is a constant, hence

$$2V \frac{\partial V}{\partial R} = -\frac{C}{R^2}$$

or

$$\frac{\partial V}{\partial R} = -\frac{1}{2}\frac{V}{R}, \tag{4.42}$$

and

$$A = \frac{3}{4}\frac{V}{R}, \qquad B = -\frac{1}{4}\frac{V}{R}, \tag{4.43}$$

and

$$A = -3B. \tag{4.44}$$

8. Effect on proper motions: general considerations

The tangential effect is normally studied as an angular yearly proper-motion effect, which is of particular interest in astrometric studies. To reduce (4.33) to angular measure we proceed as follows. We take into account that

$$1 \text{ km/sec} = \frac{1 \text{ a.u./year}}{4.74},$$

i.e., the second equation of (4.33) may be written as

$$T = r\left(\frac{A}{4.74}\cos 2l + \frac{B}{4.74}\right) \text{a.u./year.} \tag{4.45}$$

The value of 1 a.u. at a distance of r parsecs appears as the parallax of an angle $(1/r)''$. Hence (4.45) in angular measure becomes

$$\mu = \left(\frac{A}{4.74}\cos 2l + \frac{B}{4.74}\right) ''/\text{year}, \tag{4.46}$$

which is sometimes written as

$$\mu = P\cos 2l + Q, \tag{4.47}$$

where

$$P = \frac{A}{4.74}, \qquad Q = \frac{B}{4.74}. \tag{4.48}$$

For relatively small values of r the galactic rotation effects in proper motion are independent of the distance. On the other hand, the radial velocity effects increase with the distance. Radial velocities have, therefore, played an important role in confirming the existence of galactic rotation and have established accurate values of $A\bar{r}$ for groups of stars. A may then be obtained if $\bar{r}$ is known; any error in the value of $\bar{r}$ fully affects the resulting value of A. Although proper motion effects obviate this difficulty, systematic errors have severely limited the accuracy with which A and B can be found for proper motions.

The following value of A and B may be recorded here, as a consensus of numerous, but by no means final, studies:

$$A = +.015 \text{ km/sec/parsec} = +0''.0032 \text{ per year},$$
$$B = -.010 \text{ km/sec/parsec} = -0''.0021 \text{ per year}.$$

These figures indicate a state of motion intermediate between a solid and Kepler rotation. In these studies the sun's deviation from circular motion has been allowed for by including the solar motion terms (Section 3).

The same figures yield

$$\frac{V}{R} = A - B = +0.025 \text{ km/sec/parsec}.$$

For an assumed distance of 10,000 parsecs to the galactic center, V is found to be 250 km/sec in satisfactory agreement with results obtained from globular clusters, whose radial velocities may be assumed to reflect the galactic circular velocity at the sun's location.

Also

$$\frac{\partial V}{\partial R} = -(A + B) = -0.005 \text{ km/sec/parsec},$$

i.e., in our vicinity the circular velocity appears to decrease by 5 km/sec for an increase of 1,000 parsecs in the distance from the galactic center.

If it is desired to determine also the *direction* of the galactic center from proper motion or radial velocity data, $l - l_0$ should be substituted for l, where l is the longitude of the star, and l_0 that of the galactic center counted from an adopted zero point. In this case the relations (4.33) become

$$\begin{aligned} R.V. &= rA \sin 2(l - l_0) \\ &= rA \cos 2l_0 \sin 2l + rA \sin 2l_0 \cos 2l \end{aligned} \tag{4.49}$$

$$\begin{aligned} T &= r\{A \cos 2(l - l_0) + B\} \\ &= r\{A \cos 2l_0 \cos 2l + A \sin 2l_0 \sin 2l + B\} \end{aligned} \tag{4.50}$$

and 4.46 becomes

$$\begin{aligned} \mu &= P \cos 2(l - l_0) + Q \\ &= P \cos 2l_0 \cos 2l + P \sin 2l_0 \sin 2l + Q. \end{aligned} \tag{4.51}$$

At present the direction of the galactic center appears to be so well known from other sources that it is neither necessary nor desirable to introduce it as an unknown in the above expressions for galactic rotation.

In practice, values of A are determined from radial velocities and proper motions; values of B can be determined from proper motions only. In using measures of radial velocity, solar motion has first to be allowed for or included in a comprehensive solution. In using measures of proper motion, solar motion and precession have to be taken into account. In both cases the individual motions of stars act as "cosmic errors" and complicate matters further.

9. Dependence on galactic latitude

The above formulae hold in the galactic plane; they may be extended to any galactic latitude b. We assume the galactic rotation to depend only on the distance to an axis of rotation, through the galactic center, perpendicular to the galactic plane. In this case the quantity r in the expressions for the radial and tangential velocity components is replaced by $r \cos b$. The radial compo-

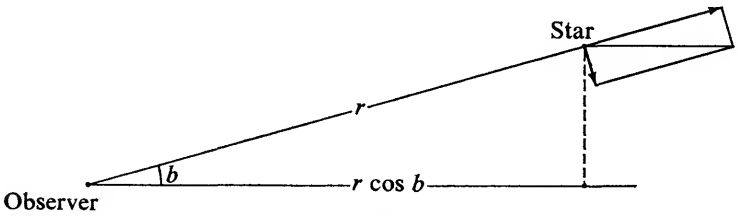

Fig. 4.9. *Effect of galactic latitude on components of galactic rotation.*

nent, to be understood as parallel to the galactic plane, now yields two components, one along the line of sight and one in galactic latitude. These components are obtained from the "radial" component by multiplying it by cos b and sin b, respectively.

We thus obtain the following effects:

Along the line of sight: $Ar \sin 2l \cos^2 b$ (4.52)

In proper motion in galactic longitude

(great circle): $P \cos 2l \cos b + Q \cos b$ (4.53)

In galactic latitude: $-\frac{P}{2} \sin 2l \sin 2b$ (4.54)

10. Galactic rotation terms in equatorial coordinates

The effects of differential galactic rotation in right ascension and declination are obtained by a rotation from the galactic to the equatorial coordinate system: i.e.,

Effect in right ascension (great circle):

$$P(\cos 2l \cos b \cos \phi + \tfrac{1}{2} \sin 2l \sin 2b \sin \phi) + Q \cos b \cos \phi,$$

Effect in declination: (4.55)

$$P(\cos 2l \cos b \sin \phi - \tfrac{1}{2} \sin 2l \sin 2b \cos \phi) + Q \cos b \sin \phi,$$

where ϕ is the "parallactic" angle counted from the galactic latitude circle to the declination circle.

These equations have been used in a variety of forms. They may be written as

$$fP + hQ, \qquad gP + jQ, \tag{4.56}$$

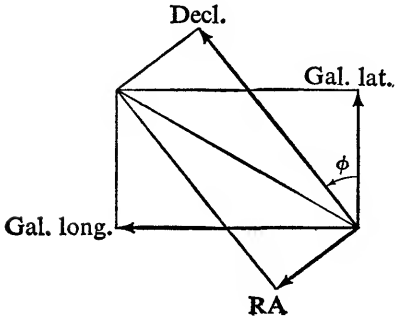

Fig. 4.10.
Relation between galactic and equatorial components of differential galactic rotation.

where

$$\begin{aligned} f &= \cos 2l \cos b \cos \phi + \tfrac{1}{2} \sin 2l \sin 2b \sin \phi, \\ g &= \cos 2l \cos b \sin \phi - \tfrac{1}{2} \sin 2l \sin 2b \cos \phi, \\ h &= \cos b \cos \phi, \\ j &= \cos b \sin \phi. \end{aligned} \tag{4.57}$$

The quantities f, g, h, j have been tabulated.[7]

C. ANALYSIS OF PROPER MOTIONS FOR PRECESSION, SOLAR MOTION AND GALACTIC ROTATION

It goes without saying that comprehensive analyses of proper motions for precession, solar motion, and galactic rotation will obliterate any systematic stellar motion that follows the same analytical law as the precession. Lunisolar and planetary precession imply a rotation of the stars about the pole of the ecliptic and the pole of the equator, respectively. Since equator and ecliptic are at an appreciable angle with the galactic circle, any rotation of the galactic system may thus be separated from the precessional effects.

If it is desired to analyze proper motions for precession, solar motion, and galactic rotation (and possible to do so) the following formulae may be used:

$$\begin{aligned} X \sin \alpha - Y \cos \alpha + \Delta k \cos \delta + \Delta n \sin \alpha \sin \delta + fP + hQ &= \mu_\alpha \cos \delta, \\ X \cos \alpha \sin \delta + Y \sin \alpha \sin \delta - Z \cos \delta + \Delta n \cos \alpha + gP + jQ &= \mu\delta, \end{aligned} \tag{4.58}$$

in which $\Delta k = \Delta m - \Delta e - \Delta l$ (Chapter 3, Section 3).

If material is homogeneous enough to warrant a constant $\left(\frac{\bar{h}}{r}\right)$ or a value that is a simple analytical function of the position on the sphere and does not conflict with the galactic rotation function, the various constants in the formulae can be derived if sufficient material is available. A least-squares solution will give the values for the following constants and combinations of constants,

From the right ascension equations: $X, Y, \Delta k, \Delta n, P, Q.$

From the declination equations: $X, Y, Z, \Delta n, P, Q.$

A combined solution would give all seven unknowns. However, separate solutions are desirable because of possible systematic errors in the proper motions that may affect the two coordinates quite differently.

[7] A. N. Vyssotsky and Emma T. R. Williams, *An Investigation of Stellar Motions, Together with Second McCormick Catalogue of Proper Motions* (Publications of the Leander McCormick Observatory, Vol. 10), University of Virginia, 1948. Appendix F gives a tabulation of the quantities f, g, h, and j.

Truly independent determinations of precessional corrections from stellar proper motions, differential galactic rotation, and solar motion should go always hand in hand. It is true that the constants P, A, and D can often be obtained from radial velocity observation, the first, however, not without considerable systematic uncertainty. The accuracy with which the various constants in the equations can be determined depends on (1) the number of objects, (2) their uniformity of distribution over the sky, (3) the cosmical accuracy of the proper motions, i.e., the accuracy with which an individual star or group of stars represents the hypothesis of precession, differential galactic rotation, and solar motion, (4) the observational accuracy of the proper motions. As far as precessional corrections, differential galactic rotation, and systematic errors in the fundamental system are concerned, objects of high cosmical accuracy are most useful, i.e., objects of small mean parallax.

The further analysis of Δk in terms of its component corrections is beyond the scope of this book, as are more sophisticated determinations of the unknowns in which the longitude of the galactic center is considered unknown and special attention is paid to possible systematic errors of a periodic nature in the proper motions.

A limitation is placed on any study of absolute proper motions by systematic errors in their reference system. Systematic errors of a periodic nature are most serious, as solar motion, precession, and galactic rotation contain first and second harmonics depending on right ascension and declination.

II

PLANE ASTROMETRY

5 Relation Between Sphere and Plane. Tilt and Refraction

Since the earliest days of astronomy stellar positions have been determined by measuring absolute right ascensions and declinations (Chapter 3, Section 1). This fundamental approach to spherical astrometry has been extended toward fainter stars by measuring positions on photographic plates. Wide-angle photographs yield plane coordinates, which are then reduced to spherical (equatorial) coordinates. The principles involved, but not the practical details, are discussed in this chapter.

Long-focus photographs are particularly suited for studying small areas of the sky—those, say, not extending beyond about 0.01 radian (0°.57). Such studies include the parallaxes and proper motions of single and multiple stars, which are best studied in the plane. However, the spherical approach is needed for long-range stellar paths, for astrometric studies of extended objects such as star clusters, and for relating the motions of widely separated objects.

The technique and reduction methods of plane long-focus astrometry are presented in Chapters 6 and 7, respectively.

1. Standard coordinates

Because we are primarily concerned with the portrayal of a portion of the celestial sphere on an *image plane* registered by a photographic plate, we shall briefly survey the general relationships between spherical coordinates and the corresponding coordinates on a plane tangent to the sphere.[1] We shall consider portrayal by an ideal objective, free from errors, which would result in a central (sometimes called gnomonic) projection from the optical center of the objective on the tangential plane. The plane *tangential* (also called *standard*

[1] Arthur König, "Astrometry with Astrographs", *in* W. A. Hiltner, ed., *Astronomical Techniques* (Stars and Stellar Systems, Vol. II). University of Chicago Press, 1962, pp. 461–486.

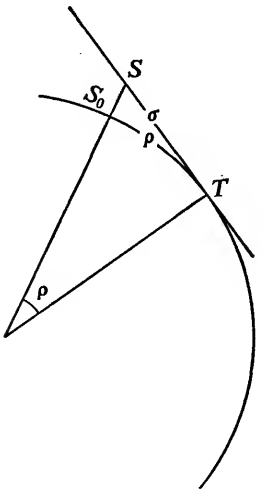

Fig. 5.1. *Plane coordinates. Cross section of sphere and plane. T = tangential point; S = central projection on plane of star S_0 on sphere.*

or *ideal*) coordinate system is defined as lying in the plane tangent to the sphere, the tangent point T being the origin of coordinates, with right ascension α_0 and declination δ_0 (Fig. 5.1).

The axis y is tangent to the hour circle through T, and its positive direction is the direction in which the distance of T to the celestial north pole is $<180°$. The axis x is perpendicular to the y-axis, and is counted positive in the direction of increasing right ascension (Fig. 5.2).

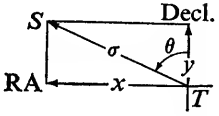

Fig. 5.2.
Tangential or standard coordinate system, as seen from inside of celestial sphere.

A point S_0 on the celestial sphere or on its image—the sphere whose radius equals the focal length of the telescope—corresponds, therefore, to the plane rectangular coordinates x and y of a point S, that point being the central projection of S_0 on the tangential plane or on its image, the photographic plate, which is assumed to be parallel to the tangential plane. We shall refer to these plane coordinates by their most commonly used designation, *standard coordinates*.

The unit of length is the radius of the celestial sphere or that of its image—the focal length. This keeps the formulae simple. When, later, we wish to introduce the focal length F, expressed in millimeters, the pure numbers x and y change to xF and yF, expressed in millimeters.

2. Relation between standard and equatorial coordinates

The linear distance σ on the plate corresponding to the spherical distance ρ from star to tangential point, is given by

$$\sigma = \tan \rho. \tag{5.1}$$

Hence the third order difference between the plane and the spherical distance amounts to $\rho^3/3$. In most long-focus work ρ rarely exceeds 0.005 radian, or 17′, and the above maximum value of difference proves to be less than 0″.01. Often ρ is rather less, and the above third order difference may be neglected. For extended fields, however, appropriate conversions are required, which we shall now derive.

Let α, δ and α_0, δ_0 be the right ascension and declination of star and tangential point respectively. The general relation between the standard coordinates x, y and the equatorial coordinates $\Delta\alpha = \alpha - \alpha_0$ and $\Delta\delta = \delta - \delta_0$ of a star relative to the tangential point T are derived as follows. The rectangular components or standard coordinates are given by

$$x = \tan \rho \sin \theta, \tag{5.2}$$

$$y = \tan \rho \cos \theta, \tag{5.3}$$

where θ is the position angle of the segment ρ (or σ) (Fig. 5.2).

Apply the cosine, sine, and extended cosine rules to the spherical triangle STP, formed by star, tangential point, and celestial north pole (Fig. 5.3):

$$\cos \rho = \sin \delta \sin \delta_0 + \cos \delta \cos \delta_0 \cos \Delta\alpha, \tag{5.4}$$

$$\sin \rho \sin \theta = \cos \delta \sin \Delta\alpha, \tag{5.5}$$

$$\sin \rho \cos \theta = \sin \delta \cos \delta_0 - \cos \delta \sin \delta_0 \cos \Delta\alpha, \tag{5.6}$$

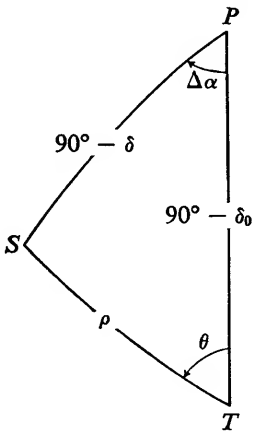

Fig. 5.3. *Spherical triangle formed by star S, tangential point T, and north pole P.*

from which, by dividing (5.5) and (5.6) by (5.4), respectively, and substituting in (5.2) and (5.3),

$$x = \frac{\cos\delta \sin\Delta\alpha}{\sin\delta \sin\delta_0 + \cos\delta \cos\delta_0 \cos\Delta\alpha}, \tag{5.7}$$

$$y = \frac{\sin\delta \cos\delta_0 - \cos\delta \sin\delta_0 \cos\Delta\alpha}{\sin\delta \sin\delta_0 + \cos\delta \cos\delta_0 \cos\Delta\alpha}. \tag{5.8}$$

3. Reduction from standard to equatorial coordinates

We shall now express $\Delta\alpha$ and δ in terms of x and y (and δ_0). Equation (5.8) may be written as

$$y(\sin\delta \sin\delta_0 + \cos\delta \cos\delta_0 \cos\Delta\alpha) = \sin\delta \cos\delta_0 - \cos\delta \sin\delta_0 \cos\Delta\alpha$$

or

$$\sin\delta\,(\cos\delta_0 - y \sin\delta_0) = \cos\delta\,(y \cos\delta_0 + \sin\delta_0) \cos\Delta\alpha,$$

whence

$$\tan\delta = \frac{\sin\delta_0 + y \cos\delta_0}{\cos\delta_0 - y \sin\delta_0} \cos\Delta\alpha. \tag{5.9}$$

The quantity $\Delta\alpha$ may be found by writing (5.7) as

$$\sin\Delta\alpha = \frac{x}{\cos\delta}(\sin\delta \sin\delta_0 + \cos\delta \cos\delta_0 \cos\Delta\alpha)$$

$$= x(\tan\delta \sin\delta_0 + \cos\delta_0 \cos\Delta\alpha)$$

or (see 5.9), since

$$\cos\Delta\alpha = \tan\delta \frac{\cos\delta_0 - y \sin\delta_0}{\sin\delta_0 + y \cos\delta_0}, \tag{5.10}$$

we find

$$\sin\Delta\alpha = x\left\{\tan\delta \sin\delta_0 + \tan\delta \cos\delta_0 \frac{\cos\delta_0 - y \sin\delta_0}{\sin\delta_0 + y \cos\delta_0}\right\}$$

$$= x \tan\delta \frac{\sin^2\delta_0 + y \sin\delta_0 \cos\delta_0 + \cos^2\delta_0 - y \sin\delta_0 \cos\delta_0}{\sin\delta_0 + y \cos\delta_0},$$

whence

$$\sin\Delta\alpha = \frac{x \tan\delta}{\sin\delta_0 + y \cos\delta_0}. \tag{5.11}$$

Also, by dividing (5.11) by (5.10)

$$\tan\Delta\alpha = \frac{x}{\cos\delta_0 - y \sin\delta_0}. \tag{5.12}$$

For small values of $\Delta\alpha$, another rigorous form of equation (5.9), which does not contain $\Delta\alpha$, may be preferred. Squaring (5.10) and (5.11) and adding, yields

$$1 = \frac{\tan^2 \delta}{(\sin \delta_0 + y \cos \delta_0)^2} \{x^2 + (\cos \delta_0 - y \sin \delta_0)^2\}$$

or

$$\cot^2 \delta = \frac{x^2 + (\cos \delta_0 - y \sin \delta_0)^2}{(\sin \delta_0 + y \cos \delta_0)^2}.$$

Now

$$\sin^2 \delta = \frac{1}{1 + \cos^2 \delta},$$

hence

$$\sin^2 \delta = \frac{1}{1 + \dfrac{x^2 + (\cos \delta_0 - y \sin \delta_0)^2}{(\sin \delta_0 + y \cos \delta_0)^2}}$$

or

$$\sin^2 \delta = \frac{(\sin \delta_0 + y \cos \delta_0)^2}{(\sin \delta_0 + y \cos \delta_0)^2 + x^2 + (\cos \delta - y \sin \delta)^2},$$

which reduces to

$$\sin^2 \delta = \frac{(\sin \delta_0 + y \cos \delta_0)^2}{1 + x^2 + y^2}.$$

Hence

$$\sin \delta = \frac{\sin \delta_0 + y \cos \delta_0}{\sqrt{1 + x^2 + y^2}}. \tag{5.13}$$

Formulae (5.12) or (5.11) and (5.9) or (5.13) are therefore suitable for reducing standard coordinates to equatorial coordinates. In practice, an approximate tangential point, defined, say, by a star or group of stars, may be substituted for the true tangential point; the error thus introduced is normally negligible, representing a minute tilt effect (Section 6).

4. Series developments for reduction from equatorial to standard coordinates and vice versa

Formulae (5.7) and (5.8) may be developed into series whose first and second order terms are easily derived.

For small values of $\Delta\alpha$, replacement of $\cos \Delta\alpha$ by 1 yields denominators of 1.

For the small numerators we replace $\sin \Delta\alpha$ by $\Delta\alpha$ and (5.7) becomes

$$x = \Delta\alpha \cos \delta = \Delta\alpha \cos (\delta_0 + \Delta\delta),$$

which for small values of $\Delta\delta$ may be written as

$$x = \Delta\alpha(\cos \delta_0 - \Delta\delta \sin \delta_0).$$

Hence

$$x = \Delta\alpha \cos \delta_0 - \Delta\alpha \, \Delta\delta \sin \delta_0. \tag{5.14}$$

Similarly we write (5.8) as follows;

$$y = \sin(\delta - \delta_0) + (1 - \cos \Delta\alpha) \cos \delta \sin \delta_0$$

or to a high degree of approximation,

$$y = \Delta\delta + \tfrac{1}{4}(\Delta\alpha)^2 \sin 2\delta_0. \tag{5.15}$$

The reverse expressions, up to and including quadratic terms, are also easily found. We write (5.14) as follows:

$$\Delta\alpha \cos \delta_0 = x + \Delta\alpha\, \Delta\delta \sin \delta_0$$

or

$$\Delta\alpha = x \sec \delta_0 + \Delta\alpha\, \Delta\delta \tan \delta_0.$$

The quantities $\Delta\alpha$ and $\Delta\delta$ on the right hand side of these equations, may, to a high degree of approximation, be replaced by $x \sec \delta_0$ and y, and we find

$$\Delta\alpha = x \sec \delta_0 + xy \sec \delta_0 \tan \delta_0. \tag{5.16}$$

Similarly, by writing (5.15) as

$$\Delta\delta = y - \tfrac{1}{4}(\Delta\alpha)^2 \sin 2\delta_0$$

and replacing $\Delta\alpha$ by $x \sec \delta_0$, we find

$$\Delta\delta = y - \frac{x^2}{2} \frac{\sin \delta_0 \cos \delta_0}{\cos^2 \delta_0}$$

or

$$\Delta\delta = y - \frac{x^2}{2} \tan \delta_0. \tag{5.17}$$

Formulae (5.16) and (5.17) are useful in calculations concerning the positions of asteroids and comets (Chapter 7, Section 9).

For more accurate computational purposes formulae (5.7) and (5.8) may be transformed to:

$$\begin{aligned} x &= \Delta\alpha \cos \delta_0 - \Delta\alpha\, \Delta\delta \sin \delta_0 + \tfrac{1}{6}(\Delta\alpha)^3 \cos \delta_0 (3 \cos^2 \delta_0 - 1) + \ldots, \\ y &= \Delta\delta + \tfrac{1}{4}(\Delta\alpha)^2 \sin 2\delta_0 + \tfrac{1}{2}(\Delta\alpha)^2\, \Delta\delta \cos 2\delta_0 + \tfrac{1}{3}(\Delta\delta)^3 + \ldots, \end{aligned} \tag{5.18}$$

and conversely,

$$\begin{aligned} \Delta\alpha &= x \sec \delta_0 + xy \sec \delta_0 \tan \delta_0 - \tfrac{1}{3}x^3 \sec^3 \delta_0 + xy^2 \sec^2 \delta_0 \tan^2 \delta_0 + \ldots, \\ \Delta\delta &= y - \tfrac{1}{2}x^2 \tan \delta_0 - \tfrac{1}{2}x^2 y \sec^2 \delta_0 - \tfrac{1}{3}y^3 + \ldots. \end{aligned} \tag{5.19}$$

Another formulation is the following:

$$\begin{aligned} x &= \Delta\alpha \cos \delta + \tfrac{1}{6}(\Delta\alpha)^3 \cos \delta (3 \cos^2 \delta - 1) + \tfrac{1}{2}\Delta\alpha(\Delta\delta)^2 \cos \delta + \ldots, \\ y &= \Delta\delta + \tfrac{1}{4}(\Delta\alpha)^2 \sin 2\delta + \tfrac{1}{3}(\Delta\delta)^3 + \ldots, \end{aligned} \tag{5.20}$$

and conversely,

$$\begin{aligned} \Delta\alpha &= x \sec \delta - \tfrac{1}{6}x^3 \sec \delta (\sec^2 \delta - 3) - \tfrac{1}{2}xy^2 \sec \delta - \ldots, \\ \Delta\delta &= y - \tfrac{1}{2}x^2 \tan \delta - \tfrac{1}{3}y^3 \ldots. \end{aligned} \tag{5.21}$$

Formulae (5.18)–(5.21) are given here without proof.

5. Effect of plate tilt

To evaluate the effects of plate tilt, which result when the plane photographic plate is not quite perpendicular to the optical axis of the objective, we first introduce the so-called base, or "optical center," T' of the plate, i.e., the point at which a perpendicular from the center of the objective falls on the plate.[2] For a tilt τ the optical center T' of the plate is at a distance τ from the ideal origin of the standard coordinates, i.e., from the tangential point, T, since the radius of the circle (i.e., the focal length) is taken as unity.

The point S is now portrayed as a point S'. We shall now evaluate the effect of the plate tilt τ on the standard coordinates of S, referred to T. Let σ and σ' be the distances from S and S' to the line of intersection of the ideal and the actual tangential plane as measured on the ideal and actual planes, respectively.

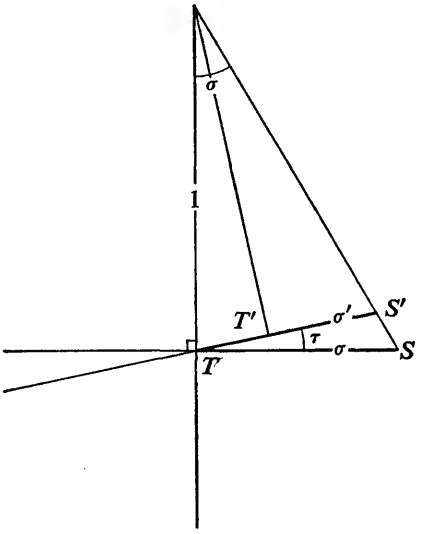

Fig. 5.4. *Effect of plate tilt τ on measured position S', compared with ideal position S.*

It is seen from Figure 5.4 that

$$\frac{\sigma}{\sigma'} = \frac{\sin(90^\circ + \sigma - \tau)}{\sin(90^\circ - \sigma)} \tag{5.22}$$

or

$$\frac{\sigma}{\sigma'} = \frac{\cos(\tau - \sigma)}{\cos\sigma} = \cos\tau + \sin\tau\tan\sigma.$$

[2] F. Schlesinger, *The Trigonometrical Parallaxes of 851 Stars*, (Transaction of the Astronomical Observatory of Yale University, Vol. 8.) New Haven, 1936. "Introduction," pp. (3)–(14).

If τ and σ are small, we have

$$\frac{\sigma}{\sigma'} = 1 + \tau\sigma$$

or

$$\frac{\sigma'}{\sigma} = 1 - \tau\sigma$$

whence

$$\sigma - \sigma' = \tau\sigma^2. \tag{5.23}$$

Hence the correction for tilt to be applied to the measured distance perpendicular to the intersection of ideal and actual plane is the product of the square of this distance and the tilt. Since τ is small, the coefficients σ may be considered identical with σ' on the right side of equation (5.23), and also in subsequent relations in this section.

To obtain the effect on the standard coordinates, we proceed as follows. Let β be the position angle of the point S' at a distance σ' from the tangential point T (Fig. 5.5). The "optical center" of the plate T' has a distance τ from

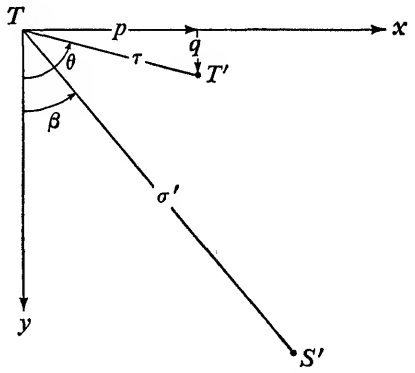

Fig. 5.5. *Relation between position S′ and optical center T′ of plate.*

the tangential point in position angle θ. The rectangular coordinate of T' and of S' are p, q and x, y, respectively: i.e.,

$$p = \tau \sin\theta, \qquad q = \tau \cos\theta, \tag{5.24}$$

and

$$x = \sigma \sin\beta, \qquad y = \sigma \cos\beta, \tag{5.25}$$

replacing σ' by σ.

The tilt between the segment σ and the corresponding segment σ' on the plate is reduced to $\tau \cos(\theta - \beta)$ as is easily seen from the spherical triangle

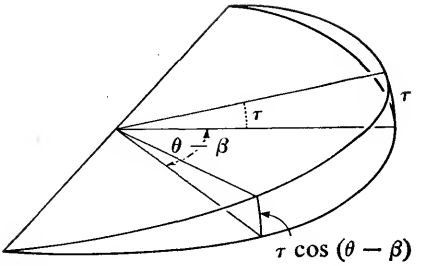

Fig. 5.6. *Tilt effect for position at an angle of* $(\theta - \beta)$ *from optical center of plate.*

(Fig. 5.6, also Fig. 1.6). Hence the tilt correction along the radius vector σ', amounts to

$$\tau\sigma^2 \cos(\theta - \beta) = \tau\sigma^2(\sin\theta \sin\beta + \cos\theta \cos\beta)$$

or, after substituting (5.24) and (5.25),

$$\sigma(px + qy). \tag{5.26}$$

The x and y components of the total tilt correction are given by multiplying the total correction by $\sin\beta = x/\sigma$ and $\cos\beta = y/\sigma$, respectively:

$$\begin{aligned} &\text{Tilt effect in } x: \quad px^2 + qxy, \\ &\text{Tilt effect in } y: \quad pxy + qy^2. \end{aligned} \tag{5.27}$$

6. Effect of refraction

We shall now turn to the effect of refraction on a limited area of the sky, such as is portrayed on a photographic plate. In particular, we shall study the change of refraction with zenith distance and its effect on the determination of stellar positions. Assuming the simple tangent relation we have

$$r = R \tan\zeta \tag{2.22}$$

and

$$r + \Delta r = R \tan(\zeta + \Delta\zeta).$$

Note that

$$\frac{d \tan\zeta}{d\zeta} = 1 + \tan^2\zeta,$$

$$\frac{d^2 \tan\zeta}{d\zeta^2} = 2 \tan\zeta(1 + \tan^2\zeta) = 2 \tan\zeta + 2 \tan^3\zeta,$$

$$\begin{aligned} \frac{d^3 \tan\zeta}{d\zeta^3} &= 2(1 + \tan^2\zeta) + 6 \tan^2\zeta(1 + \tan^2\zeta) \\ &= 2 + 8 \tan^2\zeta + 6 \tan^4\zeta. \end{aligned} \tag{5.28}$$

Hence, using the Taylor series development,

$$\frac{\Delta r}{R} = \Delta\zeta(1 + \tan^2\zeta) + (\Delta\zeta)^2(\tan\zeta + \tan^2\zeta) + \Delta\zeta^3\left(\frac{1}{3} + \frac{4}{3}\tan^2\zeta + \tan^4\zeta\right) + \cdots$$

or

$$\frac{\Delta r}{\Delta\zeta} = R\left[(1 + \tan^2\zeta) + \Delta\zeta(\tan\zeta + \tan^2\zeta) + \Delta\zeta^2\left(\frac{1}{3} + \frac{4}{3}\tan^2\zeta + \tan^4\zeta\right) + \right]. \quad (5.29)$$

The principal term in the change of refraction with zenith distance yields a contraction $R(1 + \tan^2\zeta)$. We shall discuss this term later for the case of small fields (Chapter 6, Section 2). Meanwhile, to obtain a general idea about the effect of changing refraction with altitude, let us limit ourselves to observations within 45° from the zenith, and calculate the maximum effect for $\zeta = 45°$ for which $\tan\zeta = 1$. We then have

$$\frac{\Delta r}{\Delta\zeta} = R\left(2 + 2\Delta\zeta + \frac{8}{3}\Delta\zeta^2 + \cdots\right). \quad (5.30)$$

The principal term amounts to $2R = 0.00058$, corresponding to a uniform contraction in ζ amounting to one part in about 1,700.

The second term amounts to $2R\Delta\zeta$, a further contraction, which increases with the zenith distance. This term represents the quadratic effect of the refraction or the zenith distance. For a $\Delta\zeta$ of 0.1 radian (5°.7) it amounts to 0.000058 radians, or 1″.2, leading to a maximum deviation from linearity of 0.0000145 radians, or 0″.3.

The third term amounts to

$$\tfrac{8}{3}R\Delta\zeta^2.$$

For a $\Delta\zeta$ of 0.1 radian (5°.7) this effect amounts to 0.0000078 radians, or 0″.16.

For extended areas of the sky, photographed with a wide-angle camera, the nonlinear effects of refraction must be taken into account. The effect of refraction over wide-angle plate areas of the sky has been studied, for example, by Schlesinger and Barney.[3] For small areas, the nonlinear effects may generally be ignored (Chapter 7).

7. Effect of aberration

The maximum value of the effect of aberration is a simple harmonic term of the form 20″.49 sin θ, the value of θ depending on the relative position of star

[3] Frank Schlesinger and Ida Barney, *Catalogue of the Positions and Proper Motions of 10,358 Stars*, (Transactions of the Astronomical Observatory of Yale University, Vol. 9.) New Haven, 1933. "Introduction", pp. (3)–(35).

and sun. For any other location $\Delta + \theta\Delta$, the aberration is $20''.49 \sin(\theta + \Delta\theta)$. The change of aberration with θ may be written as

$$20''.49 \left\{ \Delta\theta \cos\theta - \frac{(\Delta\theta)^2}{2} \sin\theta - \frac{(\Delta\theta)^3}{6} \cos\theta + \cdots \right\}. \tag{5.31}$$

The first term represents a scale effect whose maximum value amounts to 0.0001. Again we are interested in the nonlinear parts of the expression only. Limiting ourselves to the quadratic term, we see that maximum effect is given by $-10''.2(\Delta\theta)^2$. For $\Delta\theta = 0.01$, the maximum quadratic effect is $0''.001$ and the corresponding maximum deviation from linearity over the range $\Delta\theta = 0.01$ would be $0''.00025$, a completely negligible quantity. For $\Delta\theta = 0.1$, the maximum quadratic effect is $0''.1$, and may have to be allowed for. In neither case would it be necessary to take into account the cubic term.

Optical distortion also plays a role in the determination of stellar positions, but the study and application of its effects are beyond the scope of an introductory treatise.

Magnitude and spectral type affect the position of the photographic image. Their effects are of two kinds, (1) the unavoidable spectral elongation due to residual atmospheric dispersion, and (2) elongation due to imperfect collimations in the optical system. Less serious is the effect of differences in scale for stars of different magnitude and spectra, although these effects should, if possible, be taken into account in a number of high-precision problems.

[4] W. Dieckvoss, "Precise Photographic Measurement of Star Positions," *Sky and Telescope*, 24 (1962): 198–202.

6 Long-Focus Photographic Astrometry: Technique

In several long-focus problems the material consists of photographic plates on which the position of the star in which we are interested—the "central" star—is referred to a "background" of three or more reference stars. The classic example is the parallax work done with the largest existing refractor (focal length 19.37 meters, aperture 102 cm) at the Yerkes Observatory near the beginning of the century. The necessary techniques of observing, measuring, and calculating were developed by Frank Schlesinger, who succeeded in obtaining parallaxes with an accuracy not achieved before.[1] His methods of long-focus photographic astrometry are basic and complete; only minor improvements remained possible.

There is also the study of the relative positions of the components of double stars, first developed by Hertzsprung.[2] Both Schlesinger and Hertzsprung had visual refractors; they used panchromatic emulsions and a yellow filter (thus eliminating the blue light) to obtain sharp images in the color for which the objective was corrected.

This chapter deals with a description of the long-focus photographic technique.

1. The long-focus refractor; focal ratio, scale value, refraction

The long-focus refractor normally has a focal ratio between $f = 15$ and $f = 20$. The achromatic objective usually consists of a convex crown-glass

[1] Frank Schlesinger, *Probleme der Astronomie* (Seeliger Festschrift) Berlin, Springer Verlag, 1924, pp. 422–437; and his "Photographic Determinations of Stellar Parallax Made with the Yerkes Refractor: I [and] II," *The Astrophysical Journal*, 32 (1910): 372–387; 33 (1911): 8–27.

[2] E. Hertzsprung, *Photographische Messungen von Doppelsternen von 1914.0 bis 1919.4.* (Publikationen des Astrophysikalischen Observatoriums zu Potsdam, Vol. 24, No. 75), Potsdam, 1920.

Table 6.1. SPECIFICATIONS OF 24-INCH OBJECTIVE OF SPROUL VISUAL REFRACTOR

Component	Radii of Curvature*	Thickness and Spacing
Front lens (flint)	+284.20 inches +101.82 inches	Central thickness: 1.33 inches Spacing between lenses: 0.005 inch
Rear lens (crown)	+101.82 inches −457.15 inches	Central thickness: 1.85 inches

* + = convex toward source; − = concave toward source.

Wave Length	Refractive Indices	
	Crown	Flint
C	1.510484	1.605533
λ 5614	1.514290	1.612663
F	1.518980	1.621876
G	1.524140	G′ 1.631756
h	1.526685	1.637993

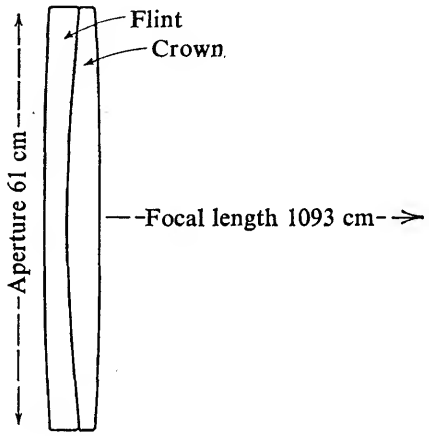

Fig. 6.1. *Diagram of Sproul 24-inch objective.*

lens and a concave flint-glass lens, which may be very close together or separated by as much as several centimeters. See, for example, the specifications for the objective of the Sproul refractor, as given in Table 6.1. The aperture of the Sproul refractor is 24 inches (61 cm), the focal length 36 feet (1,093 cm), and the focal ratio $f = 18$ (Fig. 6.1).

The scale value in the focal plane is defined as the number of seconds of arc per millimeter; for a focal length of F mm, the scale value is $206{,}265/F$ seconds of arc/mm. For the Sproul refractor the scale value is 1 mm = 18″.87, or 0.053 mm for 1 second of arc. To illustrate this, the focal image of the moon is nearly 4 inches across and fills the greater part of the useful field portrayed on the photographic plates of 5 × 7 inches (13 × 18 cm).

A more precise definition of scale value involves atmospheric refraction. As shown in Chapter 2, Section 6, at moderate zenith distances the atmos-

pheric refraction at zenith distance ζ may be represented to a high degree of approximation by the formula

$$R \tan \zeta, \qquad (2.22)$$

where R, the atmospheric refraction at $\zeta = 45°$, is the refraction constant.

Because of atmospheric refraction, any vertical angular distance suffers a minute contraction, whose first-order term is represented by the factor $R(1 + \tan^2 \zeta)$ (Chapter 5, Section 6); any horizontal distance, measured along the great circle, suffers a contraction R. For a wide range in wavelength in the visual spectrum, R is close to 60″; hence the scale reduction in the zenith amounts to a factor 0.00029 (0.029%). The scale value in use for various telescopes refers to the zenith and includes the factor 0.00029, to allow for the contraction caused by refraction. Relative to the zenith, there is no additional first-order horizontal scale reduction, while the additional vertical reduction due to refraction is given by the term $R \tan^2 \zeta$, which is tabulated in Table 6.2, together with its effect on the Sproul scale value.

Table 6.2. ADDITIONAL SCALE REDUCTION FOR SPROUL REFRACTOR

ζ	Additional Vertical Scale Reduction	Addition to Sproul Vertical Scale Value	ζ	Additional Vertical Scale Reduction	Addition to Sproul Vertical Scale Value
0°	0.00000	0″.0000	40°	0.00020	0″.0038
10	.00001	″.0002	50	.00041	″.0077
20	.00004	″.0008	60	0.00087	0″.0164
30	0.00010	0″.0019			

In practice, the scale value may refer to the pitch (revolution) of the screw of a measuring engine; this pitch is generally very close to 1 mm or a simple fraction thereof (Section 6). For example, the scale values at the zenith for the Sproul refractor are 18″.8733 for the Gaertner long-screw measuring machine and 18″.8723 for the St. Clair–Kasten long-screw measuring machine in use at the Sproul Observatory.[3] These values vary slightly with the focal setting of the telescope and the observing temperature. Except in special problems, or at unusually large zenith distances, differential refraction is neglected and the rounded-off scale value 18″.87 is used.

2. Coma; Rayleigh's criterion

Limitations of attainable positional accuracy in extended star fields are to a great extent due to optical field errors, which may vary with the temperature.

[3] K. Aa. Strand, "Photographic Observations of Double Stars Made with the 24-inch Sproul Refractor," *The Astronomical Journal*, 52 (1946): 3, 1946.

The principal off-axis aberration of many existing long-focus objectives is coma, which results both in scale and magnitude effects on the image-plane.[4] If one uses rectangular coordinates in the image plane, the intersection of any ray differs from the ideal point $(0, y_0)$ by quantities Δx and Δy, which are

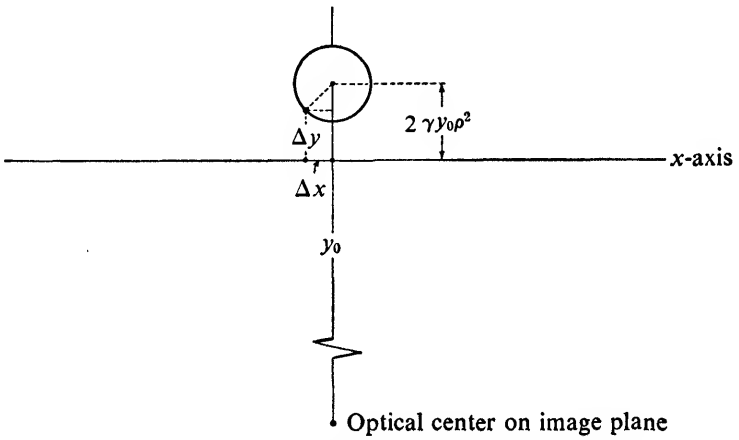

Fig. 6.2. *Coma as function of polar coordinates ρ and θ of lens element. Radius of comatic circle is $\gamma y_0\rho^2$.*

functions of ρ and θ, the polar coordinates of the point in the objective through which the ray passes. The coma is given by

$$\Delta x = \gamma y_0\rho^2 \sin 2\theta, \qquad \Delta y = \gamma y_0\rho^2(2 + \cos 2\theta); \tag{6.1}$$

that is, the rays passing through a zone of the objective of radius ρ intersect the image plane in a circle of radius $\gamma y_0\rho^2$, whose center is at a distance $2\gamma y_0\rho^2$ from the ideal image point $(0, y_0)$. Hence the "flare" due to coma varies linearly with the distance from the optical center and with the square of the diameter of the largest zone of the objective through which the light is allowed to pass. To obtain highest optical quality, therefore, from an objective that has coma error, it may be necessary to limit the size of the field, and a reduction of the aperture may prove even more effective. A comparison of plates of the star cluster NGC 1039 taken on one night with the Sproul refractor at full (61 cm) and at reduced (30.5 cm) aperture shows strikingly improved images, off-center, for the smaller aperture, accompanied by a scale reduction of 0.0005. Plates taken through a coarse-wire objective grating (Chapter 10, Section 3) show a magnitude-coma scale effect of -0.00008 ± 0.00001 (p.e.)

[4] John Strong, *Concepts of Classical Optics*, San Francisco and London, W. H. Freeman and Company, 1958.

for an increase of one magnitude at full aperture, and -0.000015 ± 0.00001 at 30.5-cm aperture.[5]

Possible sources of systematic error are improper or changing collimation and focus. Maladjustment of focus results in displacements relative to the optical axis, the size of the displacements depending on the distance of the plate from the focal plane, the distance of the star from the optical axis, and the brightness of the star. Plates taken with the Yerkes refractor,[6] showed a shift of 0".01 for each millimeter that the plate was outside the focal plane, for a difference of one magnitude at a distance of 11′ from the optical axis. The displacement was such that the brighter of two stars was shifted toward the optical axis, relative to the fainter star, on either side of the focal plane. Since plates with extreme positive and negative parallax factors in right ascension (Chapter 8) are taken at dusk and dawn respectively, systematic differences in focus may easily occur if the same focal setting is used throughout any one night, or if only partial adjustment is made, say at midnight. The possible effect on such sensitive data as stellar parallax could be serious.

The dome can heat up quite appreciably on a hot day, and, if no proper ventilation is provided, one must expect, on opening the dome, a very important temperature gradient for an hour or so after sunset. Good ventilation should be considered a prerequisite for good seeing: not only ventilation between the inside of the dome and the outside, but also between the inside of the telescope tube and its surroundings. At Sproul Observatory the two armholes just below the objective cell are opened in the daytime, and three ventilating fans installed in the windows of the dome are operated when needed. In the daytime the telescope is kept in a horizontal position, to avoid the extremes of temperature within the dome.[7]

According to Rayleigh an optical instrument may be considered perfect if the difference between the longest and the shortest optical paths at the focus does not exceed one quarter of a wavelength. It can be shown that such an optical system will tolerate a limited range of focal adjustment. All images (visual or photographic) obtained within $4f^2\lambda$ of the focus of a theoretically perfect objective are equally good. In this expression λ is the wavelength that corresponds to the minimum focal length, and f is the focal ratio. Generally, for long-focus refractors, Rayleigh's limit is between 0.5 and 0.7 mm; for the Sproul refractor ($f = 18$) it is 0.7 mm.

It is important to keep the optical performance of the telescope as constant as possible. The remounting of an objective may lead to a systematic error of the nature of a color equation. Any slight lateral maladjustment of the lens

[5] Philip A. Ianna, "On Aberrations and Field Errors," *Vistas in Astronomy*, 6 (1965): 93–123.

[6] See footnote 1, p. 85.

[7] Sarah Lee Lippincott, "Observations of Seeing," *Vistas in Astronomy*, 6 (1965): 125–129.

has its effect on the position of the stars as a function of the color. At Sproul Observatory the lens was taken out of its cell in 1941, because of maladjustment, and again in 1949, when the old aluminum cell was replaced with a fine-grain cast-iron cell.

It has been established that plates taken over the interval 1937–1941 are subject to a color equation in the sense that over this interval the position of an M0-star was displaced $+''.046 \pm ''.005$ in the direction of right ascension relative to that of an A0 star. A very much smaller color equation was introduced in 1949, negligible for all practical purposes.[8]

3. Photographic technique: magnitude compensation, atmospheric dispersion

Guiding the telescope is accomplished by using a double-slide plate carrier, permitting an accurate slow motion of the plateholder. Residual guiding error is minimized by aiming at magnitude compensation. In positional studies of a central star referred to a limited number of fainter background stars, this may be accomplished by reducing the brightness of a central star by means of a small rotating sector in front of the plate. The Sproul Observatory has a set of 43 sectors, with extinctions ranging in steps very close to 0.2 mag. up to 8.3 mag. Sector openings of less than about 2.5 percent (extinction 4 stellar mag.) lead to a slight increase in positional error and should generally be avoided. Coarse diffraction gratings, in front of the objective, may be used to provide faint companion images, symmetrically placed on each side of the star images (Chapter 10, Section 3). Both sectors and gratings play an important role in reducing differences in the apparent sizes of star images, with a resulting increase in the ultimate accuracy of measurement.

Except at the zenith, each star appears as a spectrum whose blue end is closer to the zenith than is the red end. For stars of different spectral types

Table 6.3. ATMOSPHERIC REFRACTION AND DISPERSION

λ	R	Dispersion per 100 Å	λ	R	Dispersion per 100 Å
4000 Å	61″.34	−0″.108	6500 Å	60″.06	−0″.021
4500	60″.89	− ″.072	7000	59″.96	− ″.017
5000	60″.58	− ″.050	7500	59″.89	− ″.014
5500	60″.33	− ″.037	8000	59″.83	−0″.011
6000	60″.19	−0″.028			

[8] Sarah Lee Lippincott, "Accuracy of Positions and Parallaxes Determined with the Sproul 24-inch Refractor," *The Astronomical Journal*, 62 (1957): 55–69.

the energy distribution is different; moreover, the spectra differ in brightness. For positional work, the spectral range should be reduced, in order to have as nearly monochromatic images as possible. The approach to monochromatism is obtained by the triple combination of objective, emulsion, and filter. Sharp, round star images are obtained as long as the effective radiation is within Rayleigh's criterion for focal accuracy.

Color effects are due primarily to dispersion in our atmosphere, but imperfect collimation of the objective may contribute its share also. The refraction constant R and its dispersion per 100 Å are tabulated in Table 6.3.

4. Photovisual technique: focal curve, emulsion, and filter; Bergstrand effect

Proper choice of emulsion and filter keeps the range of light close to the wavelength corresponding to the minimum focal length of the focal curve (also called color-curve, achromatization-curve, or secondary spectrum) of the objective. The photographic position still depends on the residual energy distribution of the star's spectrum, as filtered by the objective (transparency and focal curve), filter, and emulsion. The effective wavelengths of the star images depend on the spectrum and, to some extent, on the magnitude; however, with proper choice of filter and emulsion, this dependence may be reduced to a minimum.

The rapid decrease in atmospheric dispersion toward longer wavelengths gives an advantage to the photographic technique as applied with visual refractors—referred to as "photovisual technique." As an illustration, the Sproul visual refractor with its aperture of 61 cm has its minimum focal length of 1,093 cm for λ 5607. A minus-blue (No. 12) Wratten filter is used in contact with the 5 × 7-inch plate, eliminating practically all radiation on the blue side of approximately λ 5100. A suitable range of radiation is recorded by the photographic plate by using the Eastman G-type emulsion, for which the sensitivity is greatest at λ 5650 but extends hardly beyond λ 6000. Sharp images are obtained with effective wavelengths ranging only from about λ 5480 for a blue star of spectral type A to about λ 5525 for a red star of spectral type M. This corresponds to a small difference in refraction constant of $\Delta R = 0''.016$ at an altitude of 45°. The A star is comparatively that much closer to the zenith than the M star.

In addition, there is a delicate effect which was first noted by Bergstrand[9] for positions obtained on ordinary photographic emulsions: the photographic position for one and the same spectrum depends on the brightness. This is explained by the contribution of radiations of different colors to the formation

[9] O. Bergstrand, "Uber die Wirkung der Atmosphärischen Dispersion auf die Bestimmung der Jährlichen Parallaxen der Fixsterne," *Astronomische Nachrichten*, 167 (1905): 241–254.

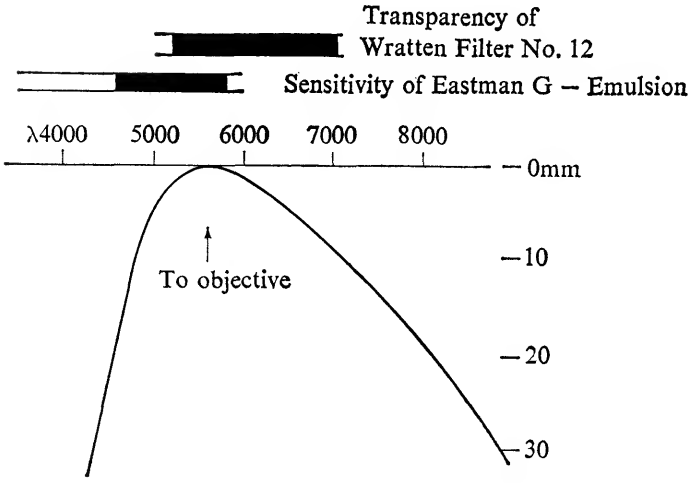

Fig. 6.3. *Focal curve of Sproul 24-inch objective.*

of the photographic star image. Generally, the distribution of these relative intensities is asymmetrical with respect to the wavelength. Initially, only a limited range of radiation is effective, but with increased exposure or brightness other radiations begin to contribute to the formation of the photographic image. For one and the same stellar spectrum the relative contribution of the different colors changes gradually with increasing exposure or brightness. The resulting change in effective wavelength or color depends on the character of the focal curve and selective absorption of the objective and on the type of emulsion and filter.

Observations with coarse gratings (Chapter 10) as well as theoretical studies have yielded effective wavelengths for well-exposed images obtained with the Sproul refractor, using different emulsions and filters (Table 6.4).

Table 6.4. SPROUL REFRACTOR EFFECTIVE WAVELENGTHS

Emulsion	Filter	Spectral Type			
		A		M	
		Obs.	Theor.	Obs.	Theor.
Eastman G	Wratten No. 12	λ 5482	λ 5508	λ 5525	λ 5552
Eastman C	Wratten No. 12	5767	5667	5844	5803
Eastman G	Wratten No. 8	—	5440	—	5522

Agreement between observation and theory is good for the G,12 combination, but indicates a systematic difference for C,12. The differences are not surprising in view of the various uncertainties, such as spectral energy distribution and formation of stellar images. There is fair agreement for the differences in effective wavelengths, and the corresponding differences in refraction constants (Table 6.5). There appears to be a slight change in the theoretically

Table 6.5. SPROUL REFRACTOR RELATIVE REFRACTION CONSTANTS

Emulsion	Filter	$\Delta\lambda$ (M − A)		ΔR (M − A)	
		Obs.	Theor.	Obs.	Theor.
Eastman G	Wratten No. 12	+43 Å	+ 44 Å	−″.016	−″.016
Eastman C	Wratten No. 12	+77	+136	−.024	−.043
Eastman G	Wratten No. 8	—	+ 82	—	−.030

determined effective wavelength with increasing brightness, but not enough to make the Bergstrand effect a matter of serious concern in the Sproul photovisual technique.

Although the values of $\Delta\lambda$ and ΔR for an extreme spectral range $M - A$, are comparatively small, constancy of technique, in terms of emulsion and filter, is obviously desirable, particularly in studying small displacements of stars.

5. Residual dispersion in right ascension and declination

Even with the best possible spectral compensation, small differences in effective wavelength are likely to remain. It is advisable to avoid any variation in this residual systematic error, such as would be caused by a large variation in hour angle. Let ΔR be the difference in refraction constant for a certain pair of wavelengths. Assuming the refraction and hence the dispersion to vary with $\tan \zeta$, the dispersion component in right ascension (see 2.25) is given by

$$\Delta R \sin t \cos \phi \sec \zeta, \tag{6.2}$$

where t is the hour angle and ϕ is the latitude; for observations near the meridian, the formula (see 2.28) may be written as

$$\Delta R t \cos \phi \sec (\phi - \delta). \tag{6.3}$$

Although for observations near the meridian the refraction and hence the dispersion in declination are practically constant, the component in right ascension depends strongly on the hour angle. For observations not exceeding an hour angle of 1 hour, the change in the dispersion effect in declination is

negligible. In right ascension the dispersion effect is very nearly proportional to the hour angle and changes signs at the meridian; an increase in altitude corresponds to a shift toward the meridian. For latitude 45° and $\Delta R = +0''.01$ (a decrease of 27 Å at λ 5500) the values are given in Tables 6.6 and 6.7.

Table 6.6. DISPERSION EFFECT IN RIGHT ASCENSION FOR $\Delta R = +0''.01$

Declination	Hour Angle				
	60^m E.	30^m E.	Meridian	30^m W.	60^m W.
−20°	−0″.0046	−0″.0022	0″.0000	+0″.0022	+0″.0046
0°	− ″.0027	− ″.0013	″.0000	+ ″.0013	+ ″.0027
+20°	− ″.0021	− ″.0010	″.0000	+ ″.0010	+ ″.0021
+40°	− ″.0019	− ″.0009	″.0000	+ ″.0009	+ ″.0019
+60°	−0″.0019	−0″.0009	0″.0000	+0″.0009	+0″.0019

Table 6.7. DISPERSION EFFECT IN DECLINATION FOR $\Delta R = +0''.01$

Declination	Hour Angle				
	60^m E.	30^m E.	Meridian	30^m W.	60^m W.
−20°	+0″.0224	+0″.0216	+0″.0214	+0″.0216	+0″.0224
0°	+ ″.0104	+ ″.0101	+ ″.0100	+ ″.0101	+ ″.0104
+20°	+ ″.0049	+ ″.0047	+ ″.0047	+ ″.0047	+ ″.0049
+40°	+ ″.0010	+ ″.0010	+ ″.0009	+ ″.0010	+ ″.0010
+60°	+0″.0026	+0″.0027	+0″.0027	+0″.0027	+0″.0026

Variations in the flexure of the objective and possible relative displacement of the two lens components may further cause prismatic effects having the same effect as refraction.

It is customary to limit the photographic observations as much as possible to the meridian. These hour-angle restrictions are particularly stringent for the ordinary photographic technique, less so in photovisual work.

6. Measurement

Long-focus astrometric problems are customarily studied in rectangular coordinates x and y that coincide closely with the directions of right ascension and declination of the equatorial coordinate system. The rectangular coordi-

nates are in the tangential coordinate system, which has already been described in Chapter 5.

The positions of star images in any one coordinate may be obtained with a precision long-screw measuring machine. The plate is oriented by two or more star images and is mounted on a carriage which can be moved along precision sliding ways. The plate is viewed with a long-power (say 20×) microscope mounted on a second carriage by means of a nut which fits a long horizontal precision screw, perpendicular to the sliding ways. The screw has a pitch of, say, 1 mm; by turning the screw and moving the plate carriage, the positions in one coordinate of stars may be measured over the entire plate. Instead of direct viewing, the projection method may be used. The microscope contains a vertical wire for bisecting the star images (and a horizontal one to indicate the center of the field), assuming that the centroid of the image represents the position of the star. At one end the screw is provided with a graduated dial, so that the amount of turning, and hence the distance moved, can be read and recorded to 0.001 mm (1μ).

We shall be primarily concerned with problems in which the position of a central star is referred to a background of three or more reference stars. Two successive settings are made on each image; the central star is usually measured twice. The plates are measured in four positions, differing by 90° each, representing the direct and reversed directions of the rectangular celestial coordinates; the averages of the direct and reversed values in each coordinate are thus reasonably free from systematic errors of bisection, which will vary with the measurer and the intensity of the photographic image. It is customary to record the measurements to 0.001 mm, but to carry out averages and further calculations to 0.0001 mm. Measuring machines with two screws perpendicular to each other are also used.

The diameter of a well-defined, sharp, black star image is about one to two seconds of arc or even more. The measured position of a star image may be obtained with an accuracy of about one percent of the diameter of the image; photoelectric scanning may be expected to yield even higher accuracy.

With the Sproul refractor, the relative location of two star images of the same diameter is obtained with a probable error of ±0.002 mm, or about ±0″.04. An increase in the number of exposures on any one night permits a further reduction in the probable error to ±0″.02. One may reach an accuracy of ±0″.01 if observations covering many exposures on several nights are combined.

Experience has shown that the positional accuracy is almost independent of atmospheric turbulence or "seeing," provided that inferior definition is avoided. Apart from such obvious image qualities as symmetry, the most important requirement for high positional accuracy is that the images shall

be well blackened, i.e., give a good representation of the position of the star; the sharpness of the image is of secondary importance.

Astrometric series of plates often extend over several decades. It is not always feasible or advisable to measure all the plates of a series during a limited span of time. When measurements are made at different times, the stability of the measuring technique is of prime importance, and experience has shown that it is generally quite stable. Repeated measurements have seldom revealed systematic differences of more than 0.001 mm in the measured positions of the central star against the reference background; most of these systematic differences are below 0.0005 mm. Whenever desirable or necessary, the "personal equation" of different measurers may be established and allowed for. The personal equation represents the inherent unavoidable differences among different measurers in ascertaining the location of the centroid of the star images, differences which are not necessarily completely eliminated by reversal.

The various sources of errors will be further discussed in Sections 2 and 5 of Chapter 8.

7. Looking into the future

The rapid increase in the sensitivity of photographic emulsions has already resulted in a minor revolution over the past several decades, in that photographs are now obtained with exposure times only a few percent of those required three or four decades ago. The current image-tube experiments indicate even greater reductions in exposure times. The advantages of greatly reduced exposure times are obvious—fainter stars may be reached and multiple exposures may be made. Short periods of atmospheric stability may be utilized, leading, for example, to greater photographic resolving power for close double stars.

Although the long-focus refractor has, up to the present time, appeared to be the instrument par excellence for problems of long-focus photographic astrometry, the construction of the new 152-cm quartz reflector of the U.S. Naval Observatory is ushering in a new era in this field. A reflector can cover the whole optical range of electromagnetic radiation. This particular instrument should have a more nearly constant optical figure than most of the existing instruments. Because of its larger aperture and complete achromatism it should provide a vast increase in our knowledge of parallaxes and orbital motions of much fainter stars than can now be reached. It will undoubtedly lead to an extension of our knowledge of intrinsically faint stars and of stars of low mass.

The future will certainly put the current photographic method in a different perspective. Improved measuring techniques, involving photoelectric evalu-

ation of the location of the star image and automatic recording, are also to be expected.

Meanwhile, the long-focus telescopes with either micrometer or interferometer attachments still continue to be significant in the visual realm, with their high resolving power, as the observer continues visual measurements of close double stars—a necessary supplement to the photographic method.

The photographic era, a revolutionary development only a century ago, has led to the current techniques and methods of long-focus photographic astrometry that are successfully being continued by surface observations.

There is little reason to question the continued usefulness of long-focus telescopes mounted on platform earth, and it will prove interesting and instructive to witness the development of the comparative advantages and disadvantages of these and telescopes which may be mounted on artificial space platforms.

Suggested readings

K. Aa. Strand, "Determination of Stellar Distances," *Science*, 144 (1964): 1299–1309. (Also available as a United States Naval Observatory Reprint.)

Peter van de Kamp, "Astrometry with Long-focus Telescopes," *in* W. A. Hiltner, ed., *Astronomical Techniques* (Stars and Stellar Systems, Vol. II). University of Chicago Press, 1962, pp. 487–536.

7 | Stellar Paths. Reduction Methods

The long-focus photographic method is particularly useful in making a high-precision study of the path of a star. If the star is under observation for parallax, useful information may be obtained in a few years; if it is under observation for orbital motion, a long period of time—several decades or even centuries—may be necessary to obtain the required observational material. In all cases the path of the star is referred to and measured against a background of virtually fixed reference stars, usually only three or four in number. Although the largest known parallactic displacement for a star is less than 1″, there are numerous stars whose annual proper motion exceeds 1″. The largest known annual motion is 10″.3, for Barnard's large-proper-motion star. Appreciable displacements are the rule, at least for the more interesting nearby stars. The measured positions must be properly adjusted or so reduced as to permit a precise analysis of the star's path.

For an extended stellar path, an increasing disparity between rectangular and spherical coordinates develops, which may be represented to a high approximation as a slowly changing orientation of the equatorial with respect to the rectangular coordinate system, amounting to

$$\Delta\theta = \Delta\alpha \sin \delta \qquad (2.18)$$

where $\Delta\alpha$ is the projection of the path in the x-coordinate measured in right ascension, and δ is the declination. In comparing results expressed in rectangular and in equatorial coordinates, the above change in position angle must be kept in mind, and secular effects should be considered, especially for stars of large proper motion situated at high declination; the effect on the components of the annual parallactic motion is negligible.

The difference between spherical and plane portrayal of a stellar path 1000″ long remains below 0″.01, and is therefore generally negligible.

1. Scale, orientation, and tilt effects

The principal geometric effects on the measured positions are changes in scale and orientation resulting from the following causes.

Observational
Instrumental (measuring machine, telescope)
Spherical (refraction, aberration)
Cosmic
Proper motions of reference and orientation stars

Accidental errors in the angle of orientation may be kept well below 0.0002 radians when orienting by star images. Proper motions of the orientation stars may introduce a systematic effect; a yearly change in orientation of the order of 0.0001 is not excluded. To avoid a progressive change in orientation and its effect on the measurements, the proper motions of the orientation stars should be well enough known that they may be allowed for. Variations in scale due to changes in temperature and barometric pressure are negligible for the present purpose.

The linear scale effect due to refraction is 0.00029, and is incorporated in the scale value of the telescope (Chapter 6, Section 1). The linear scale effect due to aberration is at most 0.0002, and its possible effect on parallax is negligible. Because of the small angular extent of long-focus plates, the small changes in refraction and aberration may be considered as linear functions of the position of the star on the plate, and the nonlinear terms may be ignored (Chapter 5, Sections 6 and 7).

The effect of plate tilt is generally negligible for long-focus instruments (Chapter 5, Section 5). Recall that p and q are the standard coordinates of the base, or optical center, of the plate, referred to the tangential point. (Chapter 5, Sections 1 and 5.) The resulting corrections are

$$px^2 + qxy \text{ in } x, \qquad qy^2 + pxy \text{ in } y. \tag{5.27}$$

For an extreme x or y of 20′ and a value of 1′ for p and q, the quadratic terms in the above expressions would be only 0″.002.

For the Sproul 24-inch telescope, with the plateholder in normal position, i.e., the long dimension parallel to the equator, the tilt amounts to $p = 7$ mm west, and $q = 11$ mm north, of the geometrical plate center. Or, in angular measure, $p = 2'.2$ and $q = 3'.5$. For an extreme x or y of 20′, the corresponding tilt effect is less than 0″.01.

2. Standard frame; plate constants

When comparing the different plates of a series of observations of the same field, all that is necessary is to reduce the measurements to a common origin, scale, and orientation by a linear transformation. This is provided by a set of n reference stars, at least three but rarely more than four. The plates yield tangential, or *standard*, coordinates in the image plane that are closely oriented with the directions of right ascension and declination (Chapter 5, Section 2).

Let X', Y' and x', y' be the measured coordinates of central and reference stars as obtained at the measuring machine and expressed in 0.0001 mm. (Chapter 6, Section 6.) In order to permit a comparison of measured positions on different plates, a reduction is made to a *standard frame* based on the reference stars. Its coordinates are admittedly and intentionally approximate: they may be taken as the positions of the reference stars referred to the equator of any convenient epoch (2000 is now commonly used) and rounded off to 0.01 mm. The standard frame is simply an idealized or fictitious "standard plate," to whose origin, scale, and orientation all other plates in the series are reduced. There is no particular reason to select and prefer one particular plate as the standard plate, as has often been done. Were the positions on any plate known to be without error, such a plate might truly be a standard plate, and thus represent an ideal standard frame. Since this is never true, and since the reference stars are not fixed, the standard frame provides a more elegant reference system than any single plate, for in a sense it represents all plates. A transfer to any other standard frame can always be easily accomplished (see Section 4 of this chapter).

Ordinarily there are only minute differences in scale between the different plates. At the measuring machine, the orientation of all plates is adjusted as closely as possible to that of the standard frame by means of suitably located orientation stars, which may include reference stars. The zero point of the measurements is arbitrary and, of course, differs for successive exposures. As a rule the same approximate zero point is used for the first exposure on any one plate.

The coordinates of the standard frame will be denoted by the subscript s; the positions x_s and y_s, defining the standard frame of reference, are relative to their mean position, i.e.,

$$[x_s] = [y_s] = 0. \tag{7.1}$$

All measured positions can now be reduced to the scale, orientation, and origin of the reference frame (x_s, y_s) through plate constants a, b, and c, which are given by the linear equations of condition for each reference star,

$$a_x x_s + b_x y_s + c_x = x_s - x', \qquad a_y x_s + b_y y_s + c_y = y_s - y'. \tag{7.2}$$

A least-squares solution gives

$$\begin{aligned} a_x &= \frac{[y_s^2][x_s(x_s - x')] - [x_s y_s][y_s(x_s - x')]}{[x_s^2][y_s^2] - [x_s y_s]^2}, \\ b_x &= \frac{[x_s^2][y_s(x_s - x')] - [x_s y_s][x_s(x_s - x')]}{[x_s^2][y_s^2] - [x_s y_s]^2}, \\ c_x &= -\frac{[x']}{n}, \end{aligned} \tag{7.3}$$

and similar expressions for a_y, b_y, and c_y.

For the central star the position X and Y reduced to the standard frame is given by

$$X = X' + a_x X_0 + b_x Y_0 + c_x, \qquad Y = Y' + a_y X_0 + b_y Y_0 + c_y, \quad (7.4)$$

where X_0 and Y_0 are adopted values of X and Y. Thus the position X_0, Y_0 is *rigorously* corrected for plate constants, but the values of X and Y obtained through the relation (7.4) remain uncorrected to the extent of

$$\begin{aligned} &a_x(X - X_0) + b_x(Y - Y_0) \qquad \text{in } x, \\ &a_y(X - X_0) + b_y(Y - Y_0) \qquad \text{in } y. \end{aligned} \quad (7.5)$$

Generally a and b are below 0.0002, so that X_0, Y_0 need not be known to more than one or two tenths of a millimeter, and the quantities in (7.5) are therefore negligible.

3. Dependences: plate solutions, dependence center, and dependence background

Schlesinger has shown that, for linear plate constants, time may be saved—but above all, insight gained—by expressing the reduced position as an explicit linear function of the measured coordinates.[1] The necessary transformation is obtained by substituting equations (7.3) in equations (7.4), which leads to

$$\begin{aligned} X = X' + \left\{ \frac{X_0\{x_s[y_s^2] - y_s[x_s y_s]\} + Y_0\{y_s[x_s^2] - x_s[x_s y_s]\}}{[x_s^2][y_s^2] - [x_s y_s]^2} \right. \\ \left. \times (x_s - x') \right\} - \frac{[x']}{n}, \end{aligned} \quad (7.6)$$

$$\begin{aligned} Y = Y' + \left\{ \frac{X_0\{x_s[y_s^2] - y_s[x_s y_s]\} + Y_0\{y_s[x_s^2] - x_s[x_s y_s]\}}{[x_s^2][y_s^2] - [x_s y_s]^2} \right. \\ \left. \times (y_s - y') \right\} - \frac{[y']}{n}. \end{aligned}$$

The resulting reduction statement, regardless of the zero point of the measured coordinates, therefore is

$$X = X' + [D_i(x_s - x')_i], \qquad Y = Y' + [D_i(y_s - y')_i], \quad (7.7)$$

where $i = 1, \ldots, n$. The quantities

$$D_i = \frac{X_0\{x_{si}[y_s^2] - y_{si}[x_s y_s]\} + Y_0\{y_{si}[x_s^2] - x_{si}[x_s y_s]\}}{[x_s^2][y_s^2] - [x_s y_s]^2} + \frac{1}{n}, \quad (7.8)$$

are named *dependences*. It is obvious that $[D] = 1$, and, because of the least-

[1] F. Schlesinger, "Photographic Determinations of Stellar Parallax Made with the Yerkes Refractor, III, IV, V, VI, VII," *The Astrophysical Journal*, 33 (1911): 161–184, 234–259, 353–374, 418–430; 34 (1911): 26–36.

squares procedure, that $[D^2]$ is a minimum. In the plate-constant method, X and Y are implicit functions of (x') and (y'); the dependence method provides an explicit expression which greatly simplifies the reduction calculations.

The *dependence reductions* (7.7) may be written as follows:

$$X = [Dx_s] + X' - [Dx'], \qquad Y = [Dy_s] + Y' - [Dy']. \tag{7.9}$$

The position $[Dx_s]$ and $[Dy_s]$ defines a point close to the central star, which is rigorously corrected for plate constants and is called the *dependence center;* $[Dx']$ and $[Dy']$ are the measured *dependence background.* Note that the dependences are simply the barycentric coordinates of the central star with respect to the reference stars.

The dependence method leaves only a small segment uncorrected, the so-called *plate solution,* sometimes called *offset:*

$$\xi = X' - [Dx'], \qquad \eta = Y' - [Dy'], \tag{7.10}$$

which remains uncorrected to the small amount given in (7.5). Theoretically, the plate solutions should vanish for the position X_0, Y_0, but, because of the limited number of decimals in D, small plate solutions exist for this position. Because of their explicit use in the dependence reduction method, it is convenient to substitute the plate solution ξ and η in the reduced positions, so that

$$X = [Dx_s] + \xi, \qquad Y = [Dy_s] + \eta. \tag{7.11}$$

The zero point of the measurements is eliminated for the plate solutions; the coordinates of the standard frame, the quantities x_s and y_s used in the computation of the dependence center, refer to their mean.

The plate solutions, of course, can be made vanishingly small by using a sufficient number of decimal places, say five or more, in the dependences. However, if the plates are carefully oriented, the plate constants are factors less than 0.0002, and their effect on the plate solutions is well below that of the observational errors (see equations 7.5). If the uncorrected plate solutions are kept sufficiently small, say less than 0.5 mm, the plate-constant reduction obtained is rigorous—within the errors of observation and even of those of calculation. Thus, with careful orientation, it is advantageous to permit the values of the plate solutions to fall within a given range, so that the same set of dependences, calculated for one position X_0, Y_0 of the central star, can be used in the reduction of a large number of exposures and generally need not be expressed to more than three decimal places. This is the great advantage of the dependence method, as compared with the reduction by plate constants.

The dependence method has another advantage: it reveals the relative significance, or the weight, of the positions of the individual reference stars. The dependence method gives no information about the linear plate constants, which are eliminated; however the plate constants are of no particular signifi-

cance. The situation is entirely different in more sophisticated reductions involving more than a simple linear transformation. If quadratic or higher terms and other parameters such as magnitude and color are introduced, a larger number of reference stars becomes necessary and various plate constants must be used.

Lest there be any misunderstanding or misapprehension we repeat and stress that, with careful orientation, the dependence method yields results which are *identical* with those obtained with linear plate constants.

4. Change of dependences

There are problems, such as conventional parallax determinations, in which the path of the central star is small enough to be covered by one set of dependences. In these problems the plate solutions as such, i.e., the positions with respect to the dependence background of the reference stars, may be used to study the path of the star, and no further reduction is necessary. But there are other problems in which it is necessary to use more than one dependence center, either because of appreciable change in the position of a central star due to proper motion, or because it is desired to study the relative position of two or more widely separated stars on the same plate. In all such cases a reduction to the origin of the standard frame is recommended.

For a central star with appreciable proper motion, successive dependence sets are so chosen that the dependence center is kept close to the central star. As before, the uncorrected segments, or plate solutions, ξ, η, are kept sufficiently small that, mainly through careful orientation, rigorous linear plate-constant reduction is obtained within the errors of observation for the duration of each dependence set. Since many measured positions are reduced by the same set of dependences, the economy of the dependence method is maintained, and it remains a desirable substitute for the plate-constant method.

In many long-focus problems (parallax, mass ratio, perturbation, perspective acceleration) there is no need to know the accurate positions of the reference stars. If, however, the position and proper motion of the central star or stars as such are of importance, accurate knowledge of the positions and proper motions of the reference stars is ultimately necessary. The required data can be obtained by referring the reference stars to a more comprehensive group of stars. In this case an eventual reduction (Δx_s, Δy_s) to a more precise reference system requires the addition of $[D\Delta x_s]$ and $[D\Delta y_s]$ to the dependence centers $[Dx_s]$ and $[Dy_s]$.

5. Calculation of dependences

A set of dependences for an initial position X_0, Y_0, and the standard frame (x_s, y_s), may be computed by the linear formula:

$$D_i = f_i X_0 + g_i Y_0 + \frac{1}{n}. \tag{7.12}$$

Here

$$f_i = \frac{x_{si}[y_s^2] - y_{si}[x_s y_s]}{[x_s^2][y_s^2] - [x_s y_s]^2},$$

and (7.13)

$$g_i = \frac{y_{si}[x_s^2] - x_{si}[x_s y_s]}{[x_s^2][y_s^2] - [x_s y_s]^2}$$

with the control equations,

$$[f x_s] = 1 \quad \text{and} \quad [g y_s] = 1. \tag{7.14}$$

The quantities D_i must satisfy the equations

$$[D] = 1, \qquad [Dx_s] = X_0, \qquad [Dy_s] = Y_0. \tag{7.15}$$

The first equation must be rigorous, in order to provide accurate elimination of the zero point of the measured coordinates. The calculated dependence center, $[Dx_s]$, $[Dy_s]$, must equal the position X_0, Y_0 within the errors due to rounding off the dependences.

In practice it will be found convenient to adopt for X_0 and Y_0 the position in a certain year. For any other year the dependences can then be easily computed through the use of their annual variations, D, which are given by

$$\Delta D_i = f_i \mu_X + g_i \mu_Y. \tag{7.16}$$

Here μ_X and μ_Y are the rectangular components of the yearly proper motion of the central star; the control equations are

$$[\Delta D] = 0, \qquad [\Delta D x_s] = \mu_X, \qquad [\Delta D y_s] = \mu_Y. \tag{7.17}$$

By means of these formulae an ephemeris for both dependences and dependence centers is easily computed. For plates taken with the 24-inch Sproul refractor (scale 1 mm = 18″.87), x_s and y_s are used to 0.01 mm; the scale and orientation errors of the adopted standard frame are usually below a factor 0.0001. Using two decimals in X_0 and Y_0, the dependences are computed to four decimals, but rounded off to three, always taking care that their sum shall rigorously equal unity. The dependence centers are computed to 0.0001 mm.

The rounding-off to three places in the dependences leads to values of the plate solutions that are rarely over 0.05 mm near the dependence epoch. By spacing the dependence centers not more than about 1 mm apart in each coordinate, the solutions seldom exceed 0.5 mm, and errors due to extreme orientation (and scale) constants are rarely above 0.0001 mm.

6. Geometric accuracy: choice of configuration of reference stars

The chief consequence of the central star's proper motion is the varying accuracy of its geometrical fixation due to its changed location within the configuration. We shall neglect the possible variation in intrinsic positional accuracy of each reference star with its location on the photographic plate. The geometrical accuracy of the reduced position of the central star depends on the dependences for the reference stars. Let ϵ be the mean error of a measured position x' (or y'); then the mean error E of the reduced position of the central star is given by

$$E^2 = \epsilon^2\{1 + [D^2]\}. \tag{7.18}$$

We shall refer to the quantity

$$1 + [D^2] \tag{7.19}$$

as the *inverse weight*, which is thus indicative of the accuracy of the reduced position, the mean error of unit weight being ϵ. For a central star of appreciable proper motion, the dependences change and result in a corresponding change in accuracy for the changing dependence background. Writing

$$D_t = D_0 + t\Delta D, \tag{7.20}$$

the inverse weight becomes

$$1 + [D_0^2] + 2t[D_0\Delta D] + t^2[\Delta D^2], \tag{7.21}$$

reaching a minimum value for

$$t_m = -\frac{[D_0\Delta D]}{[\Delta D^2]}. \tag{7.22}$$

Calling the dependences at this epoch D_m, the inverse weight at any other time is given by

$$1 + [D_m^2] + (t - t_m)^2[\Delta D^2]. \tag{7.23}$$

For any investigation spread over a limited time interval, the greatest accuracy is maintained if the position of greatest dependence accuracy is reached about the middle of that interval. If the interval is not more than a few decades, it is generally not difficult to find an appropriate configuration for which the dependences do not vary too much over the interval and, in any case, remain positive.

The absolute minimum value of $[D_m^2]$ in the configuration occurs at the origin, defined by

$$[x_s] = [y_s] = 0,$$

where each of the dependences equals $1/n$. For any central star, therefore, to insure a satisfactorily small $[D^2]$, it is important to choose a configuration whose origin will not lie too far off the path of the star. As a rule $1 + [D^2]$ proves to be between 1.3 and 1.4.

Table 7.1. ACCURACY ON BACKGROUNDS OF THREE AND MORE STARS (EQUAL DEPENDENCES)

n	Inverse Weight $1 + [D^2]$	Relative Error	n	Inverse Weight $1 + [D^2]$	Relative Error
3	1.333	1.031	7	1.143	0.956
4	1.250	1.000	8	1.125	0.949
5	1.200	0.981	...	...	...
6	1.167	0.967	∞	1.000	0.895

Even for a central star at the origin, the accuracy of the reduced position does not increase appreciably with the number of reference stars. This is illustrated in Table 7.1. Considering the extra work involved, little is gained by using more than four reference stars, except, of course, in reductions involving more than a linear transformation (Section 3).

In a limited problem, such as a conventional parallax determination, nothing is therefore more desirable than a configuration that has a limited number of stars and approximately equal dependences and limited areal extent. A smaller configuration results in higher astrometric accuracy because it limits the effect of errors due to refraction, plate-emulsion, coma and measuring machine (see Chapter 8, Section 5, footnote 9).

Graphical methods are useful for initial exploration and evaluation of the dependences of different configurations of reference stars; they are particularly effective for three-star combinations.[2] For three reference stars, the

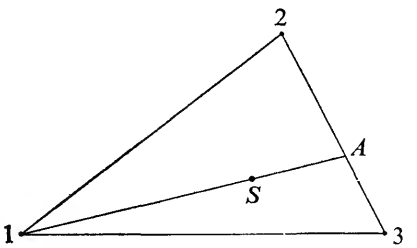

Fig. 7.1. *Graphical evaluation of dependences for three reference stars.*

dependences may be simply measured, as illustrated in Figure 7.1, where S is the central star and 1, 2, and 3 the three reference stars. By measuring the

[2] Frank Schlesinger, "A Short Method for Deriving Positions of Asteroids, Comets, etc., from Photographs," *The Astronomical Journal*, 37 (1926): 77–84. L. J. Comrie, "Note on the Reduction of Photographic Plates," *Journal of the British Astronomical Association*, 39 (1929): 203–209.

lengths of the segments $1A$, SA, $2A$, and $3A$, directly on the photographic plate if desired, the dependences are found from

$$D_1 = \frac{SA}{1A}$$

$$D_2 + D_3 = 1 - D_1$$

$$\frac{D_2}{D_3} = \frac{3A}{2A}.$$

Obviously, two other approaches are available.

For a central star with considerable proper motion, the effect of each reference star on its reduced position changes with time; thus secular effects due to magnitude, color, and proper motion are introduced. The first two can be kept at a minimum by limiting the range of magnitude and spectrum for the reference stars; the dispersion effects can be minimized by photography in the longer wavelengths. In long-range astrometric problems the effect of the proper motion of the reference stars becomes important (see Chapter 9).

The choice of reference stars is thus determined by several considerations. Generally one need have little concern about the proper motions and parallaxes of the reference stars; almost any set of faint stars represents an acceptably close approximation to a fixed background. The choice depends largely on the exposure time to be used and on the limitations imposed by the required magnitude compensation.

For a short-term problem, it may be desirable to use a relatively small configuration, with the corresponding advantage of increased astrometric accuracy.[3] Even in this case, however, it is wise to provide for possible extension to a longer period of time. This can, of course, be done by starting with a larger long-range configuration, even though its positional accuracy may be less. An alternative approach is to make a transition from a smaller to a larger configuration whenever future developments warrant such a procedure (Chapter 9).

7. Long-range problems; transition from one configuration to another

For a star of appreciable proper motion which is to be observed over a long interval, the configuration chosen (avoiding stars near the edge of the plate) should be large enough that the same reference system may serve well for as long a time as possible. The size of the telescopic field and the photographic plate limits the lifetime of maximum usefulness of any configuration, but if a configuration which the central star has recently entered is chosen, long use can be made of the reference system. The importance of a reference star in a

[3] J. Schilt, "The Dependence of the Errors in Relative Star Positions on the Distances of the Comparison Stars," *The Astronomical Journal*, 48 (1939): 53–64.

long-range problem should be judged not only by its present dependence value but by the annual dependence changes as well. The advantage of having one long-range reference system more than offsets the possible temporary occurrence of negative dependences at the beginning and end of its period of usefulness.

When planning measurements for a region that is to be observed for a long time, one should make a survey of potential configurations. The proper motion of the central star should be known, so that its future path can be traced with accuracy. After magnitude compensation and exposure time have been considered several possible configurations are likely to be found, all of them satisfying the condition that at some time in the future the path of the central star will pass close to the center of the configuration.

In any long-term astrometric problem it is therefore important to study carefully every possible choice of reference stars, so that one will not be faced with early obsolescence of the configuration chosen but, instead, will have a good foundation for both present and future use. Other things being equal, greatest astrometric accuracy is reached with a small configuration of stars. A larger configuration may often be preferred because of its longer life and, of course, the practical choice of reference stars is limited by the availability of stars in the region being studied.

The addition of reference stars leads, of course, to increased accuracy of the plate constants, which in turn leads to a greater accuracy of the reduced position of the central star. Since linear plate-constant reduction and dependence reduction are mathematically equivalent, it follows that the addition of a reference star leads to a new distribution of the dependences that always has a correspondingly lower value for $[D^2]$. This value equals the old value only if the dependence of the additional star is zero; if not, $[D^2]$ must be smaller, even though a negative dependence for another star may have appeared. The addition of another reference star may be of little or no value at any given time, as would be demonstrated by a small, or even negative, dependence value. The eventual transition to a reference system involving the inclusion of one additional star is most conveniently carried out at about the time of vanishing dependence value for that star. The most economical procedure is to select a star of potential future importance, but to refrain from measuring the star until its dependence value has become appreciably positive. By measuring and reducing a sufficient number of common backgrounds at that time, any reductions of earlier plates to the new frame may be evaluated with adequate accuracy. This problem is further discussed in Chapter 9.

8. Positions of planets, comets, asteroids, and satellites

Because stellar paths remain for many years within the confines of a single reference configuration of limited areal extent, they are ideally suited to the

long-focus technique. The astrometric problem is entirely different for such rapidly moving objects as planets, comets, and artificial satellites. In dealing with them the methods of spherical astrometry must be used: i.e., it is necessary to have the basic observations expressed in spherical (equatorial) coordinates. Nevertheless, the reduction methods developed for long-focus photographic astrometry may be used to advantage, particularly the dependence method.[4]

We limit ourselves to an object referred to n (usually three or four) reference stars with known positions, i.e., equatorial coordinates:

$$\alpha_{si} \quad \text{and} \quad \delta_{si} \quad (i = 1, 2, \ldots, n).$$

We define $\Delta\alpha$ and $\Delta\delta$ as the relative values of α and δ, referred to the tangential point. We assume that the diameter of the reference system does not exceed a few degrees. We measure the position x_i', y_i' for the reference stars $(i = 1, 2, \ldots, n)$ and the position (X_c', Y_c') for the central object.

We shall limit ourselves to reduction by linear plate constants. This is equivalent to expressing the reduced position as

$$X_c = [Dx_s], \qquad Y_c = [Dy_s]. \tag{7.24}$$

Here D are the dependences expressed to enough decimal places to make the dependence reduction rigorous, and x_s and y_s are the adopted standard coordinates (Chapter 5) of the standard frame defined by the reference stars, relative to their geometric center.

As a first approximation the reduced position α, δ of the central star may obviously be written as

$$\alpha_c = [D\alpha_s], \qquad \delta_c = [D\delta_s] \tag{7.25}$$

where α_s, δ_s represent the equatorial standard frame formed by the reference stars: or, in practice, the adopted equatorial coordinates of the reference stars.

To obtain a more rigorous reduction, we must make allowance for the difference between the spherical and plane coordinates. It is generally sufficient to neglect third- and higher-order terms and limit ourselves to the relations (5.14 and 5.15) derived in Chapter 5. The corresponding equatorial coordinates $\Delta\alpha$, $\Delta\delta$ are normally referred to the tangential point and the relations between rectangular and spherical coordinates are

$$x = \Delta\alpha \cos \delta_0 - \Delta\alpha\Delta\delta \sin \delta_0, \tag{5.14}$$

$$y = \Delta\delta + \tfrac{1}{4}(\Delta\alpha)^2 \sin 2\delta_0, \tag{5.15}$$

limiting ourselves to quadratic terms only. Here x, y are the standard coordinates referred to the tangential point. In practice it is convenient and customary to refer x, y to the geometric center of the reference stars. We may substitute this point for the tangential point, thereby introducing what

[4] See footnote 2, page 107.

amounts to a small tilt effect. This effect generally may be considered negligible as long as the geometric center is not too far removed from the tangential point.

We may, therefore, write for the central object,

$$\begin{aligned} X_c &= \Delta\alpha_c \cos\delta_0 - \Delta\alpha_c\Delta\delta_c \sin\delta_0, \\ Y_c &= \Delta\delta_c + \tfrac{1}{4}(\Delta\alpha_c)^2 \sin 2\delta_0, \end{aligned} \tag{7.26}$$

and for the reference stars ($i = 1, 2, \ldots, n$):

$$\begin{aligned} x_{si} &= \Delta\alpha_{si} \cos\delta_0 - \Delta\alpha_{si}\Delta\delta_{si} \sin\delta_0, \\ y_{si} &= \Delta\delta_{si} + \tfrac{1}{4}(\Delta\alpha_{si})^2 \sin 2\delta_0, \end{aligned} \tag{7.27}$$

or, substituting in (7.24),

$$\begin{aligned} \Delta\alpha_c \cos\delta_0 - \Delta\alpha_c\Delta\delta_c \sin\delta_0 &= [D\{\Delta\alpha_s \cos\delta_0 - \Delta\alpha_s\Delta\delta_s \sin\delta_0\}], \\ \Delta\delta_c + \tfrac{1}{4}(\Delta\alpha_c)^2 \sin 2\delta_0 &= [D\{\Delta\delta_s + \tfrac{1}{4}(\Delta\alpha_s)^2\} \sin 2\delta_0], \end{aligned} \tag{7.28}$$

which may be written as

$$\begin{aligned} \Delta\alpha_c &= [D\Delta\alpha_s] + \{\Delta\alpha_c\Delta\delta_c - [D\Delta\alpha_s\Delta\delta_s]\} \tan\delta_0, \\ \Delta\delta_c &= [D\Delta\delta_s] - \tfrac{1}{4}\{(\Delta\alpha_c)^2 - [D\Delta\alpha_s^2]\} \sin 2\delta_0. \end{aligned} \tag{7.29}$$

Since $[D] = 1$, the left-hand side and first terms on the right-hand side of these formulae (7.29) may be reduced to "absolute" right ascension by adding on both sides the equatorial coordinates of the tangential point, so that,

$$\begin{aligned} \alpha_c &= [D\alpha_s] + \{\Delta\alpha_c\Delta\delta_c - [D\Delta\alpha, \Delta\delta_s]\} \tan\delta_0, \\ \delta_c &= [D\delta_s] - \tfrac{1}{4}\{(\Delta\alpha_c)^2 - [D\Delta\alpha_s^2]\} \sin 2\delta_0. \end{aligned} \tag{7.30}$$

So much for ideal theory. In practice the dependences may be used to three or even two places; they may well have been obtained graphically (Section 6). In this case (7.24) becomes

$$X_c = [Dx_s] + \xi, \qquad Y_c = [Dy_s] + \eta, \tag{7.11}$$

where

$$\xi = X_c' - [Dx'], \qquad \eta = Y_c' - [Dy']. \tag{7.10}$$

The plate solutions ξ, η must be added to (7.30), and we have:

$$\begin{aligned} \alpha_c &= [D\alpha_s] + \xi \sec\delta_0 + \{\Delta\alpha_c\Delta\delta_c - [D\Delta\alpha_s\Delta\delta_s]\} \tan\delta_0, \\ \delta_c &= [D\delta_s] + \eta - \tfrac{1}{4}\{(\Delta\alpha_c)^2 - [D(\Delta\alpha_s)^2]\} \sin 2\delta_0. \end{aligned} \tag{7.31}$$

In general, therefore, the computed equatorial position α, δ of the central star equals the dependence mean equatorial position, plus the values for the plate solution (reduced to small circle in right ascension) of the reference stars, plus corrections depending on the relative position of central and reference stars. If desired, the former correction may be obviated by calculating the dependences to four or five places. The latter corrections depend on the value of δ_0 and on the values of $\Delta\alpha$, $\Delta\delta$ for central and reference stars. Tabulations

are found in various places. Abbreviated versions are given in Tables 7.2 and 7.3 for

$$\begin{aligned} R &= \Delta\alpha\Delta\delta && \text{in seconds of time} \\ S &= \tfrac{1}{4}(\Delta\alpha)^2 \sin 2\delta_0 && \text{in seconds of arc.} \end{aligned} \tag{7.32}$$

Hence

$$\begin{aligned} \alpha_c &= [D\alpha_s] + \xi \sec \delta_0 + \{R_c - [DR_s]\} \tan \delta_0, \\ \delta_c &= [D\delta_s] + \eta - \{S_c - [DS_s]\}. \end{aligned} \tag{7.33}$$

Table 7.2. $R = \Delta\alpha\,\Delta\delta$ (IN SECONDS OF TIME)

$\Delta\delta$	$\Delta\alpha$					
	1^m	2^m	3^m	4^m	5^m	6^m
	s	s	s	s	s	s
5′	0.09	0.18	0.26	0.35	0.44	0.52
10′	0.18	0.35	0.52	0.70	0.87	1.05
15′	0.26	0.52	0.78	1.05	1.31	1.57
20′	0.35	0.70	1.05	1.40	1.74	2.09
25′	0.44	0.87	1.31	1.74	2.18	2.62
30′	0.52	1.05	1.57	2.09	2.62	3.14
35′	0.61	1.22	1.83	2.44	3.05	3.66
40′	0.70	1.40	2.09	2.79	3.49	4.19
45′	0.78	1.57	2.36	3.14	3.93	4.72

Table 7.3. $S = \frac{1}{4}(\Delta\alpha)^2 \sin 2\delta_0$ (IN SECONDS OF ARC)

δ_0	$\Delta\alpha$						δ_0
	1^m	2^m	3^m	4^m	5^m	6^m	
5°	0″.2	0″.7	1″.5	2″.7	4″.3	6″.1	85°
10°	0″.3	1″.3	3″.0	5″.4	8″.4	12″.1	80°
15°	0″.5	2″.0	4″.4	7″.8	12″.3	17″.7	75°
20°	0″.6	2″.5	5″.7	10″.1	15″.8	22″.7	70°
25°	0″.7	3″.0	6″.8	12″.0	18″.8	27″.1	65°
30°	0″.8	3″.4	7″.6	13″.6	21″.3	30″.6	60°
35°	0″.9	3″.7	8″.3	14″.8	23″.1	33″.2	55°
40°	1″.0	3″.9	8″.7	15″.5	24″.2	34″.8	50°
45°	1″.0	3″.9	8″.8	15″.7	24″.5	35″.3	45°

From the known values of $\Delta\alpha$, $\Delta\delta$ for the reference stars, the values $\Delta\alpha_c$, $\Delta\delta_c$ for the central star needed for calculating the corrections R and S may be obtained with sufficient accuracy by the approximations

$$\begin{aligned} \Delta\alpha_c &= [D\Delta\alpha_s], \\ \Delta\delta_c &= [D\Delta\delta_s]. \end{aligned} \tag{7.34}$$

Another expression may be obtained by using the relations

$$\Delta\alpha = x \sec\delta_0 + xy \sec\delta_0 \tan\delta_0, \tag{5.16}$$

$$\Delta\delta = y - \tfrac{1}{2}x^2 \tan\delta_0, \tag{5.17}$$

again limiting ourselves to quadratic terms. By writing the above formulae for both central star and reference stars, we derive

$$\begin{aligned} \Delta\alpha_c &= [D\Delta\alpha] + \{X_c - [Dx_s]\} \sec\delta_0 + \{X_cY_c - [Dx_sy_s]\} \sec\delta_0 \tan\delta_0, \\ \Delta\delta_c &= [D\Delta\delta] + \{X_c - [Dy_s]\} - \tfrac{1}{2}\{X_c^2 - [Dx_s^2]\} \tan\delta_0, \end{aligned} \tag{7.35}$$

whence, after simple transformation

$$\begin{aligned} \alpha_c &= [D\alpha_s] + \xi \sec\delta_0 + \{X_cY_c - [Dx_sy_s]\} \sec\delta_0 \tan\delta_0, \\ \delta_c &= [D\delta_s] + \eta - \tfrac{1}{2}\{X_c^2 - [Dx_s]^2\} \tan\delta_0. \end{aligned} \tag{7.36}$$

8 | Proper Motion and Parallax

The first use of the long-focus photographic technique was for the determination of annual parallaxes, and it is still used for that purpose. Schlesinger began this work at the Yerkes Observatory in 1903, and other observatories gradually followed his example: among the first were the McCormick, Allegheny, Mount Wilson, Sproul, Dearborn, and Van Vleck observatories in the United States, the Greenwich Observatory in England, the Cape Observatory in South Africa, the Stockholm Observatory in Sweden, and the Bosscha Observatory in Indonesia; the most recent additions have been Lick and Flagstaff in the United States. With the exception of Mount Wilson, Bosscha, and Flagstaff, the telescopes are refractors, visual or photographic. Although most parallax determinations so far have been limited to stars brighter than the twelfth magnitude, the recent programs started with the Lick refractor and the United States Naval Observatory reflector in Flagstaff permit an extension toward fainter stars.

1. At the telescope

Parallax work has stringent hour-angle requirements. At the Sproul Observatory, photographs are rarely taken more than one hour off the meridian. A survey of 30 parallax determinations,[1] involving some 3,000 plates, reveals little range in the average hour angle at different times of the night; the algebraic average is within one minute of time of the meridian. The maximum systematic difference in hour angle, comparing dawn and dusk observations, amounts to less than twenty minutes of time. The corresponding differential dispersion effect in right ascension is slightly more than $0''.001$ for an extreme difference in spectrum, A to M, (Chapter 6, Section 5). This material therefore is systematically well compensated for dispersion effects.

[1] Peter van de Kamp and Sarah Lee Lippincott, "Summary of Thirty Sproul Parallaxes," *The Astronomical Journal*, 55 (1950): 89–93.

Besides equalizing the magnitude of the central star, whenever required, with the average magnitude of the reference stars, it is desirable to have a small dispersion in the magnitudes of the reference stars. No magnitude error need generally be feared if both the compensation between central star and reference stars are below half a magnitude. Since guiding error occurs mostly in the direction of diurnal motion, a slight elongation of the exposures in the direction of right ascension is well-nigh unavoidable; this is not a serious matter as long as the elongation is not asymmetrical.

At most observatories plates are taken near extreme parallactic displacement only (shortly after dusk and before dawn) and generally only right ascension displacements are used, since they cover the greater part of the parallactic displacement.

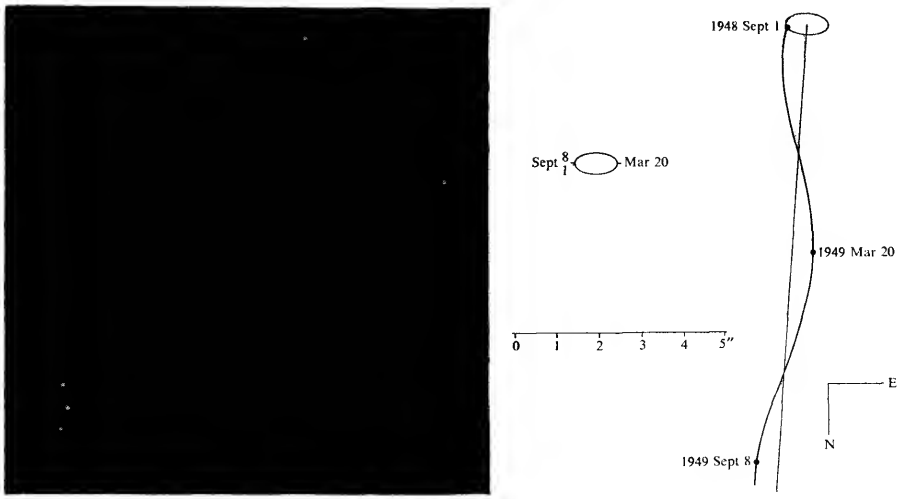

Fig. 8.1. *Barnard's star is notable for its large proper motion (10".3 yearly) and parallax (".53). Photographs of Barnard's star were taken with the Sproul refractor at three successive epochs of extreme parallactic displacement, separated by approximately half a year each. The brightness of Barnard's star, apparent magnitude 9.7, was reduced by two magnitudes by a rotating sector, to provide approximate equality with the two background stars in the upper right of the portion of the field illustrated.*

In this composite print the three photographs have been superimposed. The "fixed" background stars each give one image, whereas Barnard's star gives three separate images, showing displacement both south-north (proper motion) and east-west (parallax), which may be checked against the diagram. The orientation is inverted, corresponding to that ordinarily presented by the astronomical telescope.

The Sproul 24-inch refractor has a focal length of 10.93 meters (36 feet) and therefore has a scale of 1" = 0.053 mm at the focal plane. The original plates have here been enlarged approximately eleven times, to yield a scale close to 1" = 0.6 mm.

2. Plate weight: plate, night, and measurement errors; double plates; night weights

Increase in positional accuracy on any one night at the Sproul Observatory is obtained by increasing the number of exposures per plate and the number of plates. Each plate contains from one to four exposures, spaced a millimeter, or more apart; plate weights are assigned, depending on quality and number of exposures, according to the following schedule, suggested by long experience.

Table 8.1. ADOPTED PLATE WEIGHTS

Image Quality	No. of Exposures			
	4	3	2	1
Good	1.4	1.2	1.0	0.7
Fair	1.2	1.0	0.7	0.5
Poor	1.0	0.7	0.5	0.3

This weighting system takes into account the effect of a *plate error*, common to the successive exposures on any one plate and mostly due to emulsion shifts. Reduction of film errors is obtained by the use of "double" plates, obtained by turning the same photographic plate 180° in its own plane between the two successive sets of exposures, representing the two single plates. The two sets of exposures for the central star are close together on the emulsion; here the effects of a general film shift are virtually equal and are opposite for the two successive sets of exposures. The double-plate procedure is especially desirable for large configurations, where plate error is to a great extent responsible for the decreased positional accuracy of single sets of exposures.

The useful number of plates on any one night is limited by the *night errors*, which may be due to refraction anomalies. These errors are assumed constant during all the exposures of the same field within the same night. For the Sproul Observatory Dr. Land has found an average value of $\pm 0''.0124$ (probable error) for the night error, and an average accidental plate error, which includes film, image, and measurement errors, of $\pm 0''.0274$ (p.e.) when reduced to unit weight.[2] Plate error and night error combine into an error of $\pm 0''.030$ (p.e.) for one plate of unit weight (two good exposures). This value therefore represents the accuracy obtained from one good plate with two exposures,

[2] Gustav Land, "Systematic Errors in Astrometric Photographs," *The Astronomical Journal*, 51 (1944): 25–29.

for the position of the central star relative to the background of reference stars.

The accidental error of *measurement* of a plate is found to be about ±0.0008 mm or ±0″.015 (p.e.). This is part of the observed plate error of ±0″.0274 (p.e.) mentioned above; the true plate error is therefore ±0″.023 (p.e.). The average of two measurements of a plate increases the effective plate weight by a factor 1.15, three measurements by 1.25. The gain due to remeasurements is limited, and, generally, the additional effort is not warranted, apart from its value as a test of the stability of the measuring machine and the evaluation of personal equation between different measurers.

The law of diminishing returns, as enforced by the night errors, makes it advisable to introduce a *night weight* (*p*).[3] For example, total plate weights of 5 and 10, are reduced to effective night weights of only 3 and 4 because of the existence of night errors. A total plate weight of 5 therefore yields an error ±0″.017 (p.e.), while a total plate weight of 10 reduces the error no further than ±0″.015 (p.e.). Hence, whenever exposure times are sufficiently short, two double plates, but no more, are exposed; the single component plates have three or four exposures each. In this way a night weight of three is obtained; more material for any one night is generally not warranted. The resulting positional accuracy (p.e.) is about 0″.02, which may be regarded as the practical limiting accuracy for any one night. Measurements of relative photographic positions of stars close together, such as visual double stars, are less affected by plate and night errors, and an appreciably higher accuracy may be obtained (Chapter 10, Section 3).

Often it will be desirable to obtain a very high accuracy, for example, in studying the systematic behavior of residuals from a solution for parallax and proper motion, which may represent orbital motion. In this case the positional results obtained on several nights may be combined into average values, referred to as normal points, or normal places. Apart from the presence of systematic errors that may remain constant for several nights, weeks, or longer periods, a probable error of ±0″.010 or even smaller may be obtained for the normal places.

3. Analysis for proper motion and parallax

To determine proper motion and parallax we proceed as follows. The central star has been measured on a background of faint reference stars; the reduced positions refer to the dependence background of these faint stars; the resulting values for proper motion and parallax of the central star are relative to the reference background.

[3] Peter van de Kamp, "On the Weight of Astrometric Photographs," *The Astronomical Journal*, 51 (1945): 159–160.

Average values of the plate solution ξ and η are formed for the different exposures on each plate. Means for each night are formed and added to the corresponding dependence center, $[Dx_s]$, $[Dy_s]$, thus yielding positions X and Y, which hold for the standard frame, (x_s, y_s). The standard frame and the measured portions hold for the equator of any convenient epoch, for example, the year 2000 (see Chapter 7, Section 2).

The equations of condition for a uniform rectilinear heliocentric path are

$$X = c_X + \mu_X t \qquad Y = c_Y + \mu_Y t. \tag{8.1}$$

Here c_X, c_Y is the heliocentric position at a certain zero epoch, for example, 1950.000; μ_X, μ_Y is the yearly proper motion; the time t in years is counted from the adopted zero epoch. The unit of time is the solar or Besselian year, which begins when the right ascension of the mean sun is 280°. The Besselian fraction of the year, τ, is given in the *American Ephemeris and Nautical Almanac*.[4]

The equations of condition for the corresponding geocentric path are

$$X = c_X + \mu_X t + \pi P_\alpha \qquad Y = c_Y + \mu_Y t + \pi P_\delta. \tag{8.2}$$

Here, π is the relative parallax; P_α and P_δ are the parallax factors in right ascension (reduced to great-circle measure) and declination (Chapter 3, Section 4).

The positions X and Y for each night are often corrected for provisional values of the unknowns c, μ, and π. This may be done to facilitate the calculations, but also to inspect the material for possible orbital motion. The equations of condition are assigned a night weight p, in accordance with the total plate weight and an assumed night error (Section 2). The least-squares solutions are carried out to obtain the differential corrections, which are afterward added to the provisional values, to yield the final values of c, μ, and π. All calculations are carried out in units of 0.0001 mm; the final results for the unknowns are reduced to seconds of arc by multiplying by the scale value (1 mm = 18″.87 for the Sproul refractor).

4. Reduction from relative to absolute parallax

The relative parallax must now be reduced to absolute by adding a correction representing the dependence weighted mean parallax of the reference stars. This correction may be obtained by evaluating the spectral parallax of each reference star, through its apparent magnitude and assumed absolute magnitude. Generally a statistical correction that takes into account galactic latitude is applied instead. At the Sproul Observatory the following procedure is used. If the spectral types are known, the secular parallax of the reference

[4] Published annually by the United States Government Printing Office, Washington, D.C.

stars is taken from Table 8.VII in Vyssotsky and Williams' proper motion investigation[5] and reduced to annual parallax for an assumed solar velocity of 20 km/sec by multiplying by 0.237. If the spectral types are not known, Table 8.I of the same study is used. For stars fainter than the eleventh magnitude the values of the annual parallax are taken from Table 8 in Binnendijk's study of proper motions.[6]

For most long-focus photographic parallax determination the values for the reduction from relative to absolute parallax range between 0".001 and 0".005.

5. Results

The results obtained by long-focus parallax determination have been summarized by Jenkins.[7] More than six thousand stars are listed, representing some ten thousand separate parallax determinations. The vast majority of these determinations are based on some twenty to thirty plates spread over a few years, the resulting probable errors averaging close to $\pm 0''.010$.

It is obvious that the parallax method has its limitation in probing stellar distances. Beyond twenty parsecs, i.e., for stars with a parallax of less than 0".05, the relative error of a parallax determination becomes uncomfortably large. This is especially true of double stars, for which a relative error in the parallax appears threefold in the sum of the masses (Chapter 11, Section 5). Parallax determinations of many apparently bright but distant stars generally lead to frustrating results and are of statistical value only. The promising and valuable determinations are those of "nearby" stars, the bulk of which are first detected as faint stars of large proper motion. The vast majority of these large-proper-motion stars prove to have large parallaxes, and are therefore rewarding subjects for parallax observations.

A useful list of stars nearer than twenty parsecs has been compiled by Gliese,[8] in which basic data are listed in addition to the parallax values. Gliese lists 915 stars, with a total of 1,094 components, known to have annual parallaxes of more than 0".05. The parallaxes, of all these stars, and hence the distances, have been determined, but with a percentage of error that may be as great as 20 percent at a distance of 20 parsecs. The parallaxes and distances

[5] A. N. Vyssotsky and Emma T. R. Williams, *An Investigation of Stellar Motions, Together with Second McCormick Catalogue of Proper Motions* (Publications of the Leander McCormick Observatory, Vol. 10) University of Virginia, 1948, p. 33, table 8.I; p. 36, table 8.VII.

[6] L. Binnendijk, "Mean Parallaxes of Faint Stars, Derived from a Combination of the Pulkovo and Radcliffe Catalogues of Proper Motions," *Bulletin of the Astronomical Institutes of the Netherlands*, 10 (1943): 15, table 8.

[7] L. F. Jenkins, *General Catalogue of Trigonometric Stellar Parallaxes*, New Haven: Yale University Observatory, 1952. *Supplement*, 1963.

[8] W. Gliese, "Katalog der Sterne näher als 20 Parsek für 1950.0." *Astronomisches Rechen-Institut in Heidelberg, Mitteilungen Serie A*, Nr 8 (1957): 1–89.

of stars nearer than 5 parsecs are generally known with a probable error of 2 percent or even less.

Analyses of sources of errors in extensive series of parallax determinations have been made: for example, by Alden and by Land, who investigated the 1,323 parallaxes observed at the Southern Station of the Yale Observatory from 1925 to 1935.[9] They found that there was a significant increase in the probable error of unit weight as the size of the reference configuration increased, and that smaller, less blackened exposures and very small sector openings also increased the error. Dr. Land suggests that the average probable error of unit weight of $\pm 0''.0245$ for the Yale parallaxes could be reduced to $\pm 0''.0188$ if all contributing sources of systematic effects could be eliminated in the observational technique. An optimum exposure time of 60 to 75 seconds is found to yield highest positional accuracy. This is because the refraction oscillations have a period of roughly one minute; asymmetry of the images results from shorter and longer exposures.

6. Trend to higher precision: attainable accuracy

The "classical" parallax determinations with long-focus refractors are based on some twenty to thirty plates, spread over five to seven successive observing seasons, and yield probable errors of about $\pm 0''.01$ for the relative parallax. Gradually a tendency has developed to increase the span of time and number of plates in individual parallax determinations, and thus increase the accuracy. This has resulted both from a desire for greater accuracy of the parallaxes and because of long-range problems that are now studied by means of the long-focus photographic techniques, such as masses and mass-ratios (Chapter 11), and unresolved astrometric binaries (Chapter 12). Increasing the number of plates—up to several hundred in certain cases—has resulted in obtaining probable error values as low as $\pm 0''.002$.

There is evidence for a probable "year error" of about $\pm 0''.002$ in the Sproul astrometric positions, an error that appears to set a limit to the accuracy attainable in any one year. Although an error of this size is acceptable in such problems as that of long-period orbital motion of appreciable amplitude, it would, as a possible seasonal error, put severe limitations on the attainable accuracy in parallax determinations. Systematic errors having a period of one year would be serious because of their obvious effect on parallax determinations and on perturbations with periods close to one year. For normal points based on six or more multiple exposure photographs of relative positions of

[9] Harold L. Alden, *The Probable Errors of Yale Parallax Plates*, (Transactions of the Astronomical Observatory of Yale University, Vol. 15, part 2) 1948. Gustav Land, *Systematic Effects in the Probable Errors of the Yale Parallaxes*, (Transactions of the Astronomical Observatory of Yale University, Vol. 15, part 3) 1948.

double-star components (Chapter 10, Section 3), the quantity $\pm 0''.002$ also appears to represent the ultimate in positional accuracy obtainable for yearly normal positions with the long-focus photographic technique.

Because the Sproul Observatory plates are taken without special regard to the time of the night, the material is not limited to extreme parallax factors in right ascension. As a result there is on the average more than the usual range of parallax factors in declination and the parallax values determined from the declination measures are of some significance, at least statistically; on the average the weight of the parallax determinations in declination (y) is 15 percent of those in right ascension (x). In nearly all cases, first, separate least-squares solutions in x and y are made for parallax and proper motion (and sometimes orbital motion). The separate parallax values generally are in satisfactory agreement and the adopted results for each star are based on the combined normal equations. An average difference of $+0''.001 \pm 0''.001$ is found at Sproul Observatory for the independent parallax determinations of 85 stars from the two coordinates in the sense right ascension *minus* declination. This systematic difference is small enough to give us some reassurance on the subject of systematic errors in parallaxes.

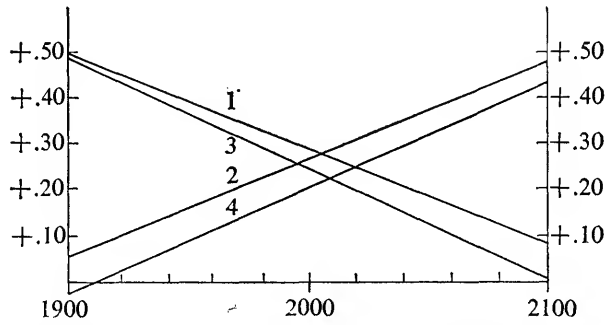

Fig. 8.2. *Dependence paths for four-star reference configuration of BD + 5°1668.*

The Sproul values of the parallaxes, reduced to absolute, average $+0''.003 \pm 0''.001$ (p.e.) more than the values given in the *General Catalogue of Trigonometric Stellar Parallaxes* and its supplement.[10]

7. Precision parallaxes: example, BD + 5°1668

An example of a parallax determination of particularly high accuracy is given by the star of large proper motion BD + 5°1668 (7^h24^m4, $+5°32'$, 1900; vis.

[10] See footnote 7, page 120.

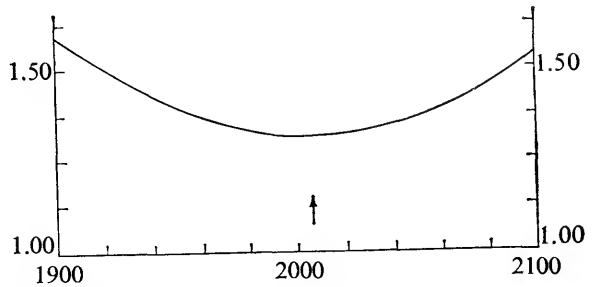

Fig. 8.3. *Inverse weight for position of BD + 5°1668 at different epochs.*

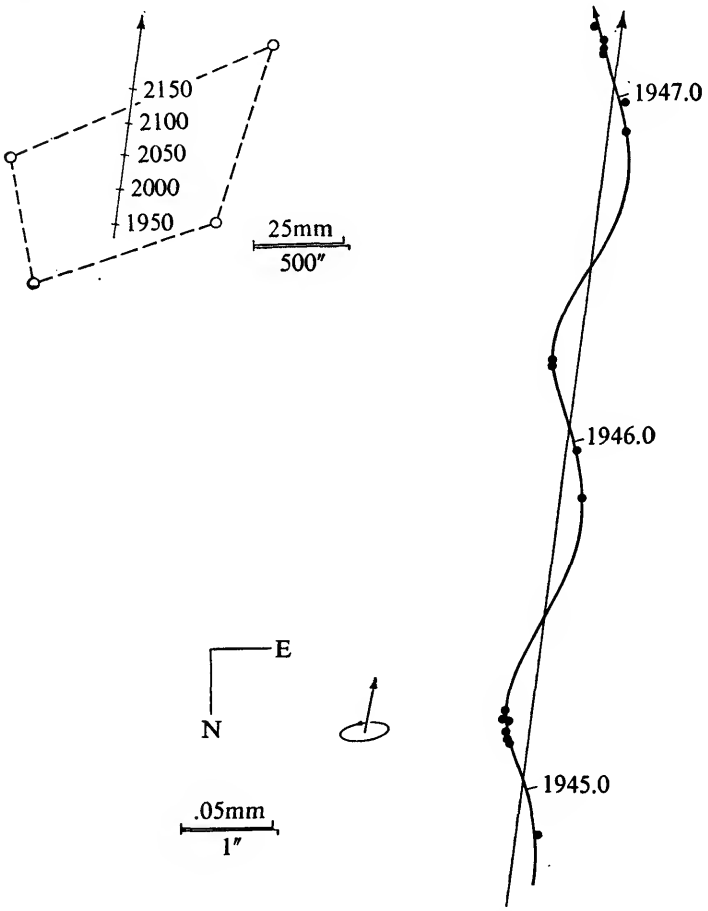

Fig. 8.4. *Proper motion and parallax of BD + 5°1668.*

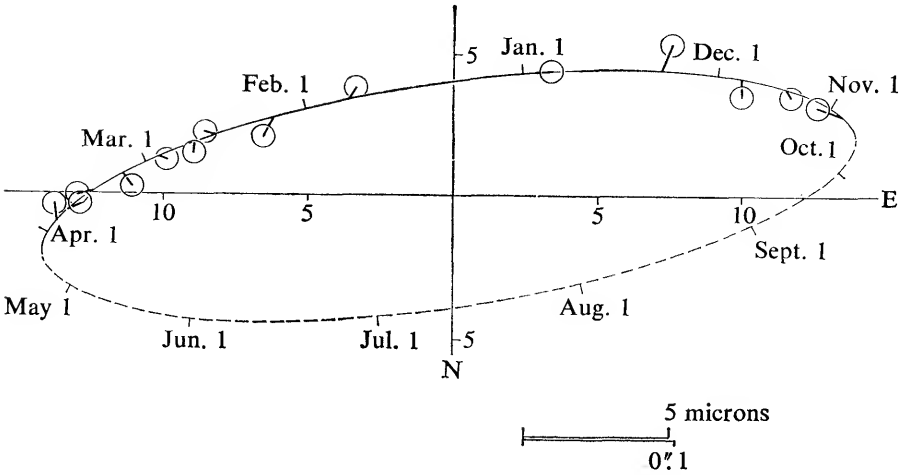

Fig. 8.5. *Normal places (1937–1947) of parallax displacements of BD + 5°1668.*

mag. 10.1, sp. M4, $\mu = 3''.72$ in 170°).[11] A parallax determination has now been made from the material obtained with the Sproul refractor from 1937 to 1965 (Figures 8.2, 8.3, 8.4, 8.5). Four reference stars were used; because of the large proper motion the dependences were changed yearly (Table 8.2).

Table 8.2. BD + 5° 1668 DEPENDENCES AND INVERSE WEIGHT
(Greatest geometric accuracy is reached in the year 2007.)

Epoch	Dependences				Inverse Weight $1 + [D^2]$
	1	2	3	4	
1920	.457	.094	.434	.015	1.407
1940	.415	.137	.387	.061	1.344
1960	.372	.180	.340	.108	1.298
1980	.330	.223	.293	.154	1.268
2000	.287	.266	.246	.201	1.254
2020	.244	.309	.199	.248	1.256
2040	.202	.352	.152	.294	1.274
2060	.160	.395	.104	.341	1.308
2080	.117	.438	.057	.388	1.359
2100	.075	.481	.010	.434	1.425

[11] Peter van de Kamp, "Parallax and Proper Motion of BD + 5° 1668," *The Astronomical Journal*, 53 (1948): 229–233. [This paper covers the first decade of the observations; later data are as yet unpublished.]

Measurements were made on 718 plates with 2444 exposures, taken on 194 nights; the total night weight amounts to 510. The resulting values for the relative parallax are:

Right ascension:	$+0''.2623 \pm 0''.0021$
Declination:	$+0''.2759 \pm 0''.0112$
Combined:	$+0''.2627 \pm 0''.0020$

The combined value is adopted for further use.

To reduce the relative values to absolute we add the parallax of the reference background (Section 4). For the average visual magnitude 10.1 of the reference stars, and the galactic latitude $+12°$, the mean secular parallax is $0''.0135$. Assuming a solar velocity of 20 km/sec, an annual parallax of $0''.0032$ is found. When reduced to absolute the Sproul value for the parallax of BD $+ 5°1668$ is therefore $+0''.266$, in excellent agreement with other photographic values $+0''.263 \pm 0''.008$ (Van Vleck), $+0''.264 \pm 0''.010$ (McCormick), and $+0''.262 \pm 0''.008$ (Yale).

The residuals after allowing for parallax and proper motion are small; they are represented by a probable error of unit weight of only $\pm 0''.031$. The residuals do not appear to be random; they strongly indicate a systematic displacement of the star, varying with the time. Such a periodic pattern of the residuals may be attributed to the presence of an unseen companion object of low mass (Chapter 12).

Suggested readings

K. Aa. Strand, "Trigonometric Stellar Parallaxes," *in* his *Basic Astronomical Data* (Stars and Stellar Systems, Vol. III). University of Chicago Press, 1963, pp. 55–63.

9 Quadratic Time-Effects. Secular Acceleration. Transitions.

Series of astrometric plates taken over a long period of time unavoidably involve secular terms, owing to the proper motions of both central and reference stars. The proper motion of the central star results in linear time changes in the dependences of the reference stars, and these changes in turn result in a linear time change in the dependence-mean proper motion of the system of reference stars. The principal result is a quadratic time effect, which must be carefully evaluated in order to separate it from a true secular proper motion effect or from a long-range perturbation effect. In long-range problems knowledge of the proper motions of the reference stars is therefore mandatory. In addition there is a secular change in parallax, which generally is of less concern.

Quadratic time effects must also be considered if it is desired to compare stellar paths measured on different reference systems.

1. Spurious secular acceleration and parallax effects

The effect of the proper motion and parallax of the reference stars on the reduced position of a central star changes with the time along the stellar path. The effect is most simply expressed through the changes in dependences, rather than through plate constants.

The plate reduction of a measured position may be written as

$$X = [Dx_s] + X' - [Dx'], \tag{9.1}$$

limiting ourselves to one coordinate. Here X' and x' represent the measured positions of central and reference stars. Full plate-constant reduction is insured by changing the dependence sufficiently often; hence the measured positions x' may be assumed to have been made in the coordinate system defined by the positions x_0 of the reference stars at an arbitrary zero epoch. Hence, in the usual notation,

$$x' = x_0 + \mu_x t + \pi P_\alpha. \tag{9.2}$$

The ideal reference system (x_0) would have neither proper motion nor parallax, in which case the reduced position would be

$$[Dx_s] + X' - [Dx_0]. \tag{9.3}$$

Compared with the ideal, fixed reference stars, an effect

$$-[D(x' - x_0)] \tag{9.4}$$

is therefore introduced into the reduced position X of the central star. This effect may be written as

$$-t[D\mu_x] - P_\alpha[D\pi]. \tag{9.5}$$

The first term represents a uniformly accelerated motion,

$$-t[D_0\mu_x] - t^2[\Delta D\mu_x]. \tag{9.6}$$

This is, with the opposite sign, the motion of the reference background, consisting of the reflected dependence mean proper motion at the zero epoch, $-[D_0\mu_x]$, and the reflected secular acceleration of this background, amounting to $-2[\Delta D\mu_x]$ yearly.

The second term of expression (9.5) represents a uniformly changing annual parallax of

$$-P_\alpha[D_0\pi] - P_\alpha t[\Delta D\pi]. \tag{9.7}$$

This is, with the opposite sign, the effect of a uniformly changing annual parallax, consisting of the negative dependence mean parallax at the zero epoch, $-[D_0\pi]$, and the negative yearly secular change of this mean parallax, $-[\Delta D\pi]$.

The apparent secular changes in proper motion and parallax caused by the reference stars may be quite appreciable and may well be of the same order of size as the true secular changes in these quantities.

2. True secular acceleration

For a nonaccelerated motion, the perspective secular changes along and perpendicular to the radius vector are simply the centrifugal and Coriolis accelerations in the rotating coordinate system defined by the radius vector joining sun and star:

1. Perspective secular change in the line of sight equals centrifugal acceleration:

$$r\left(\frac{d\theta}{dt}\right)^2, \tag{9.8}$$

a quantity which is, of course, always positive.

2. Perspective secular change perpendicular to the line of sight equals Coriolis acceleration:

$$-2\frac{dr}{dt}\frac{d\theta}{dt}. \tag{9.9}$$

The angular value of the Coriolis acceleration, as viewed from the sun, is given by

$$-2\frac{dr}{dt}\frac{d\theta}{dt}\frac{1}{r}. \tag{9.10}$$

We shall next express the yearly secular changes in conventional astronomical units. The distance r is expressed in parsecs [1 parsec (psc) = 206,265 astronomical units (a.u.)]; the radial velocity V and its annual change ΔV are expressed in km/sec; the proper motion μ and its annual change $\Delta\mu$ are expressed in seconds of arc/year. Recall that 1 a.u./year = 4.74 km/sec; parallax $p'' = 1/r$ (psc). We now have the relations

$$\frac{dr}{dt} = \frac{V}{4.74 \times 206{,}265}, \tag{9.11}$$

$$\frac{d\theta}{dt} = \frac{\mu}{206{,}265}, \tag{9.12}$$

$$\frac{d^2\theta}{dt^2} = \frac{\Delta\mu}{206{,}265}. \tag{9.13}$$

Substituting in (9.8) and (9.10) and replacing r by $1/p$, we find

$$\Delta V = +2.30 \times 10^{-5}\frac{\mu^2}{p}\ \text{km/sec/year}, \tag{9.14}$$

$$\Delta\mu = -2''.05 \times 10^{-6} V\mu p/\text{year}. \tag{9.15}$$

For the sake of completeness, we add the expression for the secular change in parallax:

$$-\frac{1}{r^2}\frac{dr}{dt}, \tag{9.16}$$

or in conventional units,

$$\Delta p = -1''.02 \times 10^{-6} V p^2/\text{year}. \tag{9.17}$$

Both true and spurious acceleration are ordinarily small, but the accumulated effects increase with the square of the time and therefore become significant as time goes by.

The observed secular acceleration may be used for deriving the radial velocity V independent of the Doppler shift.[1] This procedure permits, in principle at least, a determination of the gravitational redshift, by correcting the observed redshift for the value of the radial velocity as determined geo-

[1] Jan H. Oort, "The Mass of van Maanen's Star," *Bulletin of the Astronomical Institutes of the Netherlands*, 6 (1932): 287.

metrically from the observed perspective acceleration and the well-known values of the proper motion and parallax.

In practice the situation is not favorable, since the secular changes in the proper motion and also in the parallax are unavoidably tied up with the apparent secular changes caused by the reference stars (Sections 1 and 6).

3. Application to Barnard's star

The above secular changes are largest for Barnard's star, $17^h55^m.4$, $+4°33'$ (1950), visual magnitude 9.54, spectrum M5V, for which

$$V = -108 \pm 2.5 \text{ km/sec (p.e.)},$$

$$\mu = 10''.31 \text{ (mostly in declination)},$$

$$p = 0''.545 \pm 0''.003.$$

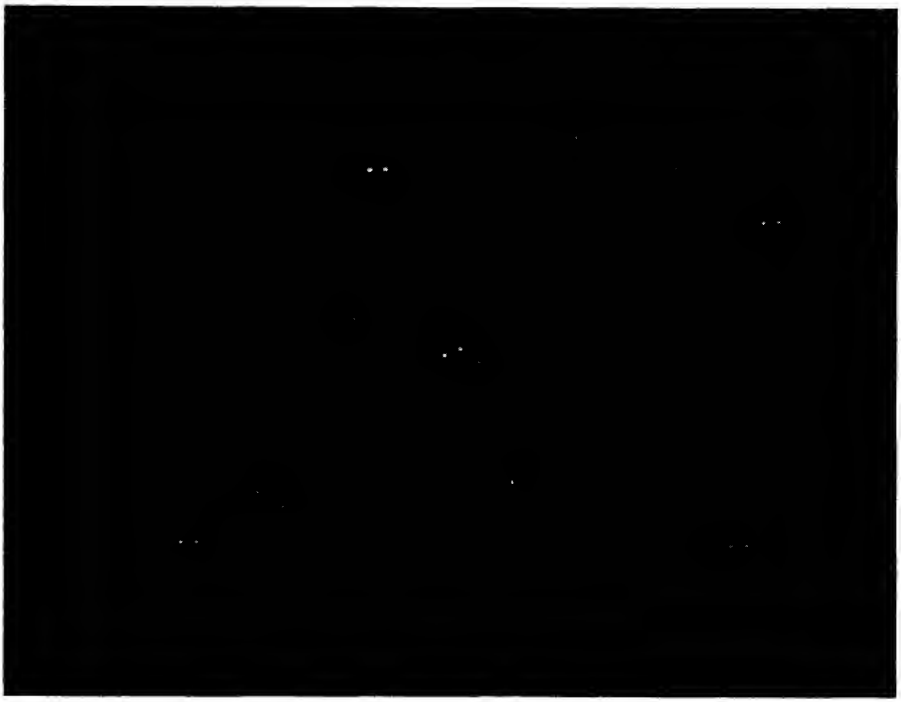

Fig. 9.1. *Proper motion of Barnard's star from July 31, 1938 to June 24, 1939. The recent epoch is to the left of the early one; the motion is mostly in declination (10".3 yearly). The scale of this photograph (1 mm = 11".6) is approximately one and a half times that of the original films. The exposures of two hours each were made by Roy W. Delaplaine with the twenty-four inch refractor of the Sproul Observatory, Swarthmore College. The focal length of the telescope is 10.93 meters, the scale 1 mm = 18".87.*

The corresponding yearly secular changes amount to

$$\Delta V = +0.0046 \text{ km/sec},$$

$$\Delta\mu = +0''.00124 \pm 0''.00003,$$

$$\Delta p = +0''.000032.$$

A recent study[2] based on intensive photographic material, covering the interval 1916–1961, has yielded a value for the acceleration that is in close agreement with the predicted value:

$$\Delta\mu = +0''.00119 \pm 0''.00004.$$

A more detailed presentation, in summary form, follows. The predicted values of the yearly acceleration are $-0''.00010$ and $+0''.00123$ in right ascension and declination, respectively. The probable error, $\pm 0''.00003$, of the predicted acceleration in declination could be reduced appreciably if the radial velocity were more accurately known.

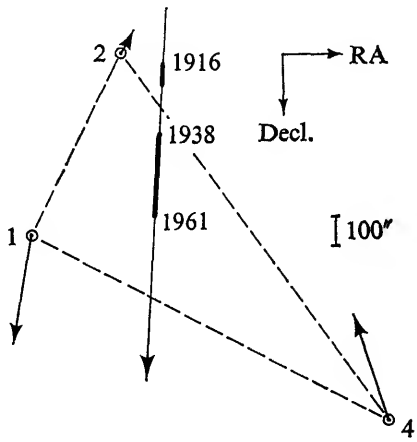

Fig. 9.2. *Path of Barnard's star. Reference stars and their proper motions per 10,000 years.*

Barnard's star has been photographed with the Sproul 24-inch refractor, the parallax series of 24 plates taken in the years 1916–1919 being followed by a series covering the interval 1938–1961 and totaling 2316 plates. The positions of Barnard's star were measured relative to a background of three reference stars. The reduced positions were combined into yearly means; after correcting for parallax, at least-squares solution yields a value for the proper

[2] Peter van de Kamp, "Perspective Secular Acceleration of Barnard's Star," *The Astronomical Journal*, 67 (1962): 284–285; and his "Astrometric Study of Barnard's Star," *Ibid.* 68 (1963): 515–521.

motion and an observed *apparent acceleration* of $+0''.00012 \pm 0''.00005$ (RA) and $+0''.00051 \pm 0''.00002$ (Decl.) which has to be corrected as follows.

Because of the large proper motion of Barnard's star, the weights, or dependences, of the reference stars change rapidly with time. The resulting secular changes of the dependence background create spurious secular changes in proper motion and parallax. For the present only the proper motion effects are of interest. The *spurious acceleration* amounts to $-2[\Delta D\mu_x]$ in RA and $-2[\Delta D\mu_y]$ in declination, respectively (Section 1). Here the ΔD are the yearly changes in the dependences of the reference stars; μ_x and μ_y, their proper motion components. The relevant data are given in Table 9.1. The proper

Table 9.1. BARNARD'S STAR. CHANGING REFERENCE BACKGROUND

Reference Star	μ_x	μ_y	ΔD
1	$-0''.0078$	$+0''.0365$	+0.0114
2	$+0''.0009$	$-0''.0018$	−0.0144
4	$-0''.0096$	$-0''.0350$	+0.0030

motions of the reference stars, relative to a background of 24 faint stars, were obtained from two pairs of plates over a 44-year interval.

The spurious acceleration amounts to $+0''.00026 \pm 0''.00003$ and $-0''.00067 \pm 0''.00003$ in RA and declination, respectively. Correcting for this effect, we find the *true perspective acceleration* to be $-0''.00014 \pm 0''.00006$ (RA) and $+0''.00118 \pm 0''.00004$ (decl.), which is in good agreement with the predicted values.

4. Transition between two reference systems: accuracy of transition function[3]

We shall now consider one central star measured on two different configurations numbering n and N reference stars respectively; generally n and N would be not more than 3 or 4. For observations made at the same epoch the transition from the n-star to the N-star background is given by the quantity (see Chapter 7, Section 3),

$$X_N - X_n = [Dx_s]_N - [Dx_s]_n + \xi_N - \xi_n,$$

or symbolically

$$X_{N-n} = [Dx_s]_{N-n} + \xi_{N-n}. \tag{9.18}$$

[3] Peter van de Kamp, "On the Transition from One Reference Background to Another in Long-range Astrometric Problems," *The Astronomical Journal*, 52 (1947): 226–229.

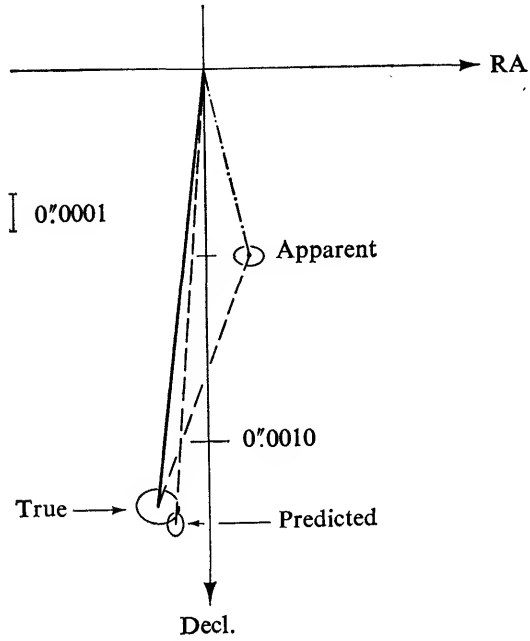

Fig. 9.3. *Perspective secular acceleration of Barnard's star. The true acceleration is found by correcting the observed apparent acceleration for the spurious acceleration. The small ovals represent the probable errors of the results.*

Apart from errors of observation the transition value changes with the time, since both the dependences and the positions of the reference stars do. As full plate constant reduction for any measured transition is ensured, we shall study the transition function by assuming the *measured* positions to be in the coordinate systems defined by the *true* positions (x_0) of the reference stars at an arbitrary zero epoch. The geocentric positions of the reference stars at any time t are represented by

$$x' = x_0 + \mu_x t + \pi P_\alpha. \tag{9.19}$$

Here μ_x is the annual proper motion, π the annual parallax, P_α the parallax factor. Since $\xi = X' - [Dx']$, substitution leads to

$$X_{N-n} = \{X' + [D(x_s - x_0 - \mu_x t - \pi P_\alpha)]\}_{N-n}. \tag{9.20}$$

If we now refer the values (x_0) for both sets of reference stars to the *same* origin, then $X'_N = X'_n$ so that finally:

$$X_{N-n} = \{[Dx_s] - [Dx_0] - t[D\mu_x] - P_\alpha[D\pi]\}_{N-n} \tag{9.21}$$

in which the first term is appreciable and the others, representing ξ_{N-n}, are small. It is practically impossible to evaluate a priori the last three terms

since x_0, μ_x, and π are difficult to obtain. It thus is necessary to derive the function from measured transition values.

Within the accuracy required by the dependence ephemeris the central star has a constant proper motion, and the momentary heliocentric dependences may be considered linear functions of the time

$$D = D_0 + t\Delta D \tag{7.20}$$

where the time t in years is counted from an arbitrary zero epoch; ΔD represents the yearly dependence changes. Substitution of (7.20) in (9.21) gives:

$$X_{N-n} = \{[D_0(x_s - x_0)] + t[\Delta D(x_s - x_0)] - t[D_0\mu_x] - t^2[\Delta D\mu_x] - P_\alpha[D_0\pi] - tP_\alpha[\Delta D\pi]\}_{N-n}. \tag{9.22}$$

The first three terms represent a linear function of the time, the fourth term an acceleration, and the last two terms an annual parallactic fluctuation, whose amplitude is a linear function of the time. If the last two terms can be ignored the transition function becomes a quadratic function of the time, and this quadratic effect will often prove negligible. If in addition the reference stars were motionless, the transition would still be a linear function of the time, because of the inherent approximate character of the standard frame.

In considering a possible transition from one configuration to another it becomes necessary to consider the accuracy of the measured transition. We shall limit ourselves to the case where each individual transition value is derived from measurements on one and the same plate, so that the error of the central star does not enter. The transition accuracy increases with the number of plates for which common reductions are made; of particular interest is the change with time in geometric weight, owing to the dependence changes. A careful study is helpful in determining the most desirable time interval and the number and epochs of individually measured transition values from which to derive the transition function. From the latter, transition values of adequate accuracy may then be extrapolated wherever needed to reduce other measurements.

In practice the adopted dependences do not change continually with the time; however, for purposes of computation the use of discrete dependence sets gives the same observed values of the transition function. For one dependence set the last three terms of (9.22) are constant within the errors of observation, hence an average transition value based on several plates holds for the average epoch of these plates. For rapidly changing dependences the range in the second and third term would generally be so small that the average plate epoch could be identified with the dependence epoch.

Let ϵ be the mean error of a measured position x', then the mean error E of one measured transition is given by

$$E^2 = \epsilon^2\{[D^2]_n + [D^2]_N\}. \tag{9.23}$$

Or, we can say the accuracy of the transition is represented by the inverse weight:

$$[D^2]_n + [D^2]_N, \tag{9.24}$$

the mean error of unit weight being ϵ. For three stars in each configuration, having equal dependences, this inverse weight amounts to .67; for four stars it would be .50. It should be kept in mind that for the transition value the "night errors" partially cancel out.

Since the heliocentric values D are linear functions (7.20) of the time, (9.24) can be written as

$$[D_0^2]_n + [D_0^2]_N + 2t\{[D_0\Delta D]_n + [D_0\Delta D]_N\} + t^2\{[\Delta D^2]_n + [\Delta D^2]_N\}. \tag{9.25}$$

Thus the inverse weight of the transition is a quadratic function of the time; the minimum value, i.e., the greatest accuracy, is reached for the epoch

$$t_m = -\frac{[D_0\Delta D]_n + [D_0\Delta D]_N}{[\Delta D^2]_n + [\Delta D^2]_N}. \tag{9.26}$$

A more favorable accuracy exists if the two configurations have one or more reference stars in common. Denoting the dependence differences for the common stars by d, the inverse weight of the transition amounts to

$$[D^2] + [d^2], \tag{9.27}$$

the first term referring to the stars differing in the two configurations. For this case the time of greatest accuracy of transition is reached at

$$t_m = -\frac{[D_0\Delta D] + [d_0\Delta d]}{[\Delta D^2] + [\Delta d^2]}, \tag{9.28}$$

where d_0 represents the dependence differences at the zero epoch and Δd the annual changes.

5. Addition of reference stars

The addition of one or more stars to a configuration always leads to an increase in geometric accuracy. (See also Chapter 7, Section 7.) The inverse weight of the reduced position is $1 + [D^2]$. Of the different possible sets of dependences for which $[D] = 1$, the conventional one based on a least-squares solution for plate constants gives a minimum value for $[D^2]$, so that the inverse weight of the reduced position is a minimum. The addition of one reference star to the configuration must lead to a new distribution of $[D]$ for which now $[D^2]$ is a minimum. This new minimum value could at most equal the old value if the dependence of the additional star were zero; if not, it must be smaller, even though slightly negative dependences for other stars may have made their appearance.

The addition of stars to a configuration may, however, lead to such a

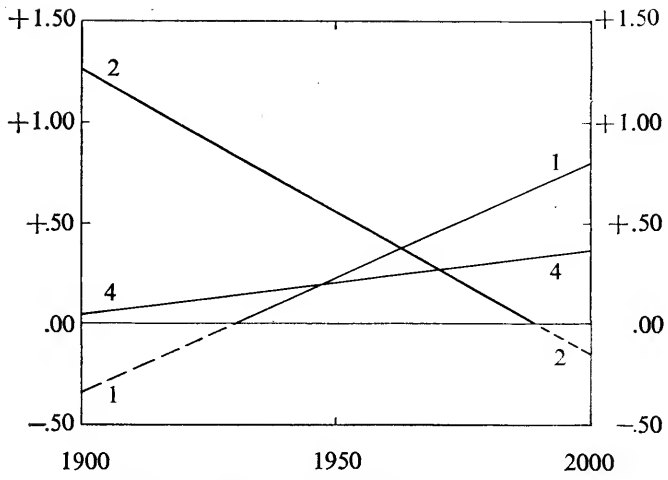

Fig. 9.4. *Dependence paths for reference stars in the three-star configuration 124 for Barnard's star.*

minute increase in accuracy that for reasons of economy it would be wiser to postpone action till some future period, when adequate transition values could still be extrapolated for the earlier material.

6. Addition of one reference star: example, Barnard's star

A special case is that of adding one reference star. If we count the time t from the epoch at which the dependence of the additional reference star becomes positive, the dependences D_0 and hence the quantities $[D_0x_0]$ and $[D_0\mu_x]$ are identical for both configurations for $t = 0$. Ignoring the parallaxes of the reference stars the transition function reduces to

$$X_{N-n} = \{[D_0x_s] + t[\Delta D(x_s - x_0)] - t^2[\Delta D\mu_x]\}_{N-n}. \tag{9.29}$$

The inverse weight of the transition may be written as

$$t^2\{\Delta D^2 + [\Delta d^2]\}, \tag{9.30}$$

which obviously is zero at the time when the dependence of the additional star crosses the zero value. At that time the transition function reduces to the difference between the dependence centers of the two standard frames, which for identical dependence sets represents the difference in origin for the two standard frames, save for rounding off errors imposed by the rigorous conditions $[x_s] = 0$. For all practical purposes there is little reason to measure the additional star near the epoch of zero dependence value.

In the 1940's an examination[4] of the available reference stars for an astro-

[4] Peter van de Kamp, "Present and Future Reference Configurations for Barnard's Star," *The Astronomical Journal*, 52 (1947): 229–233.

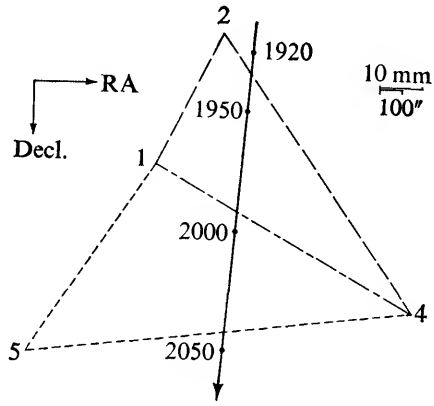

Fig. 9.5. *Reference stars and path of Barnard's star.*

metric study of Barnard's star led to the choice of stars 1, 2, and 4 (see Section 3). Maximum geometric accuracy for the reduced position of Barnard's star was reached in 1962, when $1 + [D^2] = 1.35$. However, the dependence of star 2 is decreasing rapidly; it will fall below +0.100 in the year 1981, and become negative in 1988 (Fig. 9.4). The addition of a new reference star is thus necessary; star number 5 appears to be in a suitable location (Fig. 9.5). The configuration 1245 will have a longer useful life than 124, since the dependence of star 2 will not drop below +0.100 until the year 2012 and will not become negative until 2027 (Fig. 9.6). Maximum geometric accuracy

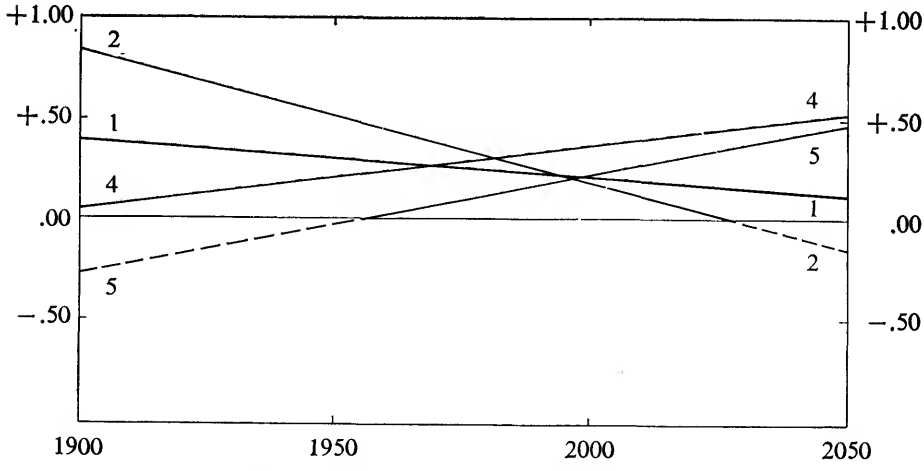

Fig. 9.6. *Dependence paths for reference stars in the four-star configuration 1245 for Barnard's star.*

for the reduced position of Barnard's star in the configuration 1245 will be reached in 1989, when $1 + [D^2] = 1.27$.

The relevant data for Barnard's star are listed in tables 9.2 and 9.3 and

Table 9.2. BARNARD'S STAR. DEPENDENCES AT DIFFERENT EPOCHS

Configuration	Reference Star	1900	1950	2000	2050
124	1	−0.327	+0.242	+0.810	+1.379
	2	+1.265	+0.545	−0.174	−0.894
	4	+0.062	+0.213	+0.364	+0.515
1245	1	+0.392	+0.299	+0.206	+0.113
	2	+0.843	+0.512	+0.180	−0.152
	4	+0.038	+0.211	+0.384	+0.558
	5	−0.273	−0.022	+0.230	+0.481

Table 9.3. INVERSE WEIGHT OF CONFIGURATIONS 125 AND 1245 AND OF TRANSITION BETWEEN THESE CONFIGURATIONS

Epoch	$1 + [D^2]$		Transition 124–1245
	124	1245	
1920	1.98	1.67	.306
30	1.72	1.56	.144
40	1.52	1.47	.053
50	1.40	1.40	.005
60	1.35	1.34	.010
70	1.36	1.30	.064
80	1.44	1.27	.172
90	1.60	1.27	.332
2000	1.82	1.28	.543

illustrated in Figures 9.2–9.8. Figures 9.4, 9.6, and 9.7 present the changes in the dependences with time, also called *dependence paths*. Figure 9.8 shows the changes with time of the inverse weight of the reduced positions of Barnard's star with respect to each of the two configurations and to the transition between them. These graphs as well as Figure 9.5 aid in understanding the choice of the first reference system 124 and in choosing the epoch

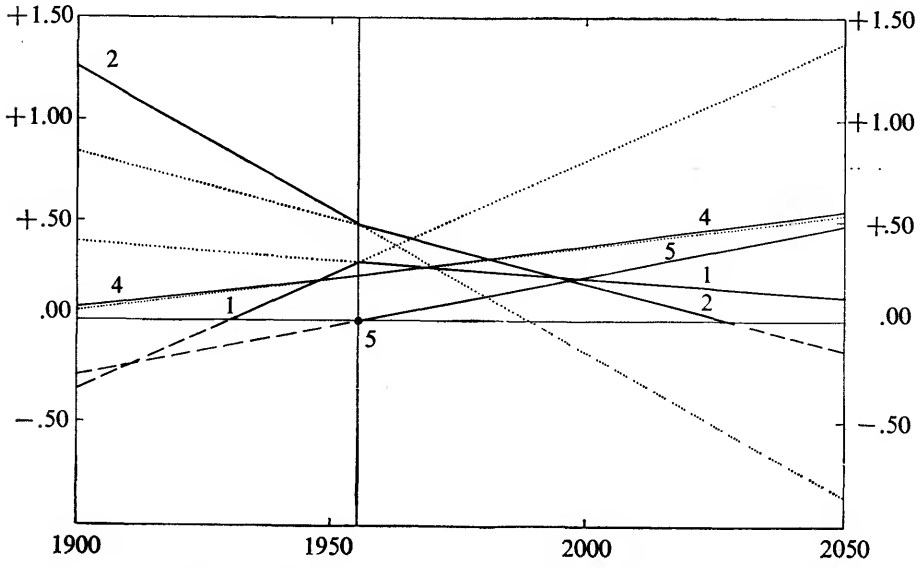

Fig. 9.7. *Dependence paths for reference systems 124 and 1245 for Barnard's star.*

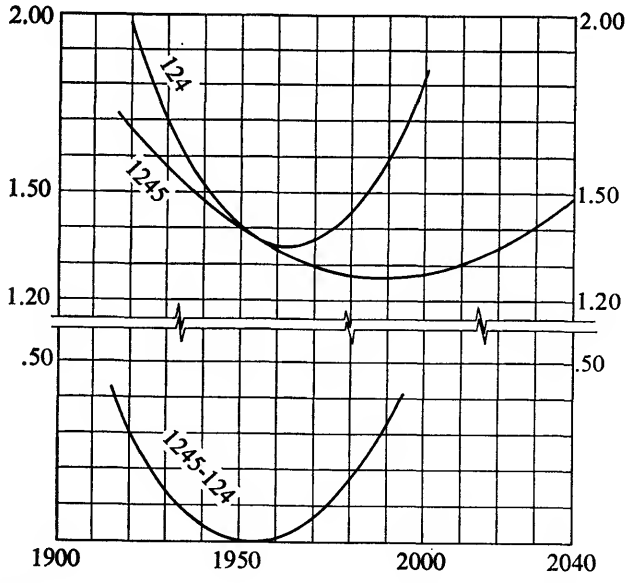

Fig. 9.8. *Inverse weight of reduced positions for Barnard's star* (above), *and of transition between reference systems 124 and 1245* (below).

at which a transition to the new reference system 1245 may be made. From 1945 to 1965 both configurations may be considered equivalent, the two dependence backgrounds differing by a transition value of very high observational weight. The dependence of star 5 did not become positive until 1954 and will not reach the value +0.100 until 1972. Hence there was little reason for measuring star 5 at first, and we had the advantage, practical and economic, of measuring only three reference stars until the middle nineteen-sixties. At that time it became desirable to shift to configuration 1245 and hence star 5 has been measured since 1966. The earlier measurements, all referred to the configuration 124, may be reduced to the configuration 1245 by establishing the transition function (9.29) from measurements at appropriately chosen epochs.

Sometime early in the twenty-first century another transition will have to be considered, since star 2 and, later, star 1 will lose their usefulness, as indicated by their dependence paths.

10 Visual Binaries

1. Introduction

The very abundance of physical double stars, or binary stars, classifies them as an important group of objects, deserving study for their own sake. In addition, they serve a utilitarian purpose in furnishing a means of obtaining stellar masses.

Historically, the first discoveries and studies of binaries were made by visual techniques,[1] which led to the designation "visual binaries." It would not be inappropriate to replace the designation *visual* by *astrometric*, i.e., the two-dimensional projection on the plane of the sky. Ideally, of course, the complete study of a binary orbit should be both *astrometric and spectroscopic.* Selection effects favor the spectroscopic discovery of short-period binaries among bright stars and the astrometric discovery of long-period binaries.

We shall limit ourselves to the astrometric technique and methods. Visual, photographic, and interferometer surveys have yielded "close" binaries that, as a rule, have proved to be physical pairs. Proper-motion surveys have revealed the so-called proper-motion binaries, which are characterized by the nearly identical proper motions of stars that may be widely separated. Although proper-motion binaries with components of nearly equal magnitudes and moderate separation are easily detected, binaries with large magnitude differences are more difficult to observe and large numbers undoubtedly remain to be discovered.

Visual observation of close astrometric binaries with appreciable magnitude differences is very difficult, and the orbital motion of the brighter component, or of the photocenter, becomes a valuable aid to discovery.

The most important orbital elements are the semi-axis major a (in seconds of arc) and the period of revolution P (in sidereal years). If, in addition, the

[1] P. Muller, "Techniques for Visual Measurements," *in* W. A. Hiltner, ed., *Astronomical Techniques* (Stars and Stellar Systems, Vol. II), University of Chicago Press, 1962, pp. 440–460.

parallax p'' is known the linear value of a in astronomical units is a''/p''. The combined mass of the two components A and B is then obtained through the relation[2]

$$M_A + M_B = \frac{4\pi^2}{G}\frac{a^3}{P^2} \tag{10.1}$$

in cgs units, where G is the constant of gravitation. In terms of the astronomical unit for distance, sun's mass, and sidereal year, $G = 4\pi^2$, and we have the simple harmonic relation[3]

$$M_A + M_B = \frac{a^3}{P^2}. \tag{10.2}$$

The separate masses may be obtained by locating the center of mass through its nonaccelerated motion on a background of other stars. The mass ratio of double star components can be measured as the inverse ratio of the scale of the observed orbital displacements of the components relative to the center of mass. The latter is revealed through its uniform rectilinear motion relative to a background of reference stars. If the total mass of the binary system is known, the separate masses may thus be obtained. This type of work has been done both through micrometer and meridian-circle observations. At present, the procedures commonly followed are those of long-focus photographic astrometry. The observed positions are represented by three terms: the uniform rectilinear motion of the center of mass, the annual parallactic motion, and the orbital motion of either or both components, which, combined with the known relative orbit of the two components, yields the mass ratio, commonly represented by the fractional mass

$$\mathrm{B} = \frac{M_B}{M_A + M_B} \tag{10.3}$$

of the fainter component.

It frequently happens that the photographic images of the two components are blended. In this case the semi-axis major α of the so-called *photocentric* orbit may be measured. The following relation exists:

$$\alpha = (\mathrm{B} - \beta)a \tag{10.4}$$

where a is the semi-axis major of the relative orbit of the two components and β is the relative luminosity of the fainter component,

$$\beta = \frac{l_B}{l_A + l_B}. \tag{10.5}$$

Provided β is known from visual observations, the mass ratio, B, may still be derived:

[2] Peter van de Kamp, *Elements of Astromechanics*, San Francisco and London, W. H. Freeman and Company, 1964, equation 2.43.

[3] *Ibid.*, equation 2.45.

$$B = \frac{\alpha}{a} + \beta. \tag{10.6}$$

The determination of mass-ratio, both for resolved and unresolved astrometric binaries, will be discussed in Chapter 11.

2. Astrometric observations

Long-focus telescopes and accessories are the best instruments with which to obtain the basic information for visual binaries: primarily and ideally, the relative location of the two components at different epochs.

The original visual techniques that were carried out with some type of micrometer, or even by using the meridian circle, have been supplemented by several others. The multiple-exposure photographic technique (Section 3), has proved to be very accurate and remarkably free from systematic errors, provided the photographic images are well separated. For pairs of equal magnitude, accurate photographic measures are obtained down to separations of 2″ or even less. For unequal pairs, the lower limit of successful separation is higher, say 3″ or 4″, with objective gratings used to provide magnitude compensation. The photographic method for well-separated images is superior to the visual method. Visual observations of double stars separated by more than 3″ or 4″ generally cannot be justified. Such measures are likely to do more harm than good when they are included in orbit calculations. On the other hand, separations from 2″ down to the resolving power of the telescope, provide the range *par excellence* for micrometer observations.

Interferometer techniques are successfully applied to pairs too close for the direct visual technique. Measures down to 0″.04 have been made.

All methods yield an attainable accuracy of about 0″.01, or even smaller, if proper precautions are taken. Although systematic errors may easily creep in if the methods are used beyond the range of their capabilities, the position angles are generally relatively free from systematic errors.

Experiments with image-tube techniques may be expected to yield accurate measures and resolving power in the hitherto exclusive domain of the visual observer. With the image intensifier, exposure times are shortened and brief periods of good seeing may be utilized. Photoelectric scanning methods appear very promising.

The position of the fainter secondary component (B) relative to the brighter primary (A) of a visual binary is generally expressed in polar coordinates, as the separation, or distance ρ, in seconds of arc, and the position angle θ in degrees, counted from north through east. These quantities may be observed directly or derived from the corresponding rectangular components

$$\Delta\alpha \cos\delta = \Delta x \qquad \text{and} \qquad \Delta\delta = \Delta y,$$

such as are commonly measured by the photographic method.

The following relations exist:

$$\begin{aligned} \Delta\alpha \cos\delta &= \Delta x = \rho \sin\theta, \\ \Delta\delta &= \Delta y = \rho \cos\theta; \end{aligned} \tag{10.7}$$

$$\rho = \sqrt{(\Delta x)^2 + (\Delta y)^2},$$

$$\theta = \arctan \frac{\Delta x}{\Delta y}. \tag{10.8}$$

To permit a comparison of observations at different epochs all position angles are reduced to a standard equator, say of the year 2000. The position angle at epoch t is corrected to the equator of epoch 2000 by adding (equation 3.2),

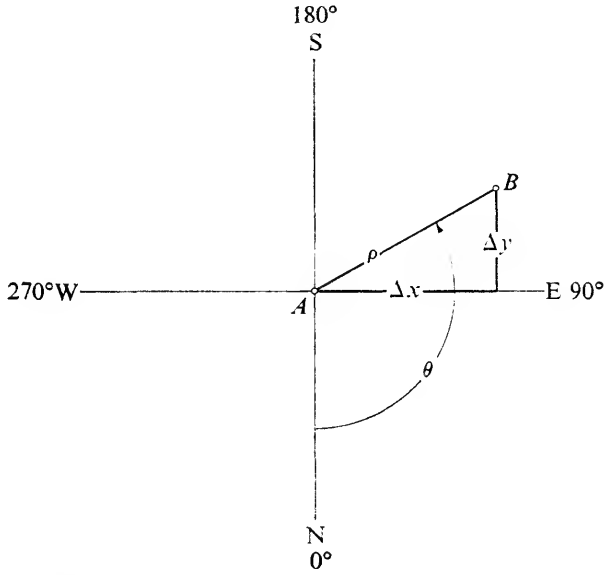

Fig. 10.1. *Relative position of double-star components.*

$+0^{\circ}0056 \sin\alpha \sec\delta(2000 - t)$ for precession, and $+0^{\circ}00417\, \mu_\alpha \sin\delta(2000 - t)$ for proper motion, where μ_α is the annual proper motion in right ascension expressed in seconds of time. The latter correction follows from equation (2.18) by replacing $\Delta\alpha$ by $(2000 - t)\, \mu_\alpha$.

3. Multiple-exposure technique

The photographic technique has proved to be extremely accurate for the measurement of wide pairs—about 3″ and wider. The precise technique of long-focus photographic measurements of double stars was first developed by

E. Hertzsprung,[4] with the visual refractor of 12.5-meter focal length of the Potsdam Observatory during the years 1914–1919. This type of observation has been continued by others, notably by K. Aa. Strand.[5] Again the photovisual technique has yielded positional results of extreme accuracy.

The photographic method is limited to doubles with separations exceeding about 0.15 mm on the plate. Below this limit it is, in general, difficult to obtain satisfactory exposures. The neighboring images affect each other, causing either a diminution or an increase in the separation between the images. Hence there is every reason to observe the "close" double stars visually, either by micrometer or by interferometer, and to limit the photographic observations to wider pairs for which the images are clearly separated on the photographic plate.

In observing the relative positions of the components of a resolved astrometric binary by the photographic method, the magnitude error is compensated by the use of a coarse grating in front of the objective. Such a grating produces diffraction images symmetrically located with respect to the central image; these images can be given any desired intensity with respect to the central image by proper choice of the thickness of the bars and of their spacing.

The linear separation, Δ, between the central and nth-order images in the focal plane is given by the formula

$$\Delta = \frac{nF\lambda}{l + d}, \tag{10.9}$$

where F is the focal length, λ the effective wavelength, l the width of the space between the bars, and d the width of a bar. The extinction in magnitudes for the central image is

$$5 \log \frac{l + d}{l}. \tag{10.10}$$

The difference in magnitude between the nth-order and central image is given by

$$\Delta m = 5 \left(\log \frac{nl\pi}{l + d} - \log \sin \frac{nl\pi}{l + d} \right). \tag{10.11}$$

The diffraction images are really spectra; in the photovisual technique, however, the first- and even higher-order spectra look like star images because of the narrow range in wavelength (Chapter 6, Section 3).

[4] E. Hertzsprung, *Photographische Messungen von Doppelsternen von 1914.0 bis 1919.4* (Publikationen des Astrophysikalischen Observatoriums zu Potsdam, Vol. 24, No. 75), Potsdam, 1920.

[5] K. Aa. Strand, *Photographic Measurements of Six Double Stars and the Computation of Their Orbits with Special Attention to These Measurements* (Leiden Annals, Vol. 18, Pt. 2), 1937; and his "Photographic Observations of Double Stars Made with the 24-inch Sproul Refractor," *The Astronomical Journal*, 52 (1946): 1–21.

By employing a grating for which the first- or higher-order spectra of the brighter component are of approximately the same intensity as the central image of the fainter component, a compensation for possible magnitude error is provided by using the mean of the measured positions of the two spectral images instead of the central image. So long as the difference in intensity between the images does not exceed half a magnitude, the magnitude error is usually negligible; it is therefore sufficient to have a limited number of gratings, producing first-order spectra that are a whole number of magnitudes fainter than the central image. For example, in his work with the Sproul refractor, Strand used four gratings, made of duraluminum, giving differences of 1, 2, 3, and 4 magnitudes, respectively, between the central image and the first-order spectra (Figs. 10.2 and 10.3).

Multiple exposures are taken; each plate has two rows of exposures, in a west-to-east sequence parallel to the daily motion. After a series of about thirty to forty exposures has thus been obtained, either manually or by some automatic device, the telescope is given a small shift in declination, and the double star itself or a neighboring bright star is used to impress a trail giving the equator of the date. As a rule, a second row of exposures is then taken, followed by a second trail. The exposure times never exceed 30 seconds; on the other hand, no exposures below 3 seconds are used.

The relative position of the two components is obtained from the difference in $\Delta\alpha \cos \delta$ (Δx) and $\Delta\delta(\Delta y)$, measured, for example, on a precision long-screw machine. In each coordinate the plates are measured with the film turned toward the microscope and also through the glass, the plate being turned 180° between the two measures around an axis parallel to the vertical bisecting wire in the microscope. This eliminates errors arising from inaccuracy in the orientation between the axis of the screw, the bisecting wire, and the motion of the plate carriage at right angles to the screw.

For an average plate with forty to fifty measured exposures, the relative position Δx, Δy of the two components is obtained with a probable error of $\pm 0''.006$. Part of this error, about $\pm 0''.004$, is the personal error of the measurer; it affects the distances rather than the position angles. As a rule, the error in orientation arising from inaccuracies in the trail is below 0°.01 for any one plate and would therefore be less than $0''.002$ for a pair with a separation of $10''$.

One good photographic exposure with a long-focus refractor yields about the same accuracy as one visual measure with the micrometer. More than a hundred visual observations are required to obtain an accuracy comparable to that of one photographic plate, taken and measured as described above. These visual observations are all independent measures, each representing a single night's observations by one observer, and the mean result is considered to be made up of observations by many observers with different tele-

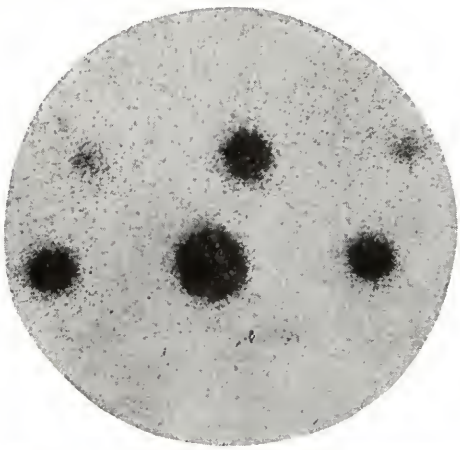

Fig. 10.2. *A 5-second exposure of Castor, enlarged 75×. The separation of the components is 3″.74, or 0.198 mm on the plate. The first-order spectra are 1 magnitude fainter than the central image. Photographed December 1, 1939, by K. Aa. Strand, with the Sproul 24-inch refractor, aperture reduced to 13 inches, Eastman IV-G emulsion, Wratten No. 12 (minus blue) filter. Scale of original photo: 1 mm = 18″.87.*

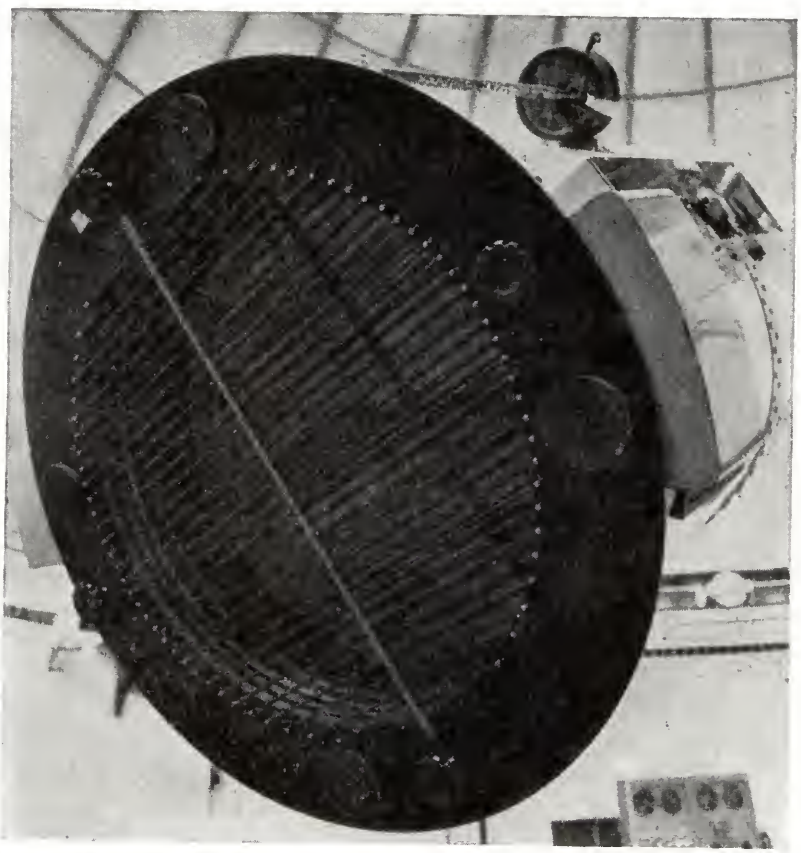

Fig. 10.3. *Objective of 26-inch refractor at the U.S. Naval Observatory, with an objective grating in front. (Official U.S. Navy photograph.)*

scopes. In visual observations of double stars, systematic and personal errors are appreciable; generally not more than a few settings make a single night's observation, and not more than three or four observations each year are warranted.

The superiority of photographic observations is even more pronounced if the distances are considered. The visually observed distances between the components may be off as much as 0″.06, even though they represent the mean of many observers with different telescopes. The systematic errors in visual measures do not cancel out, even over several decades, and may be found to depend on the separation of the components. For example, in the case of 70 Ophiuchi, the visual distances have been found to be systematically too small when the separation is over 2″.5 and systematically too large when the separation is less than 2″.5. Such a result may be due to one observer, who may have observed the star for several decades. In general, in very bright pairs such as γ Virginis, for example, the visual measurements of distances are too large. Systematic errors are not entirely absent in photographic measures, but they are only about one-tenth as large, and their effect can be partly eliminated by repeated measurements of the same plate by different persons. In other words, photographic measurements take us one decimal further. It pays to have forty to fifty measurable images on each plate, to take four to six plates each year, and thus reach a potential accuracy of about $\pm$0″.002 to $\pm$0″.003 (p.e.).

Gratings consisting of a limited number of thin wires and noncircular diaphragms are used for double stars with components differing greatly in brightness.[6] Although the validity of this unusual approach is not yet well established the technique has been applied, for example, to the double star Sirius, whose components differ more than ten magnitudes in brightness; their separation ranges from 3 to more than 11 seconds of arc.[7]

4. Apparent orbit

The determination of the orbit of a celestial object involves its orientation in space. The earth's orbital motion complicates the observed orbital motion of planets and comets. The latter complication is conspicuously absent from the *relative orbit* of the components of a binary star.

We shall limit ourselves to the astrometric approach to binaries, or the study of orbits as seen projected on the sky, i.e., perpendicular to the line of sight. We shall distinguish between *resolved* and *unresolved astrometric binaries*, depending on whether the components are observed separated or blended.

[6] G. B. van Albada, "Telescope Diaphragms for the Observation of Faint and Fairly Close Binary Components," *Contributions from the Bosscha Observatory*, No. 6 (1958): 3–29.

[7] Sarah Lee Lippincott and Michael D. Worth, "The Double Star Sirius," *Sky and Telescope*, 31 (1966): 4–6. See also footnote 6.

The relative orbit in its own plane is referred to as the *true orbit*, its orthogonal projection on the plane of the sky is the *apparent orbit*. The latter is obtained from observations of the relative positions obtained at different epochs; the first step is to draw the apparent orbit through the inherently imperfect observations in such a manner that it represents the projection of Keplerian motion. That is to say, the apparent ellipse has to obey the law of equal areas. Ideally, the observations should cover at least one full period of revolution. If not, an attempt is made to complete the apparent orbit on the basis of the observed part of the orbit.

To permit a more accurate drawing of the orbit it is generally desirable to make two diagrams—one of the position angle θ and one of the distance or separation ρ, both plotted against the time t, i.e., the epoch of observation. These diagrams permit an examination of the internal consistency and reveal extreme discordances of the observations. Normal places may be used by combining several observations. Except for very short periods the observations are usually combined into weighted means for each year. Visual and photographic observations are kept separate, and different weights are assigned to the corresponding normal points. For a general statement we may say that photographic normal places have about ten times the weight of visual normal places. In visual observations of double stars the distances are generally much less reliable than the position angles. Hence, whenever possible, the visual distances are not used, in combination with more recent photographic observations, only the position angles.

The projected law of areas requires that $\rho^2(d\theta/dt) = \text{constant}$: $d\theta/dt$ may be expressed in radians per year; the quantity $\rho^2(d\theta/dt)$ is called the areal constant. By drawing smooth interpolation curves through the normal places the quantities ρ and $d\theta/dt$ can be read off for a number of epochs, and the constancy of $\rho^2(d\theta/dt)$ tested. Thus the reliability of the observations is revealed, and the interpolation curves may be adjusted to some extent, in order to yield more nearly equal values of $\rho^2(d\theta/dt)$ for different times. Adjusted interpolation curves are used to draw the apparent orbit, which most nearly satisfies the law of areas.

5. Orbital elements: dynamical and geometric

The true orbit in space of the companion relative to the primary are defined by seven elements that fall into three groups.

Dynamical elements. P = period, e = eccentricity, T = epoch of periastron passage. P and T are usually expressed in years. The mean motion in degrees per year is denoted by

$$n = \frac{360^\circ}{P}.$$

Scale of orbit (i.e., semi-axis major or mean distance a, the average between periastron and apastron distances). For visual binaries this element is expressed in seconds of arc and may be converted to linear measure (astronomical units) if the parallax p is known, by the relation

$$a(\text{a.u.}) = \frac{a''}{p''}.$$

The dynamical elements P, e, and T, and the scale a determine the position in the true orbit. It is often useful to introduce the *unit orbit*, defined by the dynamical elements only, which is converted into the true orbit by applying the scale factor a.

Orientation elements (Fig. 10.9). Ω represents the position angle of the ascending node—i.e., the point on the intersection of the orbital plane and the plane of the sky at the primary—at which the companion recedes from us. In the absence of appropriate radial-velocity observations the ascending node cannot be distinguished and Ω refers simply to that nodal point for which $\Omega < 180°$.

ω, sometimes referred to as "longitude of periastron," is the angle in the plane of the true orbit from the ascending node (or nodal point) to periastron, in the direction of orbital motion.

i is the inclination of the orbital plane to the plane tangent to the sky. For direct motion, i.e., position angles increasing with the time, i is between 0° and 90°, for retrograde motion $90° < i < 180°$.

If $i = 0°$ or 180°, Ω is taken to be 0°, and the position angle of periastron is ω for direct ($i = 0°$), $360° - \omega$ for retrograde ($i = 180°$) motion.

If $e = 0$, take $\omega = 0°$, and T as the epoch of nodal passage.

It is logical and convenient to carry out the derivation of the true orbit from the apparent orbit in two steps. First, derive the dynamical elements, then derive the scale and the orientation elements, either by geometric or by analytical methods.

Scale and orientation elements are the "conventional" *geometric elements;* these four elements may be transformed into other "natural" geometric elements (Section 9).

The designation *Campbell elements* is used to include the dynamical elements P, e, and T, the scale a, and the orientation elements Ω, ω, and i.

6. Keplerian motion; elliptical rectangular coordinates

The location in an elliptical orbit is determined by the three *dynamical elements:* period P, eccentricity e, epoch of periastron passage T, plus the epoch of observation t. This is called Kepler's problem and the solution is easily followed by introducing Kepler's *auxiliary circle,* which is located in

the orbital plane tangent to the orbit in periastron and apastron and from which the elliptical orbit may be derived by the foreshortening factor $\sqrt{1-e^2}$ perpendicular to the major axis. The radius of Kepler's circle is therefore equal to the semi-axis major a of the orbit.

The angular coordinate of the position in the ellipse is the *true anomaly* v counted from periastron in the direction of orbital motion. The position of the corresponding location in the auxiliary circle is measured at the center by the *eccentric anomaly*, E, also counted from periastron in the direction of orbital motion. It is convenient to introduce the *unit orbit* and the *unit circle*, for which $a = 1$. The radius vector FS is the projection of the radius vector FS', which sweeps over equal areas of the circle in equal intervals of time. The area of the unit circle is π, and is swept over in one period P. Hence the area $FS'P$ in the unit circle, covered in the time $t - T$ since periastron passage, amounts to $\pi(t-T)/P = n/2(t-T)$. This area may be expressed as the difference between the sector $S'OP$ and the triangle $OS'F$, i.e.,

$$S'OP - OS'F = FS'P,$$

or

$$\frac{E}{2} - \frac{e \sin E}{2} = \frac{n}{2}(t - T)$$

whence

$$E - e \sin E = n(t - T). \tag{10.12}$$

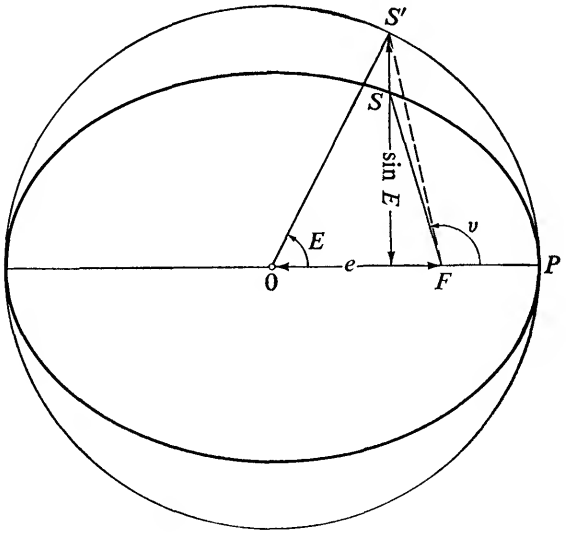

Fig. 10.4. *Kepler's problem. Relation between position S on unit orbit and corresponding position S' on auxiliary unit circle.*

The right-hand side of the equation is also called the *mean anomaly* M, and thus we arrive at *Kepler's equation*

$$E - e \sin E = M, \tag{10.13}$$

a transcendental functional relation between E, e and M.

E as a function of M and e has been tabulated.[8]

To obtain the position in the orbit from E, we proceed as follows: v may be calculated from[9]

$$\tan \frac{v}{2} = \sqrt{\frac{1+e}{1-e}} \tan \frac{E}{2}, \tag{10.14}$$

and r from

$$r = a(1 - e \cos E),$$

and thus the position in the orbit is known.

It is convenient to introduce the *elliptical rectangular coordinates* x, y, in the *unit orbit*, given by

$$\begin{aligned} x &= \cos E - e, \\ y &= \sin E \sqrt{1 - e^2}. \end{aligned} \tag{10.15}$$

Since

$$\begin{aligned} r \cos v &= a(\cos E - e), \\ r \sin v &= a \sin E \sqrt{1 - e^2}, \end{aligned} \tag{10.16}$$

the elliptical rectangular coordinates in the orbit of semi-axis major a are thus given by

$$\begin{aligned} r \cos v &= ax, \\ r \sin v &= ay. \end{aligned} \tag{10.17}$$

Tables exist for x and y as functions of e and M, so that E need not even be computed.[10]

7. Relation between true and apparent orbits

Projection of the Keplerian motion yields an elliptical motion for the secondary, which still obeys the law of areas with respect to the primary, although this is not at the focus of the apparent ellipse. The center of the apparent ellipse corresponds to the projected center of the true ellipse.

[8] J. J. Åstrand, *Hülfstafeln zur leichten und genauen Auflösung des Kepler'schen Problems*, Leipzig, Wilhelm Engelmann, 1890.

[9] Peter van de Kamp, *Elements of Astromechanics*, San Francisco and London, W. H. Freeman and Company, 1964, equation 1.47.

[10] *Tables of X and Y* (Union Observatory Circular Number 71), 1927. Otto G. Franz and Betty F. Mintz, *Tables of x and y Rectangular Coordinates* (Astronomical Papers Prepared for the Use of The American Ephemeris and Nautical Almanac, Vol. 19, Pt. 1) U.S. Government Printing Office, 1964.

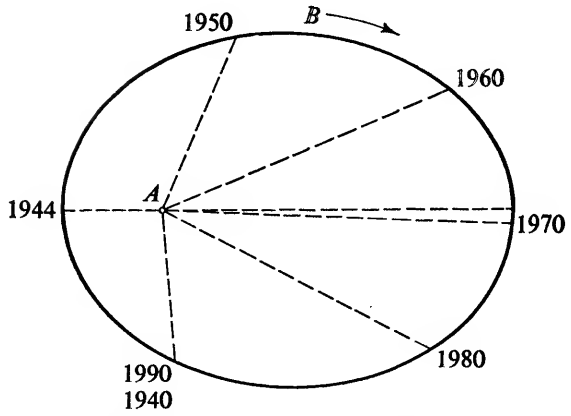

Fig. 10.5. *Keplerian motion in true orbit for the visual binary Sirius.*

Generally no valid analysis of the orbit can be made till the part of the orbit that has been covered is sufficient to permit an acceptable estimate of the course of the apparent orbit through its complete revolution. The degree of completeness of the analysis depends on the apparent size of the orbit and the accuracy and the time covered by the observations.

The adjusted apparent ellipse may now be analyzed and the orbital elements determined. The diameter of the apparent ellipse passing through the primary is the projected major axis of the true orbit; the extremes of this diameter are periastron and apastron. Any line parallel to the intersection of the true and apparent orbits, the so-called line of nodes, remains parallel and is not foreshortened in the apparent ellipse. Any line perpendicular to the line of nodes remains perpendicular, but its length is foreshortened in the apparent ellipse

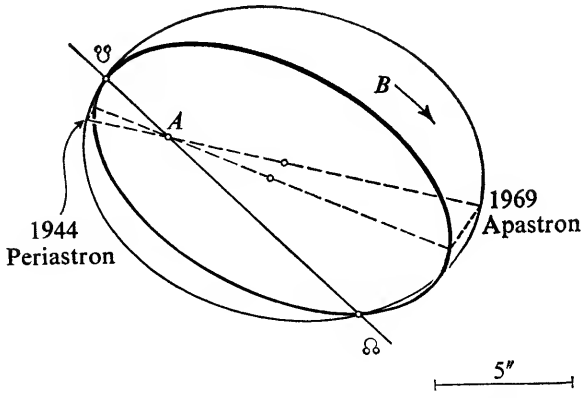

Fig. 10.6. *Relation between true and apparent orbits of the visual binary Sirius.*

by the factor cos i. The auxiliary Kepler circle appears as an auxiliary Kepler ellipse (Section 9).

There are different ways in which to derive the orbital elements; we shall outline the natural and most frequently used methods of analysis. Most of them require first a determination of the dynamical elements, and we therefore consider this problem first.

8. Derivation of dynamical elements

From apparent orbit.—The period P is measured from the graph in which the position angle θ is plotted against the epoch of observation. If more than one revolution has been completed, the derivation is quite straightforward. If less than one revolution has been completed, the interpolation curves for ρ and θ may be extrapolated, always trying to satisfy the relation $\rho^2(d\theta/dt) = \text{const.}$ In this way the period may be estimated and the apparent ellipse is thus also tentatively completed.

The eccentricity e is measured from the apparent ellipse as the ratio of the lengths, primary-center and periastron-center; this ratio is not changed by projection.

The epoch of periastron passage T is obtained from the interpolation curve for θ by measuring the position angle of periastron passage as revealed by the projected major axis of the true ellipse.

The above procedure is inadequate in certain cases, particularly when the inclination of the orbit is near 90°: the apparent ellipse may then be very slender, or may appear as a straight line, so that the law of areas can no longer be used.

In these cases, and also for any general case, another approach may be used. Instead of studying the apparent ellipse and its implicit time element, it is equally (and often more) convenient and profitable to make use of the so-called time-displacement curves.[11]

From time-displacement curves.—Project the apparent orbital motion in any chosen direction, and plot this projection as a function of the time. Generally it is natural and convenient to study the projection of the apparent orbital motion in the two coordinates, right-ascension (x) and declination (y), and plot these projected motions against the time. This is completely analogous to the orbital study of spectroscopic binaries, where there is no other choice but to study the orbital motion in the one coordinate available to the spectroscopic observer, namely the line of sight. The visual-double-star observer has two coordinates at his disposal, as contrasted with the one coordinate available

[11] Peter van de Kamp, "Two Graphical Procedures for Evaluating the Eccentricity of an Astrometric Double Star Orbit"; *also*, "The Relation Between the Eccentricity and the Slopes at Periastron and Apastron in the Displacement and Velocity Curves of Binaries," *The Astronomical Journal*, 52 (1947): 185–189.

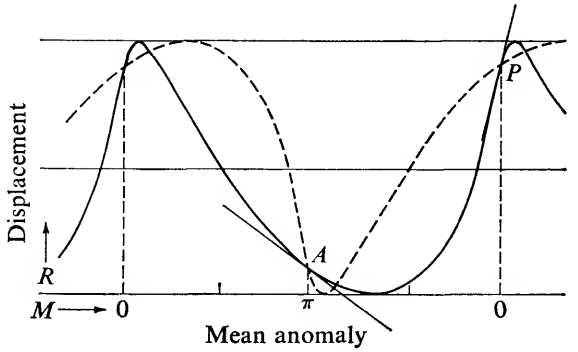

Fig. 10.7. *Graphical evaluation of periastron P, apastron A, and eccentricity e from slope of time-displacement curves at periastron and apatron. The curve illustrated is cos E + 0.174 sin E, corresponding to e = 0.7.*

to the spectroscopic observer. The latter has one radial velocity curve; the visual observer has two displacement curves, whose combination gives the projection of the three-dimensional orbital motion on the two-dimensional plane of the sky.

The advantage of using displacements (and velocities) plotted against the time is that the best known observed datum, the time, enters explicitly. Periastron and apastron are located by the fact that their mean anomalies differ by 180° and their ordinates are equal and opposite when referred to the center of the orbit. Periastron and apastron are conveniently located by making a copy of the displacement curve, reversing it along the central line representing the center of the orbit and shifting the reversed curve half a period along the time axis. Generally two pairs of intersections result (Fig. 10.7). Of these the single intersection on the shorter, steeper branch and the central intersection on the longer branch represent periastron and apastron, respectively.

The slopes of any displacement curve represent projected velocities dR/dt. The ratio of the true velocity vectors at periastron and apastron is $-(1 + e)/(1 - e)$, their directions being opposite. Since this ratio remains the same in projection, the ratio of the slopes $(dR/dt)_P$ and $(dR/dt)_A$ at periastron and apastron respectively amounts to $-(1 + e)/(1 - e)$, for any displacement curve, including those of astrometric orbits seen on edge. We thus cannot only distinguish periastron from apastron, but also derive the eccentricity of the orbit, independently of the focus, through the relation

$$e = \frac{(dR/dt)_P + (dR/dt)_A}{(dR/dt)_P - (dR/dt)_A}. \tag{10.18}$$

The method becomes unreliable when periastron and apastron are close to the extreme amplitudes—this occurs if the major axis is at a small angle with the line of nodes—for any spectroscopic orbit and for any astrometric orbit with a high inclination. In this case a combination of graphical and analytical methods may be used to derive the eccentricity from the observed cosine of the eccentric anomaly for selected values of the mean anomaly (see fn. 11).

This analysis of time-displacement curves is equally applicable to resolved and to unresolved astrometric binaries, provided, of course, that in the latter the orbital motion of the center of light is appreciable and well separated from the proper motion and parallax of the system. Although the time-displacement curve method may often be superfluous for resolved binaries, it is of particular significance for unresolved binaries, for which the conventional geometric derivation of the eccentricity is awkward or fails, but the time-displacement curve methods are effective, accurate, and generally applicable.

9. Derivation of geometric elements; Thiele-Innes constants

After the dynamical elements have been obtained by either of the methods outlined above, the geometric elements may be determined by either geometric or analytic methods.

Geometric method.—This is often referred to as Zwiers' method, although it was independently presented by Henry Norris Russell in a slightly different form.[12] We follow essentially Russell's presentation. The projected minor axis is obtained as the conjugate diameter of the orthogonal projection of the true major axis. The projection of the auxiliary or Kepler circle has as conjugate diameters the projection of the major axis and the projection of the minor axis increased in the ratio

$$k = \frac{1}{\sqrt{1 - e^2}},$$

e having been previously measured. The projection of the auxiliary circle, with conjugate diameters a_1 and b_1, may be readily constructed. It is called the *auxiliary ellipse* and has semi-axes α (major) and β (minor). Its major axis is the only diameter of the auxiliary circle, which appears unforeshortened, and its length 2α is therefore equal in length, $2a$, to the major axis of the true orbit and parallel to the line of nodes, thus yielding the elements a and Ω. The cosine of the inclination i of the true orbit is given by the ratio of the

[12] H. F. Zwiers, "Ueber eine Neue Methode zur Bestimmung von Doppelsternbahnen," *Astronomische Nachrichten*, 139 (1895): 369–380. H. N. Russell, "A New Graphical Method of Determining the Elements of a Double-Star Orbit," *The Astronomical Journal*, 19 (1898): 9–10.

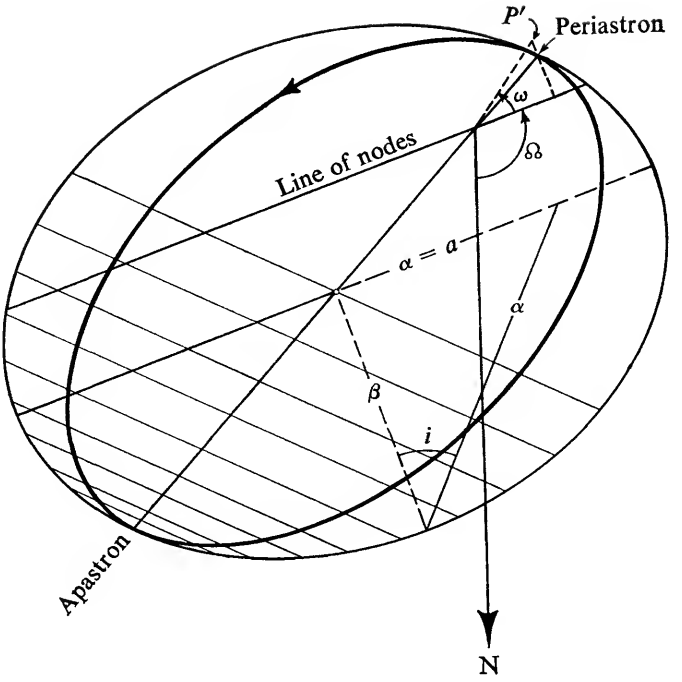

Fig. 10.8. *Apparent* (heavy line) *and auxiliary Kepler ellipse with semi-axes* α *(major) and* β *(minor). Evaluation of conventional geometric elements:* $e = 0.71$: $k = 1.40$; $i = 40°$; $\omega = 36°$; $\Omega = 114°$.

minor to the major axes of the auxiliary ellipse, i.e., $\cos i = \beta/\alpha$, which may be constructed.

All orbital distances perpendicular to the line of nodes are foreshortened by the factor $\cos i$. If we wish, we can therefore construct the true ellipse by applying the factor $1/\cos i$ perpendicular to the line of nodes to all points of the apparent orbit. In particular we may thus construct the unprojected position P' of the periastron in the true orbit, and hence measure the angle ω.

In practice this geometric method relies on analytical procedure also.[13]

Analytic method.—An extremely elegant approach is the widely used Thiele-Innes method. Recall that for a position in the apparent orbit

$$\begin{aligned} \Delta\alpha \cos\delta &= \Delta x = \rho \sin\theta, \\ \Delta\delta &= \Delta y = \rho \cos\theta. \end{aligned} \tag{10.7}$$

For position in the true orbit

$$ax = r\cos v, \qquad ay = r \sin v. \tag{10.17}$$

[13] W. M. Smart, *Spherical Astronomy*, Cambridge University Press, 1960, pp. 351–355.

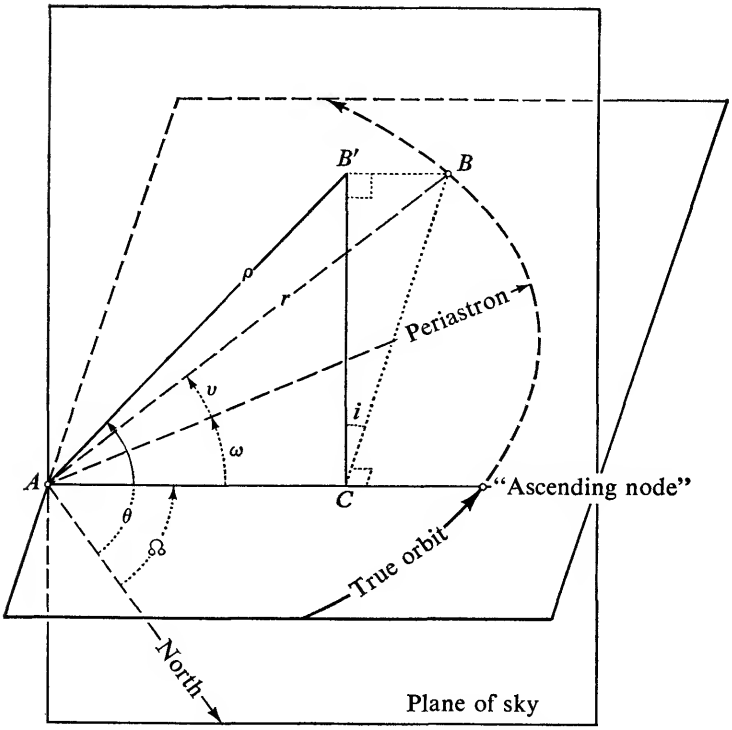

Fig. 10.9. *Relation between polar coordinates in apparent and true orbits.*

The two sets of polar coordinates are related as follows (Fig. 10.9):

$$\begin{aligned} AC &= \rho \cos(\theta - \Omega) = r \cos(\upsilon + \omega), \\ B'C &= \rho \sin(\theta - \Omega) = r \sin(\upsilon + \omega) \cos i. \end{aligned} \tag{10.19}$$

Working out these relations we find

$$\Delta x = Bx + Gy, \qquad \Delta y = Ax + Fy \tag{10.20}$$

where

$$\begin{aligned} B &= a(\cos\omega \sin\Omega + \sin\omega \cos\Omega \cos i), \\ A &= a(\cos\omega \cos\Omega - \sin\omega \sin\Omega \cos i), \\ G &= a(-\sin\omega \sin\Omega + \cos\omega \cos\Omega \cos i), \\ F &= a(-\sin\omega \cos\Omega - \cos\omega \sin\Omega \cos i). \end{aligned} \tag{10.21}$$

In these formulae x and y are the elliptical rectangular coordinates in the unit orbit (Section 6): they are functions of the dynamical elements only; B, A, G, and F contain the scale a and the three orientation elements. These four *geometric* elements are also called natural elements, or Thiele-Innes constants,

and are related to the conventional geometric elements through the relations 10.21. The designation Thiele-Innes elements includes both the dynamical elements P, e, and T and the Thiele-Innes constants B, A, G, and F.

The natural elements have a simple geometric meaning. Note that at periastron

$$x = 1 - e, \qquad y = 0,$$

hence

$$\Delta x_P = B(1 - e), \qquad \Delta y_P = A(1 - e), \tag{10.22}$$

and at apastron

$$x = -1 - e, \qquad y = 0,$$

hence

$$\Delta x_A = B(-1 - e), \qquad \Delta y_A = A(-1 - e). \tag{10.23}$$

Hence the coordinates of the center of the apparent orbit are

$$\Delta x_c = -Be, \qquad \Delta y_c = -Ae, \tag{10.24}$$

and the coordinates of periastron, referred to the *center* of the apparent orbit are B, A.

For $E = 90°$, we have

$$x = -e, \qquad y = \sqrt{1 - e^2},$$

hence

$$\Delta x_{90°} = -Be + G\sqrt{1 - e^2}, \qquad \Delta y_{90°} = -Ae + F\sqrt{1 - e^2}. \tag{10.25}$$

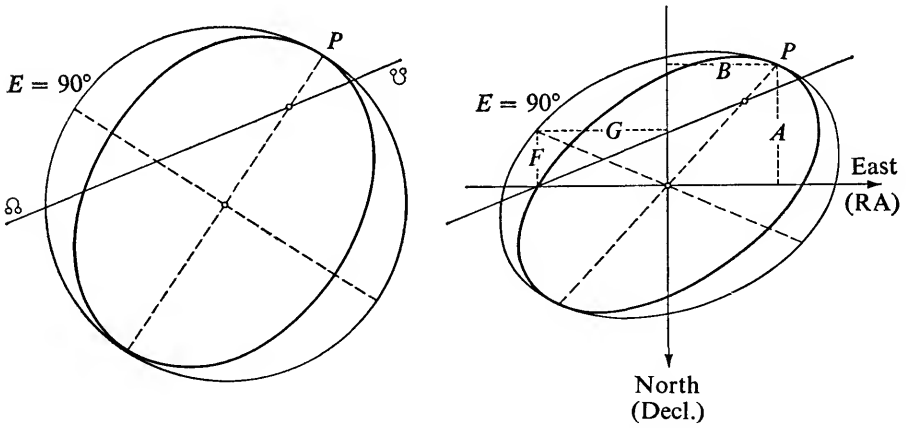

Fig. 10.10. (Left) *True orbit and auxiliary Kepler circle.* (Right) *Apparent orbit and auxiliary Kepler ellipse in equatorial (rectangular) coordinate system. The Thiele-Innes constants are the projected rectangular equatorial coordinates of periastron and of the point $E = 90°$ of the auxiliary circle.*

Hence the coordinates of the point $E = 90°$ on the apparent orbit referred to the *center* are

$$\Delta x_{90°} = G\sqrt{1 - e^2}, \qquad \Delta y_{90°} = F\sqrt{1 - e^2}, \tag{10.26}$$

while the corresponding coordinates on the auxiliary Kepler ellipse are G, F.

10. Derivation of conventional from natural geometric elements

The conventional geometric elements are derived as follows:
Relations (10.21) yield

$$\begin{aligned} A + G &= a(1 + \cos i)\cos(\omega + \Omega), \\ A - G &= a(1 - \cos i)\cos(\omega - \Omega), \\ B - F &= a(1 + \cos i)\sin(\omega + \Omega), \\ -B - F &= a(1 - \cos i)\sin(\omega - \Omega), \end{aligned} \tag{10.27}$$

hence we find ω and Ω from

$$\tan(\omega + \Omega) = \frac{B - F}{A + G},$$

where $\sin(\omega + \Omega)$ has the same sign as $B - F$,

$$\tan(\omega - \Omega) = \frac{-B - F}{A - G}, \tag{10.28}$$

where $\sin(\omega - \Omega)$ has the same sign as $-B - F$.

Hence the quadrants of $\omega + \Omega$ and $\omega - \Omega$ are unambiguously determined since $a(1 + \cos i)$ or $a(1 - \cos i)$ cannot be negative. However, we may add 360° to $\omega + \Omega$ (or to $\omega - \Omega$) and thus obtain two solutions

$$\omega, \Omega \quad \text{and} \quad \omega \pm 180°, \qquad \Omega \pm 180°.$$

Unless a distinction is possible, the solution for which $\Omega < 180°$ is adopted.

To obtain a and i we apply the theorems of Apollonius for the ellipse.

1. *The sum of the squares of any two conjugate diameters equals the sum of squares of the axes.*

2. *The area between the parallelograms on any two conjugate diameters equals that of the rectangle of the axes.*

Applying these theorems to the auxiliary ellipse we find

$$a^2(1 + \cos^2 i) = A^2 + B^2 + F^2 + G^2 = 2k \tag{10.29}$$

$$a^2 \cos i = AG - BF = m. \tag{10.30}$$

We introduce the auxiliary quantities k and m and also

$$j^2 = k^2 - m^2 \tag{10.31}$$

and find

$$a^2 = j + k \tag{10.32}$$

$$\cos i = \frac{m}{a^2}. \tag{10.33}$$

It has been found practical to determine the dynamical elements P, e, and T geometrically from photographic and visual normal places combined since generally the photographic normal places alone cover too short a part of the orbit. Next the geometric elements B, A, G and F are determined from a least-squares solution based on the photographic normal places alone. The dynamical elements P, e, and T are given slight variations to test the stability of the solution and, if possible, to establish the set of elements that give the best fit,—as shown, for example, by a minimum value of the sum of the squares of the residuals, $O - C$. A simultaneous least-squares solution for corrections to all seven elements may be made if the available accuracy warrants such a procedure. Final residuals may be given both in x and y and in ρ and θ; the residuals in position angle may be stated in angle as well as in arc, i.e., $\rho_{\text{comp}} \sin (\theta_{\text{obs}} - \theta_{\text{comp}})$.

11. Results: example, Krüger 60

More or less reliable orbits of several hundred visual binaries have been published. Of the numerous examples we mention the orbital determinations by Strand of several "classical" binaries, such as η Cas, γ Vir, ξ Boo, 70 Oph and others.[14]

Catalogues of orbits as well as new orbits and other information regarding visual binaries are published frequently.[15]

In accurate long-term problems the perspective change in the apparent orbit due to motion of the center of mass in the line of sight must be taken into account. In the future this feature of orbital analysis will become more and more important. An example of the required reduction is the orbital analysis of the visual binary 61 Cygni.[16]

[14] K. Aa. Strand, *Photographic Measurements of Six Double Stars . . .* , 1937. (See footnote 5.)

[15] Robert G. Aitken, *New General Catalogue of Double Stars within 120″ of the North Pole*, Carnegie Institution of Washington, 1932, 2 vols. Hamilton M. Jeffers and Willem H. van den Bos with Frances M. Greeby, *Index Catalogue of Visual Double Stars, 1961.0* (University of California, Publications of the Lick Observatory, Vol. 21, Pts. 1 and 2), 1963. Charles E. Worley, *A Catalogue of Visual Binary Orbits* (Publications of the United States Naval Observatory, second series, Vol. 18, Pt. 3), Washington, D.C., Government Printing Office, 1963. P. Muller, *Circulaire d'Information*, Union Astronomique Internationale, Commission des Etoiles Doubles, 1954 to date. (Issued irregularly.)

[16] A. Fletcher, "Note on the Effect of Proper Motion on Double Star Measures"; *also* "The Binary System 61 Cygni," *Monthly Notices of the Royal Astronomical Society*, 92 (1931): 119–121, 121–131.

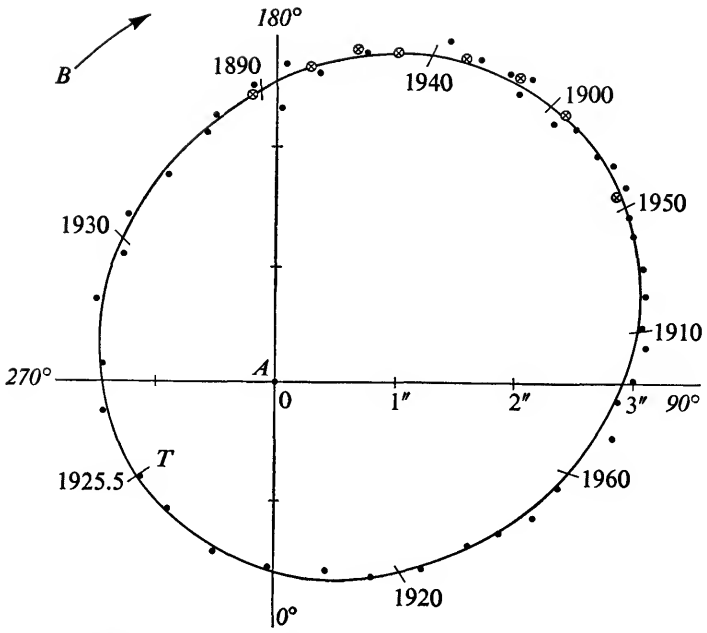

Fig. 10.11. *Apparent orbit of the visual binary Krüger 60:* ● = *visual observations;* ⊗ = *photographic observations.*

Figure 10.11 shows the apparent orbit of the visual binary Krüger 60, based on observations extending from 1890 to 1949. A graphical determination of the dynamical elements yields

$$P = 44\overset{y}{.}6, \qquad e = 0.41, \qquad T = 1925.64$$

The photographic observations yield

$$B = -1\overset{''}{.}964 \pm 0\overset{''}{.}004 \text{ (p.e.)}$$
$$G = -1\overset{''}{.}261 \pm 0\overset{''}{.}007 \text{ (p.e.)}$$
$$A = +1\overset{''}{.}343 \pm 0\overset{''}{.}004 \text{ (p.e.)}$$
$$F = -1\overset{''}{.}993 \pm 0\overset{''}{.}007 \text{ (p.e.)}$$

from which we find

$$a = 2\overset{''}{.}412 \pm 0\overset{''}{.}005$$

$$\left.\begin{aligned} \omega &= 217\overset{\circ}{.}8 \\ \Omega &= 161\overset{\circ}{.}1 \\ i &= 164\overset{\circ}{.}5 \end{aligned}\right\} \text{2000 equator.}$$

For a parallax of $+0\overset{''}{.}253$, the sum of the masses is found to be 0.43 times the sun's mass; a mass ratio of 0.626 to 0.374 as found by the methods de-

scribed in Chapter 11, yields masses of 0.27 and 0.16 times the sun's mass for the components A and B.[17] Photographs and a diagram illustrating the mass ratio of Krüger 60 are given in Chapter 11, Section 4.

12. Perturbations

For several binaries the residuals from the best possible orbit have revealed systematic deviations, which point to a perturbation caused by a third component, close to one of the visible components. Although perturbations have been noticed even in visual measures, it is obvious that the chances for discovery are immensely increased by the accurate photographic technique.

In these cases the systematic behavior of the residuals in both coordinates is analyzed for Keplerian motion, care being taken to provide corrections to the orientation elements of the "large" orbit. After the orbital motion in the "small" orbit has been determined, the original observations are corrected for the perturbation and the elements for the large orbit are recomputed. From the analysis it cannot be determined whether the third body is close to the visual primary or secondary component; this can be determined only by measuring the orbital motion on an astrometric background of other stars (see Chapter 12).

Suggested readings

R. G. Aitken, *The Binary Stars*. New York and London, McGraw-Hill Book Company, 1935. (Reprinted by Dover Publications, New York.)

W. H. van den Bos, "Orbit Determinations of Visual Binaries," *in* W. A. Hiltner, ed., *Astronomical Techniques* (Stars and Stellar Systems, Vol. II). University of Chicago Press, 1962, pp. 537–559.

Peter van de Kamp, "Visual Binaries," *in Encyclopedia of Physics*, Berlin, Springer-Verlag, Vol. 50 (1958), pp. 187–224.

Peter van de Kamp, "Double Stars (Robert Grant Aitken Lecture)," *Publications of the Astronomical Society of the Pacific*, 73 (1961): 389–409.

[17] Sarah Lee Lippincott, "Parallax and Orbital Motion of Krüger 60," *The Astronomical Journal*, 58 (1953): 135–141.

11 Orbital Motion. Parallax and Mass Ratio

1. Resolved Astrometric Binaries

For orbital motion, another term has to be added to the equations of condition of the stellar path. For a resolved binary the geocentric equations (8.2) hold for the barycenter, and the positions of the brighter component A and the fainter component B referred to the barycenter are as follows:

Orbital effect of A in x-coordinate: $-\mathrm{B}\Delta x$,

Orbital effect of A in y-coordinate: $-\mathrm{B}\Delta y$,

Orbital effect of B in x-coordinate: $(1 - \mathrm{B})\Delta x$,

Orbital effect of B in y-coordinate: $(1 - \mathrm{B})\Delta y$.

Here B is the fractional mass $M_B/(M_A + M_B)$ of the companion in terms of the combined mass of primary and companion, and Δx, Δy, is the relative position of the secondary B referred to the primary A. Hence, limiting ourselves to the primary component, the equation of condition for the geocentric position of the primary are

$$\begin{aligned} X &= c_X + \mu_X t + \pi P_\alpha - \mathrm{B}\Delta x, \\ Y &= c_Y + \mu_Y t + \pi P_\delta - \mathrm{B}\Delta y. \end{aligned} \tag{11.1}$$

We recall that the relative positions of the two components in the apparent orbit may be written as

$$\begin{aligned} \Delta x &= Bx + Gy, \\ \Delta y &= Ax + Fy. \end{aligned} \tag{10.20}$$

Here x and y are the elliptical rectangular coordinates in the unit orbit (i.e., unit semi-axis major), which are functions to the dynamical elements P, e, and T. (Chapter 10, Section 6); B, A, G, and F are the "natural" geometric elements, or Thiele-Innes constants, which are related to the conventional geometric element a, Ω, ω, i (Chapter 10, Sections 9 and 10). Thus

Δx and Δy may be calculated if the orbital elements of the relative orbit of the two components are known.

Another, more elegant and often more revealing, form of equations (11.1) is obtained as follows:[1] the orbits of primary and secondary are similar; the semi-axis major α of the orbit of the primary is related to the semi-axis major a of the relative orbit of primary and companion by $\alpha = \mathrm{B}a$; the phases in the respective orbits differ by 180°.

We may write the orbital displacements for the primary as follows:

$$\begin{aligned} &\text{Orbital displacement in } x: \quad -\mathrm{B}\Delta x = -\frac{\alpha}{a}(Bx + Gy), \\ &\text{Orbital displacement in } y: \quad -\mathrm{B}\Delta y = -\frac{\alpha}{a}(Ax + Fy), \end{aligned} \tag{11.2}$$

or

$$\begin{aligned} &\text{Orbital displacement in } x: \quad \left(-\frac{B}{a}x - \frac{G}{a}y\right)\alpha = Q_\alpha \alpha, \\ &\text{Orbital displacement in } y: \quad \left(-\frac{A}{a}x - \frac{F}{a}y\right)\alpha = Q_\delta \alpha. \end{aligned} \tag{11.3}$$

The quantities Q_α and Q_δ are named "orbital factors"; they are the projected values in right ascension (reduced to great circle) and declination of the radius vector barycenter-primary for unit orbit. The orbital factors are analogous to the parallax factors; the latter refer to the star's parallactic orbit, the former to the star's own apparent orbit. Q_α and Q_δ may be expressed as follows:

$$Q_\alpha = (b)x + (g)y, \qquad Q_\delta = (a)x + (f)y, \tag{11.4}$$

where

$$\begin{aligned} (b) &= -\cos\omega \sin\Omega - \sin\omega \cos\Omega \cos i, \\ (a) &= -\cos\omega \cos\Omega + \sin\omega \sin\Omega \cos i, \\ (g) &= +\sin\omega \sin\Omega - \cos\omega \cos\Omega \cos i, \\ (f) &= +\sin\omega \cos\Omega + \cos\omega \sin\Omega \cos i. \end{aligned} \tag{11.5}$$

These "orientation factors" are related to the Thiele-Innes constants as follows:

$$\begin{aligned} B &= -(b)a, \qquad G = -(g)a, \\ A &= -(a)a, \qquad F = -(f)a. \end{aligned} \tag{11.6}$$

We thus obtain the following equations of condition for the observed geocentric positions of the primary:

$$X = c_X + \mu_X t + \pi P_\alpha + \alpha Q_\alpha, \qquad Y = c_Y + \mu_Y t + \pi P_\delta + \alpha Q_\delta. \tag{11.7}$$

[1] Peter van de Kamp, "Note on the Photographic Determination of Stellar Masses," *The Astronomical Journal*, 51, (1945): 161–162.

2. Unresolved astrometric binaries; photocentric orbit

In many binaries the distance between the components is below the resolving power of the photographic plate, in which case no separation is possible, and a composite image results. These photographically unresolved astrometric binaries are important, since so many interesting objects fall in this group. We can measure the position of the composite image, but these questions arise: What do we measure? What do the measures signify?

The smallest star images on long-focus photographs are rarely below 1″ in diameter. Blended exposures of components separated by 1″, or sometimes even more, generally present circular images. This is certainly true for magnitude differences of 2 or more. A close companion may be too faint to be detected visually or spectroscopically, but it affects the center of light by pulling it toward the barycenter. A self-luminous companion, even though photographically not resolved, will generally draw the center of light toward the center of mass. For periods of half a century and more there might be no danger of photographic blending, except for stars of small parallax. However, blending is generally to be expected for periods up to several decades, except possibly for a few of the very nearest stars. The blended image of the unresolved binary may appear circular, and the orbit of the center of the image will generally be smaller than the actual perturbation orbit described by the primary. Since the dimensions of this orbit are a measure of the mass of the companion, observations of a blended image thus generally yield a lower limit for the mass of the companion.

If the companion is very much fainter, or when its image is not blended with that of the primary, the measured positions, of course, refer to the primary.

We assume that the measured position of the blended image represents the weighted center of light-intensity, or *photocenter*, of the components. In this case the fractional distance β of the primary to the photocenter, in terms of the distance between the two components, is given by

$$\beta = \frac{l_B}{l_A + l_B}. \tag{10.5}$$

Here l_A and l_B are the luminosities of the components. Or, if we introduce the difference in magnitude Δm, companion minus primary, we have (Table 11.1),

$$\beta = \frac{1}{1 + 10^{(0.4)\Delta m}}. \tag{11.8}$$

Experiments made at the Yerkes Observatory with artificial binaries show systematic deviations from the theoretical relation.[2] For separations of less

[2] R. G. Hall, Jr., "Photographic Blending of Images of Unresolved Binaries," *The Astronomical Journal*, 55 (1951): 215–218.

Table 11.1. THEORETICAL RELATION BETWEEN Δm AND β

Δm	β	Δm	$\Delta\beta$
0.0	0.500	2.0	0.137
0.5	0.387	3.0	0.060
1.0	0.285	4.0	0.025
1.5	0.201	5.0	0.010
2.0	0.137	6.0	0.006

than 0.12 mm there is a discrepancy beginning at about $\Delta m = 2^{m}0$; for larger values of Δm the observed value of β is less than the theoretical value, reaching the value zero at $\Delta m = 4^{m}0$ (Fig. 11.1).

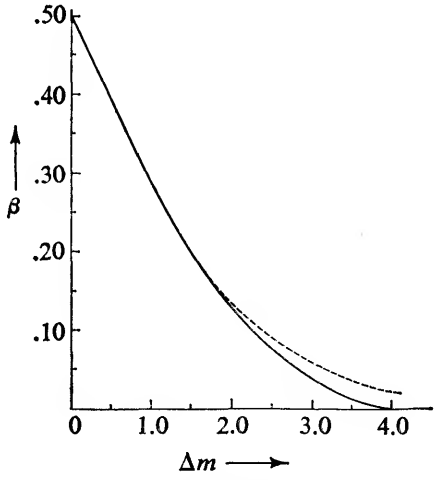

Fig. 11.1. *Relation between Δm and β: theoretical,* dotted line; *observed,* solid line.

The fractional difference of photocenter to barycenter is therefore $B - \beta$, and the semi-major axis of the photocentric orbit relative to the barycenter is

$$\alpha = (B - \beta)a. \qquad (10.4)$$

Referred to the barycenter, the orbits of primary, companion, and photocenter are all similar to the orbit of companion relative to primary in the ratios B, $1 - B$, and $B - \beta$ (Fig. 11.2). Note that α has the sign of $B - \beta$. A positive value for α indicates that photocenter and companion are on opposite sides of the barycenter; a negative value, that they are on the same side. Except

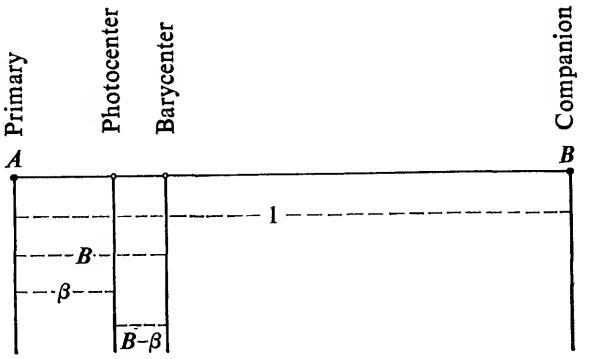

Fig. 11.2. *Relative spacing between components, barycenter, and photocenter for photographically unresolved binaries.*

for the abnormal possibility that $\beta - \mathrm{B} > \mathrm{B}$, i.e., a comparatively luminous companion of low mass, the photocentric orbit is always smaller than the orbit of the primary (Chapter 12, Section 4).

The orbital displacement of the photocenter is represented by

$$-(\mathrm{B} - \beta)\Delta x, \qquad -(\mathrm{B} - \beta)\Delta y;$$

but the form αQ_α, αQ_δ remains of particular value because of the explicit way in which α appears.

The formulae for analyzing the geocentric positions of the photocenter for proper motion, parallax, and orbital motion are therefore

$$\begin{aligned} X &= c_X + \mu_X t + \pi P_\alpha - (\mathrm{B} - \beta)\Delta x, \\ Y &= c_Y + \mu_Y t + \pi P_\delta - (\mathrm{B} - \beta)\Delta y, \end{aligned} \tag{11.9}$$

or, also,

$$X = c_X + \mu_X t + \pi P_\alpha + \alpha Q_\alpha, \qquad Y = c_Y + \mu_Y t + \pi P_\delta + \alpha Q_\delta. \quad (11.7)$$

3. Proper motion, parallax, and mass ratio

As a rule, parallax and mass ratio are determined simultaneously, using formulae (11.1), (11.7), or (11.9). If both components are visible and well separated on the photographic plate, the orbit need not be known; Δx and Δy are directly furnished by the measurements, and B is obtained through formulae (11.1). Or, if the orbital elements of the relative orbit are known, Δx and Δy may be calculated, and B or $\mathrm{B} - \beta$ may be obtained with the aid of formulae (11.1) or (11.9).

In general, only the primary or the photocenter of the blended primary and secondary is measured; in this case formulae (11.7) are most conveniently used, assuming the relative orbit to be known. The dynamical and orientation ele-

ments are used to compute the orbital factors Q_α and Q_δ. From material covering a sufficiently extended part of the orbit, a least-squares solution yields values of π and α.

If the measured positions refer to a primary component whose image is considered unaffected by a well-separated or a very faint companion, then the value α yields directly a determination of the quantity $B = \alpha/a$, i.e., the fractional mass $M_B/(M_A + M_B)$ of the companion in terms of the combined mass of primary and companion. If the measured positions refer to the blended image of primary and companion, the resulting photocentric orbital displacements yield a determination of

$$B - \beta = \frac{\alpha}{a}. \tag{11.10}$$

The expression

$$B = \frac{\alpha}{a} + \beta \tag{10.6}$$

shows explicitly how the total error of B depends on errors in α, a, and β. For large, well-established orbits the fractional accuracy of α is simply transferred to B. For small or provisional orbits the accuracy of B is also limited by the accuracy of a, while for blended images it is directly affected by any uncertainty in β, which in turn depends on the accuracy of Δm and on the reliability of the assumed theoretical relation between β and Δm.

In the 1930's the first serious attempts were made at accurate photographic determinations of parallax and mass ratio. Twenty to thirty plates seemed hardly adequate; gradually fifty to sixty plates were used for combined parallax and mass-ratio determinations, yielding probable errors of $\pm 0''.005$ for the relative parallax and something like 2 percent for the mass ratio. For accurate mass-ratio determinations as many as two hundred or more plates have been used, with resulting decrease in the probable errors of the parallax to $\pm 0''.003$ or even $\pm 0''.002$, while the mass ratio has often been found with an error of 1 percent or even less.[3]

4. Examples: 99 Herculis; Krüger 60

As an illustration we will first consider the binary 99 Herculis (ADS 11077; $18^h3^m.2$, $+30°33'$, 1900).[4] This star was photographed at the Sproul Observatory during the years 1915–1917, and again from 1937 on. The period is 56 years; periastron was passed in 1942; hence sufficient orbital motion for an accurate mass-ratio determination is covered by the 89 plates taken on 38

[3] Peter van de Kamp, "Masses of Visual Binaries," *The Astronomical Journal*, 59 (1954): 447–454.

[4] L. Binnendijk, "A Determination of the Parallax and Mass-ratio of 99 Herculis," *The Astronomical Journal*, 54 (1948): 21–23.

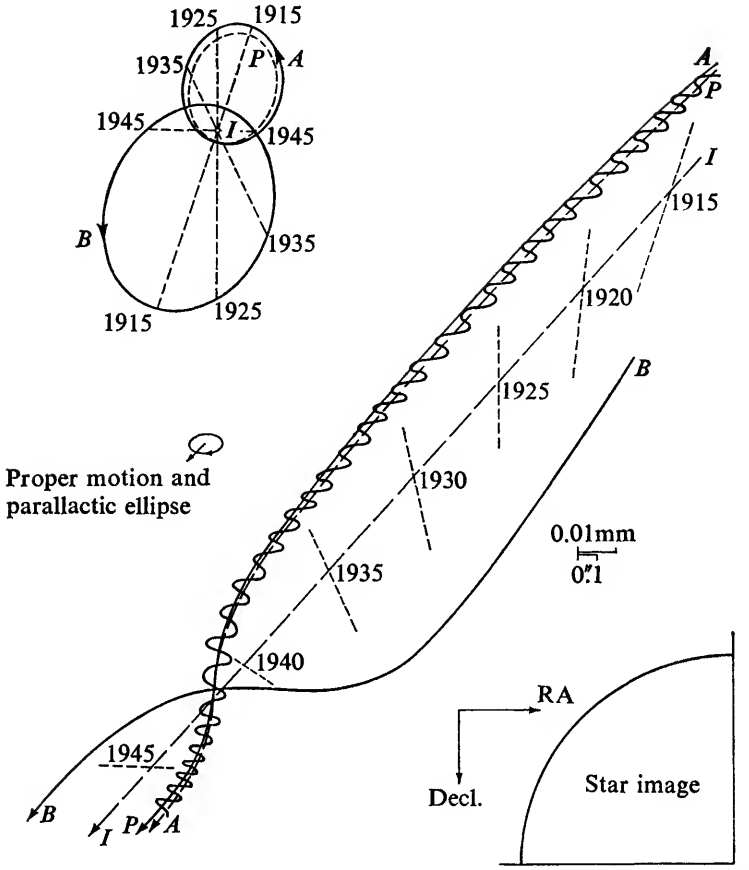

Fig. 11.3. *Heliocentric and geocentric paths and orbital motions* (upper left) *of the components A and B and the photocenter P of 99 Herculis, relative to center of mass I. From photographs with the Sproul refractor. Enlarged* **500** *times.*

nights between 1915 and 1947. Because of the small proper motion of 99 Herculis (μ = 0".12 in 301°), the same set of dependences, covering the entire interval, could be used for the three reference stars.

The image of 99 Herculis was reduced to close equality, 10.1 mag., with that of the reference stars by the use of a rotating sector of 1.0 percent opening. The separation of the components never exceeded 1".5, or about .08 mm; the difference in magnitude between the components is 3.4 mag.

The mean positions for each night were represented by equation (11.7) in which the orbital factors were computed from the elements for the relative visual orbit of companion and primary:

$$P = 56^{y}.0 \qquad e = 0.76 \qquad T = 1942.00$$
$$\Omega = 55°.8 \qquad \omega = 105°.0 \qquad i = 32°.0.$$

The results for π and a from a combined solution of the RA and Decl. material are

$$\pi = +0''.069 \pm 0''.006,$$
$$a = +0''.344 \pm 0''.009.$$

The relative orbit gives $a = 1''.03$; using formula (10.6) we obtain

$$B = +0.334 + \beta.$$

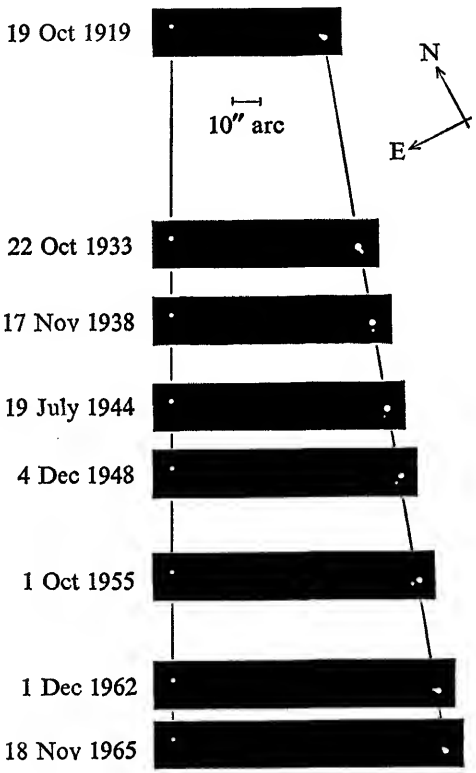

Fig. 11.4. *Proper motion and orbital motion of the components* A *and* B *of the visual binary Krüger 60, relative to the optical companion Krüger 60.*

With the value of 3.40 for Δm we derive $\beta = 0.040$; hence B = 0.374 with a probable error ± 0.009 due to the astrometric determination of α.

The sum of the masses is computed by means of the harmonic relation

$$M_A + M_B = a^3/P^2, \qquad (10.2)$$

where a is the semi-axis major of the relative orbit, expressed in astronomical units, P the period in years; the masses are referred to the sun's mass as a unit.

Combining the above value of the parallax with others, a value of 0".055 is adopted for the parallax of 99 Herculis, yielding 2.0⊙ for the sum of the masses of the components. Hence the mass of 99 Herculis A is 1.3⊙, that of 99 Herculis B is 0.7⊙, where ⊙ is the mass of the sun.

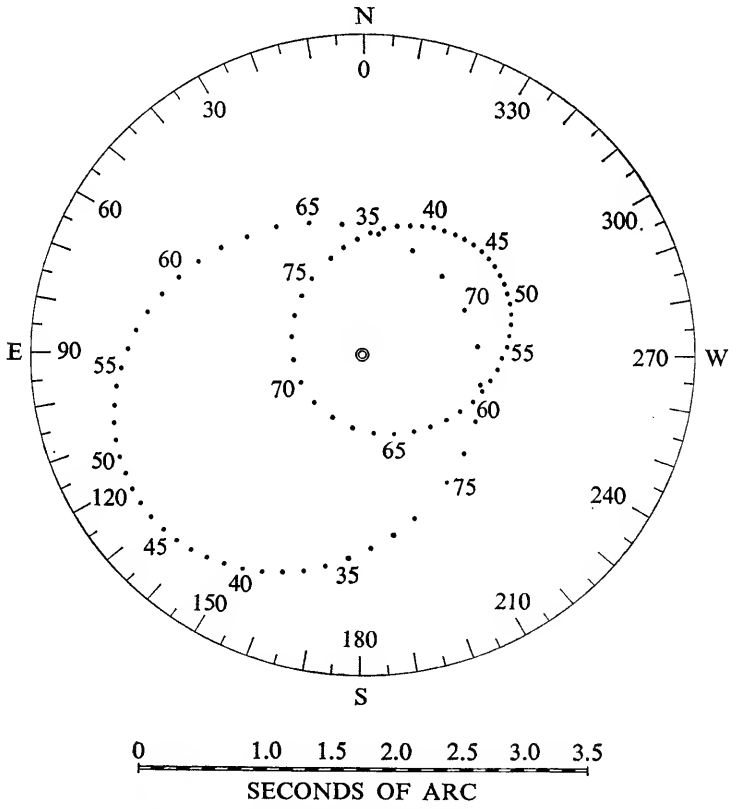

Fig. 11.5. *Orbital motion of the components* A *and* B *of the binary Krüger 60, relative to their barycenter.*

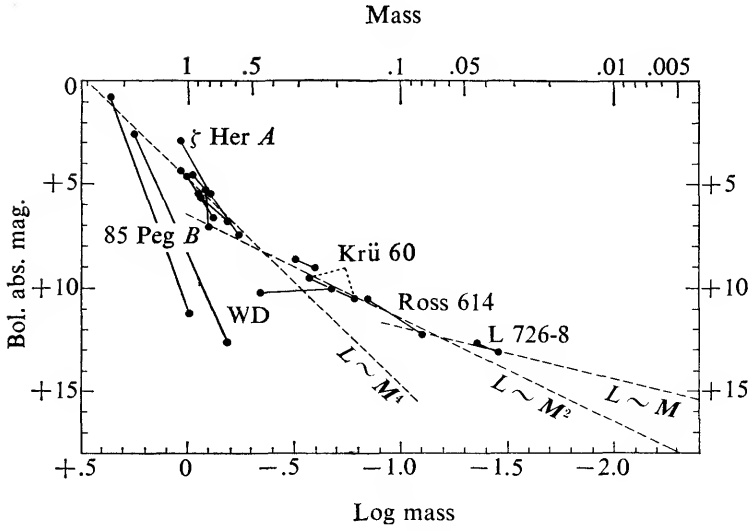

Fig. 11.6. *Mass-luminosity relation for visual binaries.*

Another illustration is given for the visual binary Krüger 60 AB[5] (see also Chapter 10, Section 11).

A series of photovisual photographs (Fig. 11.4) shows the proper motion and orbital motion of the components A and B (right) of the visual binary Krüger 60, referred to the optical companion C (left) from exposures made with the McCormick 26-inch refractor (1919 and 1933) and the Sproul 24-inch refractor (1938–1965).

The exposures have been oriented so that the proper motion of the barycenter of A, B relative to C is horizontal; they have been shifted to align the exposures of C vertically. The vertical spacings are a linear function of the epoch of observation and result in a rectilinear arrangement of the barycenter of the successive exposures of A, B.

The proper motion of the barycenter amounts to

$$\mu = ''.90 \quad \text{in} \quad \theta = 245°$$

or

$$\mu_\alpha \cos\delta = -''.811, \qquad \mu_\delta = -''.385.$$

Note that the summer exposure of 1944 shows a morning parallactic displacement of nearly 0″.4, relative to the other evening exposures.

Figure 11.5 shows orbital motion of components A (small orbit) and B (large orbit) relative to their barycenter. The position of B relative to A may be read from the compass rose.

[5] James F. Wanner, "The Visual Binary Krüger 60," *Sky and Telescope*, 33 (1967): 16–17.

5. Mass-luminosity relation for visual binaries

Stellar masses of visual binaries are therefore accurate only for comparatively nearby stars. Generally the mass ratio may be measured more accurately than the sum of the masses, since any error in the parallax appears threefold in the sum of the masses. Thus we cannot claim to know more than about thirty stellar masses accurately, i.e., with probable errors less than about 10 percent. A relation between mass and bolometric luminosity has been established for astrometric binaries, as shown in Figure 11.6. This relation resembles closely, in fact it is, the main sequence relation, its striking exceptions, in our current state of knowledge, being the white dwarfs Sirius B, Procyon B, and o^2 Eridani B. Other deviations that appear to be well established are the bright component of ζ Herculis, which appears overluminous for its mass, and the faint component of 85 Pegasi, which is underluminous for its mass.

The mass-luminosity relation for brighter main sequence stars may be represented by the relation $L \sim M^4$. For the red dwarfs, $L \sim M^2$ seems more appropriate while $L \sim M$ may even be indicated toward the faint end of the mass-luminosity relation.

The past decade has witnessed considerable progress in our knowledge of the fainter portion of the mass-luminosity relation. Whereas before 1955 the smallest mass known was that of Krüger 60 B(0.16$\odot$), Ross 614 A,B has since yielded masses of 0.14$\odot$ and 0.08$\odot$, and the components of L 726-8 are found to have masses of only 0.044$\odot$ and 0.035$\odot$.[6]

[6] D. L. Harris III, K. Aa. Strand, and C. E. Worley, "Empirical Data on Stellar Masses, Luminosities, and Radii," *in* K. Aa. Strand, ed., *Basic Astronomical Data* (Stars and Stellar Systems, Vol. III) University of Chicago Press, 1963, pp. 273–292. Peter van de Kamp, "Parallax, Orbital Motion and Mass of the Visual Binary L726-8," *The Astronomical Journal*, 64 (1959): 236–240. See also footnote 3, p. 170.

12 Perturbations. Spectroscopic and Eclipsing Binaries

1. Introduction

The study of unresolved astrometric binaries includes the discovery and subsequent determination of photocentric orbits revealed through perturbations. These perturbations may be manifested as the "variable" proper motion of a star previously considered single, or as an irregularity in the Keplerian motion of a visual binary, which thus proves to have a third component.

The discovery of unresolved astrometric binaries dates back to 1844, when Bessel deduced the existence of the unseen companions of Sirius and Procyon from perturbations in the paths of these stars: the companions were seen visually later. Bessel's classical deduction occurred two years before the discovery of Neptune from perturbations in the path of Uranus. Perturbations in the orbital motions of some known binaries led to the discovery of further unseen companions in these systems; here the classical cases are ζ Cancri (1880) and ξ Ursae Majoris (1907). All these discoveries were based on visual observations, and were accidental discoveries rather than results of a planned program.

In this century, the photographic technique, with its high positional accuracy, is being used for systematic studies by the method that had proven to be so fruitful for Sirius and Procyon. For the past four decades, the paths of apparently single stars have been followed by the methods of long-focus photographic astrometry, but even these methods have definite limitations. Perturbations of short periods have small amplitudes, which are not easily found. Perturbations of longer periods will not reveal any sensible deviation from uniform rectilinear motion in a short time; an increase in the time immensely increases the chance of discovery.

In the study of a perturbation, where no a priori orbital elements are known, it is convenient to use the following formulae for the orbital displacements:

$$\begin{aligned} \alpha Q_\alpha &= \alpha(b)x + \alpha(g)y = (B)x + (G)y, \\ \alpha Q_\delta &= \alpha(a)x + \alpha(f)y = (A)x + (F)y. \end{aligned} \tag{12.1}$$

The dynamical elements P, e, and T are represented by the elliptical rectangular coordinates x and y in the unit orbit. The geometric elements (B), (A), (G), and (F) refer to the observed photocentric orbit of the unresolved system, and are given in parentheses to distinguish them from the geometric elements B, A, G, and F, which refer to the relative orbit of the two components. They are related to the orientation factors and to the Thiele-Innes constants as follows:

$$\begin{aligned} (B) &= -\left(\frac{\alpha}{a}\right) B = \alpha(b) = \alpha(-\cos\omega \sin\Omega - \sin\omega \cos\Omega \cos i), \\ (A) &= -\left(\frac{\alpha}{a}\right) A = \alpha(a) = \alpha(-\cos\omega \cos\Omega + \sin\omega \sin\Omega \cos i), \\ (G) &= -\left(\frac{\alpha}{a}\right) G = \alpha(g) = \alpha(+\sin\omega \sin\Omega - \cos\omega \cos\Omega \cos i), \\ (F) &= -\left(\frac{\alpha}{a}\right) F = \alpha(f) = \alpha(+\sin\omega \cos\Omega + \cos\omega \sin\Omega \cos i). \end{aligned} \tag{12.2}$$

The general formulae for analyzing the positions of the photocenter for proper, parallactic, and orbital motion are, therefore,

$$\begin{aligned} X &= c_X + \mu_X t + \pi P_\alpha + (B)x + (G)y, \\ Y &= c_Y + \mu_Y t + \pi P_\delta + (A)x + (F)y. \end{aligned} \tag{12.3}$$

These formulae are useful if the dynamical elements are known: for example, from spectroscopic information. They are particularly suitable if nothing whatsoever is known about the orbital elements. This is the case, par excellence, resulting from the discovery and subsequent study of an astrometric binary revealed by variable proper motion. First, the observed positions are corrected for provisional values of proper motion and parallax, aiming for the adopted proper motion to be as close as possible to that of the barycenter. The remainders are then analyzed for orbital motion; successive approximations are generally necessary.

2. Orbital analysis

The dynamical elements may be determined by Zwiers' method, which in this case involves locating the invisible focus or barycenter. This procedure may be awkward, and a different method is therefore recommended. Instead of the apparent orbit, we study its projection on any coordinate; right ascension or declination or any other. This procedure has been used for "linear" orbits as they are represented by all spectroscopic binaries and by certain visual orbits

seen edgewise. However, the principle of the method is also applicable to any "open" visual or photocentric orbit. This method has been described in Chapter 10, Section 8.

With the set of dynamical elements P, e, and T thus obtained, x and y are computed and the observations represented by the general formulae for orbital displacement. An analysis of the equations yields the four geometric elements (B), (A), (G), and (F), from which the scale α and the three orientation elements Ω, ω, and i may be computed. Successive approximations are used and, as for resolved binaries, the dynamical elements are varied, in order to test the stability of the results. Although it is possible to solve simultaneously for differential corrections to all orbital elements and to parallax and proper motion, such a procedure is hardly warranted at the current stage of this problem. The process of variations is certainly to be preferred and has the great advantage of remaining in close touch with the real worth of the available material.

3. General considerations

The discovery and study of photographically unresolved binaries consist of two parts: (1) establishing the existence of deviations which cannot be accounted for by proper motion and parallax and (2) determining the photocentric orbit from these deviations. While it may be relatively simple to detect initial deviations, the second step is much more difficult.

Thousands of parallax determinations of "single" stars have been made, and, with few exceptions, it has always been possible to represent the observed positions satisfactorily by uniform proper motion and a parallactic orbit of appropriate size. Moreover, no increase in the probable error of unit weight has been found for stars of large parallax. This general absence of observable orbital motion may often be due to a negligible value of the semi-major axis of the photocentric orbit. For example, α is zero if both components have the same mass and the same luminosity. However, even with an appreciable value of α, orbital motion may not be found because of the small number of plates, twenty or thirty, and the short time interval, often only 2 years, employed in conventional parallax determinations. If the period is short, the amplitude of the photocentric orbit may be too small to be detected. If the period is long, more time is required to detect orbital motion. Moreover, the orbital motion may be partly absorbed in the parallactic and the proper motions, or it may be temporarily or accidentally disguised through gaps in the series of observations. The conventional parallax determinations are generally neither suitable for the discovery of orbital motion nor affected by any existing orbital motion.

For any thorough investigation it is desirable to go beyond the extent and also beyond the occasional repetition of conventional parallax series. Observa-

tions over an interval of several decades are desirable; the chances of discovery depend on the particular portion of the orbit in which the star happens to be. Even for shorter periods an extended observational series is in order, to insure complete coverage of the orbit; plates should be taken without particular regard to the parallax factor, in order to insure as complete and uniform a distribution in time as possible. The narrow hour-angle requirements of the observations cause annual gaps of at least 6 or 7 months, which in turn may result in spurious periods; with limited accuracy, scattered position in successive cycles of a short-period orbit may be interpreted as an orbit with a period a multiple of the actual one unless plates are also taken in close temporal succession. The danger of interpreting a long-period orbit by a spurious short period exists also. So long as the binary is not resolved, the analysis lacks the control of the harmonic relation $a^3/P^2 = \boldsymbol{M}_A + \boldsymbol{M}_B$, which for resolved binaries may serve as a guide for the period. The danger of interpreting a limited initial set of residuals by a fortuitous orbit should always be avoided through additional observations.

A satisfactory orbit is generally not obtained until all phases of the orbit have been covered. Correct dynamical interpretation is aided by the fact that the Keplerian motion is, as a rule, observed in two coordinates. The blending of the two components and variability of either component remain potential sources of error in any analysis of a photocentric orbit.

4. Dynamical interpretation; mass function

The analysis of the astrometric orbit of an unresolved binary gives two data of principal interest—the period P (years) and the semi-axis major α (reduced to astronomical units). In the case of a completely dark companion or in that of sufficient separation of the components, $\alpha = Ba$, and we derive the mass function

$$\frac{\alpha^3}{P^2} = B^3(\boldsymbol{M}_A + \boldsymbol{M}_B). \tag{12.4}$$

Compare this with the mass function for a spectroscopic binary with one component visible:

$$B^3 \sin^3 i(\boldsymbol{M}_A + \boldsymbol{M}_B). \tag{12.5}$$

We may write (12.4) as follows:

$$\boldsymbol{M}_B = \alpha P^{-2/3}(\boldsymbol{M}_A + \boldsymbol{M}_B)^{2/3}. \tag{12.6}$$

By making an assumption about the sum of the masses or about the mass of the primary, complete knowledge of the separate masses is obtained. Generally, however, we do not know whether the observed orbit refers to the pure image of the primary or to the photocenter of primary and companion. If it refers

to the latter, $\alpha = (B - \beta)a$, and our knowledge about the masses is limited to the mass function

$$\frac{\alpha^3}{P^2} = (B - \beta)^3(M_A + M_B). \tag{12.7}$$

Thus a combined astrometric and spectroscopic study becomes significant wherever there is appreciable inclination, e.g., in eclipsing binaries, since the astrometric study furnishes the inclination i, while the spectroscopic study may not be influenced by the blend effect β. In such a combined study the mass function $B^3(M_A + M_B)$ and the ratio β/B may be determined. So long as the companion remains unseen, visually or spectroscopically, the masses of the components cannot be rigorously derived. With a reasonable assumption about $(M_A + M_B)$, however, a value for B, and hence β, can be found, and corresponding values of M_A and M_B derived.

So long as the astrometric information is not supplemented by spectroscopic data, we remain in the dark as to the evaluation of the luminosity correction β. Generally, therefore, we are confronted with the interpretation of the mass function, which contains the three unknowns M_A, M_B, and β. We may write the mass function as follows:

$$M_B - \beta(M_A + M_B) = \alpha P^{-2/3}(M_A + M_B)^{2/3}. \tag{12.8}$$

This expression gives a lower limit for the mass of the companion, for an adopted value of the combined mass. Note that the astrometric observations alone do not yield the sign of α; hence the above expressions for the mass function have the double sign. In order to interpret the observations, we generally make different assumptions for the sum of the masses $(M_A + M_B)$, which will then yield different limiting values for the mass of the companion.

If we take $B - \beta$ positive, we find the following limiting values for the masses of the components: upper limit primary: $M_A + \beta(M_A + M_B)$; lower limit companion: $M_B - \beta(M_A + M_B)$.

If $B - \beta$ is negative, we find the following limiting values for the masses of the components: lower limit primary: $M_A - (1 - \beta)(M_A + M_B)$; upper limit companion: $M_B + (1 - \beta)(M_A + M_B)$. Hence, without additional information, the absolute size of the photocentric orbit fails to distinguish between the two components. A minimum value of the mass is always found for that component that is revealed as the perturbing influence on the photocenter, i.e., the component that is on the side of the barycenter opposite the photocenter.

Often a choice between the alternate interpretations can be made by considering the implications of the results for mass and luminosity. The definition of primary and companion implies in all cases $0 < B < 1$ and $0 < \beta < 0.5$. Any admissible value of β may satisfy the condition $0 < B - \beta < 1$, in which case the photocentric orbit is always smaller than the orbit of the primary.

The alternate interpretation is subject to the restriction that $0 < \beta - B < 0.5$. In this case the photocentric orbit may be larger than the orbit of the primary, i.e., $\beta - B > B$ or $\beta > 2B$, which implies a value of $B < 0.25$. Generally, however, the photocentric orbit is smaller than the orbit of the primary. Since the dimensions of the latter are a measure of the mass of the companion, the observations give a lower limit for the mass of the companion. One has to be very careful, therefore, about ascribing a very small photocentric orbit to the influence of a planetary companion.

5. Spectroscopic and eclipsing binaries

Although little has yet been done, astrometric research on spectroscopic and eclipsing binaries has begun. We recall the general formulae for the observed orbital displacements,

$$\text{In } x\text{: } (B)x + (G)y, \qquad \text{In } y\text{: } (A)x + (F)y, \tag{12.1}$$

where

$$\begin{aligned} (B) &= \alpha(-\cos\omega \sin \Omega - \sin\omega \cos \Omega \cos i), \\ (A) &= \alpha(-\cos\omega \cos \Omega + \sin\omega \sin \Omega \cos i), \\ (G) &= \alpha(+\sin\omega \sin \Omega - \cos\omega \cos \Omega \cos i), \\ (F) &= \alpha(+\sin\omega \cos \Omega + \cos\omega \sin \Omega \cos i). \end{aligned} \tag{12.2}$$

For both known spectroscopic and eclipsing binaries the quantities P, e, and T are more accurately determined than they could possibly be if obtained from astrometric data. For both spectroscopic and eclipsing binaries properly distributed astrometric material permits a determination of the geometric elements (B), (A), (G), and (F), or the related elements α, i, Ω, ω. Neither spectroscopic nor photometric observations yield Ω; this quantity can be determined from astrometric data only; furthermore, the spectroscopic observations do not yield i.

If, in addition to the dynamical elements, we adopt the value ω furnished by the spectroscopic or eclipsing data, the following formulae for the orbital displacements may be used:

$$\begin{aligned} \text{In } x\text{: } (B)x + (G)y &= (\alpha \sin \Omega)U - (\alpha \cos \Omega \cos i)V, \\ \text{In } y\text{: } (A)x + (F)y &= (\alpha \cos \Omega)U + (\alpha \sin \Omega \cos i)V, \end{aligned} \tag{12.9}$$

where

$$U = -x \cos\omega + y \sin\omega, \qquad V = +x \sin\omega + y \cos\omega. \tag{12.10}$$

Suitable astrometric material then yields values for α, Ω, and i. For eclipsing binaries the value of i is known, and values of α and Ω are obtained in a very simple fashion. An astrometric orbit of the eclipsing binary VV Cephei has been derived from plates obtained with the Sproul 24-inch refractor.[1]

[1] L. W. Fredrick, "The System of VV Cephei," *The Astronomical Journal*, 65 (1960): 628–643.

6. Example: Ross 614

The technique and measurement of long-focus photographic astrometry will be illustrated for the interesting astrometric binary Ross 614; $06^h24^m.3$, $-2°44'$ (1900), photovisual magnitude 11.3, spectrum M2e. An early parallax determination at the McCormick Observatory for this red dwarf star revealed variable proper motion, from which a provisional orbital motion was determined. Subsequently, a comprehensive analysis was made.[2] The combined photographic material of the Sproul (1938–1950) and McCormick (1927–1937) observatories was used. The Sproul plates were measured, using four reference stars, for which the relevant information is given in Table 12.1 (see also Fig. 12.1).

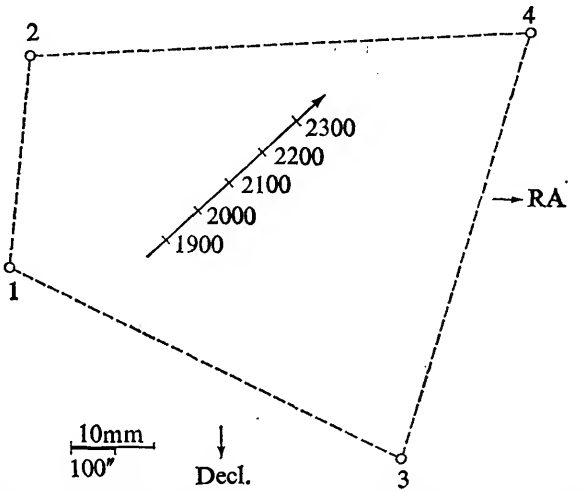

Fig. 12.1. *The astrometric binary Ross 614; reference stars and path.*

Table 12.1. REFERENCE STARS AND ROSS 614

No.	Diameter (mm)	Photo-visual Mag.	Spectrum	x_s (mm)	y_s (mm)	Dep. (1940)	ΔD/Year
1	0.127	11.4	F0	−27.52	+08.25	0.340	−0.00052
2	0.126	11.4	F5	−25.97	−17.70	0.288	+0.00001
3	0.112	11.6	F8	+19.78	+30.84	0.253	−0.00034
4	0.098	11.8	G:	+33.71	−21.39	0.119	+0.00085
Ross 614	0.130	11.3	M2e	− 7.79	+ 2.97	—	—

[2] S. L. Lippincott, "The Astrometric Binary, Ross 614 A, B—Visual Resolution and Masses of the Components," *The Astronomical Journal*, 60 (1955): 379–382.

Table 12.2. ROSS 614: DEPENDENCES AND INVERSE WEIGHT

Epoch	Dependences				Inverse Weight $1 + [D^2]$
	1	2	3	4	
1900	0.361	0.288	0.266	0.085	1.291
2000	0.309	0.289	0.232	0.170	1.261
2100	0.257	0.290	0.198	0.255	1.254
2200	0.205	0.291	0.164	0.340	1.269
2300	0.153	0.292	0.130	0.425	1.306

Because of the appreciable proper motion, two sets of dependences were used over the interval 1938–1950. The change of dependences and of the geometric accuracy (inverse weight) of the measured positions are illustrated in Table 12.2 and Figures 12.2 and 12.3. Maximum geometric accuracy will

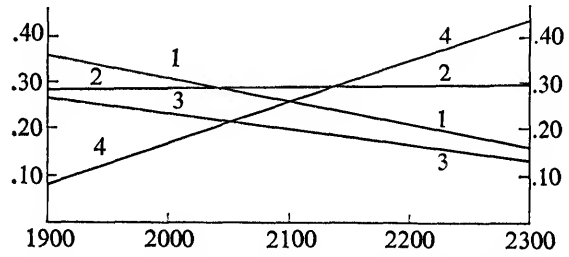

Fig. 12.2. *Dependence paths for four-star reference configuration of Ross 614.*

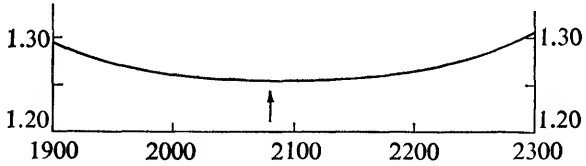

Fig. 12.3. *Inverse weight of position of Ross 614 at different epochs.*

be reached in the year 2083, when the minimum value of 1.253 will be reached for the inverse weight. The same reference system can therefore be effectively used for several centuries to come.

The Sproul material consists of 309 plates, with 933 exposures, distributed over 92 nights and representing a total weight of 191. Since the Sproul material did not cover a sufficiently large interval for a good determination of the orbital motion, it was combined with published material from the McCormick Observatory. This material was based on measurements made on a system of

five reference stars, all different from the Sproul reference stars. After correcting for a provisional value of the parallax, the McCormick measurements were reduced to the Sproul reference system by means of a linear transition derived from a graphical adjustment and checked by appropriate measurements of the transition function (Chapter 9).

Analysis of combined Sproul and McCormick material yielded the following results for the photocentric orbit of the, then, unresolved astrometric binary:

Dynamical elements: $P = 16.5$ years, $e = 0.36$, $T = 1933.2$.

Geometric elements:

$(B) = +0''.2166$, $\omega = 48°.4$,

$(A) = +0''.1162$, $\Omega = 27°.1$,

$(G) = +0''.0055$, $i = 52°.4$,

$(F) = -0''.2606$, $a = +0''.306 \pm 0''.006$ (p.e.) $= 1.22$ a.u.

See also Figures 12.4 and 12.5.

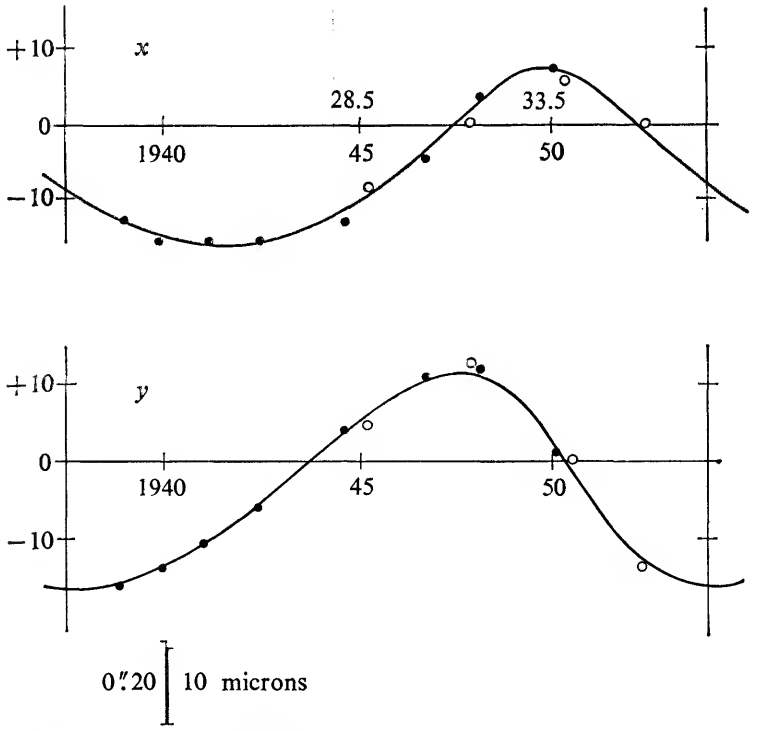

Fig. 12.4. *Ross 614. Time-displacement curves in right ascension and declination:* ● = *Sproul normal points;* ○ = *McCormick normal points.*

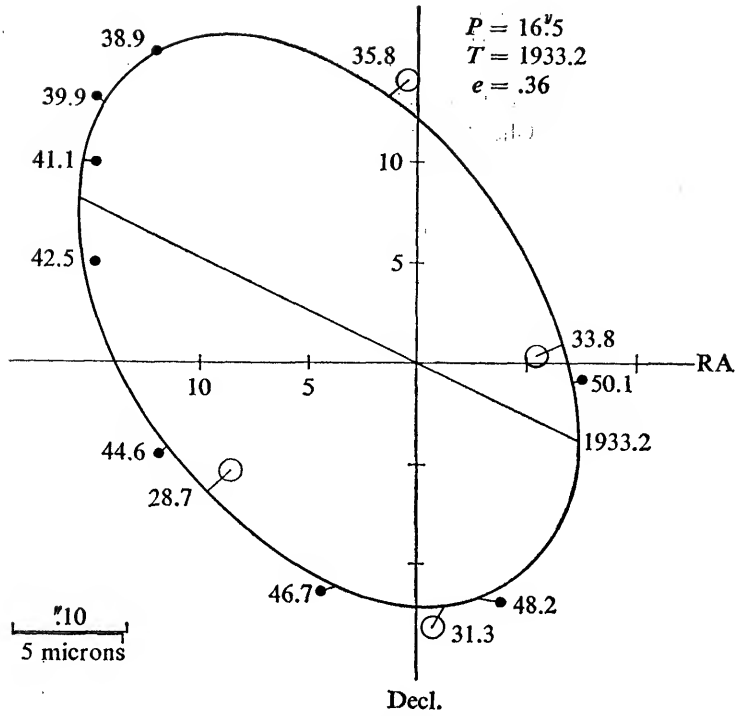

Fig. 12.5. *Photocentric orbit of Ross 614.* ● = *Sproul normal points;* ○ = *McCormick normal points. The radius in each case indicates the probable error.*

After correction for orbital motion, the Sproul material yielded a value of 0".991 for the proper motion in position angle 134° of the barycenter, and a value of +0".2468 ± 0".0024 (p.e.) for the relative parallax. Combining the latter value with determinations made elsewhere, an absolute parallax of +0".251 ± 0".0024 was derived, which was used to compute the linear value of the semi-axis major of the photocentric orbit. The resulting lower limit for the mass of the companion therefore is

$$M_B - \beta(M_A + M_B) = \alpha P^{-2/3}(M_A + M_B)^{2/3} = 0.189(M_A + M_B)^{2/3}\odot.$$

In 1955, Ross 614 was visually and photographically resolved with the Hale reflector of Palomar Observatory by Walter Baade: distance $\rho = 1".19$, position angle $\theta = 36°$, estimated magnitude difference 3.5. The predicted value for the displacement Δ of the photocenter from the barycenter was 0".372, the position angle 217°.5 (Fig. 12.6). Hence

$$B - \beta = \frac{\Delta}{\rho} = \frac{\alpha}{a} = 0.31,$$

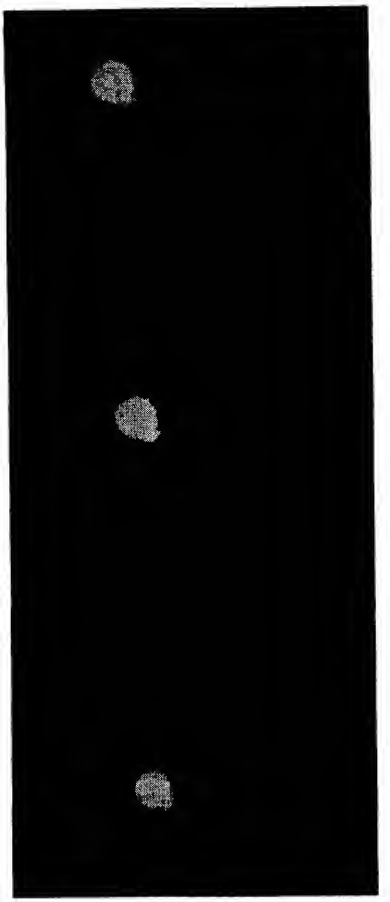

Fig. 12.6.
Three successive 5-second exposures of Ross 614, taken by W. Baade with the 200-inch Hale telescope, March 23, 1955. Scale of original photo 1 mm = 11".12. Enlarged 28×.

from which $a = 3.90$ a.u. and $M_A + M_B = a^3/P^2 = 0.22\odot$. The photovisual magnitudes of Ross 614A and B are 11.3 and 14.8, respectively; the value $\Delta m = 3.5$ yields $\beta = 0.04$. Hence B = 0.35 and, finally, $M_A = 0.14\odot$ and $M_B = 0.08\odot$. In this particular case, the principal uncertainty in the mass determination lies in the measured value of ρ. The apparent orbits of the components A, B and of the photocenter P are shown in Figure 12.7. Proper motion and parallactic and photocentric orbits are shown in Figure 12.8. The resulting path over the two decades 1938.0–1958.0 is illustrated in Figure 12.9.

7. Example: Barnard's star

The secular acceleration of Barnard's star was discussed in Chapter 9, Section 3. After correcting the observed path of Barnard's star for proper motion,

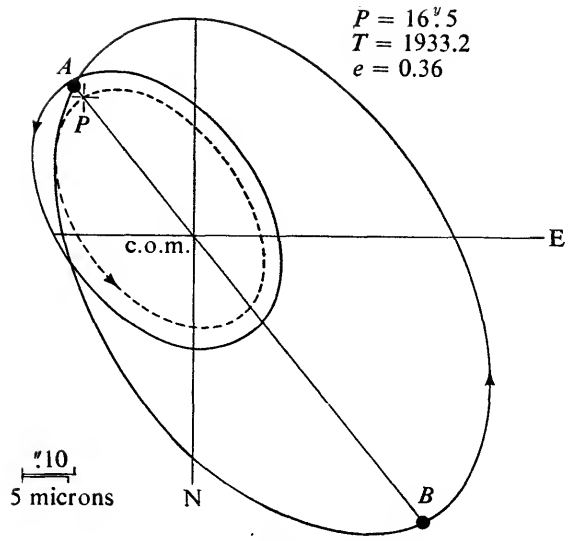

Fig. 12.7. *Orbits of components and of photocenter of Ross 614. The positions of* A, B, *and* P *are shown for March 23, 1955, the date of the visual discovery of Ross 614B.*

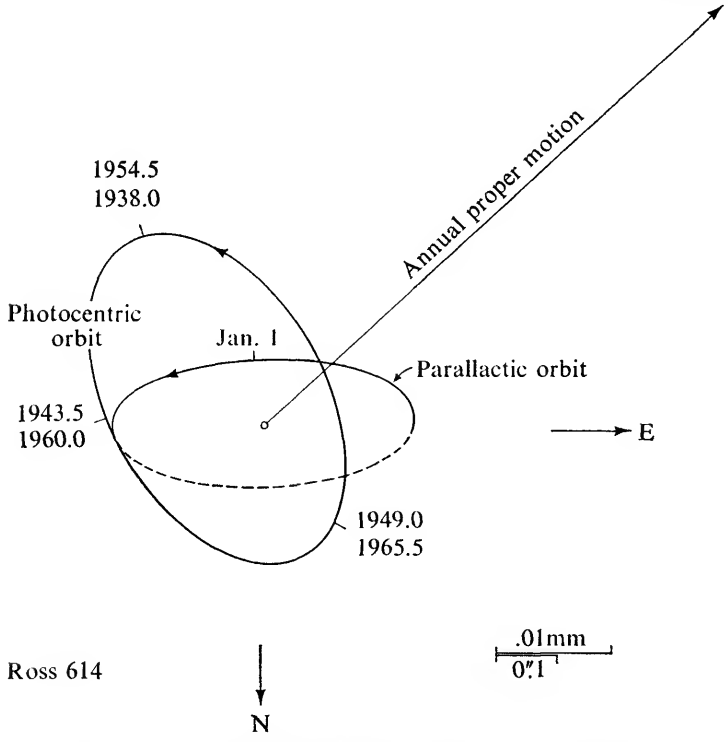

Fig. 12.8. *Annual proper motion, parallactic, and photocentric orbits of Ross 614. Since the observations are always made close to the meridian, only the full-drawn half of the parallactic orbit is accessible to observation.*

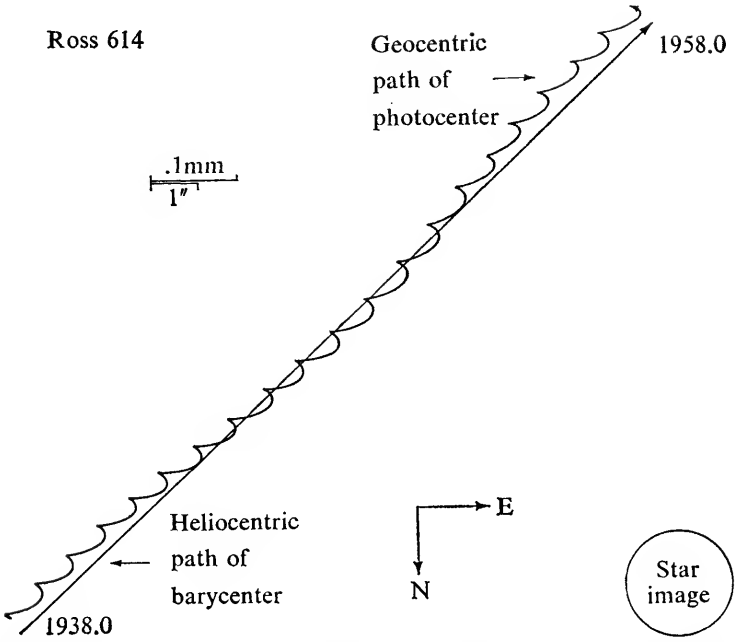

Fig. 12.9. *Path of Ross 614. The straight line refers to the heliocentric path of the barycenter. The helical line represents the geocentric path of the photocenter.*

acceleration, and parallax, residuals are left which strongly indicate a systematic displacement of the star, varying with the time.[3]

The available material consisted of 2,413 plates, with 8,260 exposures, distributed over 609 nights in the interval 1916–1962, and representing a total weight of 1,621. The material was grouped into 99 normal points, which after careful study were combined into yearly mean residuals. The systematic pattern thus revealed admits of no simpler explanation than that a perturbation has been caused by an unseen companion of Barnard's star. The time-displaced relations (Figure 12.10) may be represented by a Keplerian motion with the following elements:

Dynamical elements:	$P = 24$ years,	$e = 0.6$, $T = 1950$
Geometric elements:	$(B) = +0''.011$,	$(A) = +0''.001$,
	$(G) = +0''.019$,	$(F) = -0''.011$

The probable error of the geometric elements is $\pm 0''.002$. The geometric elements yield a value of $\alpha = 0''.0245$ for the semi-axis major of the pertur-

[3] Peter van de Kamp, "Astrometric Study of Barnard's Star," *The Astronomical Journal*, 68 (1963): 515–521.

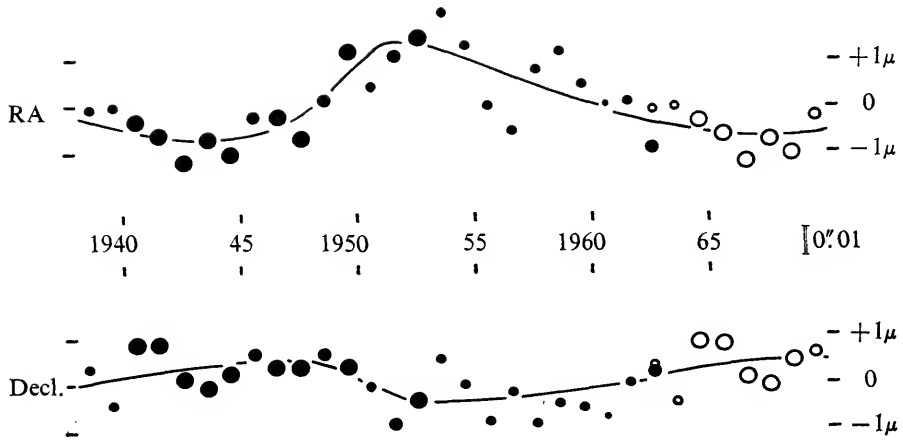

Fig. 12.10. *Yearly means of Barnard's star, averaging 96 plates and weight 80. Time-displacement curves for P = 24ᵘ, e = 0.6, T = 1950.*

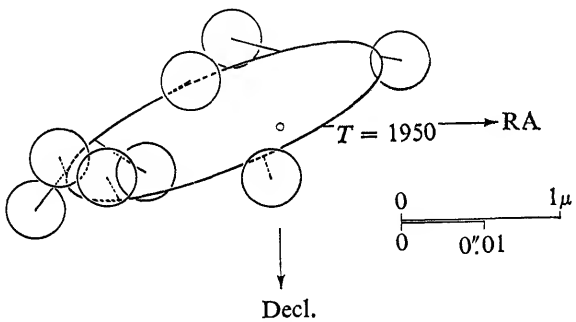

Fig. 12.11. *Apparent orbit of Barnard's star around center of mass. Eight normal points of average weight 203. Radii of circles indicate probable errors.*

bation orbit, and the inclination is $i = \pm 77°$. The observed orbit is illustrated in Figure 12.11, where the yearly mean positions have been combined into eight normal points of average weight 203.

To obtain a dynamical interpretation we assume a mass of $\boldsymbol{M} = 0.15\odot$ for Barnard's star, which is in close agreement with the known masses for stars of comparable magnitude and color. This leads to a value of

$$[0.15 \times (24^2)]^{1/3} = 4.42 \text{ a.u.},$$

or 2″.41 for the semi-axis major of the relative orbit of Barnard's star and a companion of comparatively much smaller mass $\boldsymbol{m}$. Assuming no blending effect of Barnard's star and its unseen companion, we may write

$$\frac{m}{M} = \frac{\alpha}{a} = 0.0102.$$

Hence for $M = 0.15\odot$ we find

$$m = 0.0015\odot$$

The orbital analysis leads therefore to a perturbing mass of only 1.6 that of Jupiter: in other words, to a planet-like companion of Barnard's star.

Suggested readings

Sarah Lee Lippincott and Susan Wyckoff, "Parallax and Orbital Motion of the Astrometric Binary Mu Cassiopeiae," *The Astronomical Journal*, 69 (1964): 471–474.

Peter van de Kamp, "The Search for Perturbations in Stellar Proper Motions," *in* A. Beer and K. Aa. Strand, eds., *Hertzsprung Symposium* (Vistas in Astronomy, Vol. 8) New York, Pergamon, 1966, pp. 215–218.

13 Star Fields, Clusters, and Multiple Stars

The technique and methods of long-focus photographic astrometry are applicable to other problems involving fields of limited angular extent, where high accuracy is required. Examples of these problems are field proper motions, proper motions and internal motions of open clusters, and, finally, the measurement of the proper motions of stars with distant companions, wide doubles, and multiple stars.

1. Relative proper motions

Proper motions are measured in any rectangular coordinate system, the one that is oriented closely to the equatorial system being most convenient. The results thus obtained are directly comparable with absolute proper-motion components measured in the equatorial coordinate system and referred to the sun. The orientation is found from stars of known absolute position if they occur in the field, or by a trail. For the simple case of linear plate constants, the measured differences m_x and m_y between the positions on two plates taken at different epochs are

$$\begin{aligned} m_x &= t\mu_x + c_x + a_x x + b_x y + \delta_x, \\ m_y &= t\mu_y + c_y + a_y x + b_y y + \delta_y. \end{aligned} \tag{13.1}$$

Here t is the interval; μ_x and μ_y are the yearly proper motion and are practically equal to $\mu_\alpha \cos\delta$, μ_δ. The plate constants c_x, a_x, b_x, c_y, a_y, and b_y express differences in origin, orientation, scale, the first-order effects of precession, nutation, aberration, and refraction; δ_x and δ_y are accidental errors of observation. By using gratings, magnitude compensation may be provided. For large areas or large zenith distances, higher-order terms may have to be included.

The ideal way of determining the plate constants is from galaxies, which form an ideal frame of reference for proper motions of intergalactic objects. Until the practical advent of an extragalactic reference system, we shall have to use an intragalactic reference system based on stars. We may make use of

stars with known proper motion. If this is not feasible, the plate constants may be derived from the stars themselves. For this purpose we consider the proper motions (μ_x, μ_y) as accidental deviations from the average reference system provided by the stars; the plate constants are obtained from the conditional equations

$$m_x = c_x + a_x x + b_x y, \qquad m_y = c_y + a_y x + b_y y. \tag{13.2}$$

The probable error of one equation in each coordinate is given by

$$R = 0.6745 \sqrt{\left\{\frac{t^2[\mu^2] + \delta^2}{n - 3}\right\}}. \tag{13.3}$$

The probable errors of the plate constants a and b are given by

$$r_a = \frac{R}{\sqrt{p_a}}, \qquad r_b = \frac{R}{\sqrt{p_b}}, \tag{13.4}$$

where p_a and p_b are the weights of a and b.

In this way proper motions are obtained that are relative to the origin of an internal reference system represented by a plate-constant structure (c, a, b) in each coordinate. This reference system suffers a linear distortion term $(x\epsilon_a + y\epsilon_b)$ which is of the nature of proper motion. Here ϵ_a and ϵ_b are the true errors of the plate constants a and b, and are partly of cosmic origin. The motions referred to this reference system are thus affected by a systematic error $-(x\epsilon_a + y\epsilon_b)$, but we can only say that the plate-constant structure introduces a probable error, $\pm\sqrt{(x^2 r_a^2 + y^2 r_b^2)}$. No matter how small the errors of observation (δ_x, δ_y), the accuracy of the proper motions is definitely limited by the proper motions of the stars—by the "cosmic" errors.

Apart from this, the origin of the proper motion of the reference system remains undefined, and thus proper motions derived in this manner are called "relative." The uncertainty of the plate constants caused by proper motions is entirely analogous to the uncertainty of the precession constants determined from the observed annual variations in the equatorial position of a number of stars (see Chapter 3, Section 3).

It may be desired to take into account magnitude, coma, and color effects. This may be done by the addition of terms varying linearly with the magnitude m, with the product of m and the coordinate, and with the color index k. Formulae 13.1 then become,

$$\begin{aligned} m_x &= t\mu_x + c_x + a_x x + b_x y + d_x(m - \overline{m}) \\ &\qquad + e_x x(m - \overline{m}) + f_x(k - \overline{k}) + \delta_x, \\ m_y &= t\mu_y + c_y + a_y x + b_y y + d_y(m - \overline{m}) \\ &\qquad + e_y y(m - \overline{m}) + f_y(k - \overline{k}) + \delta_y. \end{aligned} \tag{13.5}$$

Here $\overline{m}$ and $\overline{k}$ are the mean values of m and k for the chosen reference stars.

The above formulae refer to the displacements between early and recent epochs. These displacements, corrected for plate constants, are reduced to yearly proper motions by multiplying by the scale factor (Chapter 6, Section 1) and dividing by the interval in years.

2. Absolute field proper motions

An effective transfer from relative to absolute motions can be made for faint stars in small areas photographed with a long-focus instrument and centered on a standard star whose magnitude equation can be eliminated through a rotating sector or similar device. The importance of this method for obtaining absolute motions was pointed out by Schlesinger and again emphasized by Kapteyn. The method has been further worked out, and results were obtained first by Alden and van de Kamp, and later by van de Kamp and Vyssotsky, and by Vyssotsky and Williams.[1]

3. Proper motion of clusters

The long-focus photographic technique can yield accurate proper motions for open clusters. Examples are studies of the open cluster IC 348 at the center of the ζ Persei association[2] and of the open cluster NGC 2264.[3] Such studies permit the separation of cluster and noncluster stars and may also detect the expansion of stellar associations.

4. Internal Proper Motions of Open Clusters

Extreme accuracy, based on large time intervals and rich plate material, may reveal the existence of internal proper motions that are due to both dispersion in the space motions and perspective effects. An example is the study of the nucleus IC 348 of the ζ Persei association from material obtained with both the Sproul and the McCormick long-focus refractors.[2] The probable error of the annual proper motions was $\pm 0''.0003$, the probable internal

[1] H. L. Alden and P. van de Kamp, "Solar Motion and Systematic Corrections to the Proper Motions in Declination of the Preliminary General Catalogue of Boss Derived from the Proper Motions of Faint Stars Measured on Plates Taken with the 26-inch McCormick Refractor," *Publications of the Leander McCormick Observatory*, 4 (1927): 301–330. P. van de Kamp and A. N. Vyssotsky, "A Study of the Proper Motions of 18,000 Stars Derived at the Leander McCormick Observatory," *Publications of the Leander McCormick Observatory*, Volume 7, University of Virginia, 1937. A. N. Vyssotsky and Emma T. R. Williams, "An Investigation of Stellar Motions Together with Second McCormick Catalogue of Proper Motions," *Publications of the Leander McCormick Observatory*, Volume 10, University of Virginia, 1948.

[2] L. W. Fredrick, "Proper Motions in the Nucleus of the ζ-Persei Association," *The Astronomical Journal*, 61 (1956): 437–451.

[3] S. Vasilevskis, W. L. Sanders, and A. G. A. Balz, Jr., "Membership of the Open Cluster NGC 2264," *The Astronomical Journal*, 70 (1965): 797–805.

motion $\pm 0''.0006$. Another example is the study of Praesepe[4] from plates taken with the McCormick refractor. Measurements of the central part of the Praesepe cluster yielded a probable error of $\pm 0''.00079$ and a probable internal motion of $\pm 0''.00073$, in satisfactory agreement with the still more accurate values $\pm 0''.00043$ and $\pm 0''.00040$ from measurements made on plates taken with the Rutherfurd refractor with a time interval up to 65 years.[5]

5. Distant proper-motion companions

Binaries with widely separated components, as well as multiple stars, may be studied by the methods of long-focus photographic astrometry. Long periods are the rule, and in general only a beginning has been made in this field, which demands both long-range planning and perseverance.

For the study of the path of a star and its distant proper-motion companion, the dependence method is most useful. Because of the spacing between the widely separated components, two different sets of dependences are generally needed. The slightly different dependence backgrounds must be kept in mind in interpreting any observed relative orbital motion. An example is the study of the classical visual binary σ Coronae Borealis A, B, and its companion σ Coronae Borealis c, at a distance of 633″ from A and B.[6] The relative motion of c with respect to A and B, as found from the measured paths of A, B, and c, respectively, is $+0''.0004$ in right ascension and $+0''.0071$ in declination. However, because of the proper motions (μ_x, μ_y) of the reference stars and the different dependences used for A, B, and c, the above values have to be corrected for the quantities $(D_c - D_{A,B})\mu_x = +0''.0011$ and $(D_c - D_{A,B})\mu_y = -0''.0024$, yielding a corrected value for the relative motion of c with respect to A and B amounting to $+0''.0015$ in x, and $+0''.0047$ in y.

6. Wide binaries

In this section we present certain considerations about the long-range problems concerning wide binaries. Most of the well-determined binary orbits have semi-axes major between 15 and 30 astronomical units. The virtual absence of orbits with a semi-axis major of more than 100 astronomical units does not exclude the existence of such orbits, which obviously would not be determined for centuries to come. Van Biesbroeck lists some wide binaries with well-determined parallaxes whose projected linear separations range from 7,500 to

[4] Peter van de Kamp, "A Determination of the Upper Limit of Internal Motions in the Praesepe Cluster," *The Astrophysical Journal*, 81 (1935): 297–304.

[5] Jan Schilt and John Titus, "Internal Proper Motions of the Brighter Stars in Praesepe Derived from Rutherfurd's Photographs and their Repetition," *The Astronomical Journal*, 46 (1938): 197–201.

[6] Peter van de Kamp and Julia E. Damkoehler, "Parallax and Orbital Motion of the Multiple System σ Coronae Borealis A, B, c," *The Astronomical Journal*, 58 (1953): 25–28.

44,000 astronomical units, the latter value corresponding to a period of some ten million years. At least 7 percent of all stars brighter than the fifth magnitude with an annual proper motion of more than 0″.1, have distant "proper motion" companions; the actual percentage must be much higher. Nearly all these pairs have projected separations larger than 1,000 a.u., the largest being about one-fourth parsec.

Although the majority of double stars discovered are comparatively close objects, there are also the common proper motion type and the so-called 61 Cygni type binaries whose components are widely separated and have large proper motions, slightly differing in amount and direction. The spatial proximity of such stars may often be confirmed by parallax determinations. In all these cases orbital motion must exist and it can be established if sufficiently accurate measures are made. Whether the orbit is periodic or not cannot be decided until a path of sufficient duration has been established to ascertain whether it is a part of an elliptical (periodic) or hyperbolic (nonperiodic) orbit.

A few of the stars originally classified as 61 Cygni type stars now have fairly good provisional orbits. They are listed in Table 13.1.

Table 13.1. ORBITAL DATA FOR 61 CYGNI TYPE STARS

ADS	Name	Period (years)	Semi-axis major	Parallax
14636	61 Cygni	720	24″.554	+0″.292 ± 0″.004
11632	Σ 2398	351	13″.14	+ ″.280 ± ″.004
7251	Σ 1321	687	16″.52	+ ″.163 ± ″.005
48	OΣ 547	362	6″.18	+0″.090 ± 0″.005

On the other hand, there are many stars in this class whose orbital motions are slight and virtually linear, so that even provisional orbits cannot be calculated. An example is ADS 246, Groombridge 34, (parallax 0″.278) with a present separation of some 39″ and an annual change in position angle of only 0°.08, and therefore with a period of possibly several thousand years. The binding energy of a very wide binary is so small that it can be easily overcome by a stellar encounter, the estimated limit of stability being about one-half the mean interstellar distance.

We must not exclude the possible occurrence of temporary approaches among closer pairs. We may not wish to or may not be able to wait for two stars to complete a sufficiently large part of their orbit to enable us to conclude whether this orbit is elliptical or hyperbolic. Limiting information may be derived by measuring the relative velocity, provided a satisfactory estimate of the combined mass of the two components can be made. This is to some extent putting the cart before the horse, since one of the most important uses

of double stars is the determination of stellar masses. Nevertheless, two criteria are given here for what they are worth.

The relative velocity of the two components is given by the equation of energy

$$V^2 = G(M_A + M_B)\left(\frac{2}{r} - \frac{1}{a}\right), \tag{13.6}$$

expressed in cgs units, where r is the distance between the components. In the practical units, a.u., sun's mass, and sidereal year,

$$G = 4\pi^2 \quad \text{and} \quad V^2 = 4\pi^2(M_A + M_B)\left(\frac{2}{r} - \frac{1}{a}\right). \tag{13.7}$$

which may also be written as

$$V^2 r = 4\pi^2(M_A + M_B)\left(2 - \frac{r}{a}\right). \tag{13.8}$$

Hence the condition for a parabolic orbit is the critical value

$$V^2 r = 8\pi^2(M_A + M_B). \tag{13.9}$$

Whether the orbit, therefore, is periodic or nonperiodic depends on whether the value of $V^2 r$ is below or above the critical value.

Apart from evaluating $M_A + M_B$ there is the problem of determining V and r. If parallax, proper motion, and radial velocity are known, V may be determined and the projection of r can be obtained. At best we can obtain a projected value of $V^2 r$, which will always be smaller than the true value. If this projected value is larger than the critical value, the orbit must be hyperbolic, if it is smaller, the orbit *may* be elliptical.

Another orbital criterion is given by the observed areal constant, which is

$$C = \rho w \cos \phi, \tag{13.10}$$

where ρ is the separation and w the yearly orbital motion, both in seconds of arc, and ϕ is the angle between the orbital motion and its component perpendicular to the separation.

The true areal velocity A is related to the semi-axis major a and eccentricity e by the relation:

$$4A^2 = G(M_A + M_B)a(1 - e^2), \tag{13.11}$$

in cgs units, whence, in practical units,

$$A = \pi\sqrt{(M_A + M_B)a(1 - e^2)}. \tag{13.12}$$

The areal constant is twice the angular value of the projected areal velocity. If the parallax is well determined, C may be expressed in linear measure and we may write

$$C = 2\pi \cos i\sqrt{(M_A + M_B)a(1 - e^2)}, \tag{13.13}$$

where i is the orbital inclination. Thus, if the parallax is known, we can derive a minimum value of the semi-axis major a from the relation

$$a(1 - e^2) \cos^2 i = \frac{C^2}{4\pi^2(M_A + M_B)} \tag{13.14}$$

using an estimated value of $(M_A + M_B)$.

Since in the true orbit $r + r' = 2a$, where r is the radius vector to the "empty" focus, the projected value of r yields a minimum value for the upper limit of a, an awkward bit of information.

Any adopted value of a yields, of course, a value of the period, through the harmonic relation

$$P^2 = a^3(M_A + M_B)^{-1}. \tag{13.15}$$

Take, for example, the wide double star Groombridge 34 for which the projected separation is 140 a.u., the projected linear orbital velocity 0.20 a.u./year, and the observed areal constant 28 (a.u.)^2/year. If we adopt a total mass of 0.5, the projected value of V^2r is 5.6, which falls well below the parabolic criterion, 40. A high orbital inclination may be indicated. We also find

$$a(1 - e^2) \cos^2 i = \frac{784}{2\pi^2} = 39.6, \tag{13.16}$$

i.e., a minimum value of about 40 a.u. for a.

Since $r + r' = 2a$, the projected separation of 140 a.u. yields a minimum value of 70 a.u. for the upper limit of a. With $a = 50$ a.u., the corresponding value of the period is 500 years.

7. Multiple stars

There are numerous systems, recognized as *triple*, in which the space-time dimensions of the large orbit of the third, or distant, companion are always of a much higher order than those of the smaller orbit of the close binary.

One of the best-known triple systems is the nearest star α Centauri. The visual binary, AB, has a period of 80.09 years and a semi-axis of 23.2 a.u. The companion C is at a distance of 2°11′, or a projected linear separation of 14,000 a.u., indicating a period of the order of a million years. The star α Centauri C, also called Proxima Centauri, appears to have a slightly larger parallax (0″.767 ± 0″.006) than the system AB(0″.748 ± 0″.004) according to an unpublished investigation by Gasteyer.

An example of *quadruple* system is σ Coronae Borealis, with the widely different periods of 7.974 days for the spectroscopic binary A, 1,162 years for the visual system AB, and a period of the order of a million years for the distant component c around AB. The semi-axis major of the visual orbit is 151.5 a.u., the projected separation of the distant companion c from the center of mass AB is 13,000 a.u.

An interesting *quintuple* system is ξ Scorpii-Σ 1999.[7]

Castor is a *sextuple* system. The visual binary AB has a period of 380 years and a semi-axis major of 86.1 a.u. Both A and B are spectroscopic binaries with periods of 9.21 and 1.93 days respectively. The distant companion C is an eclipsing binary with a period of 0.81 days. The projected separation of C and AB is 1,000 a.u., indicating a period of more than ten thousand years.

[7] Peter van de Kamp and Robert S. Harrington, "Parallax, Proper Motion, and Orbital Motion of the Components of the Quintuple System of Xi Scorpii-Σ 1999," *The Astronomical Journal*, 69 (1964): 402–406.

III

ANALYSIS OF OBSERVATIONS

14 Theory of Errors

This chapter and the one that follows comprise a brief survey of methods of dealing with errors of observation and of the least-squares analysis of linear equations. The aim has been to present a rigorous treatment whenever possible; if such treatment is not used, it is clearly stated. The choice and presentation of concepts and formulae have been based on practical considerations —only the most common applications of those in wide use are considered here. For comprehensive treatment see the books listed at the end of this chapter.

1. Error law; modulus of precision

Systematic errors arise from causes which either persist through a series of observations, or are governed by a determinable law.

Accidental errors arise from causes so variable and transient that the resulting errors elude tracing. We assume that positive and negative errors of the same size are equally likely, and that small errors are more likely than large errors. General reasoning, followed through mathematically, shows that the error distribution, i.e., the frequency of errors Δ, turns out to be of the form

$$F(\Delta) \sim e^{-x^2} \qquad \text{or} \qquad e^{-(h\Delta)^2}, \tag{14.1}$$

where x is proportional to the amount of the error and may be written as $h\Delta$. Here h is a measure of the spread in the errors and is named the *modulus of precision*. Thus for different error distributions the same frequency of errors $F(\Delta)$ is reached for the same value of $x = h\Delta$. The larger the value of h, the smaller the corresponding value of Δ; or, in other words, the value of Δ corresponding to a certain value of $F(\Delta)$ is inversely proportional to h. This simple, convenient relation proves to be a close approach to the actual error distribution.

We may thus write

$$F(\Delta)\, d\Delta = Ce^{-x^2}\, dx, \tag{14.2}$$

where $F(\Delta)\, d\Delta$ is the fraction of all errors between Δ and $\Delta + d\Delta$. The value of C is obtained by noting that

$$1 = \int_{-\infty}^{+\infty} F(\Delta)\, d\Delta = C \int_{-\infty}^{+\infty} e^{-x^2}\, dx. \tag{14.3}$$

The value of the integral in (14.3) may be calculated in different ways, of which one of the simplest is the following.

Write

$$\int_{-\infty}^{+\infty} e^{-x^2}\, dx = \int_{-\infty}^{+\infty} e^{-y^2}\, dy. \tag{14.4}$$

Considering x and y as rectangular coordinates, the double integral

$$\int_{-\infty}^{+\infty} \int_{-\infty}^{+\infty} e^{-(x^2+y^2)}\, dx\, dy \tag{14.5}$$

is the content of a figure of revolution, (see Fig. 14.1), which may also be expressed as

$$\int_{0}^{+\infty} 2\pi r\, e^{-r^2}\, dr \tag{14.6}$$

and may be reduced as follows:

$$\pi \int_{0}^{+\infty} e^{-r^2}\, d(r^2) = \pi e^{-r^2}\Big|_{+\infty}^{0} = \pi. \tag{14.7}$$

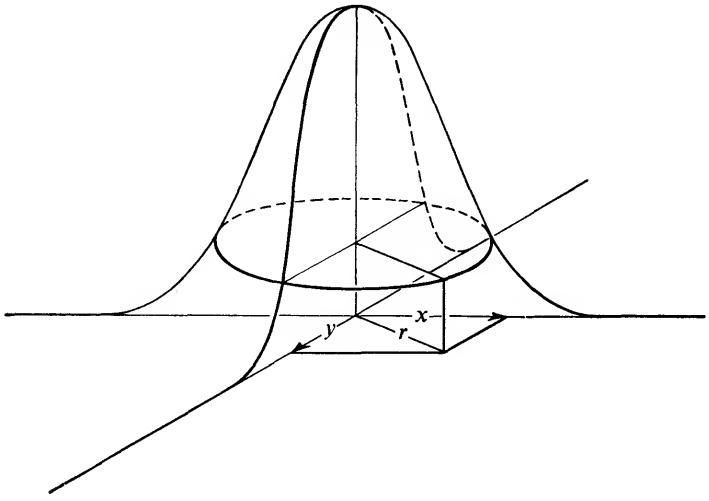

Fig. 14.1. *Proof that* $\int_{0}^{\infty} e^{-x^2}\, dx = \frac{\sqrt{\pi}}{2}$.

Hence (see 14.4)

$$\int_{-\infty}^{+\infty} e^{-x^2}\,dx = \sqrt{\pi}, \tag{14.8}$$

and also

$$\int_{0}^{+\infty} e^{-x^2}\,dx = \frac{\sqrt{\pi}}{2}. \tag{14.9}$$

Hence in (14.3)

$$C = \frac{1}{\sqrt{\pi}} \tag{14.10}$$

and we have

$$F(\Delta)\,d\Delta = \frac{1}{\sqrt{\pi}}\,e^{-x^2}\,dx \tag{14.11}$$

or, substituting $x = h\Delta$

$$F(\Delta)\,d\Delta = \frac{h}{\sqrt{\pi}}\,e^{-(h\Delta)^2}\,d\Delta. \tag{14.12}$$

$F(\Delta)$ represents the so-called *probability function*, also referred to as *normal curve*, or *Gaussian* or *Maxwellian* distribution.

2. Mean, average, and probable error

In studying and dealing with accidental errors, it is customary and convenient to have certain specific errors represent the accuracy of a series of observations. We assume that we deal with a homogeneous series: that is, that all observations have the same modulus of precision.

We recognize the

1) mean error ϵ;
2) average error η;
3) probable error r.

The theoretical values for these quantities will now be derived.

The *mean error*, or rather root-mean-square error is obtained as follows. Its square is the average value of the squares of the errors, i.e.,

$$\epsilon^2 = \frac{2h}{\sqrt{\pi}} \int_{0}^{+\infty} e^{-(h\Delta)^2}\Delta^2\,d\Delta.$$

Introduce $h\Delta = x$, i.e., $d\Delta = dx/h$. Thus

$$\epsilon^2 = \frac{2}{h^2\sqrt{\pi}} \int_{0}^{+\infty} e^{-x^2}x^2\,dx.$$

Integrating by parts, i.e.,

$$\int x\,du = xu - \int u\,dx, \qquad \text{where} \qquad u = -\frac{e^{-x^2}}{2}$$

we obtain

$$du = e^{-x^2}x\,dx.$$

We now have

$$\epsilon^2 = \frac{1}{h^2\sqrt{\pi}}\left[\frac{-xe^{-x^2}}{2}\Big|_0^{+\infty} + \int_0^{+\infty} e^{-x^2}\,dx\right] = \frac{1}{h^2\sqrt{\pi}}\,\frac{\sqrt{\pi}}{2}$$

or

$$\epsilon^2 = \frac{1}{2h^2}$$

or

$$\epsilon = \frac{1}{h\sqrt{2}} \tag{14.13}$$

The *average*, or absolute mean η, of the errors is obtained as follows:

$$\eta = \frac{2h}{\sqrt{\pi}}\int_0^{\infty} e^{-(h\Delta)^2}\Delta\,d\Delta = \frac{h}{\sqrt{\pi}}\int_0^{\infty} e^{-(h\Delta)^2}\,d\Delta^2$$

$$= \frac{1}{h\sqrt{\pi}}\int_0^{\infty} e^{-(h\Delta)^2}\,d(h\Delta)^2 = \frac{1}{h\sqrt{\pi}}\,e^{-(h\Delta)^2}\Big|_{\infty}^{0},$$

and hence

$$\eta = \frac{1}{h\sqrt{\pi}}. \tag{14.14}$$

The *probable error* is the border line between an equal number of large and small errors, considering their absolute values. In other words, in any error distribution there is an equal chance that an error may be either larger or smaller than the probable error. Hence, the probable error r is found by the condition

$$\frac{2h}{\sqrt{\pi}}\int_0^{r} e^{-(h\Delta)^2}\,d\Delta = \frac{1}{2}$$

or, substituting $x = h\Delta$,

$$\int_0^{hr} e^{-x^2}\,dx = \frac{\sqrt{\pi}}{4} = 0.4431.$$

From tabulated values for the integral, the value $hr = 0.477$ is obtained.

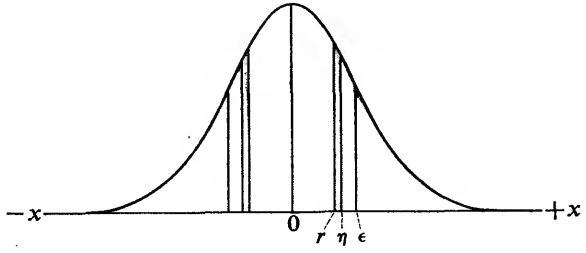

Fig. 14.2. *Probability function; probable* (r), *average* (η), *and mean error* (ϵ).

Hence

$$r = \frac{0.477}{h}. \tag{14.15}$$

Summarizing:

Mean error: $\epsilon = \dfrac{1}{h\sqrt{2}} = 1.2533\eta$

Average error: $\eta = \dfrac{1}{h\sqrt{\pi}} = 0.7979\epsilon$

Probable error: $r = \dfrac{0.477}{h} = 0.8453\eta = 0.6745\epsilon$

Table 14.1 lists the probability P of an error being smaller than t times the probable error. Table 14.2 lists the probability P of errors within certain limits

Table 14.1. PROBABILITY LESS THAN t TIMES PROBABLE ERROR

t	P	t	P	t	P
0.0	0.000	1.0	0.500	2.0	0.823
0.1	0.054	1.1	0.541	2.2	0.862
0.2	0.107	1.2	0.587	2.4	0.895
0.3	0.160	1.3	0.619	2.6	0.921
0.4	0.213	1.4	0.655	2.8	0.941
0.5	0.264	1.5	0.688	3.0	0.957
0.6	0.314	1.6	0.719	3.5	0.982
0.7	0.363	1.7	0.748	4.0	0.9930
0.8	0.411	1.8	0.775	5.0	0.99926
0.9	0.456	1.9	0.800	6.0	0.999948
1.0	0.500	2.0	0.823	7.0	0.9999977

Table 14.2. PROBABILITIES AND CHANCES IN RELATION TO PROBABLE ERROR

Between limits	P	Error larger than	P	Chance: one in
0–$0.5r$	0.264	r	0.500	2
0–r	0.500	$2r$	0.177	6
r–$2r$	0.323	$3r$	0.043	23
$2r$–$3r$	0.134	$4r$	0.007	143
$3r$–$4r$	0.036	$5r$	0.00074	1,350
$4r$–$5r$	0.006	$6r$	0.000052	19,230
$5r$–∞	0.001			

and the probability and chance that an error exceeds a certain limit, all referred to the probable error.

3. Arithmetical mean: equations of condition, residuals

We approach the principle and method of least squares through consideration of the arithmetical mean of a homogeneous series of observations.

Suppose we have a series of m observed values

$$n_1, n_2, n_3, \cdots n_m$$

of the unknown quantity x, all made under the same conditions. We may say that we have a series of observational equations, or *equations of condition*:

$$\begin{aligned} x &= n_1 \\ x &= n_2 \\ x &= n_3 \\ &\cdot \\ &\cdot \\ &\cdot \\ x &= n_m. \end{aligned}$$

For any adopted value of x, we may form the so-called *residuals* v (also named "Observed minus Computed," or simply O − C)

$$\begin{aligned} v_1 &= n_1 - x \\ v_2 &= n_2 - x \\ v_3 &= n_3 - x \\ &\cdot \\ &\cdot \\ &\cdot \\ v_m &= n_m - x. \end{aligned}$$

Obviously the algebraic sum of the residuals may be written as

$$[v] = [n] - mx. \tag{14.16}$$

Of particular interest is the so-called *arithmetical mean*

$$\bar{x} = \frac{[n]}{m}, \tag{14.17}$$

for which

$$[v] = 0. \tag{14.18}$$

In many observational problems the arithmetical mean is the preferred value and is considered the most probable. This preference proves to be related to a simple property of the residuals. If we form the sum of the squares of the residuals, we find

$$[v^2] = [(n - x)^2] = [n^2] - 2x[n] + mx^2.$$

The sum $[v^2]$ depends on the choice of x, but reaches an extreme value for

$$\frac{d[v^2]}{dx} = -2[n] + 2mx = 0,$$

i.e.,

$$\bar{x} = \frac{[n]}{m}. \tag{14.17}$$

Note that

$$\frac{d^2[v^2]}{dx^2} = +2m.$$

Thus the *arithmetical mean* corresponds to a *minimum* value for the *sum of the squares of the residuals.*

4. Error of sum of observations, of one observation, and of arithmetical mean

Let there be m observations

$$n_1, n_2, n_3, \cdots n_m$$

of the unknown quantity x. What is the accuracy of the sum N of these observations? Let the individual errors of the observations be

$$\Delta_1, \Delta_2, \Delta_3, \cdots \Delta_m.$$

Then the error Δ_N of N equals

$$\Delta_N = \Delta_1 + \Delta_2 + \Delta_3 + \cdots + \Delta_m,$$

from which we derive

$$\Delta_N^2 = [\Delta^2], \tag{14.19}$$

assuming that for a sufficiently large number of observations the error products $\Delta_1\Delta_2$, $\Delta_1\Delta_3$, etc. may be expected to cancel.

Introducing the concept of mean error ϵ we write

$$[\Delta^2] = m\epsilon^2,$$

and Δ_N^2 may be approximated by E^2 where E is the mean error of the sum N, an assumption which on the average, over many equivalent series, is justified. Hence

$$E^2 = m\epsilon^2,$$

or

$$E = \epsilon\sqrt{m}. \tag{14.20}$$

For the arithmetical mean of the m values, i.e., for the quantity N/m, the error is reduced m-fold. Hence the mean error ϵ_0 of the arithmetical mean is

$$\epsilon_0 = \frac{\epsilon}{\sqrt{m}}. \tag{14.21}$$

Comment on (14.21).—The arithmetical mean of the m values may be said to be worth m times as much as one observation; we may say that the arithmetical mean of m observation has a *weight* m. The mean error of one observation may be referred to as the mean error of unit weight. Hence the mean error of the arithmetical mean is obtained from the mean error of unit weight by dividing the latter by the square root of the weight m. Conversely the weight m equals the square of the mean error of unit weight divided by the square of the mean error of the arithmetical mean. The same relationships hold, of course, for probable errors.

We next ask, "How can we derive ϵ, and hence ϵ_0 from the residuals v from the arithmetical mean?" We proceed as follows:

For each observation the residual v from the arithmetical mean is related to the error Δ as follows:

$$\Delta = v - \Delta_0,$$

where Δ_0 is the error of the arithmetical mean. It should be stressed again that only the residuals can be evaluated, not the errors, although the difference may be slight if there are many observations, and hence, presumably, a small value of Δ_0. We find each residual squared to be

$$\Delta^2 = v^2 + \Delta_0^2 - 2v\Delta_0,$$

and the sum of the squares of all residuals is

$$[\Delta^2] = [v^2] + m\Delta_0^2, \tag{14.22}$$

the summation of the third right-hand term obviously being zero.

We now make an approximation, namely that Δ_0 equals the mean error ϵ_0 of the arithmetical mean, an assumption which on the average over many series of observations is true. Hence (14.22) becomes

$$[\Delta^2] = [v^2] + m\epsilon_0^2. \tag{14.23}$$

Now

$$[\Delta^2] = m\epsilon^2,$$

and

$$\epsilon_0^2 = \frac{\epsilon^2}{m};$$

hence

$$\epsilon^2(m - 1) = [v^2],$$

or

$$\epsilon = \sqrt{\frac{[v^2]}{m - 1}}, \tag{14.24}$$

the formula for the mean error of each observation in a series of observations. The corresponding probable error is

$$r = 0.6745\sqrt{\frac{[v^2]}{m-1}}. \tag{14.25}$$

The arithmetical mean of m observations has a *weight* $= m$. The mean error and probable error of the arithmetical mean are given by

$$\epsilon_0 = \frac{\epsilon}{\sqrt{m}} = \sqrt{\frac{[v^2]}{m(m-1)}} \tag{14.26}$$

and

$$r_0 = \frac{r}{\sqrt{m}} = 0.6745\sqrt{\frac{[v^2]}{m(m-1)}}. \tag{14.27}$$

5. Error from range of observations

Schlesinger has devised an ingenious, simple, fast method for calculating the mean, or probable error, from the range of a small number of m observations of a quantity.[1] He showed that the mean error ϵ is related to the range R, i.e., the difference between the largest and smallest value, by the formula

$$\epsilon = \frac{R}{2}\sqrt{\frac{(m+1)(m+2)}{3m(m-1)}}, \tag{14.28}$$

and hence the mean error of the arithmetical mean

$$\epsilon_0 = \frac{R}{2m}\sqrt{\frac{(m+1)(m+2)}{3(m-1)}}. \tag{14.29}$$

These formulae are a good approximation so long as m is small, say not over 6.

Table 14.3 shows the factor with which to multiply the range R in order to obtain the value of the mean, or probable error, for series of 3, 4, 5, and 6 observations.

Table 14.3. RELATION OF MEAN AND PROBABLE ERROR TO RANGE

m	3	4	5	6
ϵ/R	0.53	0.45	0.41	0.38
ϵ_0/R	0.30	0.23	0.18	0.16
r/R	0.36	0.30	0.28	0.26
r_0/R	0.20	0.15	0.12	0.11

[1] F. Schlesinger, "Computation of Probable Errors from the Range," *The Astronomical Journal*, 46 (1937): 161–162.

The probable (or mean) error itself has a probable (or mean) error, since its value is computed from a limited number of observations. It can be shown that the ratio of the probable error of the probable error to the probable error itself equals

$$\frac{0.477}{\sqrt{n}}. \tag{14.30}$$

For example, a parallax determination based on 25 observations may prove to have a probable error of 0".010, which value in turn has a probable error of 0".001.

6. Combination of errors

If a quantity is affected by different sources of error, then it can be shown that

$$\epsilon_t^2 = \epsilon_1^2 + \epsilon_2^2 + \cdots + \epsilon_m^2, \tag{14.31}$$

where ϵ_t is the total (mean) error and $\epsilon_1, \epsilon_2, \cdots \epsilon_m$ are the mean errors of the various contributing error sources. For example, if $u = x + y + z$, then the mean error of u is related to the mean errors of x, y, z by

$$\epsilon_u^2 = \epsilon_x^2 + \epsilon_y^2 + \epsilon_z^2. \tag{14.32}$$

Similarly, for the relation $u = ax + by + cz$, we have

$$\epsilon_u^2 = (a\epsilon_x)^2 + (b\epsilon_y)^2 + (c\epsilon_z)^2. \tag{14.33}$$

Corresponding relations exist, of course, for the probable errors.

Suggested readings

William Chauvenet, *Spherical and Practical Astronomy*, 5th ed. (1891). Vol. II. (Reprinted by Dover Publications, New York.)

F. B. Hildebrand, *Introduction to Numerical Analysis*. New York, McGraw-Hill, 1956.

W. M. Smart, *Combination of Observations*. Cambridge University Press, 1958.

E. T. Whittaker and G. Robinson, *The Calculus of Observations*. London and Glasgow, 1932, Blackie and Son, Ltd.

15 | Method of Least Squares

1. Principle of least squares

The principle of least squares as found for the arithmetical mean (Chapter 14) may be derived in a more general, sophisticated fashion; it is then found to have a wider significance. We recall that general mathematical reasoning leads to the probability

$$F(\Delta)\, d\Delta = \frac{h}{\sqrt{\pi}} e^{-(h\Delta)^2}\, d\Delta \qquad (14.12)$$

for an error lying between Δ and $\Delta + d\Delta$. $F(\Delta)$ represents the probability function. Suppose now that a homogeneous series of observations yields a corresponding series of conditional equations involving one or more unknowns. If the number of equations exceeds the number of unknowns the values of the unknowns must be so chosen as to yield the most probable set of residuals. We therefore adopt as the most likely set of values for the unknowns that which yields the highest combined probability for the resulting errors, i.e., the product

$$F(\Delta_1)F(\Delta_2)F(\Delta_3) \cdots F(\Delta_m) \qquad (15.1)$$

must be a maximum. This means that $[\Delta^2]$ should be a minimum, assuming homogeneous observations, all of the same modulus of precision h. This in turn implies that the sum of the squares of the residuals

$$[v^2]$$

should be a minimum.

To prove this, observe that

$$\Delta_1 = v_1 + c_1$$

and so on, where c_1 represents a small correction made in v_1 to obtain the "true" error Δ_1. We thus have

$$[\Delta^2] = [v^2] + [c^2], \qquad (15.2)$$

assuming the products cv to cancel. The most probable adjustment for $[\Delta^2]$, i.e., the minimum value of $[\Delta^2]$, must correspond to a minimum value of $[v^2]$, which is slightly smaller than $[\Delta^2]$.

2. Equations of condition; normal equations for two and more unknowns

The principle of least squares has the great advantage of being applicable to those conditional linear equations with which it is not feasible to follow the conventional procedure of using arithmetical means. This includes not only the case in which one unknown is multiplied by a different coefficient in each of many observational equations, but also that of linear equations of condition including two and more unknowns.

Consider first the conditional equations in which one unknown appears with different coefficients:

$$\begin{aligned} a_1x &= n_1, \\ a_2x &= n_2, \\ &\cdot \\ &\cdot \\ &\cdot \\ a_mx &= n_m. \end{aligned} \tag{15.3}$$

Again, for any adopted value of x, we have the residuals

$$\begin{aligned} v_1 &= n_1 - a_1x, \\ v_2 &= n_2 - a_2x, \\ &\cdot \\ &\cdot \\ &\cdot \\ v_m &= n_m - a_mx. \end{aligned}$$

We now apply the principle of least squares. The sum of the squares of the residuals is given by

$$\begin{aligned} [v^2] &= [(n - ax)^2] \\ &= [n^2] - 2x[an] + x^2[aa] \end{aligned} \tag{15.4}$$

(using the symbol aa for a^2).

A minimum value of $[v^2]$ is reached for

$$\frac{d[v^2]}{dx} = -2[an] + 2x[aa] = 0,$$

i.e.,

$$[aa]x = [an]. \tag{15.5}$$

Hence the so-called *normal equation* (15.5) yields the most probable value of x, based on the equations of condition (15.3).

For linear equations with two unknowns, we have the equation of condition

$$\begin{aligned} a_1x + b_1y &= n_1, \\ a_2x + b_2y &= n_2, \\ &\vdots \\ a_mx + b_my &= n_m. \end{aligned} \tag{15.6}$$

For the adopted values of x and y we find the residuals:

$$\begin{aligned} v_1 &= n_1 - (a_1x + b_1y), \\ v_2 &= n_2 - (a_2x + b_2y), \\ &\vdots \\ v_m &= n_m - (a_mx + b_my). \end{aligned}$$

The sum of the squares of the residuals is given by

$$\begin{aligned} [v^2] &= [\{n - (ax + by)\}^2] \\ &= [n^2] - 2[(ax + by)n] + [(ax + by)^2]. \end{aligned} \tag{15.7}$$

The principle of least squares now requires that the most probable values of x and y correspond to minimum values of $[v^2]$, i.e.,

$$\frac{d[v^2]}{dx} = -2[an] + 2[(ax + by)a] = 0$$

$$\frac{d[v^2]}{dy} = -2[bn] + 2[(ax + by)b] = 0$$

leading to the two normal equations

$$\begin{aligned} [aa]x + [ab]y &= [an], \\ [ab]x + [bb]y &= [bn], \end{aligned} \tag{15.8}$$

from which the most probable values of x and y are found. Similarly, a series of conditional equations with three unknowns, x, y, z,

$$\begin{aligned} a_1x + b_1y + c_1z &= n_1, \\ a_2x + b_2y + c_2z &= n_2, \\ &\vdots \\ a_mx + b_my + c_mz &= n_m, \end{aligned} \tag{15.9}$$

will yield three normal equations,

$$\begin{aligned} [aa]x + [ab]y + [ac]z &= [an], \\ [ab]x + [bb]y + [bc]z &= [bn], \\ [ac]x + [bc]y + [cc]z &= [cn], \end{aligned} \tag{15.10}$$

from which the most probable values of x, y, and z are found.

The procedure may be extended for linear equations of condition with any number of unknowns.

After the unknowns have thus been derived they are substituted in the equation of condition and the residuals derived. A simple arithmetical check is, of course, the following

$$[av] = 0, [bv] = 0, [cv] = 0, \cdots \tag{15.11}$$

Note that $[v]$ does not necessarily equal zero, but must equal zero (always within the rounding off errors) if all values of a, or b, or c are equal.

3. Weights; error of unit weight

So far we have assumed that all observations have been made under the same circumstances, and thus are *a priori* of equal significance or weight. We shall now consider observations of different weights. The general concept of weight is most easily understood by returning to the arithmetical mean (Chapter 14, Section 4). The mean of p observations of a series characterized by the same modulus of precision has a mean error of $1/\sqrt{p}$ times the mean error of one observation.

We recall that the arithmetical mean has the same significance, or weight, as p separate observations; the number p may be said to indicate the *weight* of the arithmetical mean. We may also relate this concept of weight to the modulus of precision (Chapter 14). Note that mean (also probable and average) errors are inversely proportional to the modulus of precision. Hence, an arithmetical mean of weight p has a modulus of precision which is $\sqrt{p}$ times as large as that of one "standard" observation.

Once the concept of weight is understood and accepted, its use may be extended and need not be limited to integer values of the weight. Although in many astronomical observations an attempt is made to collect observations of equal "unit" weight (weight obviously being a relative concept), unequal weights are frequently the rule. The reasons are: the gradual increase in precision that results from changes in techniques; instrumental, personal, and climatic limitations.

It is normal, therefore, to take into account different weights in any series of observations, which is done simply by multiplying each conditional equation by its weight p. This may be regarded either as counting the equation

p times, or as reducing all equations to the same modulus of precision corresponding with *weight unity; p* need not be an integer.

For the case of one unknown we thus have the equations of condition

$$\begin{aligned} a_1x &= n_1 \qquad \text{weight } p_1, \\ a_2x &= n_2 \qquad \text{weight } p_2, \\ &\cdots \\ a_mx &= n_m \qquad \text{weight } p_m, \end{aligned} \tag{15.12}$$

and the normal equation

$$[paa]x = [pan]. \tag{15.13}$$

In this case it can be shown that the mean error of an observation of unit weight is given by

$$\epsilon_1 = \sqrt{\frac{[pv^2]}{m-1}}, \tag{15.14}$$

and the probable error of unit weight by

$$r_1 = 0.6745\sqrt{\frac{[pv^2]}{m-1}}. \tag{15.15}$$

The quantity $[paa]$ represents the *weight* p_x of the unknown as determined by the normal equation. Hence the mean error and the probable error of x, as derived from the normal equation, are given by

$$\epsilon_x = \frac{\epsilon_1}{\sqrt{p_x}}, \tag{15.16}$$

and

$$r_x = \frac{r_1}{\sqrt{p_x}}. \tag{15.17}$$

4. Solution of normal equations; weights and errors for two and more unknowns

For two, three, and more unknowns the normal equations are similar to those derived in Section 2, except that the summation in both diagonal and cross terms takes into account the weights of the individual equations of condition.

For the case of three unknowns the normal equations are therefore,

$$\begin{aligned} [paa]x + [pab]y + [pac]z &= [pan], \\ [pab]x + [pbb]y + [pbc]z &= [pbn], \\ [pac]x + [pbc]y + [pcc]z &= [pcn], \end{aligned} \tag{15.18}$$

from which the most probable values of x, y, and z are found.

We have the arithmetical controls

$$\begin{aligned} [pav] &= 0, \\ [pbv] &= 0, \\ [pcv] &= 0. \end{aligned} \tag{15.19}$$

The normal equations may be solved in several ways. A common procedure, due to Gauss, is the following, illustrated here for the case of three unknowns.

The normal equations 15.18 may be reduced to two equations by first eliminating x, and writing

$$\begin{aligned} [pbb.1]y + [pbc.1]z &= [pbn.1], \\ [pbc.1]y + [pcc.1]z &= [pcn.1], \end{aligned} \tag{15.20}$$

where

$$\begin{aligned} [pbb.1] &= [pbb] - \frac{[pab]}{[paa]}[pab], \\ [pbc.1] &= [pbc] - \frac{[pab]}{[pan]}[pac], \\ [pcc.1] &= [pcc] - \frac{[pac]}{[paa]}[pac], \\ [pbn.1] &= [pbn] - \frac{[pab]}{[paa]}[pan], \\ [pcn.1] &= [pcn] - \frac{[pac]}{[paa]}[pan]. \end{aligned} \tag{15.21}$$

Next eliminating y:

$$[pcc.2]z = [pcn.2] \tag{15.22}$$

where

$$\begin{aligned} [pcc.2] &= [pcc.1] - \frac{[pbc.1]}{[pbb.1]}[pbc.1], \\ [pcn.2] &= [pcn.1] - \frac{[pbc.1]}{[pcc.1]}[pcn.1], \end{aligned} \tag{15.23}$$

whence

$$z = \frac{[pcn.2]}{[pcc.2]}. \tag{15.24}$$

Substitute z in the first equation of (15.20) and find y; next substitute z and y in the first equation of (15.18) and find x.

The same method of elimination may be used for any number of unknowns.

It can be shown that the *weights* of the three unknowns are given by the following quantities.

$$p_z = [pcc.2],$$
$$p_y = [pbb.2] = [pbb.1]\frac{[pcc.2]}{[pcc.1]}, \tag{15.25}$$
$$p_x = [paa.2] = [paa]\frac{[pbb.1][pcc.2]}{[pbb][pcc] - [pbc][pbc]}.$$

Other methods, beyond the scope of this book, may be used, particularly when a larger number of unknowns is involved.

Note that the weights equal the diagonal terms of the normal equations if the off-diagonal terms are zero.

We may calculate the probable error for the case of more than one unknown. It can be shown that the mean error of unit weight is given by

$$\epsilon_1 = \sqrt{\frac{[pv^2]}{m - \mu}}, \tag{15.26}$$

and the probable error of weight by

$$r_1 = 0.6745\sqrt{\frac{[pv^2]}{m - \mu}}, \tag{15.27}$$

where μ is the number of unknowns. Finally, the mean errors or the probable errors of the unknowns, are obtained as follows

$$\epsilon_x = \frac{\epsilon_1}{\sqrt{p_x}}, \qquad \epsilon_y = \frac{\epsilon_1}{\sqrt{p_y}}, \qquad \epsilon_z = \frac{\epsilon_1}{\sqrt{p_z}} \tag{15.28}$$

or

$$r_x = \frac{r_1}{\sqrt{p_x}}, \qquad r_y = \frac{r_1}{\sqrt{p_y}}, \qquad r_z = \frac{r_1}{\sqrt{p_z}}. \tag{15.29}$$

The normal equation may also be solved in a simple effective manner for the case in which the cross terms $[pab]$, $[pac]$, etc. are small compared with the diagonal terms $[paa]$, $[pbb]$, ... The approximate value of $x, y, \ldots$, may be obtained by first ignoring the cross terms, i.e., by solving $[paa]x = [pan]$, and so on. The approximate values are then used to allow for the cross terms, and a second approximation of the unknowns is found. The process is repeated until a perfect fit is obtained.

Index

Other Freeman Books

SPACETIME PHYSICS
EDWIN F. TAYLOR, Massachusetts Institute of Technology, and
JOHN ARCHIBALD WHEELER, Princeton University

The authors employ many pedagogical tools—including parables, diagrams, marginal notations and figures, and more than 100 provocative, original problems—to help the reader develop the special kind of intuition that is the basis of a true understanding of relativity.

1966, 208 pages, 141 illustrations, $4.75

INFORMATION, A SCIENTIFIC AMERICAN Book

A comprehensive review of the technology of information, this book contains all of the articles and many of the illustrations from the September 1966 issue of SCIENTIFIC AMERICAN.

1966, 232 pages, illustrated, clothbound $5.00, paperbound $2.50

WORLDS-ANTIWORLDS: Antimatter in Cosmology
HANNES ALFVEN, Royal Institute of Technology, Stockholm

A leading physicist explains a new theory of the universe based on the assumption that matter and antimatter exist in the universe in equal quantities.

1966, 110 pages, 19 illustrations, $3.50

ELEMENTS OF ASTROMECHANICS
PETER VAN DE KAMP, Sproul Observatory, Swarthmore College

In this compact introduction to astromechanics, an eminent astronomer discusses the motions of planets, single and double stars, and artificial satellites, using simple illustrations to develop the basic principles underlying these motions.

1964, 140 pages, 50 illustrations, clothbound $4.00, paperbound $2.00

PHYSICAL GEODESY
WEIKKO A. HEISKANEN, Isostatic Institute of the International Association of Geodesy, and HELMUT MORITZ, Technical University of Berlin

Theoretical in orientation and intuitive in approach, this book covers both standard topics and recent developments.

Publication date: February 1967

CONCEPTS OF CLASSICAL OPTICS
JOHN STRONG, The Johns Hopkins University

Useful for either text or reference purposes, this volume contains seventeen appendixes, consisting of essays written by authorities on topics of research interest.

1958, 692 pages, 414 illustrations, $9.50

W. H. FREEMAN AND COMPANY

660 Market Street, San Francisco, California 94104
Warner House, 48 Upper Thames Street, London, E. C. 4

VAN DE KAMP

Principles of Astrometry

FREEMAN